



TECHNISCHE  
UNIVERSITÄT  
MÜNCHEN



PHYSIK-DEPARTMENT  
Institut für Theoretische Physik  
Lehrstuhl Prof. Dr. Andrzej J. Buras

---

# Quark-Flavour Phenomenology of Models with Extended Gauge Symmetries

Dissertation von

**Maria Valentina Carlucci**

---

München, Mai 2013





TECHNISCHE UNIVERSITÄT MÜNCHEN  
Fakultät für Physik  
Institut für Theoretische Elementarteilchenphysik  
Lehrstuhl T31 Prof. Dr. Andrzej J. Buras

# Quark-Flavour Phenomenology of Models with Extended Gauge Symmetries

**Maria Valentina Carlucci**

Vollständiger Abdruck der von der Fakultät für Physik der Technischen Universität  
München zur Erlangung des akademischen Grades eines

**Doktors der Naturwissenschaften (Dr. rer. nat.)**

genehmigten Dissertation.

**Vorsitzender:** Univ.-Prof. Dr. Lothar Oberauer

**Prüfer der Dissertation:** 1. Univ.-Prof. Dr. Andrzej J. Buras, i.R.  
2. Hon.-Prof. Dr. Wolfgang F. L. Hollik

Die Dissertation wurde am 27.05.2013 bei der Technischen Universität München  
eingereicht und durch die Fakultät für Physik am 11.06.2013 angenommen.



*Sarebbe tutto più semplice se non ti avessero inculcato questa storia del finire da qualche parte, se solo ti avessero insegnato, piuttosto, a essere felice rimanendo immobile. Tutte quelle storie sulla tua strada. Trovare la tua strada. Andare per la tua strada. Magari invece siamo fatti per vivere in una piazza, o in un giardino pubblico [...]*

Alessandro Baricco, *City*



# Abstract

Gauge invariance is one of the fundamental principles of the Standard Model of particles and interactions, and it is reasonable to believe that it also regulates the physics beyond it. In this thesis we have studied the theory and phenomenology of two New Physics models based on gauge symmetries that are extensions of the Standard Model group. Both of them are particularly interesting because they provide some answers to the question of the origin of flavour, which is still unexplained. Moreover, the flavour sector represents a promising field for the research of indirect signatures of New Physics, since after the first run of LHC we do not have any direct hint of it yet.

The first model assumes that flavour is a gauge symmetry of nature,  $SU(3)_f^3$ , spontaneously broken by the vacuum expectation values of new scalar fields; the second model is based on the gauge group  $SU(3)_c \times SU(3)_L \times U(1)_X$ , the simplest non-abelian extension of the Standard Model group. We have traced the complete theoretical building of the models, from the gauge group, passing through the non-anomalous fermion contents and the appropriate symmetry breakings, up to the spectra and the Feynman rules, with a particular attention to the treatment of the flavour structure, of tree-level Flavour Changing Neutral Currents and of new CP-violating phases. In fact, these models present an interesting flavour phenomenology, and for both of them we have analytically calculated the contributions to the  $\Delta F = 2$  and  $\Delta F = 1$  down-type transitions, arising from new tree-level and box diagrams.

Subsequently, we have performed a comprehensive numerical analysis of the phenomenology of the two models. In both cases we have found very effective the strategy of first to identify the quantities able to provide the strongest constraints to the parameter space, then to systematically scan the allowed regions of the latter in order to obtain indications about the key flavour observables, namely the mixing parameters of the neutral  $K^0$ ,  $B^0$  and  $B_s$  meson systems and the most sensitive decay channels. The approach we have used has been oriented to the understanding of how these models will face more precise data, considering several sample scenarios with reduced uncertainties. In fact, the results of our work are complete patterns of predictions ready to be compared with the experiments of the very next future, in order to soon provide conclusive statements about the viability of the models.

## Kurzfassung

In dieser Doktorarbeit studieren wir die Erweiterung der Eichgruppe des Standardmodells der Teilchenphysik und betrachten insbesondere zwei Neue Physik Modelle: Ein Modell mit geeichter Flavoursymmetrie und ein 331 Modell. Zuerst legen wir die Theorie der Modelle von den grundlegenden Prinzipien bis zu den Feynman Regeln dar. Dann untersuchen wir die Phänomenologie mit Fokus auf den Quark-Flavoursektor: Wir berechnen die Effekte in Prozessen mit flavour-ändernden neutralen Strömen analytisch und führen eine numerische Analyse durch. Unsere Vorhersagen können mit den experimentellen Daten des LHC in naher Zukunft verglichen werden um eine endgültige Aussage über die betrachteten Modelle liefern zu können.



# Contents

<b>Abstract</b>	<b>v</b>
<b>Introduction</b>	<b>1</b>
<b>1 Flavour physics: the state of the art</b>	<b>7</b>
1.1 Theoretical tools . . . . .	7
1.1.1 Operator Product Expansion . . . . .	7
1.1.2 Penguin-Box Expansion . . . . .	8
1.2 Relevant processes . . . . .	9
1.2.1 $\Delta F = 2$ transitions . . . . .	9
1.2.2 $\Delta F = 1$ transitions . . . . .	15
1.3 Tensions in flavour observables . . . . .	20
1.3.1 The $\epsilon_K - S_{\psi K_S}$ tension . . . . .	20
1.3.2 The determination of $V_{ub}$ . . . . .	20
1.3.3 More discrepancies and anomalies . . . . .	22
1.4 Patterns of flavour violation . . . . .	24
1.4.1 The NP flavour problem . . . . .	24
1.4.2 Constrained Minimal Flavour Violation . . . . .	25
1.4.3 Minimal Flavour Violation at Large . . . . .	27
1.4.4 Beyond Minimal Flavour Violation . . . . .	29
<b>2 Theory and phenomenology of Gauged Flavour Symmetries</b>	<b>31</b>
2.1 The model . . . . .	31
2.1.1 Gauge group and field content . . . . .	31
2.1.2 Lagrangian and symmetry breaking . . . . .	36
2.2 Preliminary considerations . . . . .	41
2.2.1 Exploring the parameter space . . . . .	41
2.2.2 Spectrum . . . . .	44
2.3 Phenomenological analysis . . . . .	46
2.3.1 Impact on the observables . . . . .	46
2.3.2 Numerical analysis . . . . .	52
<b>3 Theory and phenomenology of 331 models</b>	<b>57</b>
3.1 General theory . . . . .	57
3.1.1 Gauge group and fermion representations . . . . .	57
3.1.2 Spontaneous symmetry breaking . . . . .	60

---

3.2	Aspects of the models . . . . .	70
3.2.1	Number of generations . . . . .	70
3.2.2	Peccei-Quinn symmetry . . . . .	76
3.3	The $\overline{331}$ model . . . . .	79
3.3.1	Model content . . . . .	79
3.3.2	Quark mixing and FCNCs . . . . .	82
3.4	Phenomenology of the $\overline{331}$ model . . . . .	85
3.4.1	Impact on the master functions . . . . .	85
3.4.2	Correlations . . . . .	88
3.4.3	Numerical analysis . . . . .	90
	<b>Conclusions and outlook</b>	<b>105</b>
	<b>A Feynman rules of the GFS model</b>	<b>109</b>
	<b>B Feynman rules of the <math>\overline{331}</math> model</b>	<b>113</b>
	<b>C Input Values</b>	<b>115</b>
	<b>Bibliography</b>	<b>137</b>
	<b>Acknowledgments</b>	<b>139</b>

# Introduction

“Not only God does play dice, but he sometimes confuses us by throwing them where they can’t be seen” [1]. Stephen Hawking was talking about black holes when he made this consideration, but this seems very appropriate to comment the situation after the first run of the Large Hadron Collider (LHC) at CERN: we know that there should be something beyond the Standard Model (SM) of particles and interactions, but even if we are searching better and better investigating the smallest distances ever reached, nature is not giving us any hint of what or where yet.

On March 30, 2010, the first proton-proton collisions at a center-of-mass energy of 7 TeV marked the beginning of a long-awaited new era in particle physics. And the LHC did not disappoint the expectations: on July 4, 2012, the experiments ATLAS [2] and CMS [3] announced to the world the discovery of a boson of mass 125 GeV compatible with the Higgs boson. Then, after months of prudence during which people preferred to refer to this particle as a Higgs-like, Higgs-ish or even Higgisy boson [4], CERN general director Rolf Heuer and CERN research director Sergio Bertolucci considered the evidences gathered by the experiments sufficient to break the taboo and call it ‘a’ Higgs boson. However, trying to contain the great enthusiasm for this historical discovery and to look objectively to the things, there is a *fil rouge* through all the results obtained by the LHC experiments in these first three years of data taking: the triumph of the SM. In fact, the Higgs boson we have found seems more and more compatible with its SM description, which is just little more than a toy model. Moreover, not only no hints of new particles have been found, but the measured mass of the Higgs boson seems discouraging for the most popular extensions of the SM: it suggests that the energy scale of Supersymmetry could be so high to make it hardly detectable at the LHC [5–7], it disfavors several types of composite-Higgs models [8], and it seems to put in difficulty some realizations of the Randall-Sundrum model [9–11]. Finally, on the side of precision physics, nothing in disagreement with the SM predictions has been found (for example, the branching ratio of the rare decay  $B_s \rightarrow \mu^+ \mu^-$  [12]), and the previous few weak hints of discrepancies have been withdrawn (for example, the mixing phase in the  $B_s$ -meson system [13]). “It is too early to despair, but there is more than enough to start a depression!” Guido Altarelli said, commenting the first LHC results already in 2011 [14].

The reason why this uncontested experimental success of the SM is sometimes so

frustrating is that it is well known that the SM cannot be the ultimate particle theory. Of course, the most evident aspect for which the SM is incomplete is that it does not describe everything, for example dark matter, baryogenesis, and especially gravity. In fact, the SM does not include the gravitational interaction, and, even worse, it cannot, because a quantum theory of gravity is necessarily non-renormalizable [15]. However, the absence of the gravity is not the main problem in itself, at least because phenomenologically quantum gravitational effects are not expected to play an important role below energies around the Planck mass  $M_{\text{Pl}} = \sqrt{\hbar c/2\pi G_N} \simeq \mathcal{O}(10^{19})$  GeV, but it is just this huge energy scale that leads to a severe problem in the SM. In fact, the energy scale of the electroweak interactions is set by the vacuum expectation value (vev) of the Higgs boson,  $v \simeq 246$  GeV. Now, differently from gauge boson masses and fermion masses which are protected respectively by the gauge symmetry and by an approximate chiral symmetry, the Higgs mass receives quadratic corrections which can only be limited by introducing a new explicit high-energy scale  $\Lambda$  in the theory as a cut-off. If one assumes that the SM is the only valid theory up to the gravity energy scale, the only possible cut-off is  $M_{\text{Pl}}$ . This means that the Higgs boson has a bare squared mass of  $\mathcal{O}(10^{38})$  GeV, and that there are quantum corrections of  $\mathcal{O}(10^{34})$  GeV that bring its renormalized squared mass to the electroweak scale. The fact that there are two huge effects from completely different origins that cancel almost exactly each other would be extraordinary, and usually in physics one does not believe in coincidences. This severe problem of naturalness<sup>1</sup> is known as the *gauge hierarchy problem* of the SM [17], and it clearly indicates that the SM must be extended beyond the electroweak energies. Moreover, if this were not enough, there are two other serious theoretical problems of the SM, both due to the assumption that the SM is valid up to the Planck scale: they are the vacuum instability problem [18], confirmed this year by the determination of the Higgs mass [19], and the cosmological constant problem [20]. In summary, the community of physicists believes that there is a more fundamental theory of particles and interactions at the TeV scale (they generally refer to it as New Physics, NP), which should reduce to the SM at low energies in order to explain its experimental success.

From this point of view, the most puzzling sector of the SM is the flavour sector. It provides predictions confirmed with incredible accuracy by experiments, within a few percent and often much less. Yet, it has been built totally *ad hoc* to reproduce the quark masses and mixing without any explanation about its origin, and its structure is definitely not appealing, presenting 13 free parameters (to be compared with the four parameters of the gauge sector), which span over more than five orders of magnitude. The cornerstones of the SM flavour sector are mainly the CKM description of quark mixing and CP violation [21, 22], and the suppression of the Flavour Changing Neutral Currents (FCNCs) through the GIM mechanism [23]. Generally NP models do not present these features, and in order to be in agreement

---

<sup>1</sup>We underline that in this case naturalness is not only an aesthetic criterion. Intuitively, it states that a physical theory that is valid within a certain scale range cannot be critically influenced by the behavior of nature at much lower distances. An enlightening discussion about naturalness is [16].

with the experimental constraints they need either to be pushed up to energy scales much higher than the few TeV one would need, or to be fine-tuned. This is known as the *NP flavour problem* [24]: it seems that NP presents the same flavour pattern as the SM, and this pattern has not been identified yet because the SM does not possess an exact flavour symmetry, but instead simply a flavour structure that could only be learnt from data.

What we have discussed up to now shows the twofold interest in flavour: on one hand, together with the whole Higgs sector of which it is part, it is the sector of the SM that most urgently calls for some NP, possibly explaining its origin and hierarchy; on the other hand, because of the absence of direct signals, the search for indirect signatures in precision physics, with the joint efforts of the accuracy improvements in the predictions and the high intensity in the experiments, represents a powerful tool to reveal NP imprints, and the present existence of a few tensions at the level of  $1\text{--}3\sigma$  in this sector is encouraging. The work presented in this thesis explores flavour physics in both these aspects: we analyze two NP models which pretend to explain some features of the flavour structure of the SM, in both cases making use of extended gauge symmetries, and we study their phenomenological predictions about the flavour observables. Gauge invariance is an elegant and powerful principle in physical theories; it led to the formulation both of the theory of electroweak interactions and of Quantum Chromodynamics, and to impressive successes like the prediction of the  $W$  and  $Z$  bosons or the explanation of asymptotic freedom. More generally, the success of the SM, which describes all its forces as gauge interactions, makes the gauge invariance very appealing as a starting point for building NP models.

The first model under consideration has been proposed by Grinstein, Redi and Villadoro in 2010 [25]; since it is based on the assumption that flavour is a spontaneously broken gauge symmetry, we will call it the *Gauged Flavour Symmetry (GFS) model*. The existence of three generations of fermions in the SM can be formalized by the presence in the gauge sector of a global flavour symmetry  $\mathcal{G}_f = \text{U}(3)^3$ ; of course, since the masses and mixings of quarks distinguish flavour, this symmetry should be broken, and in order to avoid the presence of Goldstone bosons it should also be gauged. This idea is very fascinating as an explanation of flavour, and for this reason it has been already explored some years ago [26–35]; nevertheless, it has never been considered really viable because in this framework the gauge bosons associated with the flavour gauge group generally mediate large FCNCs. However, with the only SM fermion content the theory is anomalous, and the authors of [25] noticed that the minimal fermion content needed to remove the anomalies automatically generates a mechanism of inverted hierarchy [36–38], for which the vevs of the flavour-breaking fields are proportional to the inverse of the SM Yukawa couplings, so that the FCNCs will be roughly proportional to positive powers of the Yukawa couplings, suppressing effectively flavour violating effects for the light generations. Therefore, the GFS model presents itself as an elegant explanation of flavour as a

fundamental symmetry of nature, with a plausible phenomenology which is definitely worth of investigation.

The second model we study is based on the extension of the left gauge symmetry of the SM from  $SU(2)_L$  to  $SU(3)_L$ ; the gauge group of this class of models is then  $SU(3)_c \times SU(3)_L \times U(1)_X$  and therefore they are known as *331 models*. A minimal version of 331 models was first introduced in 1992 by Frampton [39] and Pisano and Pleitez [40], motivated mainly by the investigation of lepton flavour violation due to the presence of a doubly-charged gauge boson. When it was pointed out that in this model the cancellation of anomalies does not happen within the single fermion generation as in the SM, and that exactly three fermion generations are needed to make the model anomaly free, it started to draw much interest. 331 models can be concretely built in many ways: in literature, besides the minimal version, one can find realizations with different quantum numbers, with right-handed neutrinos, with different Higgs sectors, with supersymmetric extensions, with further discrete symmetries and many others. In the work of this thesis we have chosen to analyze a specific version with no exotic charges and with a particularly interesting flavour phenomenology.

This thesis is organized as follows. In **Chapter 1** we collect an updated review about the different aspects of flavour physics that will be often treated throughout all the rest of the work. After introducing the theoretical basics of the study of flavour physics, in particular the Operator Product Expansion, we present a catalogue of the relevant flavour processes in their theoretical details and experimental status. Then we discuss the 1-3 $\sigma$  tensions that are present today between the SM predictions and the experimental values of some flavour observables; finally, we introduce the concept of Minimal Flavour Violation as a framework to recognize the flavour structure of NP models to be the same as the one of the SM or to identify deviations from it. **Chapter 2** is devoted to the study of the GFS model. First of all we build the model, starting from its gauge group and its non-anomalous fermion content, then performing the appropriate symmetry breaking; we list the obtained Feynman rules in **Appendix A**. Subsequently, we proceed with the phenomenological analysis: first we investigate the parameter space in order to obtain a first rough idea of the allowed regions and we discuss a realization of the model with a plausible sample point; then, we move to a deeper analysis by deriving the effects on the relevant flavour observables and studying how the model faces the flavour tensions. In **Chapter 3** we treat 331 models, starting with a general theoretical presentation that covers almost all the possible realizations. To this aim, we build the model, with its gauge and Higgs sectors, with a generic fermion content; then we analyze in detail the anomaly cancellation obtaining a systematic list of the possible quantum numbers and fermion contents. Subsequently we move to analyze the specific realization that we have chosen, which we call the  $\overline{331}$  model: we apply to it the results that we have obtained for the general case, drawing out at the end the Feynman rules that are listed in **Appendix B**; then we focus on the flavour sector discussing the tree-level FCNCs and their impact on the relevant flavour observables. The phenomenological

---

analysis consists in a first step in which we constrain the parameter space making use of the data coming from the  $B_{d,s}$  mixing<sup>2</sup>, and in a second step in which we scan the allowed regions in order to verify the effects on the other observables. In the **Conclusions** we summarize for each model the pattern of effects in the flavour sector, highlighting their strong and weak aspects and how they can be tested in order to obtain more definitive statements. The numerical quantities used in the work as input values or for comparisons are collected in **Appendix C**.

---

<sup>2</sup>Throughout all the text we have indicated the  $B^0$  meson as  $B_d$  in order to lighten the notation.



# Chapter 1

## Flavour physics: the state of the art

### 1.1 Theoretical tools

#### 1.1.1 Operator Product Expansion

The interactions relevant for flavour physics are the electroweak interactions, since they are the only ones that distinguish flavour. The hadronic processes are generated by quark interactions; quarks are bounded into hadrons through strong interactions, which are characterized by the typical hadronic energy scales of  $\mathcal{O}(1 \text{ GeV})$ , much lower than the energy scale of  $\mathcal{O}(m_W)$  characterizing the weak interactions. In order to describe the weak interactions of quarks, one needs therefore to work at low energies; however, the presence of these two widely separated scales makes the calculation of the decay amplitudes from the full Hamiltonian quite complicated, since large logarithms may appear, leading to the breakdown of ordinary perturbation theory. The problem can be solved building an effective low energy theory, and the formal framework to achieve this is known as Operator Product Expansion (OPE) [41–43].

OPE allows to write the product of two operators in the same point of the space-time as a convergent series of local operators; this means that one integrates out the high-energy effects into effective low-energy operators, separating the short-distance and long-distance contributions. The hadronic process will be described by an effective Hamiltonian

$$\mathcal{H}_{\text{eff}} = \sum_i C_i(\mu) Q_i , \quad (1.1)$$

where the  $Q_i$ 's are a complete basis of the local operators that govern the process, and the  $C_i$ 's, known as Wilson coefficients, describe the strength each of them contributes with. The mass  $\mu$  is the energy scale that separates the effects coming from different distances; the dependence from it cancels when one evaluates the amplitude of the process

$$\mathcal{A}(I \rightarrow F) = \langle F | \mathcal{H}_{\text{eff}} | I \rangle = \sum_i C_i(\mu) \langle Q_i(\mu) \rangle , \quad (1.2)$$

where the  $C_i(\mu)$  contain the short-distance perturbative contributions, while the long-distance effects are left as explicit degrees of freedom through the matrix elements  $\langle Q_i(\mu) \rangle$ , that are generally non-perturbative. In principle, the value of  $\mu$  can be chosen arbitrarily, but the convenient choice is of course the typical low scale of the considered process; the standard values are  $\mathcal{O}(m_b)$  and  $\mathcal{O}(m_c)$  for the  $B$  and  $D$  decays respectively, and  $\mathcal{O}(1-2 \text{ GeV})$  for  $K$  decays, since  $\mathcal{O}(m_K)$  would be too low for perturbative calculations; as a result, the Wilson coefficients usually include the contributions from the top quark, the  $W$  and  $Z$  bosons, and all the possible heavier NP particles.

The calculation of the Wilson coefficients is performed in the context of ordinary perturbation theory through the matching of the full theory into the effective theory, i.e. imposing the amplitude in the full theory to be reproduced by the corresponding amplitude in the effective one. Since for low energy processes the scale  $\mu$  is small, the large logarithms  $\ln(m_W/\mu)$  are compensated by the smallness of  $\alpha_s(\mu)$  in the evaluation of  $C_i(\mu)$ ; the resummation of the large logarithms can be efficiently performed using the renormalization group methods.

On the other hand, the matrix elements  $\langle Q_i(\mu) \rangle$  are evaluated by means of non-perturbative methods, such as lattice calculations,  $1/N$  expansion, QCD sum rules, chiral perturbation, heavy-quark effective theory and so on.

Exhaustive treatments about the construction of the effective low-energy theories for weak interactions can be found for example in [44] for a formal review, and [45] for a didactical approach.

### 1.1.2 Penguin-Box Expansion

As we have discussed, it is standard to set the OPE scale  $\mu$  at values of  $\mathcal{O}(1-5 \text{ GeV})$ . However, if the aim is to expose the short distance structure of flavour physics and in particular the NP contributions, it is more useful to choose a scale  $\mu_H \sim \mathcal{O}(M_W, m_t)$ , as high as possible but still low enough so that below it the physics is fully described by the SM [46]. In this case the relevant Wilson coefficients are obtained as

$$C_i(\mu) = \sum_j U_{ij}(\mu, \mu_H) C_j(\mu_H) , \quad (1.3)$$

where  $U_{ij}(\mu, \mu_H)$  are the elements of the renormalization group evolution matrix, and the coefficients  $C_j(\mu_H)$  are the ones found in the process of matching the full and the effective theory; the latter will be a linear combination of certain loop functions  $F_k$

$$C_j(\mu_H) = g_j + \sum_k h_{jk} F_k(m_t, \rho_{\text{NP}}) , \quad (1.4)$$

which will derive from the calculations of penguin and box diagrams containing the top quark and possible NP particles, and hence will depend on the parameters  $\rho_{\text{NP}}$  of the NP model; the other SM contributions will be contained in the constant term. As a consequence, the process amplitude will take the form

$$\mathcal{A}(I \rightarrow F) = P_0(I \rightarrow F) + \sum_k P_k(I \rightarrow F) F_k(m_t, \rho_{\text{NP}}) , \quad (1.5)$$

in which the coefficients  $P_i$  collect different contributions:

$$P_i(I \rightarrow F) \propto V_{\text{CKM}}^i B_i \eta_{\text{QCD}}^i, \quad (1.6)$$

where  $V_{\text{CKM}}^i$  denote the relevant combinations of elements of the flavour matrix,  $\eta_{\text{QCD}}^i$  stand symbolically for the renormalization group factors coming from  $U_{ij}(\mu, \mu_H)$ , and  $B_i$  are non-perturbative parameters deriving from the hadronic matrix elements  $\langle Q_i(\mu) \rangle$ .

The advantages of this approach, known as penguin-box expansion [47], become evident when one considers the properties of the contributions involved.

- In the SM, since the only source of flavour and CP violation is the mass matrix, which has been factored out, the master functions  $F_i$  are *universal* (i.e., process independent), and *real*.
- As there are no right-handed charged current weak interactions, in the SM only certain number of local operators is present, and hence only a particular set of parameters  $B_i$  is relevant. Similarly, if a careful treatment of the QCD corrections is performed, the factors  $\eta_{\text{QCD}}^i$  can be calculated within the SM independently from the choice of the operator basis in the effective weak Hamiltonian. In conclusion, the  $P_i$  coefficients are process dependent, but they depend only on the operator structure of the model.

The master functions, which we have generically called  $F_i$ , often known as Inami-Lim functions [48], are obtained from the calculation of the penguin diagrams (they are commonly known as  $C(m_t, \rho_{\text{NP}})$  for the  $Z$ -penguin,  $D(m_t, \rho_{\text{NP}})$  for the  $\gamma$ -penguins,  $D'(m_t, \rho_{\text{NP}})$  for the  $\gamma$ -magnetic penguin,  $E(m_t, \rho_{\text{NP}})$  for the gluon penguin,  $E'(m_t, \rho_{\text{NP}})$  for the chromomagnetic penguin), and box diagrams ( $S(m_t, \rho_{\text{NP}})$  for  $\Delta F = 2$  transitions,  $B^{\nu\bar{\nu}}(m_t, \rho_{\text{NP}})$  and  $B^{\ell^+\ell^-}(m_t, \rho_{\text{NP}})$  for  $\Delta F = 1$  transitions); the functions  $C$ ,  $D$ ,  $B^{\nu\bar{\nu}}$ ,  $B^{\ell^+\ell^-}$  are gauge dependent, and are combined into the gauge-independent functions  $X(m_t, \rho_{\text{NP}})$ ,  $Y(m_t, \rho_{\text{NP}})$ ,  $Z(m_t, \rho_{\text{NP}})$ . The result is a set of seven gauge independent functions which govern the FCNC processes, given by  $S$ ,  $X$ ,  $Y$ ,  $Z$ ,  $E$ ,  $D'$ ,  $E'$ ; the subscript '0' is used to indicate when these functions do not include QCD corrections, but in many cases these corrections at various orders have been calculated. The expressions for all the master functions at the leading order in the SM can be found in [45].

## 1.2 Relevant processes

### 1.2.1 $\Delta F = 2$ transitions

#### Formalism of the oscillation of neutral mesons

The systems of neutral meson-antimeson  $M - \bar{M}$  are described as a two-state quantum system governed by the non-hermitian Hamiltonian

$$\mathbf{H} = \mathbf{M} - i\mathbf{\Gamma} = \begin{pmatrix} M_{11} - \frac{i}{2}\Gamma_{11} & M_{12} - \frac{i}{2}\Gamma_{12} \\ M_{12}^* - \frac{i}{2}\Gamma_{12}^* & M_{11} - \frac{i}{2}\Gamma_{11} \end{pmatrix}, \quad (1.7)$$

where  $M_{21} = M_{12}^*$ ,  $\Gamma_{21} = \Gamma_{12}^*$  for the hermiticity of  $\mathbf{M}, \mathbf{\Gamma}$ , and  $M_{22} = M_{11}$ ,  $\Gamma_{22} = \Gamma_{11}$  for the CPT invariance; this kind of effective hamiltonian can describe the mixing and the decay of the mesons. In fact, it can be derived in the context of the Wigner-Weisskopf approximation [49], which permits to obtain from the fundamental hermitian Hamiltonian  $\mathcal{H}$  of the system of the mesons plus the final states  $f$  the effective non-hermitian Hamiltonian  $\mathbf{H}$  for the systems of the mesons, with

$$\mathbf{M}_{ij} = m_M \delta_{ij} + \langle i | \mathcal{H} | j \rangle + PV \sum_f \frac{\langle i | \mathcal{H} | f \rangle \langle f | \mathcal{H} | j \rangle}{m_M - E_f}, \quad (1.8a)$$

$$\mathbf{\Gamma}_{ij} = 2\pi \sum_f \delta(m_M - E_f) \langle i | \mathcal{H} | f \rangle \langle f | \mathcal{H} | j \rangle. \quad (1.8b)$$

Now,  $M, \bar{M}$  mix into the eigenstates of mass and width  $M_L, M_S$ :

$$|M_{L,S}\rangle = p |M\rangle \pm q |\bar{M}\rangle \quad \text{with} \quad \frac{p}{q} = \sqrt{\frac{M_{12} - \frac{i}{2}\Gamma_{12}}{M_{12}^* - \frac{i}{2}\Gamma_{12}^*}}, \quad (1.9)$$

whose eigenvalues are

$$\mu_{L,S} = \left( M_{11} - \frac{i}{2}\Gamma_{11} \right) \pm Q \quad \text{with} \quad Q = \sqrt{\left( M_{12} - \frac{i}{2}\Gamma_{12} \right) \left( M_{12}^* - \frac{i}{2}\Gamma_{12}^* \right)}. \quad (1.10)$$

Introducing the formal quantities

$$m_{L,S} = \text{Re}(\mu_{L,S}) = M_{11} \pm \text{Re}Q, \quad \Gamma_{L,S} = -2 \text{Im}(\mu_{L,S}) = \Gamma_{11} \mp 2 \text{Im}Q, \quad (1.11a)$$

$$m = \frac{m_L + m_S}{2} = M_{11}, \quad \Gamma = \frac{\Gamma_L + \Gamma_S}{2} = \Gamma_{11}, \quad (1.11b)$$

$$\Delta M = m_S - m_L = 2 \text{Re}Q, \quad \Delta \Gamma = \Gamma_L - \Gamma_S = -4 \text{Im}Q, \quad (1.11c)$$

the time evolution of the meson states reads

$$|M(t)\rangle = g_+(t) |M\rangle + \frac{q}{p} g_-(t) |\bar{M}\rangle, \quad (1.12a)$$

$$|\bar{M}(t)\rangle = \frac{p}{q} g_+(t) |M\rangle + g_-(t) |\bar{M}\rangle, \quad (1.12b)$$

where

$$g_{\pm}(t) = e^{-imt} e^{-\frac{\Gamma}{2}t} \left( \cos \frac{\Delta M t}{4} \cosh \frac{\Delta \Gamma t}{4} \pm i \sin \frac{\Delta M t}{4} \sinh \frac{\Delta \Gamma t}{4} \right); \quad (1.13)$$

the interpretation of these expressions is clear: starting from a pure  $M$  ( $\bar{M}$ ) state, of mass  $m$ , this self-interacts making transitions to  $\bar{M}$  ( $M$ ) with oscillations governed by the quantity  $\Delta M$ , and meanwhile the mixing of states decays according to the parameter  $\Gamma$ .

In general  $M_L, M_S$  are not CP eigenstates: this would be true only if  $|p| = |q|$ , i.e. if the phase

$$\phi = \arg \left( -\frac{M_{12}}{\Gamma_{12}} \right) \quad (1.14)$$

were zero; we will see that the quantity  $\Delta\Gamma$  is linked to this phase.

What we have discussed until now can be applied to all the systems of neutral mesons. For a specific system one can apply approximations due to the hierarchy of the parameters and consider the relevant CP-violating observables; in the following we are going to analyze the meson systems which will be considered in this work.

- **$K^0 - \bar{K}^0$  system**

For this system, experimentally one finds that  $|p/q| \sim 1 + \mathcal{O}(10^{-3})$ , and hence  $\text{Im}M_{12}^K \ll \text{Re}M_{12}^K$ ,  $\text{Im}\Gamma_{12}^K \ll \text{Re}\Gamma_{12}^K$ ; in the SM this is due to the hierarchy of the Yukawa matrix elements. These relations imply that one can write explicitly

$$\Delta M_K \simeq 2 \text{Re}M_{12}^K, \quad \Delta\Gamma_K \simeq 2 \text{Re}\Gamma_{12}^K, \quad (1.15)$$

obtaining the observable quantities as functions of the entries of the effective Hamiltonian.

As regards the CP violation in the kaon system, it is well known that the mass eigenstates  $K_S$  and  $K_L$  preferably decay to  $2\pi$  and  $3\pi$  respectively, and that the violation of this rule is a proof of indirect CP violation<sup>1</sup>. As a consequence, a relevant quantity to characterize the CP violation in the  $K^0 - \bar{K}^0$  system is

$$\epsilon_K \equiv \frac{\langle (\pi\pi)_{I=0} | K_L \rangle}{\langle (\pi\pi)_{I=0} | K_S \rangle}, \quad (1.16)$$

where selecting the states with zero strong isospin one eliminates the dependence from phase conventions [50]. Following the non-trivial derivation of [50], and including the most recent computations (see for example [51]), the theoretical formula for  $\epsilon_K$  reads

$$\epsilon_K = e^{i\varphi_\epsilon} \kappa_\epsilon \frac{\text{Im}M_{12}^K}{2\sqrt{2} \text{Re}M_{12}^K}, \quad (1.17)$$

where  $\varphi_\epsilon$  and  $\kappa_\epsilon$  parametrize the corrections due to the dropping of some small phases and contributions to the approximate formula; moreover, in order to reduce the amount of error, in this formula one can substitute the term  $2 \text{Re}M_{12}^K$  with the experimental value of  $\Delta M_K$ .

- **$B_q - \bar{B}_q$  systems**

In the case of the  $B_d$  and the  $B_s$  systems, experimentally the hierarchy  $|\Gamma_{12}^q| \ll |M_{12}^q|$  ( $q = d, s$ ) is found instead; this implies

$$\Delta M_q \simeq 2|M_{12}^q|, \quad \Delta\Gamma_q \simeq 2|\Gamma_{12}^q| \cos \phi_q \quad (1.18)$$

for the relations between the observables and the effective Hamiltonian.

---

<sup>1</sup>This kind of CP violation is called indirect as it does not proceed via explicit breaking of the CP symmetry in the decay itself, but via the mixing of states with opposite CP parity into the initial state.

For the study of CP violation in these systems, it is interesting to consider the decays to a final state  $f$ , CP eigenstate with eigenvalue  $\eta_f$ , which is accessible to both  $B_q$  and  $\bar{B}_q$  mesons (for a recent review, see [52]). In these cases one can introduce the key quantity

$$\lambda_f = \frac{q \langle f | \bar{B}_q \rangle}{p \langle f | B_q \rangle}, \quad (1.19)$$

which permits to estimate the CP violations

$$\mathcal{A}_f^{\text{dir}} = \frac{1 - |\lambda_f|^2}{1 + |\lambda_f|^2}, \quad \mathcal{A}_f^{\text{mix}} = -\frac{2 \text{Im} \lambda_f}{1 + |\lambda_f|^2}, \quad (1.20)$$

where the first one is non-vanishing in presence of CP violation in the oscillation  $B_q - \bar{B}_q$ , while the second is non-vanishing in presence of CP violation in the interference between the two possible decay channels  $B_q \rightarrow f$  and  $B_q \rightarrow \bar{B}_q \rightarrow f$ . These quantities are experimentally accessible through the measurement of the time-dependent asymmetry

$$a_{\text{CP}}(t) \equiv \frac{\Gamma(\bar{B}_q(t) \rightarrow f) - \Gamma(B_q(t) \rightarrow f)}{\Gamma(\bar{B}_q(t) \rightarrow f) + \Gamma(B_q(t) \rightarrow f)}, \quad (1.21)$$

which can be written as

$$a_{\text{CP}}(t) = -\frac{\mathcal{A}_f^{\text{dir}} \cos(\Delta M_q t) + \mathcal{A}_f^{\text{mix}} \sin(\Delta M_q t)}{\cosh\left(\frac{\Delta \Gamma_q t}{2}\right) - \frac{2 \text{Re} \lambda_f}{1 + |\lambda_f|^2} \sinh\left(\frac{\Delta \Gamma_q t}{2}\right)}. \quad (1.22)$$

In the  $B_q$  decays dominated by the  $b \rightarrow c\bar{c}s$  transition, one has simply  $\lambda_f = \eta_f e^{-i\phi_q}$ ; therefore  $\mathcal{A}_f^{\text{dir}} = 0$ , and it is common to denote the mixing-induced CP asymmetry as  $S_f$ ; it reads simply

$$S_f \equiv \mathcal{A}_f^{\text{mix}} = \eta_f \sin \phi_q \quad (1.23)$$

and permits to access directly to the phase  $\phi_q$ .

## Theoretical predictions and experimental status

The absorptive part of the  $\Delta F = 2$  effective Hamiltonian  $\mathbf{H}$ ,  $\Gamma_{12}$ , is hardly affected by NP effects in most of the models beyond the SM, since it receives contributions only from on-shell transitions; moreover, its phase can be considered negligible for all purposes. On the other hand, the dispersive part of  $\mathbf{H}$ ,  $M_{12}$ , is sensitive to new short distance dynamics, and hence the most interesting observables under the NP point of view are the ones that depend on its modulus and phase, namely the mass differences and the CP-violating parameters that we have presented. At the leading order  $M_{12}$  is just the matrix element of the  $\Delta F = 2$   $M - \bar{M}$  transition Hamiltonian:

$$M_{12}^M = \frac{\langle M | \mathcal{H}_{\text{eff}}^{\Delta F=2} | \bar{M} \rangle}{2m_M}, \quad (1.24)$$

normalized to the meson mass. In the OPE formalism, the most general effective hamiltonian for the  $\Delta F = 2$  transitions can contain eight different local operators:

$$\mathcal{H}_{\text{eff}}^{\Delta F=2} = \frac{G_F^2}{16\pi^2} \sum_{i=1}^8 C_i(\mu) Q_i, \quad (1.25)$$

$$Q_1^{\text{VLL}} = (\bar{q}_i^\alpha \gamma_\mu P_L q_j^\alpha) (\bar{q}_i^\beta \gamma^\mu P_L q_j^\beta), \quad Q_1^{\text{VRR}} = (\bar{q}_i^\alpha \gamma_\mu P_R q_j^\alpha) (\bar{q}_i^\beta \gamma^\mu P_R q_j^\beta), \quad (1.26a)$$

$$Q_1^{\text{LR}} = (\bar{q}_i^\alpha \gamma_\mu P_L q_j^\alpha) (\bar{q}_i^\beta \gamma^\mu P_R q_j^\beta), \quad (1.26b)$$

$$Q_2^{\text{LR}} = (\bar{q}_i^\alpha P_L q_j^\alpha) (\bar{q}_i^\beta P_R q_j^\beta), \quad (1.26c)$$

$$Q_1^{\text{SLL}} = (\bar{q}_i^\alpha P_L q_j^\alpha) (\bar{q}_i^\beta P_L q_j^\beta), \quad Q_2^{\text{SRR}} = (\bar{q}_i^\alpha \sigma_{\mu\nu} P_R q_j^\alpha) (\bar{q}_i^\beta \sigma^{\mu\nu} P_R q_j^\beta), \quad (1.26d)$$

$$Q_2^{\text{SLL}} = (\bar{q}_i^\alpha \sigma_{\mu\nu} P_L q_j^\alpha) (\bar{q}_i^\beta \sigma^{\mu\nu} P_L q_j^\beta), \quad Q_1^{\text{SRR}} = (\bar{q}_i^\alpha P_R q_j^\alpha) (\bar{q}_i^\beta P_R q_j^\beta), \quad (1.26e)$$

with  $\alpha, \beta$  being color indices and  $\sigma_{\mu\nu} = \frac{1}{2} [\gamma_\mu, \gamma_\nu]$ .

In the SM only the operator  $Q_1^{\text{VLL}}$  contributes, and the calculation of its matrix element and its Wilson coefficient gives, for the considered mesons,

$$(M_{12}^K)^*_{\text{SM}} = \frac{G_F^2}{12\pi^2} F_K^2 \hat{B}_K m_K m_W^2 [(V_{cs}^* V_{cd})^2 \eta_1 S_0(x_c) + (V_{ts}^* V_{td})^2 \eta_2 S_0(x_t) + 2(V_{ts}^* V_{td})(V_{cs}^* V_{cd}) \eta_3 S_0(x_t, x_c)] , \quad (1.27a)$$

$$(M_{12}^q)^*_{\text{SM}} = \frac{G_F^2}{12\pi^2} F_{B_q}^2 \hat{B}_{B_q} m_{B_q} m_W^2 (V_{tb}^* V_{tq})^2 \eta_B S_0(x_t) . \quad (1.27b)$$

The Wilson coefficients contain two non-trivial contributions. The first one consists in the Inami-Lim functions  $S_0$ , which are the loop functions obtained from the calculations of the two box diagrams that generate the  $M - \bar{M}$  transition in the SM;  $S_0(x_t)$  is the dominant contribution, and the contributions from the charm quark are totally negligible for the  $B_q$  mesons. The second is represented by the factors  $\eta_i$ ; they contain the corrections obtained from the QCD evolution from the scale  $m_W$  to the hadronic scales that characterize the meson systems; they have been evaluated at NLO [53–57] and some of them at NNLO [58, 59].

The matrix element  $\langle M | Q_1^{\text{VLL}}(\mu) | \bar{M} \rangle$  implies the appearance of the non-perturbative factors  $F_M$  and  $\hat{B}_M$ ; they represent the largest source of error in the SM predictions of the  $\Delta F = 2$  observables. While the decay constants are already known with good precision (1-3%), in the very last years significant improvements have been reached also for the other parameters [60–64]: the accuracy of  $\hat{B}_K$  has been lowered below the 3%, and in the  $B$  sector the best results are in the combinations  $F_{B_q} \sqrt{\hat{B}_q}$  (5%) and  $\xi = (F_{B_s} \sqrt{\hat{B}_s}) / (F_{B_d} \sqrt{\hat{B}_d})$  (less than 3%).

Concerning the CP violation in the  $B_d, B_s$  systems, the expression in Eq. (1.27b) shows that in the SM the phases of  $M_{12}^d$  and  $M_{12}^s$  are given only by the contributions of  $V_{td}$  and  $V_{ts}$  respectively, and hence their measurement through the mixing induced CP-asymmetries  $S_f$  provides direct access to the angles  $\beta$  and  $\beta_s$  of the unitarity triangles. The golden modes for the measurements of these phases are respectively  $B \rightarrow J/\psi K_S$  and  $B \rightarrow J/\psi \phi$ , because of their clean experimental signatures. In

presence of NP effects on  $M_{12}^q$ , separating in the new contributions the modulus  $C_{B_q}$  and the phase  $\phi_q$  according to

$$M_{12}^q = |(M_{12}^q)_{SM}| e^{2i\beta(s)} C_{B_q} e^{2i\varphi_q} , \quad (1.28)$$

the expressions of the CP-asymmetries are modified<sup>2</sup>:

$$S_{\psi K_S} = \sin(2\beta + 2\varphi_d) , \quad S_{\psi\phi} = \sin(2|\beta_s| - 2\varphi_s) . \quad (1.29)$$

These expressions can be interpreted in two ways when compared with experiments: on one hand, possible deviations of the experimental data from the SM prediction in these quantities can be attributed to NP phases; on the other hand, the agreement of the SM predictions of these observables with the experimental measurements would not exclude completely the presence of NP phases, since they could instead modify the extraction of the angles of the unitarity triangles. An example of the last possibility can be found in the so-called 2HDM $_{\overline{MFV}}$  (see Sec. 1.4.3).

Experimentally [65], the  $\Delta F = 2$  observables in the  $K$  sector are known with very high precision: the values of  $\Delta M_K$  and  $|\epsilon_K|$  present uncertainties of the 0.1% and 0.5% respectively. In the  $B$  sector, also the mass differences  $\Delta M_d$  and  $\Delta M_s$  are known within errors of less than 1%; as regards the mixing-induced CP asymmetries, while for  $S_{\psi K_S}$  we can count on a moderate uncertainty of the 3.4%, the experimental estimation of  $S_{\psi\phi}$  has been very debated in the last years (see Sec. 1.3.3), but recent measurements can be considered reliable even if they still present a huge uncertainty [66].

### The like-sign dimuon charge asymmetry

We conclude analyzing an observable involving  $\Delta\Gamma$  that is particularly interesting today due to the discrepancy between its SM prediction and its first experimental determinations. The like-sign dimuon charge asymmetry  $A_{sl}^b$  for semileptonic decays of  $b$  hadrons produced in proton-antiproton collisions is defined as

$$A_{sl}^b = \frac{N_b^{++} - N_b^{--}}{N_b^{++} + N_b^{--}} , \quad (1.30)$$

where  $N_b^{++}$  and  $N_b^{--}$  are the numbers of events containing two  $b$  hadrons that decay semileptonically via  $b \rightarrow \mu X$ , producing two positive or two negative muons respectively. It can be expressed as [67]

$$A_{sl}^b = \frac{f_d Z_d a_{sl}^d + f_s Z_s a_{sl}^s}{f_d Z_d + f_s Z_s} , \quad (1.31)$$

where  $Z_q$  are functions of the  $B_q$  mixing parameters  $\Gamma_q$ ,  $\Delta M_q$  and  $\Delta\Gamma_q$ , the quantities  $f_q$  are the production fractions for  $\bar{b} \rightarrow B_q$ , and  $a_{sl}^q$  is the charge asymmetry for the

---

<sup>2</sup>We recommend to be careful not to confuse the similar symbols  $\phi_q$ , which indicates the total phase of  $M_{12}^q$ , and  $\varphi_q$ , which is only the possible NP contribution to that phase.

“wrong-charge” (i.e. a muon charge opposite to the charge of the original  $b$  quark) semileptonic  $B_q$ -meson decay induced by oscillation:

$$a_{sl}^q = \frac{\Gamma(\bar{B}_q(t) \rightarrow \mu^+ X) - \Gamma(B_q(t) \rightarrow \mu^- X)}{\Gamma(\bar{B}_q(t) \rightarrow \mu^+ X) + \Gamma(B_q(t) \rightarrow \mu^- X)} ; \quad (1.32)$$

the latter is time-independent, and can be written as

$$a_{sl}^q = \frac{\Delta\Gamma_q}{\Delta M_q} \tan \phi_q . \quad (1.33)$$

In this way, substituting the experimental values, the like-sign dimuon charge asymmetry reads [68, 69]

$$A_{sl}^b = (0.532 \pm 0.039)a_{sl}^d + (0.468 \pm 0.039)a_{sl}^s , \quad (1.34)$$

showing explicitly the dependence on the relevant parameters  $\Delta\Gamma_q$  and  $\phi_q$ .

The most recent determination of the like-sign dimuon asymmetry, obtained in 2010 in  $6.1 \text{ fb}^{-1}$  of  $p\bar{p}$  collisions recorded with the D0 detector at a center-of-mass energy  $\sqrt{s} = 1.96 \text{ TeV}$  [70], differs by  $3.2\sigma$  from the SM prediction [71].

## 1.2.2 $\Delta F = 1$ transitions

The OPE effective Hamiltonian for the  $\Delta F = 1$  transitions  $d_i \rightarrow d_j$  is

$$\mathcal{H}_{\text{eff}}^{\Delta F=1} = \frac{4G_F}{\sqrt{2}} \sum_{i=1} C_i(\mu) Q_i , \quad (1.35)$$

$$Q_1^{(\prime)} = (\bar{d}_i^\alpha \gamma_\mu P_{L(R)} q^\alpha) (\bar{q}^\beta \gamma^\mu P_{L(R)} d_j^\beta) , \quad Q_2^{(\prime)} = (\bar{d}_i^\alpha \gamma_\mu P_{L(R)} q^\beta) (\bar{q}^\beta \gamma^\mu P_{L(R)} d_j^\alpha) , \quad (1.36a)$$

$$Q_3^{(\prime)} = (\bar{d}_i^\alpha \gamma_\mu P_{L(R)} d_j^\alpha) \sum_q (\bar{q}^\beta \gamma^\mu P_L q^\beta) , \quad Q_4^{(\prime)} = (\bar{d}_i^\alpha \gamma_\mu P_{L(R)} d_j^\beta) \sum_q (\bar{q}^\beta \gamma^\mu P_L q^\alpha) , \quad (1.36b)$$

$$Q_5^{(\prime)} = (\bar{d}_i^\alpha \gamma_\mu P_{L(R)} d_j^\alpha) \sum_q (\bar{q}^\beta \gamma^\mu P_R q^\beta) , \quad Q_6^{(\prime)} = (\bar{d}_i^\alpha \gamma_\mu P_{L(R)} d_j^\beta) \sum_q (\bar{q}^\beta \gamma^\mu P_R q^\alpha) , \quad (1.36c)$$

$$Q_7^{(\prime)} = (\bar{d}_i \sigma_{\mu\nu} P_{L(R)} d_j) F^{\mu\nu} , \quad Q_8^{(\prime)} = (\bar{d}_i \sigma_{\mu\nu} T^a P_{L(R)} d_j) G^{\mu\nu a} , \quad (1.36d)$$

$$Q_9^{(\prime)} = (\bar{d}_i \gamma_\mu P_{L(R)} d_j) (\bar{\ell} \gamma^\mu \ell) , \quad Q_{10}^{(\prime)} = (\bar{d}_i \gamma_\mu P_{L(R)} d_j) (\bar{\ell} \gamma^\mu \gamma_5 \ell) , \quad (1.36e)$$

$$Q_S^{(\prime)} = (\bar{d}_i P_{L(R)} d_j) (\bar{\ell} \ell) , \quad Q_P^{(\prime)} = (\bar{d}_i P_{L(R)} d_j) (\bar{\ell} \gamma_5 \ell) . \quad (1.36f)$$

The operators that are most sensitive to NP are the magnetic ( $Q_7^{(\prime)}$ ), chromomagnetic ( $Q_8^{(\prime)}$ ), semileptonic ( $Q_9^{(\prime)}$  and  $Q_{10}^{(\prime)}$ ), scalar ( $Q_S^{(\prime)}$ ) and pseudoscalar ( $Q_P^{(\prime)}$ ) penguins<sup>3</sup>.

<sup>3</sup> In principle there are also tensor penguins,  $Q_{T(5)} = (\bar{d}_i \sigma_{\mu\nu} d_j) (\bar{\ell} \sigma^{\mu\nu} (\gamma_5) \ell)$ , which could be relevant for some observables.

$\mathbf{B}_{d,s} \rightarrow \mu^+ \mu^-$

These decays are of particular interest among the electroweak penguin processes, because in the SM they present a double suppression, due to the FCNC transition and to the chirality suppression; moreover, beyond SM they are dominated by scalar and pseudoscalar operators, and hence they are particularly sensitive to the exchange of new scalar and pseudoscalar particles; several NP models, especially those with an extended Higgs sector, can significantly enhance the branching ratios even in the presence of other existing constraints.

The branching fraction can be expressed as [72–74]

$$\mathcal{B}(B_q \rightarrow \mu^+ \mu^-) = \frac{G_F^2 \alpha^2}{64\pi^3} F_{B_q} \tau_{B_q} m_{B_q}^3 |V_{tq}^* V_{tb}|^2 \sqrt{1 - \frac{4m_\mu^2}{m_{B_q}^2}} \times \left\{ \left(1 - \frac{4m_\mu^2}{m_{B_q}^2}\right) |C_S - C'_S|^2 + \left| (C_P - C'_P) + 2 \frac{m_\mu}{m_{B_q}} (C_{10} - C'_{10}) \right|^2 \right\}, \quad (1.37)$$

and within the SM the Wilson coefficients  $C_S$  and  $C_P$  are negligibly small, while the dominant contribution of  $C_{10}$  is helicity suppressed, so that the branching ratio becomes [75]

$$\mathcal{B}(B_q \rightarrow \mu^+ \mu^-)_{\text{SM}} = \frac{G_F^2 \alpha}{16\pi^3 \sin^4 \theta_W} F_{B_q} \tau_{B_q} m_{B_q} m_\mu^2 \sqrt{1 - \frac{4m_\mu^2}{m_{B_q}^2}} |V_{tq}^* V_{tb}|^2 Y(x_t), \quad (1.38)$$

where  $Y(x_t)$  is the relevant loop function obtained through the calculation of the penguin diagrams. The decay constraints  $F_{B_q}$  represent the main source of error in the SM prediction, but as we have discussed there has been significant progress in the computation of these quantities in recent years.

Also recently more theoretical improvements have been made in the comprehension of the  $B_s \rightarrow \mu^+ \mu^-$  decay channel in particular. First of all, experimentally the measured branching fraction is the time-averaged branching fraction, which, as first pointed out by [76–78], differs from the theoretical value because of the sizable width difference between the heavy and light  $B_s$  mesons. This requires the introduction of a correction factor:

$$\mathcal{B}(B_s \rightarrow \mu^+ \mu^-)_{\text{theor}} = \frac{1 - y_s^2}{1 + A_{\Delta\Gamma} y_s} \mathcal{B}(B_s \rightarrow \mu^+ \mu^-)_{\text{exp}}, \quad (1.39)$$

with  $y_s = \tau_{B_s} \Delta\Gamma_s / 2 \simeq 0.088$ , and

$$A_{\Delta\Gamma} = \frac{|P|^2 \cos(2 \arg(P) - \varphi_s) - |S|^2 \sin(2 \arg(S) - \varphi_s)}{|P|^2 + |S|^2}, \quad (1.40)$$

where  $P$  and  $S$  are combinations of the Wilson coefficients and  $\varphi_s$  is the possible NP phase in the  $B_s$  mixing;  $A_{\Delta\Gamma}$  can deviate from 1 beyond SM for the presence of scalar and pseudoscalar operators and new phases. It is a matter of choice to include the correction factor in the experimental value or in the theoretical calculation, provided this factor is not significantly affected by NP; including it in the

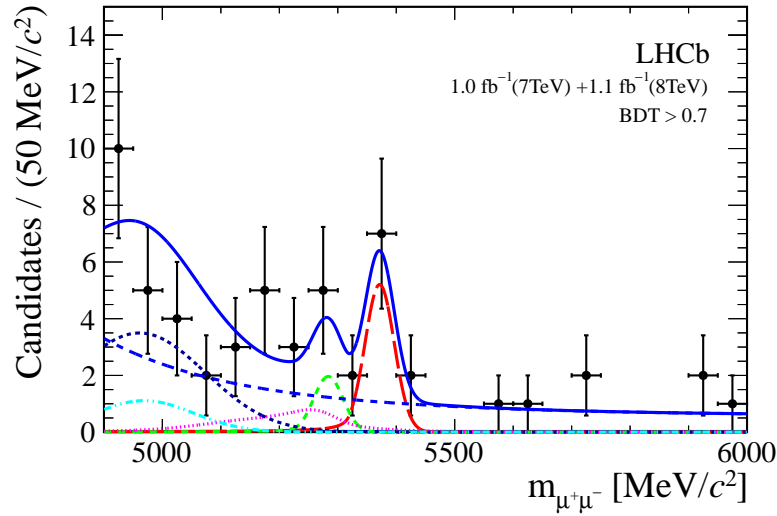


Figure 1.1: First signal of the  $B_s \rightarrow \mu^+ \mu^-$  decay, observed by the LHCb Collaboration [12]: invariant mass distribution of the selected  $B_s \rightarrow \mu^+ \mu^-$  candidates (black dots) in the combined 2011+2012 dataset. The result of the fit is overlaid (blue solid line) and the different components detailed:  $B_s \rightarrow \mu^+ \mu^-$  (red long dashed),  $B_d \rightarrow \mu^+ \mu^-$  (green medium dashed),  $B_{d,s} \rightarrow h^+ h'^-$  (pink dotted),  $B_d \rightarrow \pi^- \mu^+ \nu_\mu$  (black short dashed) and  $B_d^{(+)} \rightarrow \pi^{0(+)} \mu^+ \mu^-$  (light blue dot dashed), and the combinatorial background (blue medium dashed).

experimental branching ratio one can preserve some correlations like the ones of CMFV [79] (see Sec. 1.4.2). Moreover, it is possible to define a CP-asymmetry  $S_{\mu\mu}^s$  analogous to  $S_{\psi K_S}$  and  $S_{\psi\phi}$ :

$$S_{\mu\mu}^s = \frac{|P|^2 \sin(2 \arg(P) - \varphi_s) - |S|^2 \cos(2 \arg(S) - \varphi_s)}{|P|^2 + |S|^2}, \quad (1.41)$$

which is zero in the SM; both  $A_{\Delta\Gamma}$  and  $S_{\mu\mu}^s$  are accessible in the near future providing additional tests of NP models [80].

The first measurement of the branching fraction of  $B_s \rightarrow \mu^+ \mu^-$ , shown in Fig. 1.1, represents one of the most important results achieved by LHCb in the first LHC run [12, 81]. Using data collected in 2011 and 2012, consisting of  $1.0 \text{ fb}^{-1}$  of proton-proton collisions at  $\sqrt{s} = 7 \text{ TeV}$  and  $1.1 \text{ fb}^{-1}$  at  $\sqrt{s} = 8 \text{ TeV}$ , they have measured the signal with a significance of  $3.5\sigma$ . Their value is well compatible with the SM prediction, putting an end to the long-pursued hopes of possible excesses. At the same time, LHCb has also set a new upper bound for  $B_d \rightarrow \mu^+ \mu^-$ .

### $\bar{B} \rightarrow \mathbf{X}_s \gamma$

The inclusive channel  $\bar{B} \rightarrow X_s \gamma$  is considered particularly interesting because it provides generally a very strong constraint on extensions of the SM; in fact, the present experimental measurements have the fair accuracies of about 10% [65], that is of the same size as the available QCD corrections to the perturbative decay width

$\Gamma(b \rightarrow s\gamma)$ , and larger than the known nonperturbative corrections to the relation  $\Gamma(\bar{B} \rightarrow X_s\gamma) \simeq \Gamma(b \rightarrow s\gamma)$  [82].

The effective Hamiltonian of the  $b \rightarrow s\gamma$  transitions receives the contributions from the four-fermion operators  $Q_1 \dots Q_6$  and from the magnetic penguins  $Q_7, Q_8$ . The magnetic  $\gamma$ -penguin plays the crucial role in this decay, but the role of the dominant current-current operator  $Q_2$  is very important too, since the short distance QCD effects involving in particular the mixing between  $Q_2$  and  $Q_7$  enhance the Wilson coefficient  $C_7(\mu_b)$  significantly, so that the final branching ratio turns out to be by a factor of 3 higher than it would be at LO. A peculiar feature of the renormalization group analysis in  $\bar{B} \rightarrow X_s\gamma$  is that the mixing under infinite renormalization between the set  $Q_1 \dots Q_6$  and the operators  $(Q_7, Q_8)$  vanishes at the one-loop level [45]; consequently, in order to calculate the coefficients  $C_7(\mu_b)$  and  $C_8(\mu_b)$  in the leading logarithmic approximation, two-loop calculations are necessary. The corresponding NLO analysis requires the evaluation of the mixing in question at the three-loop level. Because of this peculiar feature, the first fully correct calculation of the leading anomalous dimension matrix relevant for this decay was obtained only in 1993 [83, 84], and the NLO correction in 1996 [85].

Going beyond the SM, also the primed operators  $Q'_7, Q'_8$  could be present. The prediction for the  $\bar{B} \rightarrow X_s\gamma$  branching ratio in the presence of arbitrary NP contributions to the Wilson coefficients  $C_7^{(\prime)}$ ,  $C_8^{(\prime)}$  can be well approximated by the expression [86]

$$\frac{\mathcal{B}(\bar{B} \rightarrow X_s\gamma)}{\mathcal{B}(\bar{B} \rightarrow X_s\gamma)_{\text{SM}}} \simeq 1 + \hat{a}_{77} \left( |C_7^{\text{NP}}|^2 + |C_7^{\prime\text{NP}}|^2 \right) + \hat{a}_{88} \left( |C_8^{\text{NP}}|^2 + |C_8^{\prime\text{NP}}|^2 \right) + \text{Re}(\hat{a}_7 C_7^{\text{NP}}) + \text{Re}(\hat{a}_8 C_8^{\text{NP}}) + \text{Re}(\hat{a}_{78} [C_7^{\text{NP}} C_8^{*\text{NP}} + C_7^{\prime\text{NP}} C_8^{\prime*\text{NP}}]) \quad , \quad (1.42)$$

where  $\hat{a}_i$  are fixed complex numbers and the Wilson coefficients have to be evaluated at a scale  $\mu = 160$  GeV. The primed Wilson coefficients  $C'_7, C'_8$  cannot interfere with the SM contributions to  $C_7, C_8$  in the branching ratio of this inclusive decay, therefore they appear only quadratically, while the NP contributions to the unprimed coefficients also appear linearly. NP contributions to  $C_7, C_8$  are thus expected to be more strongly constrained than contributions to  $C'_7, C'_8$ . However, if  $C_7^{\text{NP}}$  and  $C_8^{\text{NP}}$  are complex, the constraint from  $\mathcal{B}(\bar{B} \rightarrow X_s\gamma)$  can be relaxed to a large extent [87]. For a recent review about the last developments see e.g. [88], while the most recent experimental determination can be found in [89].

## $B \rightarrow X_s \nu \bar{\nu}$

The rare transition  $b \rightarrow s\nu\bar{\nu}$  allows a transparent study of  $Z$ -penguin and other electroweak penguin effects in NP scenarios in the absence of scalar and magnetic penguin contributions that are often dominating in the  $b \rightarrow s\ell^+\ell^-$  and  $b \rightarrow s\gamma$  transitions, as we have just discussed in the previous two sections. The most interesting decays containing this transition are the  $B \rightarrow X_s\nu\bar{\nu}$  inclusive channel and the exclusive channels  $B \rightarrow K^{(*)}\nu\bar{\nu}$ ; while the only observables in  $B \rightarrow X_s\nu\bar{\nu}$  and  $B \rightarrow K\nu\bar{\nu}$  are the respective branching ratios, the angular distribution of the  $K^*$  decay prod-

ucts in the  $B \rightarrow K^*(\rightarrow K\pi)\nu\bar{\nu}$  decay allows to extract additional information about the polarization of the  $K^*$ .

With an estimated uncertainty of less than 10%, the inclusive channel  $B \rightarrow X_s\nu\bar{\nu}$  has the theoretically cleanest branching ratio as it does not involve any form factors (see [90] for a recent analysis). It is useful to normalize this quantity to the semileptonic rate  $B \rightarrow X_c e\bar{\nu}$ , that is experimentally well known, in order to reduce the uncertainties due to the CKM matrix elements and to powers of  $m_b$ . In the SM, the expression of this ratio reads

$$\frac{\mathcal{B}(B \rightarrow X_s\nu\bar{\nu})}{\mathcal{B}(B \rightarrow X_c e\bar{\nu})} = \frac{3\alpha^2}{4\pi \sin^4 \theta_W} \frac{\kappa(0)}{f(z)\kappa(z)} \frac{|V_{ts}|^2}{|V_{cb}|^2} X^2(x_t), \quad (1.43)$$

where  $f(z)$  is the phase space factor in  $B \rightarrow X_c e\bar{\nu}$ ,  $\kappa(z)$  is the QCD correction to the semileptonic decay,  $\kappa(0)$  represents the QCD correction to the matrix element of the  $b \rightarrow \nu\bar{\nu}$  transition due to virtual and bremsstrahlung contributions, and  $X(x_t)$  is the relevant loop function; all these contributions are known with good precision.

None of these three rare decays has been observed yet, and the present experimental upper bounds on their branching ratios, obtained by ALEPH [91], are still far above the SM predictions.

### $K \rightarrow \pi\nu\bar{\nu}$

The  $K^+ \rightarrow \pi^+\nu\bar{\nu}$  and  $K_L \rightarrow \pi^0\nu\bar{\nu}$  decays are the theoretically cleanest processes among the many rare K and B decays (see [92] for a recent review). Both decays, in particular the neutral mode that in the SM is purely induced by direct CP violation, are known to offer unique possibilities to test the structure of flavour and CP violation in extensions of the SM.

The branching fractions of the two channels, as in the previous case normalized to an experimentally well known semileptonic rate in order to reduce the theoretical errors, are [93, 94]

$$\frac{\mathcal{B}(K^+ \rightarrow \pi^+\bar{\nu}\nu)}{\mathcal{B}(K^+ \rightarrow \pi^0 e^+\nu)} = \left( r_{K^+} \frac{3\alpha^2 |V_{us}|^2}{2\pi^2 \sin^4 \theta_W} \right) \times \left[ \left( \frac{\text{Im}(V_{ts}^* V_{td})}{|V_{us}|^5} X(x_t) \right)^2 + \left( \frac{\text{Im}(V_{cs}^* V_{cd})}{|V_{us}|} P_0(X) + \frac{\text{Re}(V_{ts}^* V_{td})}{|V_{us}|^5} X(x_t) \right)^2 \right], \quad (1.44)$$

$$\frac{\mathcal{B}(K_L \rightarrow \pi^0\bar{\nu}\nu)}{\mathcal{B}(K^+ \rightarrow \pi^0 e^+\nu)} = \left( r_{K_L} \frac{\tau_{K_L}}{\tau_{K^+}} \frac{3\alpha^2 |V_{us}|^2}{2\pi^2 \sin^4 \theta_W} \right) \left( \frac{\text{Im}(V_{ts}^* V_{td})}{|V_{us}|^5} X(x_t) \right)^2, \quad (1.45)$$

where  $r_{K^+}$ ,  $r_{K_L}$  summarize the isospin-breaking corrections from the original decay to the reference semileptonic one, due to quark mass effects and electroweak radiative corrections, while  $X(x_t)$  is the relevant loop function, and  $P_0(X)$  is its analogue that accounts for contributions from charm and light quark loops.

On the experimental side, for the charged mode a few candidate events have been reported by the E787 and E949 experiments at BNL [95], while only a very loose upper bound from the E391a experiment at KEK exists for the neutral mode [96].

The central value of the measured branching ratio of  $K^+ \rightarrow \pi^+ \nu \bar{\nu}$  is a factor of 2 above the SM prediction, but it is perfectly consistent with the SM, given the large experimental error at present. In the near future the NA62 experiment at CERN and the KOTO experiment at JPARC will aim to improve the sensitivity for the charged and neutral channels respectively.

## 1.3 Tensions in flavour observables

### 1.3.1 The $\epsilon_K - S_{\psi K_S}$ tension

Using the unitarity of the CKM matrix, in the SM the expression of  $\epsilon_K$  can be rewritten with a reduced number of CKM elements as

$$|\epsilon_K|^{\text{SM}} = \kappa_\epsilon \frac{G_F^2 F_K^2 \hat{B}_K m_K m_W^2}{6\sqrt{2}\pi^2 \Delta M_K} |V_{cb}|^2 |V_{us}|^2 \times \left( \frac{1}{2} |V_{cb}|^2 R_t^2 \sin 2\beta \eta_2 S_0(x_t) + R_t \sin \beta (\eta_3 S_0(x_c, x_t) - \eta_1 x_c) \right), \quad (1.46)$$

where  $R_t$  is a side of the unitarity triangle, determinable with small uncertainty as

$$R_t \equiv \frac{|V_{tb}^* V_{td}|}{|V_{cb}^* V_{cd}|} = \frac{\xi}{|V_{us}|} \sqrt{\frac{m_{B_s}}{m_{B_d}}} \sqrt{\frac{\Delta M_d}{\Delta M_s}}; \quad (1.47)$$

in this way, the CKM dependence of  $\epsilon_K$  is in  $|V_{us}|$ ,  $|V_{cb}|$ , which are fixed by tree-level processes, and in the angle  $\beta$  of the unitarity triangle.

Recently the uncertainty on the SM prediction of  $\epsilon_K$ , due to the improvements in the calculation of the corrections and in the accuracy of the non-perturbative parameters, has been reduced down to roughly the 15% [59]. This has led to notice [51, 97–99] that, using for  $\beta$  the value obtained from the measurement of  $S_{\psi K_S}$  in the SM frame, the predicted value of  $\epsilon_K$  is about  $2\sigma$  below its experimental value.

Now, believing that this tension is due to the presence of some NP, if the latter is present into  $\epsilon_K$  or into  $S_{\psi\phi}$  depends on the values of the other two tree-level-determined parameters of the CKM matrix, namely  $|V_{ub}|$  and  $\gamma$ . In fact, the  $R_t$  side can be written as

$$R_t = \sqrt{1 + \left[ \left(1 - \frac{|V_{us}|^2}{2}\right) \frac{1}{|V_{us}|} \frac{|V_{ub}|}{|V_{cb}|} \right]^2 - 2 \left(1 - \frac{|V_{us}|^2}{2}\right) \frac{1}{|V_{us}|} \frac{|V_{ub}|}{|V_{cb}|} \cos \gamma}, \quad (1.48)$$

which in the SM should be in agreement with the value obtained from the experiments and lattice according to Eq. (1.47). However, the present measurement of  $\gamma$  is affected by a large uncertainty [65], while the determination of  $|V_{ub}|$  is controversial.

### 1.3.2 The determination of $V_{ub}$

The modulus of the CKM matrix element  $V_{ub}$  can be determined at tree level through the transition  $b \rightarrow u \ell \bar{\nu}$ . However, considering the inclusive decay  $B \rightarrow X_u \ell \bar{\nu}$ , one

	Scenario 1 $ V_{ub}  = 3.23(31) \times 10^{-3}$	Scenario 2 $ V_{ub}  = 4.41(32) \times 10^{-3}$	Experiment
$10^{15} \Delta M_K$ (GeV)	3.05(43)	3.04(43)	3.484(5)
$10^{13} \Delta M_d$ (GeV)	3.65(40)	3.69(41)	3.337(33)
$10^{11} \Delta M_s$ (GeV)	1.25(14)	1.26(14)	1.164(5)
$10^3  \epsilon_K $	1.72(24)	2.25(32)	2.228(11)
$S_{\psi K_S}$	0.646(24)	0.827(31)	0.676(21)
$S_{\psi\phi}$	0.034(1)	0.046(2)	-0.001(105)
$10^4 \mathcal{B}(B^+ \rightarrow \tau^+\nu)$	0.62(14)	1.02(20)	1.15(23)

Table 1.1: SM predictions of the relevant observables in the two  $|V_{ub}|$  scenarios, compared with their experimental values.

has the difficulty of the large  $B \rightarrow X_c \ell \bar{\nu}$  background; on the other hand, for the exclusive channels, like  $B \rightarrow \pi \ell \bar{\nu}$ , the form factors have to be known. A result of these complications is that the present determinations of  $|V_{ub}|$  from inclusive and exclusive decays show a discrepancy of about  $4\sigma$  [65].

As we have discussed in the previous section, the value of  $V_{ub}$  influences sensibly the balance of the  $|\epsilon_K| - S_{\psi K_S}$  relation. In this context, taking for  $|V_{ub}|$  the average between the inclusive and the exclusive determination, with a huge uncertainty, would wash out any kind of indication from this tension of precision observables. A more useful approach is to assume that, instead of being both far from the actual value of  $|V_{ub}|$ , in the future only one between its inclusive and the exclusive determinations will reveal itself to present some large error. As a consequence, we are led to consider two limiting scenarios:

- **Scenario 1:** Exclusive (small)  $|V_{ub}|$ .

Setting the tree-level-determined parameters  $|V_{us}|$ ,  $|V_{cb}|$ ,  $\gamma$  to their central values, and using as the fourth independent input of the CKM matrix the exclusive value of  $|V_{ub}|$ , the unitarity of the CKM matrix permits to determine the value of  $\beta$ . Using the latter, one finds that  $S_{\psi K_S}$  is in agreement with data, while  $|\epsilon_K|$  is well below its experimental measurement.

As discussed in [98, 99], a sizeable constructive NP contribution to  $\epsilon_K$  would not require an increased value of  $\sin 2\beta$  relative to the experimental value of  $S_{\psi K_S}$ . NP of this type would then remove the  $\epsilon_K - S_{\psi K_S}$  anomaly in the presence of the exclusive value of  $|V_{ub}|$ .

- **Scenario 2:** Inclusive (large)  $|V_{ub}|$ .

Exploiting as in the previous case the unitarity of the CKM matrix to derive  $\beta$ , using the inclusive determination of  $|V_{ub}|$  one obtains this time that  $|\epsilon_K|$  is in good agreement with data, while  $S_{\psi K_S}$  is significantly above its experimental value.

As shown in [97, 98], a negative NP phase  $\varphi_d$  in the  $B_d$  mixing would solve the  $\epsilon_K - S_{\psi K_S}$  tension in this case, since  $\sin 2\beta$  would be larger than  $S_{\psi K_S}$ ,

implying a higher value on  $|\epsilon_K|$ , in reasonable agreement with data, and a better fit of the unitarity triangle.

This kind of analysis imply that the structure of a certain NP model could prefer a specific determination of  $|V_{ub}|$ ; then, the correlated effects on other observables, especially  $\Delta M_{s,d}$ , would represent a powerful test for such a model. This will be the case of the two models studied in this work: we will show that the GFS model selects the Scenario 1, while the  $\overline{331}$  model selects the Scenario 2.

In Tab. 1.1 we report the SM predictions for the crucial flavour observables that are sensitive to  $|V_{ub}|$  in the two scenarios; the request of the agreement with the experiment values will guide the analysis of the NP models.

### 1.3.3 More discrepancies and anomalies

#### $\Delta M_{d,s}$ versus $\epsilon_K$

Using the most recent lattice inputs, it results that the SM predictions for both  $\Delta M_d$  and  $\Delta M_s$  are slightly above the data, of about  $1\sigma$  once the hadronic uncertainties have been taken into account. While this is not a severe discrepancy in itself, it can become more problematic when also  $\epsilon_K$  is considered. In fact,  $\Delta M_{d,s}$  are often correlated with  $\epsilon_K$  in NP models, and if an enhancement of  $|\epsilon_K|$  is required, as in the case of the  $|V_{ub}|$  Scenario 1, the weak agreement of  $\Delta M_{d,s}$  with experiment could be worsened. As we will discuss in Sec. 1.4.2 and Sec. 2.3.2 respectively, this is the case of models with CMFV and of the GFS model.

#### The anomalous like-sign dimuon asymmetry

As we have anticipated in Sec. 1.2.1, the experimental value of  $A_{sl}^b$  differs by  $3.2\sigma$  from its SM prediction. In [69] a detailed model-independent analysis of NP in the  $B_{d,s} - \bar{B}_{d,s}$  mixing has been performed; it has been found that in order to reconcile  $A_{sl}^b$  with its experimental value, accounting at the same time the constraints coming from  $S_{\psi\phi}$ , NP is required not only in  $M_{12}^{d,s}$ , but also in  $\Gamma_{12}^{d,s}$ .

#### The anomaly in $\mathcal{B}(B \rightarrow D^{(*)}\tau\nu)/\mathcal{B}(B \rightarrow D^{(*)}\ell\nu)$

Based on its full data sample, in 2012 BaBar reported its improved measurements of the ratios  $\mathcal{R}(D^{(*)}) = \mathcal{B}(B \rightarrow D^{(*)}\tau\nu)/\mathcal{B}(B \rightarrow D^{(*)}\ell\nu)$ , with  $\ell = e, \mu$  [100]. With the last updates [101], their results are

$$\mathcal{R}(D)_{\text{exp}} = 0.440 \pm 0.058 \pm 0.042, \quad \mathcal{R}(D^*)_{\text{exp}} = 0.332 \pm 0.024 \pm 0.018, \quad (1.49)$$

that exceed the SM predictions [102]

$$\mathcal{R}(D)_{\text{SM}} = 0.297 \pm 0.017, \quad \mathcal{R}(D^*)_{\text{SM}} = 0.252 \pm 0.003, \quad (1.50)$$

by  $2.0\sigma$  and  $2.7\sigma$  respectively; altogether, the possibility that the measured  $\mathcal{R}(D)$  and  $\mathcal{R}(D^*)$  both agree with the SM predictions is excluded at the  $3.4\sigma$  level. These channels are particularly sensitive to charged Higgs contributions in NP models;

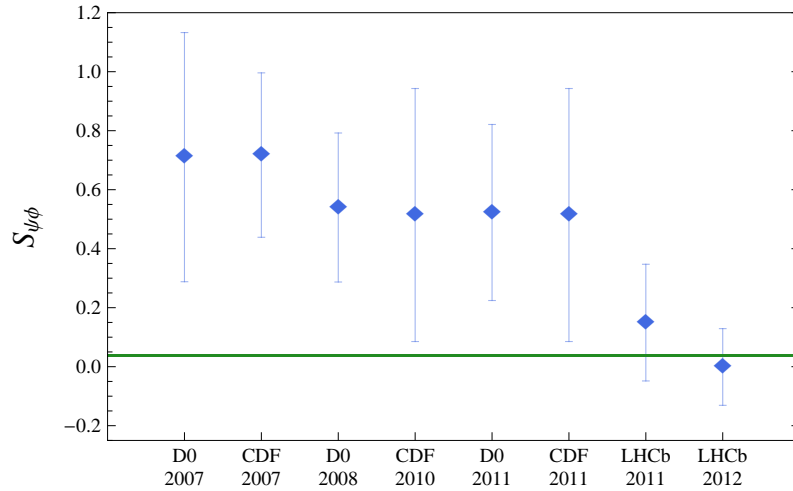


Figure 1.2: Measured values of the mixing-induced CP violation  $S_{\psi\phi}$  from various experiments in the last five years. The green band indicates the SM prediction with its  $3\sigma$  uncertainty.

models with more Higgs doublets present generally physical charged Higgs (for a review, see [103]); however, BaBar showed that for example this excess cannot be explained by a charged Higgs boson in the Type II 2-Higgs-doublet model, which results to be excluded at the 99.8% CL for any value of  $\tan\beta/m_H$ .

### $S_{\psi\phi}$ and $\mathcal{B}(B^+ \rightarrow \tau^+\nu)$ : the fading stars

At the end of 2007, CDF [104] and D0 [105] released their results about the first flavour-tagged determinations of the mixing-induced CP violation  $S_{\psi\phi}$ ; their combined measurements resulted to be larger than the SM predictions by more than  $3\sigma$  [106]. These measurements raised a great enthusiasm in the flavour community, and many speculations about NP in the  $B_s$  mixing phase were proposed. However, as can be seen from Fig. 1.2, in the following years CDF and D0 weakened their claims, and at the end of 2011 LHCb put definitely an end to the optimistic hopes of the previous years [13]. In fact, its value is in perfect agreement with the SM prediction, expecting already for 25 years the mixing-induced CP violation in  $B_s$  decays to be significantly smaller than in  $B_d$  decays. Nevertheless, from the present perspective, the measurement of  $S_{\psi\phi}$  is affected by a large uncertainty, which not only still presents the possibility of moderate enhancements, but this time also contemplates the possibility of being negative; the latter would be an even clearer signature of NP.

Another hint of NP was suspected in the last years in the branching ratio of  $B^+ \rightarrow \tau^+\nu$ . The latter is a simple tree-level decay in the SM, but the attempts to conciliate its prediction from the unitarity triangle fit with its experimental values obtained by BaBar and Belle were very puzzling [107]. In fact, the decay is generated by the transition  $\bar{b} \rightarrow \bar{u}\tau^+\nu$ , and hence the CKM element  $|V_{ub}|$  is involved, the determination of which, as we have discussed, is quite controversial; nevertheless, both with the exclusive and with the inclusive value of  $|V_{ub}|$  the SM prediction resulted

to be largely below the experimental value. Even trying to remove the dependence from  $|V_{ub}|$  by using the unitarity of the CKM matrix, so that the branching ratio depends on the CKM parameters  $|V_{ud}|$ ,  $\beta$  and  $\gamma$ , the SM prediction was still  $2.8\sigma$  lower than the measurement. Now, in 2012 both BaBar [108] and Belle [109] presented their updates about the measurement of  $\mathcal{B}(B^+ \rightarrow \tau^+\nu)$ ; in particular, the latter reported a very smaller value, such to lower the world average and weaken the tension to  $1.6\sigma$  [110].

## 1.4 Patterns of flavour violation

### 1.4.1 The NP flavour problem

In general, new sources of flavour and CP violation are present in NP models. Model-independent considerations can be developed by means of a generic effective theory approach, assuming that the energy scale of NP is a certain  $\Lambda_{\text{NP}}$  and integrating out the NP degrees of freedom; their effects will be described by higher dimensional operators  $O_i^{(d)}$  in the resulting effective Lagrangian

$$\mathcal{L}_{\text{eff}} = \mathcal{L}_{\text{SM}} + \sum_{i, d>4} \frac{c_i^{(d)}}{\Lambda_{\text{NP}}^d} O_i^{(d)}, \quad (1.51)$$

where  $c_i^d$  are unknown effective couplings.

Now, as we have discussed in the Introduction, the solution of SM gauge hierarchy problem would require some NP at a scale  $\Lambda_{\text{NP}}$  that should not exceed a few TeV. On the other hand, the term with the higher dimensional operators contains for example dimension six  $\Delta F = 2$  four-quark operators that lead to contributions to neutral meson mixing; the very good agreement between the SM predictions for meson mixing and the experimental data can then be translated into bounds for  $c_i^{(d)}/\Lambda_{\text{NP}}$ . If the coefficients  $c_i^{(d)}$  are assumed to be generic, i.e. all of  $\mathcal{O}(1)$ , then the most stringent bounds that come from CP violation in the  $K$  mixing imply for  $\Lambda_{\text{NP}}$  values of the order  $\mathcal{O}(10^4 - 10^5)$  TeV: the examination of models with generic flavour structure has shown that large new sources of flavour symmetry breaking beyond the SM are already excluded at the TeV scale [24]. The large discrepancy between these two determinations of  $\Lambda_{\text{NP}}$  is a manifestation of what in different specific NP frameworks (supersymmetry, technicolor, etc.) goes under the name of *flavour problem* [111].

These considerations have raised the interest in the understanding the flavour structure of the NP models, and in signatures of deviations of it from the flavour structure of the SM. The formalization of this solution to the flavour problem, i.e. the recognition or imposition of the SM flavour structure in a certain NP model, is called Minimal Flavour Violation (MFV), and it has been developed and analyzed in different ways during the last years; in particular, two relevant frameworks [112] are the pragmatic approach called Constrained Minimal Flavour Violation (CMFV), and a more formal approach that makes use of group methods and effective theories, and which at the same time allows more freedom. We stress however that MFV is

not a theory of flavour, since it does not provide an explanation for the hierarchical flavour structure that is already present in the SM.

### 1.4.2 Constrained Minimal Flavour Violation

CMFV can be seen as a brute-force method of extrapolating the flavour structure of the SM. It is defined by two conditions [113, 114]:

- all flavour changing transitions are governed by the CKM matrix with the CKM phase being the only source of CP violation;
- the only relevant operators in the effective Hamiltonian below the weak scale are those that are also relevant in the SM.

The use of the penguin-box expansion is very useful for the study of CMFV. In fact, the properties of universality and realness of the  $F_i$  master functions depend only on the flavour and CP structure of the SM, and the form of the  $P_i$  coefficients depends only on the operator structure of the SM. Both the flavour and CP structure and the operator structure of the SM are preserved by definition in models with CMFV, and hence the  $P_i$  are model independent within the whole class of CMFV models, while the details of the single models are contained into the master functions  $F_i$ , which maintain their universality and realness. Since the SM belongs itself to the class of CMFV, in these models the formulae of the observables will have the same form as in the SM with the only substitution  $F_i(x_t) \rightarrow F_i(x_t, \rho_{\text{NP}})$ , where the latter are obtained by the calculation of the relevant diagrams in the NP model.

#### Universal Unitarity Triangle

The analysis of the unitarity triangle provides a powerful test of the flavour pattern of CMFV in a model independent way; in fact, a triangle common to the whole class of CMFV models, known as Universal Unitarity Triangle (UUT) [113], can be built, and comparing it with the Reference Unitarity Triangle (RUT), can give information not only on the possible presence of NP, but also about its flavour structure (Fig. 1.3, left).

Once the parameters  $\lambda \equiv |V_{us}|$  and  $A = |V_{cb}|/\lambda^2$ , unaffected by NP, have been determined, the determination of the apex  $(\bar{\rho}, \bar{\eta})$  requires the knowledge of one side and one angle of the triangle, provided the CKM matrix is unitary. Two choices of sets with different characteristics are possible.

- **$R_b$  and  $\gamma$**  .  $R_b \propto |V_{ub}|$  and  $\gamma = \arg(V_{ub})$  are extracted from tree-level processes, and hence are very unlikely modified by NP. The triangle obtained with this method is the RUT.
- **$R_t$  and  $\beta$**  . With a very good approximation  $R_t \propto |V_{td}/V_{ts}|$ , while  $\beta = \arg(V_{td})$ ; the presence of the top quark implies that these can be only determined from loop processes. However, the universality of the master functions

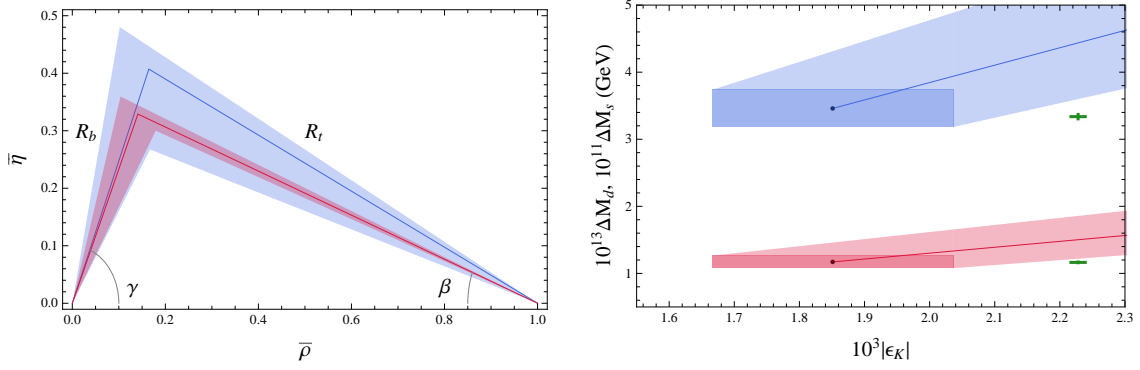


Figure 1.3: (Left) Comparison between the RUT (blue) and the UUT (red), obtained from the 2012 updated inputs. (Right)  $\Delta M_d$  (blue) and  $\Delta M_s$  (red) as functions of  $\epsilon_K$  in models with CMFV. The green crosses represent the data, while the darker regions the SM predictions.

$F(x_t, \rho_{\text{NP}})$  in CMFV models implies a model independent extraction of the ratio  $|V_{td}/V_{ts}|$  as

$$\left| \frac{V_{td}}{V_{ts}} \right| = \xi \sqrt{\frac{m_{B_s}}{m_{B_d}}} \sqrt{\frac{\Delta M_d}{\Delta M_s}} \quad \text{or} \quad \left| \frac{V_{td}}{V_{ts}} \right|^2 = \frac{m_{B_s} \tau_{B_s} F_{B_s}^2 \mathcal{B}(B_d \rightarrow \mu^+ \mu^-)}{m_{B_s} \tau_{B_d} F_{B_d}^2 \mathcal{B}(B_s \rightarrow \mu^+ \mu^-)}, \quad (1.52)$$

from measurable quantities. On the other hand, the absence of new CP-violating phases in the  $B$  mixing implies that the angle  $\beta$  can be extracted directly from  $S_{\psi K_S}$ . The triangle built in this way is common to all the models with CMFV and has been called UUT.

## Correlations and lower bounds

The flavour universality of the master functions  $F_i$  and the model independence of the parameters  $P_i$  suggest the idea of considering ratios between different observables in which at the same time the flavour pattern can be tested and the hadronic uncertainties are reduced [115]. Correlations like

$$\frac{\Delta M_d}{\Delta M_s} = \frac{m_{B_d} \hat{B}_d F_{B_s}^2}{m_{B_s} \hat{B}_s F_{B_s}^2} \left| \frac{V_{td}}{V_{ts}} \right|^2 r(\Delta M), \quad (1.53a)$$

$$\frac{\mathcal{B}(B_s \rightarrow \mu^+ \mu^-)}{\mathcal{B}(B_d \rightarrow \mu^+ \mu^-)} = \frac{m_{B_s} \tau_{B_s} F_{B_d}^2}{m_{B_s} \tau_{B_d} F_{B_s}^2} \left| \frac{V_{td}}{V_{ts}} \right|^2 r(\mu^+ \mu^-), \quad (1.53b)$$

$$\frac{\mathcal{B}(B \rightarrow X_d \nu \bar{\nu})}{\mathcal{B}(B \rightarrow X_s \nu \bar{\nu})} = \left| \frac{V_{td}}{V_{ts}} \right|^2 r(\nu \bar{\nu}) \quad (1.53c)$$

have been indicated as *standard candles of flavour physics* [79], since in CMFV  $r(\Delta M) = r(\mu^+ \mu^-) = r(\nu \bar{\nu}) = 1$  and deviations from unity can be used to recognize and parametrize different patterns of flavour violation.

Less intuitive but still simple calculations permit also to find that the observables related to the meson mixing like  $\epsilon_K$  and  $\Delta M_{d,s}$  are not only correlated, but also can only be enhanced with respect to the SM [116].

### Comparison with experiments

First of all one observes that, since in this context  $S_{\psi K_S}$  cannot receive new contributions, CMFV models prefer what we have called the Scenario 2 for  $V_{ub}$ . Now, as we have discussed, positive contributions to  $\epsilon_K$  are allowed, and hence the  $S_{\psi K_S} - \epsilon_K$  tension can be solved. Nevertheless, the enhancement of  $\epsilon_K$  would determine a correlated enhancement of both  $\Delta M_d$  and  $\Delta M_s$ , worsening the  $\Delta M_{d,s} - \epsilon_K$  tension [79] (Fig. 1.3, right).

The previous considerations, even if only qualitative, point out the difficulties that CMFV models have in accommodating the tensions in flavour data, due to the presence of few free parameters and strict correlations. A more quantitative and complete study has recently been performed [117].

### 1.4.3 Minimal Flavour Violation at Large

The flavour symmetry of the SM can be formalized in the framework of group theory. In fact, it can be identified with the largest group of unitary quark field transformations that commutes with the SM gauge Lagrangian [118, 119]

$$\mathcal{G}_q = (\text{SU}(3) \times \text{U}(1))^3, \quad (1.54)$$

i.e. a  $\text{SU}(3)$  symmetry and a phase symmetry for each electroweak multiplet:

$$\text{SU}(3)^3 = \text{SU}(3)_{Q_L} \times \text{SU}(3)_{U_R} \times \text{SU}(3)_{D_R}, \quad \text{U}(1)^3 = \text{U}(1)_B \times \text{U}(1)_Y \times \text{U}(1)_{\text{PQ}}, \quad (1.55)$$

where the three  $\text{U}(1)$  symmetries can be rearranged as the baryon number, the hypercharge, and a Peccei-Quinn symmetry [120] (see Sec. 3.2.2). In the SM this symmetry (with the exception of  $\text{U}(1)_B$ ) is explicitly broken by the two Yukawa couplings

$$\mathcal{L}_Y = -\bar{Q}_L Y_d D_R H - \bar{Q}_L Y_u U_R \tilde{H} + \text{h.c.} \quad (1.56)$$

Now, the flavour symmetry  $\mathcal{G}_q$  can be formally recovered by promoting the Yukawa matrices to *spurions*, i.e. dimensionless auxiliary fields transforming as

$$Y_u \sim (\mathbf{3}, \bar{\mathbf{3}}, \mathbf{1})_{\text{SU}(3)^3}, \quad Y_d \sim (\mathbf{3}, \mathbf{1}, \bar{\mathbf{3}})_{\text{SU}(3)^3}. \quad (1.57)$$

One defines an effective theory as satisfying the criterion of MFV if all higher-dimensional operators, constructed from SM and spurion fields, are formally invariant under the flavour group  $\mathcal{G}_q$  [119].

In practice, one can build effective couplings and higher-dimensional operators in which the only relevant non-diagonal structures are polynomials  $\mathcal{P}(Y_u Y_u^\dagger, Y_d Y_d^\dagger)$  of the two basic spurions

$$Y_u Y_u^\dagger, Y_d Y_d^\dagger \sim (\mathbf{8}, \mathbf{1}, \mathbf{1})_{\text{SU}(3)_q^3} \oplus (\mathbf{1}, \mathbf{1}, \mathbf{1})_{\text{SU}(3)_q^3}. \quad (1.58)$$

As an example of this mechanism at work, we shortly discuss the application of this formulation of MFV to a generic model with two Higgs doublets, resulting in a NP scenario called  $2\text{HDM}_{\overline{\text{MFV}}}$  [121].

### The $2\text{HDM}_{\overline{\text{MFV}}}$

In a generic model with two-Higgs doublets,  $H_1$  and  $H_2$ , with hypercharges  $Y = 1/2$  and  $Y = -1/2$  respectively, the most general renormalizable and gauge-invariant interaction of them with the SM quarks is

$$-\mathcal{L}_Y = \bar{Q}_L X_{d1} D_R H_1 + \bar{Q}_L X_{u1} U_R H_1^c + \bar{Q}_L X_{d2} D_R H_2^c + \bar{Q}_L X_{u2} U_R H_2 + \text{h.c.} , \quad (1.59)$$

where  $H_{1(2)}^c = -i\tau_2 H_{1(2)}^*$  and the  $X_i$  are  $3 \times 3$  matrices with a generic flavour structure. By performing a global rotation of angle  $\beta = \arctan(v_2/v_1)$  of the Higgs fields, the mass terms and the interaction terms are separated, but they cannot be diagonalized simultaneously for generic  $X_i$  and dangerous FCNC couplings to the neutral Higgses appear.

If the MFV hypothesis is imposed instead, the  $X_i$  are forced to assume the particular structure

$$X_{d1} = Y_d \quad (1.60a)$$

$$X_{d2} = \mathcal{P}_{d2}(Y_u Y_u^\dagger, Y_d Y_d^\dagger) \times Y_d = \epsilon_0 Y_d + \epsilon_1 Y_d Y_d^\dagger Y_d + \epsilon_2 Y_u Y_u^\dagger Y_d + \dots \quad (1.60b)$$

$$X_{u1} = \mathcal{P}_{u1}(Y_u Y_u^\dagger, Y_d Y_d^\dagger) \times Y_u = \epsilon'_0 Y_u + \epsilon'_1 Y_u Y_u^\dagger Y_u + \epsilon'_2 Y_d Y_d^\dagger Y_u + \dots \quad (1.60c)$$

$$X_{u2} = Y_u \quad (1.60d)$$

that is renormalization group invariant [121]. At higher orders in  $Y_i Y_i^\dagger$  FCNCs are generated, and in order to investigate them one can perform an expansion in powers of suppressed off-diagonal CKM elements, so that the effective down-type FCNC interaction can be written as

$$\mathcal{L}_{\overline{\text{MFV}}}^{\text{FCNC}} \propto \bar{d}_L^i [(a_0 V^\dagger \lambda_u^2 V + a_1 V^\dagger \lambda_u^2 V \Delta + a_2 \Delta V^\dagger \lambda_u^2 V) \lambda_d]_{ij} d_R^j \frac{S_2 + iS_3}{\sqrt{2}} + \text{h.c.} , \quad (1.61)$$

where  $\lambda_{u,d} \propto 1/v \text{diag}(m_{u,d}, m_{c,s}, m_{t,b})$ ,  $\Delta = \text{diag}(0, 0, 1)$ , and the  $a_i$  are parameters naturally of  $\mathcal{O}(1)$ ; this structure shows a large suppression due to the presence of two off-diagonal CKM elements and the down-type Yukawas [121], demonstrating explicitly how MFV is effective and natural.

It is remarkable that the mechanisms of flavour and CP violation do not necessarily need to be related: in MFV the Yukawa matrices are the only sources of flavour breaking, but other sources of CP violation could be present, provided that they are flavour-blind: this happens when the FCNC parameters  $a_i$  are allowed to be complex, as well as for the phases that can be present in the Higgs potential.

With a more detailed analysis the following relevant properties have been found [121]:

- the impact in  $K$ ,  $B_d$  and  $B_s$  mixing amplitudes scales with  $m_s m_d$ ,  $m_b m_d$  and  $m_b m_s$  respectively;

- new flavour-blind phases  $\phi_s = (m_s/m_d)\phi_d$  can contribute to the  $B_d$  and  $B_s$  systems, and they are not present in the  $K$  system instead.

The previous observations imply that  $\epsilon_K$  can receive only tiny new contributions while  $S_{\psi K_S}$  could be in principle sizeably modified; as a consequence, for the reasons that have been discussed in the previous section, the  $2\text{HDM}_{\overline{\text{MFV}}}$  selects the inclusive  $|V_{ub}|$ . However, in this framework a suppression of  $S_{\psi K_S}$  would determine a correlated enhancement of  $S_{\psi\phi}$ , an effect that was considered very welcome until last year, when LHCb excluded a large NP phase in the  $B_s$  mixing, putting therefore this model in difficulty [79].

The flavour-blind phases of the Higgs potential imply instead  $\phi_s = \phi_d$  [122], and could be used to remove the  $S_{\psi K_S} - \epsilon_K$  tension, but the necessary size of  $\phi_d$  would imply in turn  $S_{\psi\phi} > 0.15$ , which is  $2\sigma$  away from the LHCb central value [79].

#### 1.4.4 Beyond Minimal Flavour Violation

From the discussion in the previous two sections it results that models with CMFV and MFV seem to present visible difficulties in describing all  $\Delta F = 2$  observables in the  $K$  and  $B_{d,s}$  meson systems simultaneously. More definite conclusions will only be possible when  $|V_{ub}|$  and  $\gamma$  will be known from tree level decays with a much better precision and the lattice input will further improve. Nevertheless, these results seem to indicate that the tensions in the flavour observables could be hints of a new flavour structure different from the one of the SM. Both the models that we are going to study in this work go beyond MFV.

Models that do not satisfy the MFV hypothesis, neither by construction nor by imposition, present in general large flavour violating effects, unless fine tuning is applied or some other suppression mechanism occurs. As we will discuss, the first is the case of the  $\overline{331}$  model, the second of the GFS model.

In fact, in the  $\overline{331}$  model, in order to obtain phenomenological results in agreement with the experimental data, one needs both a quite high NP energy scale, coinciding with the mass of the FCNCs-mediating  $Z'$  new boson, and to force the mixing matrix to be very similar the CKM matrix.

On the other hand, we will see that a very elegant feature of the GFS model is that the minimal fermion content required for the theory to be consistent generates a mechanism of inverted hierarchy in the Yukawa couplings that automatically suppresses FCNCs. Nevertheless, even if this model presents a number of analogies with MFV models, the most evident of them being the fact that it is just based on the restoring of the flavour symmetry and that NP effects are controlled by the flavour group, it does not satisfy the MFV requirement: in fact, one can find a limit in which all Yukawa couplings vanish but flavour breaking effects remain finite.



# Chapter 2

## Theory and phenomenology of Gauged Flavour Symmetries

### 2.1 The model

#### 2.1.1 Gauge group and field content

As we have discussed in Sec. 1.4.3, the SM presents the large flavour symmetry  $\mathcal{G}_q = (\text{SU}(3) \times \text{U}(1))^3$ , explicitly broken by the two Yukawa couplings. This symmetry would be restored not only formally, but truly if instead of the Yukawa constant matrix there were physical fields transforming as  $(\mathbf{3}, \bar{\mathbf{3}}, \mathbf{1})$  and  $(\mathbf{3}, \mathbf{1}, \bar{\mathbf{3}})$  under  $\text{SU}(3)^3$ .

In the model that we are going to build,  $\mathcal{G}_q$  is assumed to be an exact symmetry of nature, spontaneously broken by the vevs of the two scalar fields  $Y_u$  and  $Y_d$ , which opportunely transform under it, called *flavons*. In order to avoid problematic flavour-violating Goldstone bosons, the symmetry should be gauged. Since we are interested mainly in the flavour breaking, we choose to gauge only the subgroup

$$\mathcal{G}_{\text{GFS}} = \text{SU}(3)_{Q_L} \times \text{SU}(3)_{U_R} \times \text{SU}(3)_{D_R} \quad (2.1)$$

and not to concentrate on the abelian part. We will call *GFS model* the model with these Gauged Flavour Symmetries and scalar content, and with the fermion content that we are going to introduce. In fact, we are going to discuss how new fermions have to be added in order to cancel the gauge anomalies.

#### Basic notions about anomalies

We recall here the relevant theoretical aspects of the perturbation theory anomalies, following mainly [123–125].

A symmetry of a classic theory is not necessary preserved when such theory is quantized. In fact, if a field transformation  $\phi \rightarrow \phi + \delta\phi$  leaves the classical action  $S(\phi)$  invariant, the path integral  $\int \mathcal{D}\phi e^{iS(\phi)}$  is not necessarily invariant, depending on the behavior of the measure  $\mathcal{D}\phi$ . If a symmetry of a classical theory is spoiled in its quantized version, one says that there is an *anomaly*. While an anomaly in a global symmetry is not problematic, if there were an anomaly in a gauge symmetry

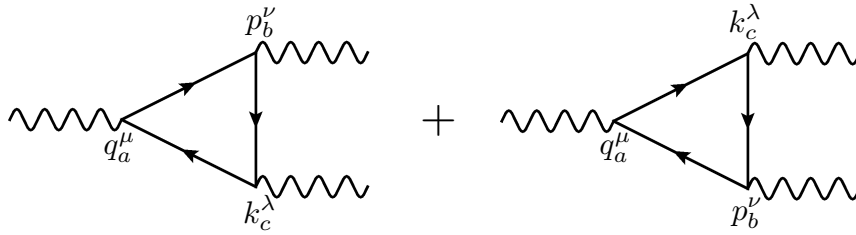


Figure 2.1: Anomalous triangular diagrams contributing to the nonconservation of the gauge current  $j_a^\mu$ .

the theory would be inconsistent, since the whole construction of a theory with local gauge invariance is based on the existence of an exact global symmetry, and results such as the presence of non-physical degrees of freedom or the non-unitarity of the  $S$ -matrix would follow. Therefore, the condition of gauge anomaly cancellation is a constraint on the construction of physical gauge theories.

Even if the transformation of the measure of the functional integral has been fully understood [126], it involves elegant but non-straightforward kind of calculations; the method of computing directly the problematic Feynman diagrams is still more clear and practical. In order to consider the general matter content of the theory, it is convenient to take all the fermion fields as massless and to merge them into a single left-handed column; for instance, if  $\psi$  is a column containing all quark and lepton fields, then one can build

$$\chi \equiv \begin{pmatrix} \frac{1}{2}(1 - \gamma_5)\psi \\ \frac{1}{2}[\mathcal{C}(1 + \gamma_5)\psi]^* \end{pmatrix}, \quad (2.2)$$

where  $\mathcal{C}$ , defined by  $\mathcal{C}\gamma_\mu^T\mathcal{C}^{-1} = \gamma^\mu$ , permits to treat right-handed fermions in the same representation of the left-handed one. When we consider the gauge group  $\mathcal{G}$  with generators  $t_a^L$  for the left-handed fermion representation and  $t_a^R$  for the right-handed one, the column undergoes the infinitesimal transformation

$$\delta\chi = i\epsilon_a T_a \chi, \quad \text{with } T_a = \begin{pmatrix} t_a^L & 0 \\ 0 & -t_a^{R*} \end{pmatrix}; \quad (2.3)$$

with these definitions one can write the fermionic vector current

$$j_a^\mu = -i\bar{\chi}T_a\gamma^\mu\chi. \quad (2.4)$$

In order to study the conservation of this current, one considers the matrix element  $\mathcal{M}$  of its divergence to create two gauge bosons

$$\int d^4x e^{-iq\cdot x} \langle p, \nu, b; k, \lambda, c | j_a^\mu(x) | 0 \rangle \propto \mathcal{M}_{abc}^{\mu\nu\lambda}(p, k), \quad (2.5)$$

which at leading order gets contributions from the two diagrams in Fig. 2.1. While with a naive calculation, by performing a shift of the internal momentum, the two

diagrams seems to cancel each other and hence the current to be conserved, treating the problem more carefully one has to notice that the two diagrams are divergent and that this shift can not be allowed by the regularization. Using dimensional regularization in order to preserve gauge invariance and the 't Hooft-Veltman definition of the  $\gamma^5$  matrix in  $d$  dimensions to perform the calculation, one finds the generally nonvanishing result

$$\langle p, \nu, b; k, \lambda, c | j_a^\mu | 0 \rangle = \frac{g^2}{8\pi^2} \epsilon^{\alpha\nu\beta\lambda} p_\alpha k_\beta \cdot \mathcal{A}^{abc} , \quad (2.6)$$

with

$$\mathcal{A}^{abc} = \text{Tr} [T^a \{T^b, T^c\}] , \quad (2.7)$$

where, as defined before,  $T^a$  is the representation of the gauge algebra on the set of all left-handed fermion and antifermion fields, and the trace denotes the sum over these fermion and antifermion species. This anomalous contribution is a consequence of the fact that in order to preserve gauge invariance one has to work in  $d$  dimensions, but  $\gamma^5$ , which is a fundamental object in chiral theories<sup>1</sup>, is an intrinsically 4-dimensional object. The following further results validate the correctness of Eq. (2.6).

- Even if the previous calculation has been developed with massless fermions, the result is correct since one can show that no fermion that is allowed by a given symmetry to have a mass can contribute to the anomaly for that symmetry [124]. It is known that mass terms for Dirac fermions are not allowed by the SM gauge symmetry and hence neither by any of its possible extensions, and therefore they contribute to the anomalies as massless fermions before the spontaneous symmetry breaking.
- The higher order corrections to the matrix element, consisting both in propagators internal to the loop and in more external currents, vanish because they make the integral sufficiently convergent to allow to shift the internal momentum without problems [127].

For the consistency of a gauge theory the current  $j_a^\mu$  must be conserved also at quantum level, and hence, as a consequence of the previous calculation, the condition for a gauge theory to be anomaly-free is  $\mathcal{A}^{abc} = 0$  when  $T_a, T_b$  and  $T_c$  run over all the generators of the gauge group. The following general results simplify this analysis.

- Of course, one needs only to consider those combinations of generators for which their product contains a singlet under the gauge group, since  $\mathcal{A}^{abc}$  obviously vanishes for all the others. For example, one can make invariants out of any number of U(1) generators, zero, two or three SU(2) generators (since  $\mathbf{2} \times \mathbf{2}$  and  $\mathbf{2} \times \mathbf{2} \times \mathbf{2}$  both contain singlets), and zero, two or three SU(3) generators.

---

<sup>1</sup>A theory is said to be *chiral* if it treats differently fields of different chiralities, if otherwise it is parity-symmetric is said to be *vector*.

- For a fermion representation that is equivalent to its complex conjugate, i.e. in which its generators are related to the ones of its complex conjugate by unitary transformations, it is straightforward to calculate  $\mathcal{A}^{abc} = -\mathcal{A}^{abc} = 0$ ; as a consequence, if the fermion content of a theory forms a representation that is real or pseudoreal, the theory is anomaly-free, and if a gauge group admits only real or pseudoreal representations (like for example SU(2), SO(10), E<sub>6</sub>), it is automatically anomaly-free for any matter content.
- Besides the fields of the gauge group, also the gravitational field should be considered. All species of fermions interact with gravitation in the same way, and the calculation of the loop graph yields to an anomaly proportional to

$$\text{Tr}[T_a] \epsilon^{\mu\nu\rho\sigma} R_{\mu\nu\kappa\lambda} R_{\rho\sigma}{}^{\kappa\lambda} ; \quad (2.8)$$

it automatically vanishes if the gauge group is non-Abelian, while, if the latter contains U(1) factors, the theory cannot be consistently coupled to gravity unless each of the U(1) generators is traceless [128].

### Anomalies in the GFS model

In order to analyze the gauge anomalies of the model in relation with its fermion content, as described in the previous paragraph, we have to consider all the possible combinations of three generators of the gauge group, except the ones that contain a single SU(3) or SU(2) factor.

- $\text{SU}(3)_{Q_L}^3$ ,  $\text{SU}(3)_{U_R}^3$ ,  $\text{SU}(3)_{D_R}^3$

All the new groups present a cubic anomaly, because the SM quarks provide non-real representations of them. In order to obtain (pseudo)real representations, one needs to add two new fermions  $\Psi_a$ ,  $\Psi_b$ , whose right-handed components  $\Psi_{aR}$ ,  $\Psi_{bR}$  transform as triplets under  $\text{SU}(3)_{Q_L}^3$ , and whose left-handed components  $\Psi_{aL}$ ,  $\Psi_{bL}$  transform as triplets under  $\text{SU}(3)_{U_R}^3$  and  $\text{SU}(3)_{D_R}^3$  respectively.

- $\text{SU}(3)_c^3$

This anomaly vanishes if the new fermions, as the ones of the SM, are vector-like with respect to  $\text{SU}(3)_c$ . This means that  $\Psi_{aL}$  and  $\Psi_{aR}$  have to belong to the same  $\text{SU}(3)_c$  representation (and hence for the number of colors one has  $N_c(\Psi_{aL}) = N_c(\Psi_{aR}) \equiv N_c(\Psi_a)$ ), as well as  $\Psi_{bL}$  and  $\Psi_{bR}$  (and hence  $N_c(\Psi_{bL}) = N_c(\Psi_{bR}) \equiv N_c(\Psi_b)$ ). Of course the simplest solutions, i.e. the singlets or the triplets ( $N_c = 1$  or  $N_c = 3$ ), are preferable, in order to obtain a more elegant and predictive theory.

- $\text{SU}(2)_E^3$

Since SU(2) has only real or pseudoreal representations, this combination is always non anomalous, independently from the fermion content.

- $\mathbf{U}(1)_{\mathbf{Y}}^3$

The contribution from the SM fermions cancels as usual, as regards the NP contributions the condition for the cancellation is

$$-N_c(\Psi_a)Y(\psi_{aR})^3 - N_c(\Psi_b)Y(\psi_{bR})^3 + N_c(\Psi_a)Y(\psi_{aL})^3 + N_c(\Psi_b)Y(\psi_{bL})^3 \equiv 0 . \quad (2.9)$$

- $\mathbf{SU}(3)_{\mathbf{Q}_L}^2 \times \mathbf{U}(1)_{\mathbf{Y}}$ ,  $\mathbf{SU}(3)_{\mathbf{U}_R}^2 \times \mathbf{U}(1)_{\mathbf{Y}}$ ,  $\mathbf{SU}(3)_{\mathbf{D}_R}^2 \times \mathbf{U}(1)_{\mathbf{Y}}$

Also the conditions for the cancellation of these anomalies give information about the hypercharge and color of the new fermions:

$$\sum_{\mathbf{3}[SU(3)_{\mathbf{Q}_L}]} (Y_{\text{SM}} + Y_{\text{GFS}}) = 3 \left( \frac{1}{6} + \frac{1}{6} \right) - N_c(\Psi_a)Y(\Psi_{aR}) - N_c(\Psi_b)Y(\Psi_{bR}) \equiv 0 , \quad (2.10a)$$

$$\sum_{\mathbf{3}[SU(3)_{\mathbf{U}_R}]} (Y_{\text{SM}} + Y_{\text{GFS}}) = 3 \left( -\frac{2}{3} \right) + N_c(\Psi_a)Y(\Psi_{aL}) \equiv 0 , \quad (2.10b)$$

$$\sum_{\mathbf{3}[SU(3)_{\mathbf{U}_R}]} (Y_{\text{SM}} + Y_{\text{GFS}}) = 3 \left( \frac{1}{3} \right) + N_c(\Psi_b)Y(\Psi_{bL}) \equiv 0 . \quad (2.10c)$$

- $\mathbf{SU}(3)_c^2 \times \mathbf{U}(1)_{\mathbf{Y}}$

Again, since the SM contribution to this anomaly regularly cancels, the NP contribution has to vanish by itself, giving the condition

$$\sum_{\mathbf{3}[SU(3)_c]} Y_{\text{GFS}} \equiv 0 , \quad (2.11)$$

where the new fermions enter or not depending if they are color triplets or singlets. This provides another relation for the hypercharges.

- $\mathbf{SU}(2)_L^2 \times \mathbf{U}(1)_{\mathbf{Y}}$

Similarly to the previous case, the NP contribution has to vanish by itself, giving

$$\sum_{\mathbf{2}[SU(2)_L]} Y_{\text{GFS}} \equiv 0 , \quad (2.12)$$

where the new fermions enter only if they are  $\mathbf{SU}(2)_L$  doublets. In the SM, given the specific hypercharges, this conditions implies that the number of quark doublets has to be the same as the one of lepton doublets; here it gives analogous information.

- $[\mathbf{Grav}]^2 \times \mathbf{U}(1)_{\mathbf{Y}}$

The condition for the cancellation of the gravitational anomaly is

$$-N_c(\Psi_a)Y(\psi_{aR}) - N_c(\Psi_b)Y(\psi_{bR}) + N_c(\Psi_a)Y(\psi_{aL}) + N_c(\Psi_b)Y(\psi_{bL}) \equiv 0 , \quad (2.13)$$

	$SU(3)_{Q_L}$	$SU(3)_{U_R}$	$SU(3)_{D_R}$	$SU(3)_c$	$SU(2)_L$	$U(1)_Y$
$Q_L$	<b>3</b>	<b>1</b>	<b>1</b>	<b>3</b>	<b>2</b>	1/6
$U_R$	<b>1</b>	<b>3</b>	<b>1</b>	<b>3</b>	<b>1</b>	2/3
$D_R$	<b>1</b>	<b>1</b>	<b>3</b>	<b>3</b>	<b>1</b>	-1/3
$\Psi_{uR}$	<b>3</b>	<b>1</b>	<b>1</b>	<b>3</b>	<b>1</b>	2/3
$\Psi_{dR}$	<b>3</b>	<b>1</b>	<b>1</b>	<b>3</b>	<b>1</b>	-1/3
$\Psi_{uL}$	<b>1</b>	<b>3</b>	<b>1</b>	<b>3</b>	<b>1</b>	2/3
$\Psi_{dL}$	<b>1</b>	<b>1</b>	<b>3</b>	<b>3</b>	<b>1</b>	-1/3
$Y_u$	$\bar{\mathbf{3}}$	<b>3</b>	<b>1</b>	<b>1</b>	<b>1</b>	0
$Y_d$	$\bar{\mathbf{3}}$	<b>1</b>	<b>3</b>	<b>1</b>	<b>1</b>	0
$H$	<b>1</b>	<b>1</b>	<b>1</b>	<b>1</b>	<b>2</b>	1/2

Table 2.1: Fermion content and quantum numbers of the GFS model.

but it does not give any additional information since it can be derived combining the new conditions for the cancellation of the mixed flavour-hypercharge anomalies.

Even if we have verified that some solutions in which there are leptons between the new fermions are possible, since we are concentrating on the quark sector, we decide to follow [25] and to assume that the new fermions are colored. The conditions for the cancellations of anomalies impose hence that they have to be all  $SU(2)_L$  singlets and fix their hypercharge. The final matter content of the GFS model is listed in Tab. 2.1.

## 2.1.2 Lagrangian and symmetry breaking

### Gauge Lagrangian

Gauging the flavour group  $SU(3)_{Q_L} \times SU(3)_{U_R} \times SU(3)_{D_R}$  implies the introduction of  $8 \times 3 = 24$  new gauge bosons  $(A_Q)_\mu^a$ ,  $(A_U)_\mu^a$ ,  $(A_D)_\mu^a$  ( $a = 1 \dots 8$ ), and three new coupling constants  $g_Q$ ,  $g_U$ ,  $g_D$ . The gauge part of the Lagrangian of the GFS model is

$$\begin{aligned}
\mathcal{L}_{\text{gauge}} &= \bar{Q}_L i \not{D} Q_L + \bar{U}_R i \not{D} U_R + \bar{D}_R i \not{D} D_R + \sum_{\substack{f=u,d \\ H=L,R}} \bar{\Psi}_f i \not{D} \Psi_f \\
&+ \frac{1}{2} (D_\mu H)^\dagger (D^\mu H) + \sum_{f=u,d} \frac{1}{2} (D_\mu Y_f)^\dagger (D^\mu Y_f) \\
&+ \sum_{F=W,B,A_f} \frac{1}{4} F_{\mu\nu} F^{\mu\nu},
\end{aligned} \tag{2.14}$$

where in the first line there are the gauge terms for the fermions, in the second for the Higgs bosons and in the third for the gauge bosons ( $F_{\mu\nu} = \partial_\mu F_\nu - \partial_\nu F_\mu + ig_F [F_\mu, F_\nu]$ )

are the usual field strength tensors of all the gauge bosons). The covariant derivative is

$$D_\mu = \partial_\mu + igI_W W_\mu + ig'Y_W B_\mu + \sum_{f=Q,U,D} ig_f N_f (A_f)_\mu ; \quad (2.15)$$

$I_W$ ,  $Y_W$  and  $W_\mu$  and  $B_\mu$  are respectively the usual quantum numbers and gauge bosons associated to the electroweak group (we are not considering QCD in these expressions); analogously,  $N_Q$ ,  $N_U$ ,  $N_D$  are the quantum numbers of the fermions with respect to the flavour group, and

$$(A_f)_\mu = \sum_{a=1}^8 (A_f)_\mu^a \frac{\lambda^a}{2} \quad (f = Q, U, D) , \quad (2.16)$$

being  $\lambda^a$ 's the Gell-Mann matrices.

### Symmetry breaking

The pattern of electroweak symmetry breaking can be implemented as usual by expanding, in the unitary gauge,

$$H = \frac{1}{\sqrt{2}} \begin{pmatrix} 0 \\ v + h \end{pmatrix} . \quad (2.17)$$

As regards the flavour breaking, a bit of manipulation is worth. The flavon fields (two complex  $3 \times 3$  matrices for a total amount of 36 degrees of freedom) can be parametrized as

$$Y_u = U_U \rho_u U_Q^\dagger , \quad (2.18a)$$

$$Y_d = U_D \rho_d U_Q^\dagger , \quad (2.18b)$$

where  $U_{Q,U,D}$  are the three unitary matrices parametrizing the 26 Goldstone modes (since the whole flavour group  $(\text{SU}(3) \times \text{U}(1))^3$  is broken to  $\text{U}(1)_B$ , there are  $9+9+8$  broken generators); in the unitary gauge  $U_{Q,U,D} = \hat{I}_3$ . Hence we are left with  $36 - 26 = 10$  degrees of freedom contained into  $\rho_u$  and  $\rho_d$ , which can be interpreted as the field excitations around the six SM masses and the four angles of the CKM matrix. In fact, we can conveniently rewrite

$$\rho_u = \Sigma_{Ru} D_u \Sigma_{Lu}^\dagger V_{\text{GFS}} , \quad (2.19a)$$

$$\rho_d = \Sigma_{Rd} D_d \Sigma_{Ld}^\dagger , \quad (2.19b)$$

where  $D_{u,d}$  are real diagonal matrices that get vevs  $Z_{u,d}$ ,  $V_{\text{GSM}}$  is a unitary matrix (we will see later how it is linked to the CKM matrix), and  $\Sigma_{Ru,Lu,Rd,Ld}$  are four unitary matrices parametrizing the remaining four angle modes. In fact, requiring the radial modes in  $\rho_{u,d}$  to be orthogonal to the Goldstone modes corresponds in the unitary gauge to the condition that cross product terms of the type  $\partial_\mu \rho A^\mu$  vanish [25]; this corresponds to the three sets of conditions

$$A_U : \quad \text{Im Tr}[\rho_u \partial \rho_u^\dagger \lambda^\alpha] = 0 , \quad \alpha = 1 \dots 9 , \quad (2.20a)$$

$$A_D : \quad \text{Im Tr}[\rho_d \partial \rho_d^\dagger \lambda^\alpha] = 0 , \quad \alpha = 1 \dots 9 , \quad (2.20b)$$

$$A_Q : \quad \text{Im Tr}[(\partial \rho_u^\dagger \rho_u + \partial \rho_d^\dagger \rho_d) \lambda^\alpha] = 0 , \quad \alpha = 1 \dots 8 , \quad (2.20c)$$

where  $\lambda^9$  is the unitary matrix. Now, if we write

$$\Sigma_X = e^{i\Pi_X} = \exp\left(i\frac{\lambda^\alpha}{2}\pi_X^\alpha\right), \quad (2.21)$$

Eq. (2.20a)-(2.20c) are 26 conditions on the 36  $\pi_X^\alpha$ , and 8 further conditions come from Eq. (2.19a)-(2.19b), leaving four independent combinations out of the  $\pi_{Ru,Lu,Rd,Ld}^\alpha$ ; we will call them  $\pi_{1,2,3,4}$  (notice that they mediate FCNCs).

In summary, the flavon fields and the breaking of the flavour symmetry can be written as

$$\begin{aligned} Y_u &= e^{i\frac{\lambda^\alpha}{2}\pi_{Ru}^\alpha} D_u e^{-i\frac{\lambda^\alpha}{2}\pi_{Lu}^\alpha} V \\ Y_d &= e^{i\frac{\lambda^\alpha}{2}\pi_{Rd}^\alpha} D_d e^{-i\frac{\lambda^\alpha}{2}\pi_{Ld}^\alpha} \end{aligned} \quad (2.22)$$

where

$$D_{u,d} = Z_{u,d} + T_{u,d} \equiv \begin{pmatrix} z_{u,d} & & \\ & z_{c,s} & \\ & & z_{t,b} \end{pmatrix} + \begin{pmatrix} t_{u,d} & & \\ & t_{c,s} & \\ & & t_{t,b} \end{pmatrix}, \quad (2.23)$$

and  $\pi_X^\alpha$  are functions of  $\pi_1, \pi_2, \pi_3, \pi_4$  with  $\langle\pi_i\rangle = 0$ ; in particular

$$\langle Y_u \rangle = Z_u V^{\text{GFS}}, \quad \langle Y_d \rangle = Z_d. \quad (2.24)$$

Concerning the mechanism for the generation of this particular symmetry-breaking pattern, it can be shown that there exists no renormalizable potential for only two bifundamentals from which the correct pattern can arise [25]. One possibility to solve this problem is to introduce a non-renormalizable potential: as long as the cut-off suppressing higher-dimensional operators is larger than the largest flavon vev, its effects can be treated as perturbations. Another possibility is to assume that  $Y_{u,d}$  are combinations of several fields transforming as bifundamentals under the flavour group.

## Mass eigenstates and interactions of fermions and gauge bosons

The most general interaction of the quarks with the Higgs fields is

$$\begin{aligned} \mathcal{L}_{\text{int}} &= \lambda_u \bar{Q}_L \tilde{H} \Psi_{uR} + \lambda'_u \bar{\Psi}_{uL} Y_u \Psi_{uR} + M_u \bar{\Psi}_{uL} U_R + \\ &\lambda_d \bar{Q}_L H \Psi_{dR} + \lambda'_d \bar{\Psi}_{dL} Y_d \Psi_{dR} + M_d \bar{\Psi}_{dL} D_R + h.c., \end{aligned} \quad (2.25)$$

where  $M_{u,d}$  are universal mass parameters and  $\lambda_{u,d}^{(\prime)}$  are coupling constants, both of which can be always chosen to be real. Building the fermion mass matrices, one finds that both the SM and new quarks mix each other separately for up-type and down-type, according to the rotations

$$\begin{pmatrix} u_{R,L}^i \\ u'_{R,L}^i \end{pmatrix} = \begin{pmatrix} c_{u(R,L)i} & -s_{u(R,L)i} \\ s_{u(R,L)i} & c_{u(R,L)i} \end{pmatrix} \begin{pmatrix} U_{R,L}^i \\ \Psi_{uR,L}^i \end{pmatrix}, \quad (2.26)$$

with

$$s_{u_{Li}} = \sqrt{\frac{C_u - (2M_u - v^2\lambda_u^2 + 2z_{u_i}^2\lambda_u'^2)}{2C_u}}, \quad (2.27a)$$

$$s_{u_{Ri}} = \sqrt{\frac{C_u + (2M_u - v^2\lambda_u^2 - 2z_{u_i}^2\lambda_u'^2)}{2C_u}}, \quad (2.27b)$$

where

$$C_u = \sqrt{(2M_u v^2 \lambda_u^2 + 2z_{u_i}^2 \lambda_u'^2) - 8M_u^2 v^2 \lambda_u^2}, \quad (2.28)$$

and  $c_{u_{(R,L)i}}$  and  $s_{u_{(R,L)i}}$  are the cosines and sines; for the down-quark sector the formulae are analogous. We obtain hence two sets of six quarks, whose masses are

$$\begin{aligned} (m_{u,d}, m_{c,s}, m_{t,b}) &= \lambda_{u,d} \frac{v}{\sqrt{2}} \left( \frac{s^{(u,d)}_{R1}}{c^{(u,d)}_{L1}}, \frac{s^{(u,d)}_{R2}}{c^{(u,d)}_{L2}}, \frac{s^{(u,d)}_{L3}}{c^{(u,d)}_{L3}} \right), \\ (m_{u',d'}, m_{c',s'}, m_{t',b'}) &= M_{u,d} \left( \frac{c^{(u,d)}_{L1}}{s^{(u,d)}_{R1}}, \frac{c^{(u,d)}_{L2}}{s^{(u,d)}_{R2}}, \frac{c^{(u,d)}_{L3}}{s^{(u,d)}_{L3}} \right); \end{aligned} \quad (2.29)$$

we identify the ones in the first row with the SM quarks, and we observe that once their masses are fixed, the masses of the new quarks are determined by the relations of inverse proportionality

$$m_{(u,d)_i} m_{(u,d)'_i} = M_{u,d} \lambda_{u,d} \frac{v}{\sqrt{2}}. \quad (2.30)$$

In this sense, considering the masses of the SM quarks as inputs, one can rewrite the formulae for the rotations and expand them for  $m_{(u,d)'_i} \gg m_{(u,d)_i}$ :

$$s_{u_{Li}} = \sqrt{\frac{m_{u_i}}{M_u} \left| \frac{\lambda_u v m_{u'_i} - \sqrt{2} M_u m_{u_i}}{\sqrt{2}(m_{u'_i}^2 - m_{u_i}^2)} \right|} \simeq \sqrt{\frac{m_{u_i}}{m_{u'_i}} \frac{\lambda_u v}{\sqrt{2} M_u}}, \quad (2.31a)$$

$$s_{u_{Ri}} = \sqrt{\frac{m_{u_i}}{\lambda_u v} \left| \frac{-\lambda_u v m_{u'_i} + \sqrt{2} M_u m_{u_i}}{(m_{u'_i}^2 - m_{u_i}^2)} \right|} \simeq \sqrt{\frac{m_{u_i}}{m_{u'_i}} \frac{\sqrt{2} M_u}{\lambda_u v}}, \quad (2.31b)$$

finding the transparent expressions for the masses

$$m_{u_i} \simeq \frac{\lambda_u v M_u}{\sqrt{2} \lambda_u' z_{u_i}}, \quad m_{u'_i} \simeq \lambda_u' v z_{u_i}; \quad (2.32)$$

the first one shows explicitly the mechanism of *inverted hierarchy* [25], for which the masses of the SM are proportional to the inverse of the vevs of the Yukawa fields, conversely to the SM in which the masses are proportional to the Yukawa couplings. On the other hand, the exotic quark masses are directly proportional to these vevs, so that the lightest partner is the one associated with the  $t$  quark. For this reason,  $m_{t'} \gg m_t$  is not necessarily a good approximation, and we can expect large corrections to the previous relations.

The presence of new exotic quarks has a relevant impact on the SM couplings. The most relevant effect can be observed in the charged current that couples to the  $W$  boson, which reads

$$\begin{aligned} \bar{u}_L(c_{u_L}V^{\text{GFS}}c_{d_L})\gamma^\mu d_L + \bar{u}_L(c_{u_L}V^{\text{GFS}}s_{d_L})\gamma^\mu d'_L \\ + \bar{u}'_L(s_{u_L}V^{\text{GFS}}c_{d_L})\gamma^\mu d_L + \bar{u}'_L(s_{u_L}V^{\text{GFS}}s_{d_L})\gamma^\mu d'_L, \end{aligned} \quad (2.33)$$

(in which we consider  $c_{u,d_L}$  and  $s_{u,d_L}$  are diagonal matrices, whose entries are  $c_{u,d_{Li}}$  and  $s_{u,d_{Li}}$ , respectively); this can be opportunely rewritten by putting SM and exotic quarks in the same vectors

$$\mathcal{U}^T = (u, c, t, u', c', t'), \quad \mathcal{D}^T = (d, s, b, d', s', b'), \quad (2.34)$$

so that it becomes

$$\bar{\mathcal{U}}_L \begin{pmatrix} c_{u_L}V^{\text{GFS}}c_{d_L} & c_{u_L}V^{\text{GFS}}s_{d_L} \\ s_{u_L}V^{\text{GFS}}c_{d_L} & s_{u_L}V^{\text{GFS}}s_{d_L} \end{pmatrix} \mathcal{D}_L, \quad (2.35)$$

showing that it is governed by a  $6 \times 6$  unitary matrix. However, if one considers only the SM quarks, the impact is very relevant: effectively the CKM matrix becomes

$$V^{\text{CKM}} = c_{u_L} \cdot V^{\text{GFS}} \cdot c_{d_L}, \quad (2.36)$$

that is not even unitary; this implies also that the GIM mechanism is broken, even if a generalized version of it is recovered after that also the exotic quarks are included.

The masses and mixings of the SM gauge bosons are unchanged. On the other hand, the vevs of the flavon fields determine the masses and the mixing of the gauge bosons. If we build a vector with the gauge bosons,

$$\chi^T = (A_Q^1, \dots, A_Q^8, A_U^1, \dots, A_U^8, A_D^1, \dots, A_D^8), \quad (2.37)$$

then the Lagrangian mass term will read

$$\mathcal{L}_{\text{mass}} = \frac{1}{2} \chi^T (\mathcal{M}_A^2) \chi, \quad (2.38)$$

where

$$\mathcal{M}_A^2 = \begin{pmatrix} M_{QQ}^2 & M_{QU}^2 & M_{QD}^2 \\ M_{UQ}^2 & M_{UU}^2 & 0 \\ M_{DQ}^2 & 0 & M_{DD}^2 \end{pmatrix}, \quad (2.39)$$

with

$$(M_{QQ}^2)_{ab} = \frac{1}{4} g_Q^2 \text{Tr} [Z_u \{\lambda^a, \lambda^b\} Z_u^\dagger + Z_d \{\lambda^a, \lambda^b\} Z_d^\dagger], \quad (2.40a)$$

$$(M_{UU}^2)_{ab} = \frac{1}{4} g_U^2 \text{Tr} [Z_u \{\lambda^a, \lambda^b\} Z_u^\dagger], \quad (2.40b)$$

$$(M_{DD}^2)_{ab} = \frac{1}{4} g_D^2 \text{Tr} [Z_d \{\lambda^a, \lambda^b\} Z_d^\dagger], \quad (2.40c)$$

$$(M_{QU}^2)_{ab} = -\frac{1}{2} g_Q g_U \text{Tr} [\lambda^a Z_u^\dagger \lambda^b Z_u], \quad (2.40d)$$

$$(M_{UQ}^2)_{ab} = (M_{QU}^2)_{ba}, \quad (2.40e)$$

$$(M_{QD}^2)_{ab} = -\frac{1}{2} g_Q g_D \text{Tr} [\lambda^a Z_d^\dagger \lambda^b Z_d], \quad (2.40f)$$

$$(M_{DQ}^2)_{ab} = (M_{QD}^2)_{ba}. \quad (2.40g)$$

In general,  $\mathcal{M}_A^2$  can be diagonalized only numerically, even if from its structure, which contains many zeroes and symmetries, some properties can be inferred, for example that  $A_U$  and  $A_D$  do not mix. Formally, one obtains the mass eigenstates of the gauge bosons

$$\hat{\chi} = \left( \hat{A}^1, \dots, \hat{A}^{24} \right) \quad (2.41)$$

through the unitary transformation

$$\chi = \mathcal{W} \hat{\chi} , \quad (2.42)$$

where  $\mathcal{W}(\hat{A}^m, A_F^a)$  are the elements of the matrix that permits to obtain the diagonal mass matrix

$$\hat{\mathcal{M}}_A^2 = \mathcal{W}^T \mathcal{M}_A^2 \mathcal{W} . \quad (2.43)$$

If the coupling of the flavour gauge bosons to the quarks is described by

$$\bar{\mathcal{U}}_i \gamma_\mu (\mathcal{G}_L^u + \mathcal{G}_R^u)_{ij,m} \mathcal{U}_j \cdot \chi_m + \bar{\mathcal{D}}_i \gamma_\mu (\mathcal{G}_L^d + \mathcal{G}_R^d)_{ij,m} \mathcal{D}_j \cdot \chi_m , \quad m = 1, \dots, 24 , \quad (2.44)$$

the rotation to the mass-eigenstates of the heavy gauge bosons redefines the couplings:

$$\bar{\mathcal{U}}_i \gamma_\mu (\hat{\mathcal{G}}_L^u + \hat{\mathcal{G}}_R^u)_{ij,k} \mathcal{U}_j \cdot \hat{\chi}_k + \bar{\mathcal{D}}_i \gamma_\mu (\hat{\mathcal{G}}_L^d + \hat{\mathcal{G}}_R^d)_{ij,k} \mathcal{U}_j \cdot \hat{\chi}_k , \quad (2.45)$$

where

$$\left( \hat{\mathcal{G}}_{L,R}^{u,d} \right)_{ij,m} = \sum_k \mathcal{W}(\hat{\chi}_m, \chi_k) \left( \mathcal{G}_{L,R}^{u,d} \right)_{ij,m} . \quad (2.46)$$

The Feynman rules of the GFS model are listed in Appendix A. We have already discussed the impact on the charged currents; of course, the couplings of quarks to the photon are protected by gauge invariance and are not modified. As regards the neutral currents, since the right handed quarks only mix with singlets of equal charge, their couplings to the  $Z$  (proportional to their electric charge) are not modified either; the coupling of left handed quarks to the  $Z$  is modified instead. Finally, the couplings of quarks to the Higgs are also modified relatively to the ones in the SM.

## 2.2 Preliminary considerations

### 2.2.1 Exploring the parameter space

The GFS model presents nine new parameters with respect to the SM (non considering the Higgs sector for the difficulties that we have explained): seven couplings  $g_{Q,U,D}$ ,  $\lambda_{u,d}^{(\prime)}$ , and two masses  $M_{u,d}$ . As a preliminary step towards a deep phenomenological flavour analysis of the GFS model, we examine the parameter space looking for indications coming from the model structure itself and the strictest experimental constraints.

- **Order of magnitudes and unphysical regions**

As regards the couplings, we assume all of them to be at most of  $\mathcal{O}(1)$  at the considered energies, in order to stay in the perturbative regime of the theory. Concerning the mass parameters, too small values can be excluded since the masses of the exotic quarks are proportional to them; on the other hand, too high values would produce effects undetectable by the present experiments; therefore, we assume them to be of  $\mathcal{O}(10^2 - 10^3)$  GeV.

In order to be consistent, from expressions in Eq. (2.31a)-(2.31b) one must obtain values  $|s_{(u,d)(L,R)i}| \leq 1$ . Even stronger constraints come observing the equivalences

$$x_{(u,d)i} = \frac{M_{u,d}}{m_{u_i}} \equiv \frac{c_{(u,d)Li}}{s_{(u,d)Ri}}, \quad y_{(u,d)i} = \frac{\lambda_{u,d}v}{\sqrt{2}m_{u_i}} \equiv \frac{c_{(u,d)Ri}}{s_{(u,d)Li}}, \quad (2.47)$$

for which the physical regions correspond to  $x_{(u,d)i}, y_{(u,d)i} \geq 1$  or  $x_{(u,d)i}, y_{(u,d)i} < 1$ ; however, the second case corresponds to  $m_{(u,d)'i} < m_{(u,d)i}$ , which can be excluded (even if, as we will discuss in the next point, not completely). These conditions impose clear bounds on  $M_{u,d}$  and  $\lambda_{u,d}$ ; however, as it can be seen in Fig. 2.2, they are significant only for  $x_{u_3}, y_{u_3}$ , and hence for  $M_u$  and  $\lambda_u$ .

Moreover, from the approximations in Eq. (2.31a)-(2.31b) it can be seen that all the sines are small, with the exception of  $s_{u(L,R)3}$  for which those approximations are not always valid.

- **Experimental bounds from the down sector**

From the expressions of the masses and the mixing sines it is evident that the ones on the up and down sector depend only on  $M_u, \lambda_u$  and  $M_d, \lambda_d$  respectively; as a consequence, looking only at quantities depending only from them it is possible to obtain constraints on the two pairs of parameters separately.

In the down sector, a strong constraint comes from the lower bounds of a possible  $b'$  quark. The most recent limits, coming from CDF [129] and CMS [130], give respectively  $m_{b'} > 372$  GeV and  $m_{b'} > 361$  GeV. However, these lower bounds are given assuming  $\mathcal{B}(b' \rightarrow Zb) = 100\%$  for  $100 \text{ GeV} \lesssim m_{b'} \lesssim 268$  GeV, and  $\mathcal{B}(b' \rightarrow Wt) = 100\%$  for  $m_{b'} = m_t + m_W = 253$  GeV, for which the  $Wt$  channel opens up. These assumptions may not apply in the GFS model, because the couplings of the  $b'$  to  $Wt$  and  $Zb$  include a suppression factor of  $s_{dL3}$ , and on the other hand the channel  $b' \rightarrow bh$  can become important [25]. Without the previous assumptions, LEP gave  $m_{b'} > 46$  GeV [131]. The constraints coming from both these limits on  $m_{b'}$  to  $M_u - \lambda_u$  are shown in Fig. 2.2 (left).

Another strict constraint comes from the fact that in the GFS model the couplings to the  $Z$  boson are not universal, in the sense that, as we have seen, they do not depend only on the charge but also on the specific generation. Since the effects are larger for heavier quarks, the most important deviations

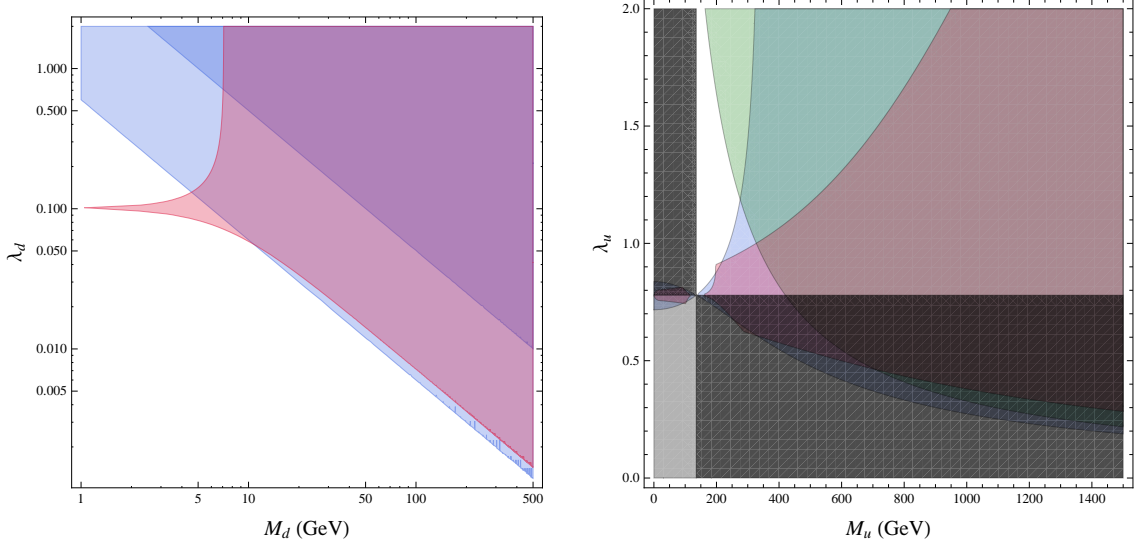


Figure 2.2: (Left) Allowed regions of parameter space in the  $M_d - \lambda_d$  plane. The blue regions corresponds to  $46 \text{ GeV} \leq m_{b'} \leq 372 \text{ GeV}$  (lighter) and  $m_{b'} > 372 \text{ GeV}$  (darker); the red region is the one allowed by the 95% CL limit on  $R_b$ . (Right) Allowed regions of parameter space in the  $M_u - \lambda_u$  plane. The dark shaded regions are not physical, while in the gray-shaded region  $m_{u'_i} < m_{u_i}$ . The green hyperbola corresponds to  $m_{t'} > 420 \text{ GeV}$ ; the red region is allowed at 95% CL by the  $S, T, U$  parameters, while the blue region is the one allowed by the bounds on  $|V_{tb}|$ .

should be found in the observable  $R_b = \Gamma(Z \rightarrow b\bar{b})/\Gamma(Z \rightarrow \text{hadrons})$ . In the GFS model it reads [25]

$$\frac{\delta R_b}{R_b^{\text{SM}}} \approx -1.8 s_{dL3}^2, \quad (2.48)$$

and the experimental global fit is  $R_b^{\text{exp}} = 0.21629 \pm 0.00066$  [65].

### • Experimental bounds from the up sector

The upper bounds on the  $t'$  mass are  $m_{t'} > 420 \text{ GeV}$  assuming  $\mathcal{B}(t' \rightarrow tX) = 100\%$  ( $m_X < 140 \text{ GeV}$ ) from ATLAS [132], and  $m_{t'} > 358 \text{ GeV}$  assuming  $\mathcal{B}(t \rightarrow Wb) = 100\%$  from CDF [133]. However, as we have discussed for  $b'$ , these assumption may not be valid in the GFS model; moreover, it can be seen from Fig. 2.2 (right) that a small region of the parameter space could be allowed for  $m_{t'}$  lower than these bounds and even for  $m_{t'} < m_t$ .

Regarding the electroweak precision tests, the exotic fermions modify the oblique corrections to the electroweak gauge bosons with respect to their SM values; the best parametrization of these effects is given by the  $S, T, U$  param-

eters [134]. In the GFS model they are given by [25]

$$S = \frac{s_{uL3}^2}{6\pi} \left[ \left( 3c_{uL3}^2 \frac{(m_{t'}^2 + m_t^2)(m_{t'}^4 - 4m_{t'}^2 m_t^2 + m_t^4)}{(m_{t'}^2 - m_t^2)^3} - 1 \right) \log\left(\frac{m_{t'}^2}{m_t^2}\right) - c_{uL3}^2 \frac{5m_{t'}^4 - 22m_{t'}^2 m_t^2 + 5m_t^4}{(m_{t'}^2 - m_t^2)^2} \right], \quad (2.49a)$$

$$T = \frac{3 s_{uL3}^2}{8\pi s_w^2 c_w^2} \frac{m_t^2}{M_Z^2} \left[ c_{uL3}^2 \left( \frac{m_{t'}^2}{m_{t'}^2 - m_t^2} \log\left(\frac{m_{t'}^2}{m_t^2}\right) - 1 \right) + \frac{s_{uL3}^2}{2} \left( \frac{m_{t'}^2}{m_t^2} - 1 \right) \right], \quad (2.49b)$$

$$U = \frac{s_{uL3}^2}{6\pi} \left[ -3 \left( c_{uL3}^2 \frac{(m_{t'}^2 + m_t^2)(m_{t'}^4 - 4m_{t'}^2 m_t^2 + m_t^4)}{(m_{t'}^2 - m_t^2)^3} - 1 \right) \log\left(\frac{m_{t'}^2}{m_t^2}\right) + c_{uL3}^2 \frac{5m_{t'}^4 - 22m_{t'}^2 m_t^2 + 5m_t^4}{(m_{t'}^2 - m_t^2)^2} \right], \quad (2.49c)$$

obtained at one loop, considering only the dominant contributions of the third family in the limit  $m_b \rightarrow 0$ . The correction to the  $T$ -parameter is generated by the violation of the custodial symmetry due to the mixing of the quark doublets with the left singlets, whose amount is proportional to  $\lambda_u$ . On the other hand, the contribution of the exotic fermions to the  $S$ -parameter is always small and its sign is not fixed, and  $U$  only affects the results in a minor way. The most recent fit for the  $S, T, U$  parameters, performed for the first time with the actual mass of the Higgs boson, gives

$$S = 0.03 \pm 0.10, \quad T = 0.05 \pm 0.12, \quad U = 0.03 \pm 0.10, \quad (2.50)$$

with correlation coefficients of  $+0.89$  between  $S$  and  $T$ , and  $-0.54(-0.83)$  between  $S$  and  $U$  ( $T$  and  $U$ ) [135].

In the up sector another important constraint comes from the CKM matrix. In fact, as we have discussed, in the GFS model the effective CKM matrix differs from the SM one and it is not unitary. The unitarity of the CKM matrix is presently tested with good accuracy only in the first two rows [65], but since they contain only light quarks, the resulting bounds are very weak. On the other hand, in the third row, looking at Eq. (2.36), the measured smallness of  $|V_{td}^{\text{CKM}}|$  and  $|V_{ts}^{\text{CKM}}|$  and the fact that  $c_{(u,d)L(1,2)} \simeq 1$  imply that  $|V_{tb}^{\text{GFS}}| = 1$  with high accuracy; hence, since also  $c_{dL3} \simeq 1$ , the direct measurement of the  $t-b-W$  coupling constrains  $c_{uL3}$ . The determination of  $|V_{tb}|$  from top decays, recently measured by CMS at 7 TeV, gives the bound  $|V_{tb}^{\text{CKM}}| > 0.92$  [136].

## 2.2.2 Spectrum

Once we have performed a first analysis of the space parameter, and before scanning the allowed regions to look for more indications from flavour physics, we choose one between the possible points in order to obtain a representative spectrum of the quarks and flavour bosons of the GFS model and make some qualitative considerations. In particular we use the following parameters.

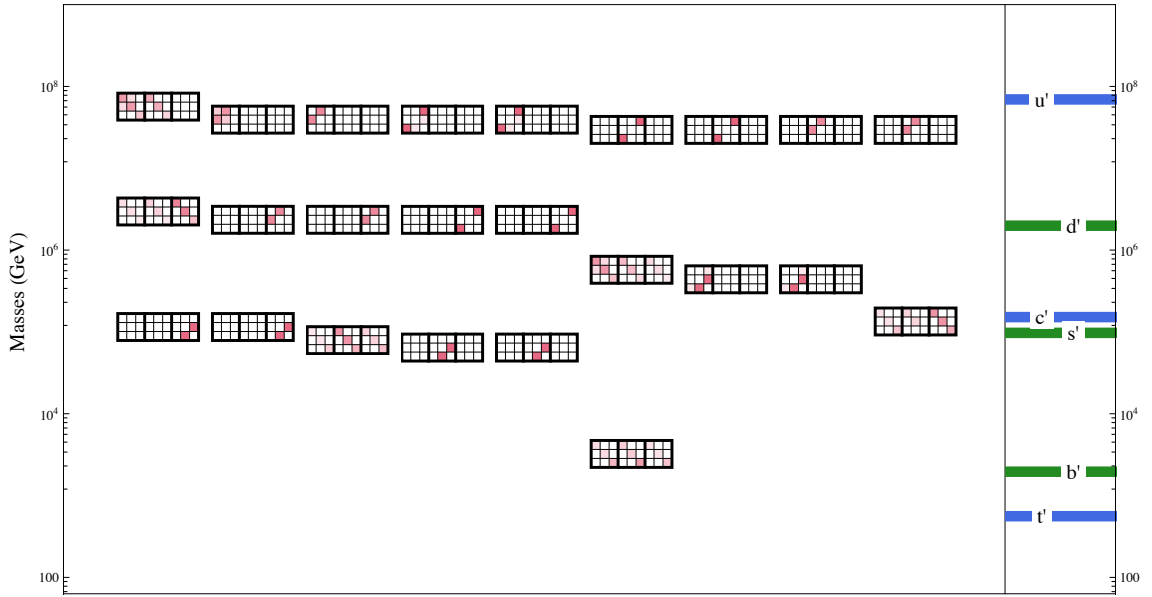


Figure 2.3: Spectrum of the flavour gauge bosons (left) and of the exotic quarks (right, blue for the up-type and green for the down-type). The position in the vertical axis of the relative rectangles and bars represents the corresponding mass. Each vector fields is represented by a set of three  $3 \times 3$  matrices (see Eq. (2.51)), each of them indicating how much they contribute to  $A_Q, A_U, A_D$  respectively: the intensity of the red color correspond to the size of each entry in the matrices (from 0 to 1).

$g_Q$	$g_U$	$g_D$	$\lambda_u$	$\lambda_d$	$\lambda'_u$	$\lambda'_d$	$M_u$	$M_d$
0.4	0.3	0.5	0.95	0.25	0.5	0.3	450 GeV	100 GeV

As we have discussed, the structure of the fermionic sector is quite rigid, since it depends only on  $\lambda_{u,d}$  and  $M_{u,d}$ ; on the other hand, also all the other parameters are involved in the gauge sector, and the fact that the diagonalization is only possible numerically makes more difficult to recognize a pattern of behavior.

As it can be seen from Fig. 2.3, in this specific case both the lightest quark states,  $t'$  and  $b'$ , have a mass of  $\mathcal{O}(1)$  TeV, so they should be within the reach of the LHC. It is important to keep in mind however that, contrarily to the models with a sequential 4th generation of quarks, their couplings to the SM  $W$  and  $Z$  bosons arise through mixing with SM left-handed fields and are suppressed by the small angles  $s_{u_{L3}}$  and  $s_{d_{L3}}$ . Due to the relation of inverse proportionality between the SM quark masses and the exotic quark masses, the spectrum of the latter presents a strong hierarchy, and the heavier quark  $u'$  has a mass of  $\mathcal{O}(10^5)$  TeV.

Regarding the flavour gauge bosons, the lightest state has a mass of  $\mathcal{O}(1)$  TeV, which is one order of magnitude lighter than the next lightest ones. In Fig. 2.3 we have also represented the contribution of each mass eigenstate to the flavour

eigenstates, with matrices according to

$$\begin{aligned}
A_Q &= \hat{A}_1 \underbrace{\left( \mathcal{W}_{1,1} \frac{\lambda^1}{2} + \dots + \mathcal{W}_{1,8} \frac{\lambda^8}{2} \right)}_{\text{1st matrix of the lightest boson}} + \dots + \hat{A}_{24} \left( \mathcal{W}_{24,1} \frac{\lambda^1}{2} + \dots + \mathcal{W}_{24,8} \frac{\lambda^8}{2} \right) , \\
A_U &= \hat{A}_1 \underbrace{\left( \mathcal{W}_{1,9} \frac{\lambda^1}{2} + \dots + \mathcal{W}_{1,16} \frac{\lambda^8}{2} \right)}_{\text{2nd matrix of the lightest boson}} + \dots + \hat{A}_{24} \left( \mathcal{W}_{24,9} \frac{\lambda^1}{2} + \dots + \mathcal{W}_{24,16} \frac{\lambda^8}{2} \right) , \\
A_D &= \hat{A}_1 \underbrace{\left( \mathcal{W}_{1,17} \frac{\lambda^1}{2} + \dots + \mathcal{W}_{1,24} \frac{\lambda^8}{2} \right)}_{\text{3rd matrix of the lightest boson}} + \dots + \hat{A}_{24} \left( \mathcal{W}_{24,17} \frac{\lambda^1}{2} + \dots + \mathcal{W}_{24,24} \frac{\lambda^8}{2} \right) .
\end{aligned} \tag{2.51}$$

The lightest boson couples to fermions through the  $\lambda^8$  flavour generator and with equal strength to left/right up/down type fermions (the unequal intensity of magnitude is compensated by the different values of the gauge couplings). Although its coupling to the third generation is the largest, the lightest vector couples also to the first two generations, which makes it accessible at the LHC. For all practical purposes it corresponds to a flavour non-universal leptophobic  $Z'$  [25]. Tevatron excludes this kind of resonances in the  $t\bar{t}$  channel only for  $m_{Z'} < 900$  GeV at 95% confidence level [137].

## 2.3 Phenomenological analysis

### 2.3.1 Impact on the observables

#### $\Delta F = 2$ transitions

In the GFS model the  $\Delta F = 2$  observables with external down-type quarks receive two kinds of new contributions at the leading order, as shown in Fig. 2.4: one from the usual SM box diagrams in which also the new up-type quarks participate, and one due to the tree-level exchange of the flavour gauge bosons. We can include these contributions in the effective Hamiltonian

$$\mathcal{H}_{\text{eff}}^{\Delta F=2} = \frac{G_F^2 m_W^2}{4\pi^2} \sum_i C_i(\mu) Q_i \tag{2.52}$$

through a modification of the Wilson coefficients

$$C_i^{(M)} = C_{i,\text{SM}}^{(M)} + \Delta_{\text{box}}^{(M)} C_i + \Delta_{\text{tree}}^{(M)} C_i , \tag{2.53}$$

where  $M$  is the meson system under consideration, and  $\mu$  is the energy scale at which the coefficient has to be evaluated.

In principle one should also consider box-diagrams with flavour gauge boson exchanges, but they are negligible with respect to the tree-level contributions. Also negligible can be considered the tree-level exchanges of the  $\pi_i$  Higgs states.

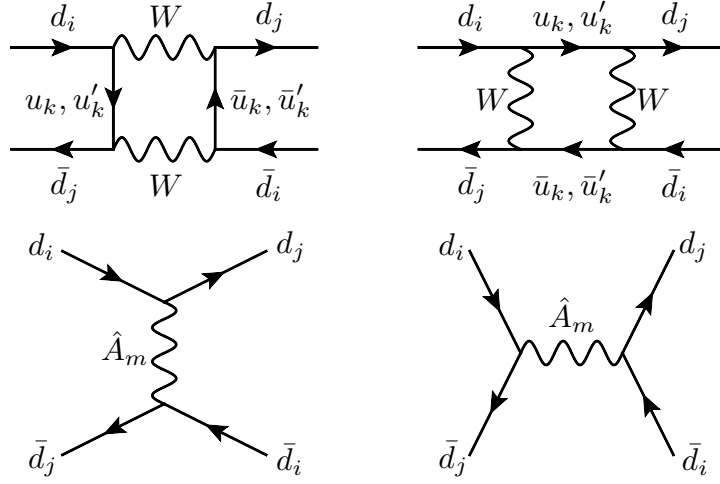


Figure 2.4: Box diagrams (upper panel) and tree diagrams (lower panel) contributing to the meson mixings  $K^0 - \bar{K}^0$ ,  $B_d - \bar{B}_d$ ,  $B_s - \bar{B}_s$ .

- **Contributions from the box diagrams**

We define the combinations of the mixing matrix

$$\lambda_i^K = (V_{\text{GFS}}^*)_{is}^* (V_{\text{GFS}})_{id}, \quad \lambda_i^{B_q} = (V_{\text{GFS}}^*)_{ib}^* (V_{\text{GFS}})_{iq}. \quad (2.54)$$

Then, for the  $K$  system, the contribution of the new box diagrams to the Wilson coefficients, that is purely of the  $VLL$  type, is

$$\begin{aligned} \Delta_{\text{box}}^{(K)} C_1^{VLL}(\mu_t) &= (c_{d_{L1}} c_{d_{L2}})^2 \sum_{i,j=1,2,3} \lambda_i^K \lambda_j^K c_{u_{Li}}^2 c_{u_{Lj}}^2 F(x_i, x_j) \\ &\quad + (c_{d_{L1}} c_{d_{L2}})^2 \sum_{i,j=1,2,3} \lambda_i^K \lambda_j^K s_{u_{Li}}^2 s_{u_{Lj}}^2 F(x'_i, x'_j) \\ &\quad + (c_{d_{L1}} c_{d_{L2}})^2 \sum_{i,j=1,2,3} \lambda_i^K \lambda_j^K \left[ c_{u_{Li}}^2 s_{u_{Lj}}^2 F(x_i, x'_j) \right. \\ &\quad \left. + s_{u_{Li}}^2 c_{u_{Lj}}^2 F(x'_i, x_j) \right]; \end{aligned} \quad (2.55)$$

the loop function [48] is

$$F(x_i, x_j) = \frac{1}{4} \left[ (4 + x_i x_j) I_2(x_i, x_j) - 8 x_i x_j I_1(x_i, x_j) \right] \quad (2.56)$$

with

$$\begin{aligned} I_1(x_i, x_j) &= \frac{1}{(1-x_i)(1-x_j)} + \left[ \frac{x_i \ln(x_i)}{(1-x_i)^2(x_i-x_j)} + (i \leftrightarrow j) \right], \\ I_2(x_i, x_j) &= \frac{1}{(1-x_i)(1-x_j)} + \left[ \frac{x_i^2 \ln(x_i)}{(1-x_i)^2(x_i-x_j)} + (i \leftrightarrow j) \right], \end{aligned} \quad (2.57)$$

and with arguments

$$x_i = \left( \frac{m_{u_i}}{M_W} \right)^2, \quad x'_j = \left( \frac{m_{u'_j}}{M_W} \right)^2; \quad (2.58)$$

the matching scale  $\mu_t$  is in the ballpark of the top quark mass<sup>2</sup>. For the  $B_q - \bar{B}_q$  mixing one has to replace  $\lambda_i^K$  by  $\lambda_i^{B_q}$  and  $c_{d_{L1}} c_{d_{L2}}$  by  $c_{d_{L1}} c_{d_{L3}}$  ( $c_{d_{L2}} c_{d_{L3}}$ ) in the case of  $q = d$  ( $q = s$ ).

These structures become more familiar by noticing that, for a fixed  $\lambda_i^M \lambda_j^M$ , we obtain the combination

$$\mathcal{F}_{ij} \equiv c_{u_{L_i}}^2 c_{u_{L_j}}^2 F(x_i, x_j) + s_{u_{L_i}}^2 s_{u_{L_j}}^2 F(x'_i, x'_j) + c_{u_{L_i}}^2 s_{u_{L_j}}^2 F(x_i, x'_j) + s_{u_{L_i}}^2 c_{u_{L_j}}^2 F(x'_i, x_j); \quad (2.59)$$

this shows the generalized GIM mechanism at work: if all fermion masses were degenerate, this combination would be independent from  $i, j$  and the unitarity of the matrix  $V_{\text{GFs}}$  would assure the disappearance of FCNCs. Moreover, these  $\mathcal{F}$  functions can be arranged in order to write the box contributions as a modification of the usual Inami-Lim functions:

$$\begin{aligned} S_0(x_t) &\longrightarrow S_t^{(K)} \equiv (c_{d_{L1}} c_{d_{L2}})^2 (\mathcal{F}_{33} + \mathcal{F}_{11} - 2\mathcal{F}_{13}) , \\ S_0(x_c) &\longrightarrow S_c^{(K)} \equiv (c_{d_{L1}} c_{d_{L2}})^2 (\mathcal{F}_{22} + \mathcal{F}_{11} - 2\mathcal{F}_{12}) , \\ S_0(x_c, x_t) &\longrightarrow S_{ct}^{(K)} \equiv (c_{d_{L1}} c_{d_{L2}})^2 (\mathcal{F}_{23} + \mathcal{F}_{11} - \mathcal{F}_{13} - \mathcal{F}_{12}) ; \end{aligned} \quad (2.60)$$

similarly for the  $B_q$  systems the analogous functions  $S_i^{(B_q)}$  are obtained by substituting  $c_{d_{L1}} c_{d_{L2}}$  with  $c_{d_{L1}} c_{d_{L3}}$  ( $c_{d_{L2}} c_{d_{L3}}$ ) in the case of  $q = d$  ( $q = s$ ); the combination of the  $\mathcal{F}_{ij}$  contributions are universal. The appearance of  $c_i$  and  $s_j$  factors introduces a new flavour dependence, breaking the SM universality of the master functions.

### • Contributions from the tree diagrams

In this case new operators, beyond the SM  $VLL$  one, are involved: for the  $K$  system the new contributions are

$$\Delta_{\text{tree}}^{(K)} C_1^{VLL}(\mu_A) = \frac{4\pi^2}{G_F^2 m_W^2} \sum_{m=1}^{24} \frac{1}{2m_{\hat{A}_m}^2} \left[ \left( \hat{\mathcal{G}}_L^d \right)_{ds,m} \right]^2 , \quad (2.61)$$

$$\Delta_{\text{tree}}^{(K)} C_1^{VRR}(\mu_A) = \frac{4\pi^2}{G_F^2 m_W^2} \sum_{m=1}^{24} \frac{1}{2m_{\hat{A}_m}^2} \left[ \left( \hat{\mathcal{G}}_R^d \right)_{ds,m} \right]^2 , \quad (2.62)$$

$$\Delta_{\text{tree}}^{(K)} C_1^{LR}(\mu_A) = \frac{4\pi^2}{G_F^2 m_W^2} \sum_{m=1}^{24} \frac{1}{2m_{\hat{A}_m}^2} \left[ 2 \left( \hat{\mathcal{G}}_L^d \right)_{ds,m} \left( \hat{\mathcal{G}}_R^d \right)_{ds,m} \right] ; \quad (2.63)$$

the energy scale  $\mu_A$  is of the order of the mass of the corresponding flavour gauge boson. The corresponding expressions for the  $B_d$  ( $B_s$ ) system are obtained by substituting  $ds$  with  $db$  ( $sb$ ) in the indices of the couplings.

<sup>2</sup>In the case of the box-diagrams involving simultaneously heavy and light particles, the correct procedure would be to integrate out first the heavy fermions and construct an effective field theory not involving them as dynamical degrees of freedom. However, as the only relevant contribution comes from the lightest exotic fermion  $t'$ , whose mass is of the same order as  $m_t$ , we can set the matching scale to be  $\mu_t$  also in this case.

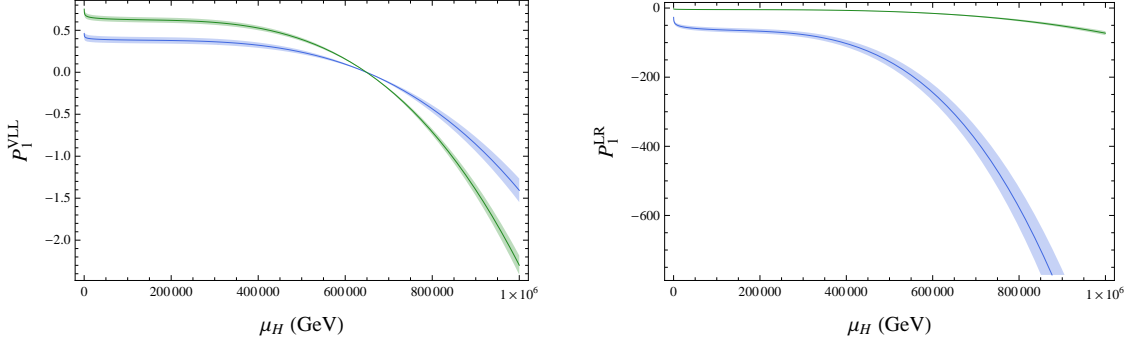


Figure 2.5: Coefficients  $P_1^{VLL}$  (left) and  $P_1^{LR}$  (right) as functions of the high energy scale  $\mu_H$ . The blue functions are valid for the  $K$  system, the green functions for the  $B_d$  and  $B_s$  systems.

	500 GeV	1 TeV	3 TeV	10 TeV
$P_1^{VLL}(\mu_H, K)$	0.392	0.384	0.373	0.363
$P_1^{LR}(\mu_H, K)$	-35.7	-39.3	-45.0	-51.4
$P_1^{VLL}(\mu_H, B_d)$	0.675	0.662	0.643	0.624
$P_1^{LR}(\mu_H, B_d)$	-2.76	-2.97	-3.31	-3.69
$P_1^{VLL}(\mu_H, B_s)$	0.713	0.698	0.678	0.659
$P_1^{LR}(\mu_H, B_s)$	-2.76	-2.97	-3.31	-3.69

Table 2.2: Central values of the relevant  $P_i$  factors for selected values of  $\mu_H$ .

### • QCD corrections

The effective Hamiltonian above has been constructed at certain high energy scales, and the renormalization group QCD evolution down to lower energy scales, at which the hadronic matrix elements are evaluated by lattice methods, has to be performed. In the GFS model this is complicated by the presence of different high scales, i.e. the mass of the  $W$  boson  $m_W$ , the masses of the neutral gauge bosons  $m_{\hat{A}_m}$ , and the masses of heavy quarks  $m_{q_i}$ .

An efficient method for the inclusion of the QCD effects in the presence of a high energy scale  $\mu_H$ , corresponding to the scale at which heavy particles are integrated out, consists in evaluating the hadronic matrix elements at this high scale instead that taking directly their low-energy scale values. The amplitude for  $M - \bar{M}$  meson mixing at the scale  $\mu_H$  is then simply given by

$$\mathcal{A}(M \rightarrow \bar{M}) = \frac{G_F^2 m_W^2}{4\pi^2} \sum_i C_i(\mu_H) \langle \bar{M} | Q_i(\mu_H) | M \rangle, \quad (2.64)$$

where the matrix element is

$$\langle \bar{M} | Q_i(\mu_H) | M \rangle = \frac{2}{3} m_M^2 F_M^2 P_i(\mu_H, M); \quad (2.65)$$

the coefficients  $P_i$  have forms of the kind

$$P_i(\mu_H, M) \sim \sum_a \eta_i^a(\mu_H, \mu_L) B_i^a(\mu_L, M) , \quad (2.66)$$

where  $\eta_i^a$  includes the renormalization-group effects from scales below  $\mu_H$ , while  $B_i^a$  represent the hadronic matrix elements obtained by lattice methods at low energy scales  $\mu_L$ . The detailed analytic formulae for the  $P_i$  coefficients have been obtained in [138]; in Fig. 2.5 and in Tab. 2.2 we have respectively shown the dependence from the high energy scale and listed some representative values for the ones relevant in the GFS model.

### • Final formulae

Putting together the results obtained in the previous points, the final expressions for the matrix elements of the  $\Delta F = 2$  transitions are

$$\begin{aligned} \langle \bar{K}^0 | \mathcal{H}_{\text{eff}}^{\Delta S=2} | K^0 \rangle = & \frac{G_F^2 m_W^2}{24\pi^2} F_K^2 \left\{ \hat{B}_K \eta_1 (\lambda_2^K)^2 S_c^{(K)} + \hat{B}_K \eta_2 (\lambda_3^K)^2 S_t^{(K)} + \right. \\ & + 2\hat{B}_K \eta_3 \lambda_2^K \lambda_3^K S_{ct}^{(K)} + \\ & + \sum_{a=1}^{24} \left[ P_1^{VLL}(\mu_{\hat{A}_m}, K) \left( \Delta_{\text{tree}}^{(K)} C_1^{VLL}(\mu_{\hat{A}_m}) + \Delta_{\text{tree}}^{(K)} C_1^{VRR}(\mu_{\hat{A}_m}) \right) \right. \\ & \left. \left. + P_1^{LR}(\mu_{\hat{A}_m}, K) \Delta_{\text{tree}}^{(K)} C_1^{LR}(\mu_{\hat{A}_m}) \right] \right\} , \end{aligned} \quad (2.67)$$

$$\begin{aligned} \langle \bar{B}_q | \mathcal{H}_{\text{eff}}^{\Delta B=2} | B_q \rangle = & \frac{G_F^2 m_W^2}{24\pi^2} F_{B_q}^2 \left\{ \eta_B \hat{B}_{B_q} \lambda_3^2(B_q) S_t^{(B_q)} + \right. \\ & + \sum_{a=1}^{24} \left[ P_1^{VLL}(\mu_{\hat{A}_m}, B_q) \left( \Delta_{\text{tree}}^{(B_q)} C_1^{VLL}(\mu_{\hat{A}_m}) + \Delta_{\text{tree}}^{(B_q)} C_1^{VRR}(\mu_{\hat{A}_m}) \right) \right. \\ & \left. \left. + P_1^{LR}(\mu_{\hat{A}_m}, B_q) \Delta_{\text{tree}}^{(B_q)} C_1^{LR}(\mu_{\hat{A}_m}) \right] \right\} . \end{aligned} \quad (2.68)$$

### More observables

#### • $B^+ \rightarrow \tau^+ \nu$ and ratios

The dominant modification of the  $B^+ \rightarrow \tau^+ \nu$  branching ratio in the GFS model is due to the different coupling of the  $W$  vertex with respect to the SM:

$$\mathcal{B}(B^+ \rightarrow \tau^+ \nu) = \frac{G_F^2 m_{B^+} m_\tau^2}{8\pi} \left( 1 - \frac{m_\tau^2}{m_{B^+}^2} \right)^2 F_{B^+}^2 |c_{uL1} V_{ub} c_{dL3}|^2 \tau_{B^+} . \quad (2.69)$$

We have assumed that the couplings of the leptons with the  $W$  boson are the same as the SM: even if we are not considering the lepton sector in our analysis, it is reasonable to assume that any NP modification can be safely negligible, as these couplings are strongly constrained by the SM electroweak analysis.

The dependence on  $F_{B_d}$  represents a significant source of error on this quantity; however, this is cancelled by considering the ratio with respect to  $\Delta M_d$  [139, 140]:

$$\begin{aligned} R_{\tau\nu/\Delta M} &\equiv \frac{\mathcal{B}(B^+ \rightarrow \tau^+\nu)}{\Delta M_d} \\ &= \frac{3\pi\tau_{B^+}}{4\eta_B \hat{B}_{B_d} S_0(x_t)} \frac{c_{uL1}^2 c_{dL3}^2}{|M_{12}^d/(M_{12}^d)_{\text{SM}}|} \frac{m_\tau^2}{m_W^2} \frac{|V_{ub}|^2}{|V_{tb}^* V_{td}|^2} \left(1 - \frac{m_\tau^2}{m_{B_d}^2}\right)^2, \end{aligned} \quad (2.70)$$

where we took  $m_{B^+} \approx m_{B_d}$ , well justified considering the errors in the other quantities.

Analogously,  $F_{B_q}$  is also the main source of the theoretical error on  $\Delta M_{B_q}$ ; when considering instead the ratio

$$R_{\Delta M_B} \equiv \frac{\Delta M_d}{\Delta M_s}, \quad (2.71)$$

the SM theoretical errors are encoded into the parameter  $\xi$  [61], which is much less affected by uncertainties with respect to the mass differences.

- **The  $b$  semileptonic CP asymmetry**

If we separate the modulus and the phase of the NP effects in the  $\Delta F = 2$  matrix elements, by writing as usual

$$M_{12}^q = (M_{12}^q)_{\text{SM}} C_{B_q} e^{2i\varphi_q}, \quad (2.72a)$$

$$\Gamma_{12}^q = (\Gamma_{12}^q)_{\text{SM}} \tilde{C}_{B_q} e^{-2i\tilde{\varphi}_q}, \quad (2.72b)$$

the contributions to the  $b$  semileptonic CP asymmetry read

$$a_{sl}^q = \left| \frac{(\Gamma_{12}^d)_{\text{SM}}}{(M_{12}^d)_{\text{SM}}} \right| \frac{\tilde{C}_{B_q}}{C_{B_q}} \sin \left( \arg \left[ -\frac{(M_{12}^d)_{\text{SM}}}{(\Gamma_{12}^d)_{\text{SM}}} \right] + 2\varphi_q + 2\tilde{\varphi}_q \right). \quad (2.73)$$

Now, in the GFS model the phase  $\tilde{\varphi}_{B_q}$  is vanishing, while  $\tilde{C}_{B_q}$  is mainly given by  $c_{uL2}^2 c_{dLb} c_{dLq} \approx 1$ ; as a result, the only modifications are provided by the contributions on  $M_{12}^q$ .

- $\bar{B} \rightarrow \mathbf{X}_s \gamma$

Similarly to the case of the  $\Delta F = 2$  transitions, the NP contributions to the Wilson coefficients in the effective Hamiltonian can be separated into two parts, as shown in Fig. 2.6: (i) the SM-like contribution from diagrams with  $W$  bosons with modified couplings to both SM and exotic up-type quarks; (ii) the contribution of flavour gauge bosons exchanges with virtual SM and exotic down-type quarks.

The first contribution has been considered in [25], where it has been shown that it could provide further information on the  $M_u - \lambda_u$  parameter space, but it actually eliminates regions already excluded by other constraints.

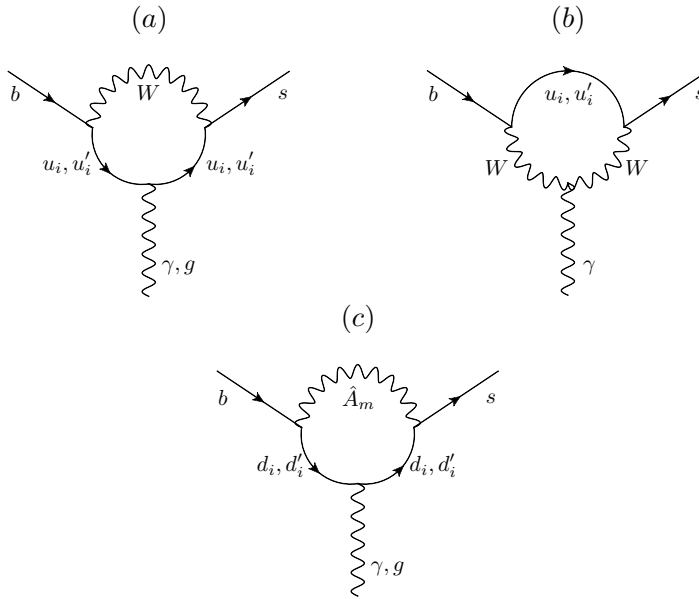


Figure 2.6: Contributions to the  $b \rightarrow s\gamma$  transition in the GFS model: from diagrams with  $W$  bosons with modified couplings (a and b) and from flavour gauge bosons exchange (c).

As regards the second contribution, the relevant Wilson coefficients were calculated within a generic framework in [141]. Applying those general formulae to the GFS model, we found that these contributions are below 1% and can be safely neglected [142]. The reason for such suppression are the See-Saw-like couplings of flavour gauge bosons to both SM and exotic fermions and the heavy flavour gauge boson masses.

### 2.3.2 Numerical analysis

The aim of our analysis is to study how the GFS model faces the flavour constraints, and to determine if it is able to relax the tensions in the flavour observables. In order to do this, we scan the allowed and significant regions of the parameter space, i.e.

$$M_u \in [400 \text{ GeV}, 1000 \text{ GeV}], \quad \lambda_u \in [0.8, 1.5], \quad (2.74a)$$

$$M_d \in [25 \text{ GeV}, 250 \text{ GeV}], \quad \lambda_d \in [0.1, 1.5], \quad (2.74b)$$

$$\lambda'_u, \lambda'_d, g_Q, g_U, g_D \in [10^{-5}, 1.1], \quad (2.74c)$$

according to the constraints and the discussions in Sec. 2.2.1. The numerical evaluation is performed iteratively, in order to fix correctly the energy scales  $\mu_t$  and  $\mu_A$  coinciding with the masses of the lightest exotic quark and of the lightest flavour gauge boson respectively.

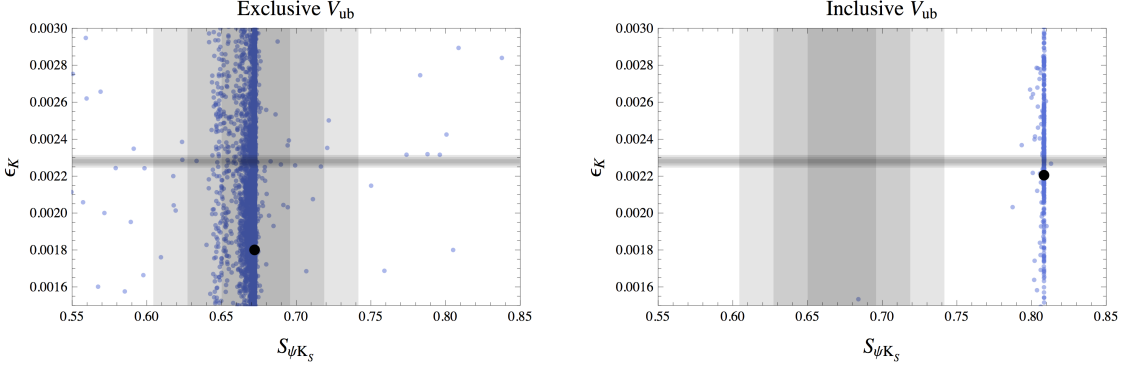


Figure 2.7:  $|\epsilon_K|$  versus  $S_{\psi K_S}$ , in Scenario 1 (left) and Scenario 2 (right) for  $|V_{ub}|$ . The shaded grey regions are the experimental  $1\sigma - 3\sigma$  error ranges, while the black points are the central values of the SM predictions.

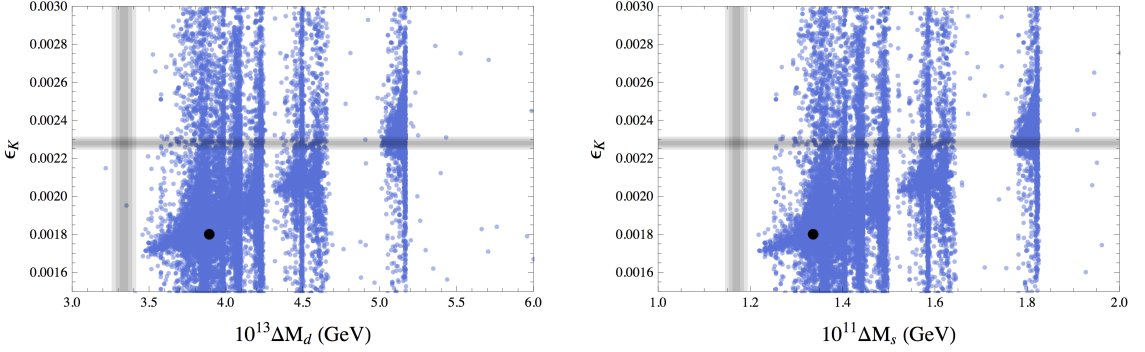


Figure 2.8:  $|\epsilon_K|$  versus  $\Delta M_d$  (left) and  $\Delta M_s$  (right). The shaded grey regions are the experimental  $1\sigma - 3\sigma$  error ranges, while the black points are the central values of the SM predictions.

- $|\epsilon_K| - S_{\psi K_S}$

The analysis of the correlation between  $|\epsilon_K|$  and  $S_{\psi K_S}$  in the GFS model permits to select one between the two scenarios of determination of  $|V_{ub}|$ .

$|\epsilon_K|$  is uniquely enhanced by the new box-diagram contributions involving exotic quarks, while it is uniquely suppressed by heavy gauge flavour boson contributions; among the latter, the  $LR$  contributions are the dominant ones, while the  $LL$  ones are safely negligible. On the other hand,  $S_{\psi K_S}$  is unaffected by the new box-diagram contributions, and this allows to see transparently the heavy gauge flavour boson contributions; the result is that it is only affected by  $LL$  contributions and can only be suppressed [142].

This means that while  $S_{\psi K_S}$  can only be slightly suppressed in the GFS model,  $|\epsilon_K|$  can be significantly both enhanced and suppressed, as can be seen from Fig. 2.7. As a consequence, this model prefers what we have called Scenario 1 for  $|V_{ub}|$ , in which  $S_{\psi K_S}$  is already in good agreement with its experimental determinations, while  $|\epsilon_K|$ , which is below its experimental value, can be

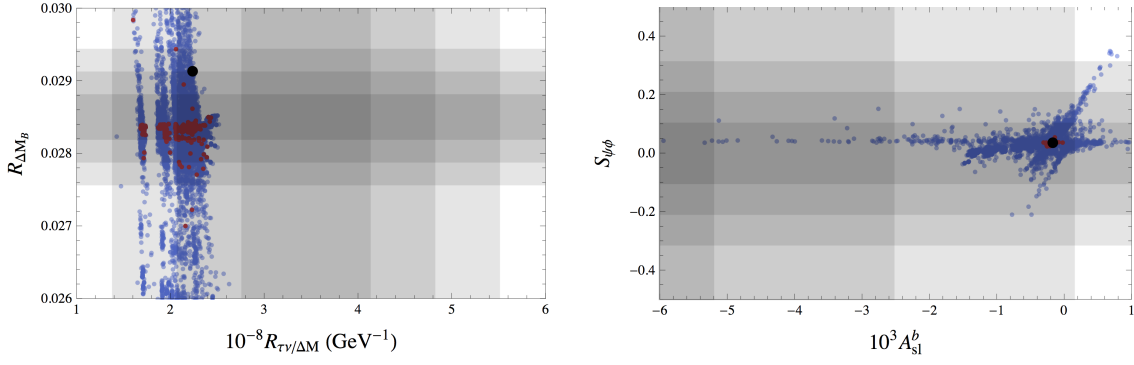


Figure 2.9:  $R_{\tau\nu/\Delta M}$  versus  $R_{\Delta M_B}$  (left) and  $S_{\psi\phi}$  versus  $A_{sl}^b$  (right). The red points are the ones for which  $\epsilon_K$  and  $S_{\psi K_S}$  are both compatible with their experimental values within the  $3\sigma$  error. The shaded grey regions are the experimental  $1\sigma - 3\sigma$  error ranges, while the black points are the central values of the SM predictions.

enhanced, as shown in the left panel of Fig. 2.7. In the right panel of the same figure it is shown how, in the GFS model, using the inclusive value of  $|V_{ub}|$  instead,  $S_{\psi K_S}$  cannot be nearly sufficiently suppressed to get closer to its experimental determination.

- $|\epsilon_K| - \Delta M_{d,s}$

$\Delta M_{d,s}$  are also uniquely enhanced by the new box-diagram contributions, but they are mostly unaffected by the heavy flavour gauge boson contributions [142].

This implies not only that the model is not able to improve the  $|\epsilon_K| - \Delta M_{d,s}$  weak tension present in the SM, but that it worsens it. In fact, as can be seen from Fig. 2.8, once we have selected the exclusive determination of  $|V_{ub}|$ , when  $\epsilon_K$  is enhanced to match its experimental value, both  $\Delta M_d$  and  $\Delta M_s$  are enhanced as well, departing more from their experimental determinations.

However, we underline how these conclusions are very sensitive to the values of the non-perturbative parameters  $F_{B_d}$  and  $F_{B_s}$ . In fact, in [142] we have shown how taking for them values reduced by 15%, close to their lower  $3\sigma$  bound, the GFS model performs much better regarding the  $|\epsilon_K| - \Delta M_{d,s}$  correlations.

- $\mathcal{B}(B^+ \rightarrow \tau^+ \nu_\tau)$

$R_{\Delta M_B}$  does not show any dependence on the new box-diagram contributions, since in the GFS model the operator structure in box-diagram contributions does not change with respect to the SM and the NP effects are the same in the  $B_d$  and  $B_s$  systems; as a result, any NP effect in this ratio should be attributed to the heavy gauge flavour boson contributions, both  $LL$  and  $LR$  [142]. On the other hand, there are no new operators contributing to  $\mathcal{B}(B^+ \rightarrow \tau^+ \nu_\tau)$ , but only the different coupling to the  $W$  boson, and hence we do not expect large modifications in this observable.

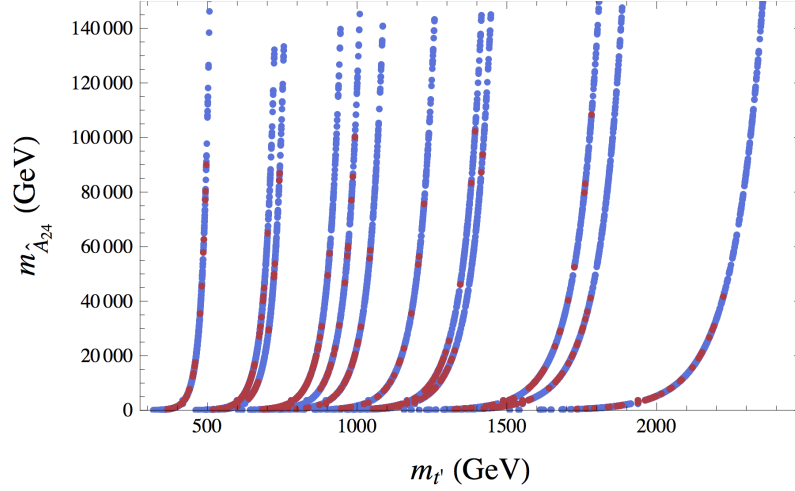


Figure 2.10: Masses of the lightest exotic quark  $t'$  and of the lightest flavour gauge boson  $\hat{A}^{24}$  of the GFS model. For the red points,  $\epsilon_K$ ,  $S_{\psi K_S}$ ,  $R_{\Delta M_B}$ ,  $R_{\tau\nu/\Delta M}$  agree with the experimental data at  $3\sigma$  level. The visible correlations corresponds to points of the parameter space with the same values of  $M_{u,d}$  and  $\lambda_{u,d}$ .

Both  $R_{\Delta M_B}$  and  $R_{\tau\nu/\Delta M}$  have small theoretical uncertainties and are therefore very useful to provide information on the parameter space of the GFS model. From Fig. 2.9 (left) we can see that the values of the GFS parameters that satisfy the  $|\epsilon_K| - S_{\psi K_S}$  constraints also improve the accordance of  $R_{\Delta M_B}$  with its measurement, but neither of them is able to significantly improve the discrepancy with the experimental value of  $\mathcal{B}(B^+ \rightarrow \tau^+ \nu_\tau)$ , that however, as we have discussed, is now less problematic due to the recent determinations.

- $A_{sl}^b$

$A_{sl}^b$  is not affected by box-diagram contributions, the  $LR$  contributions are almost completely negligible and the  $LL$  are the only relevant ones, enhancing  $|A_{sl}^b|$  towards the central value of its experimental determination. This is similar to what happens to  $S_{\psi\phi}$ : like  $S_{\psi K_S}$  it is unaffected by the new box-diagram contributions, but, differently from the latter, it depends on both  $LL$  and  $LR$  contributions; interestingly, the NP contributions interfere destructively with the SM contribution so that its sign can in principle be reversed in this model [142].

Fig. 2.9 (right) shows that the GFS model predicts only tiny deviations from the SM predictions for both  $A_{sl}^b$  and  $S_{\psi\phi}$ , especially when the indications from  $|\epsilon_K| - S_{\psi K_S}$  are taken into account. This is beneficial for  $S_{\psi\phi}$ , since the last measurements agree on a SM-like value, while concerning  $A_{sl}^b$  until now only a measurement from D0 is available, and hence an independent determination from LHCb will be very relevant in the near future.

- Masses for direct observations

The analysis of the parameter space and the constraints derived from flavour

observables in this section permit to obtain more precise estimations of reliable masses of the exotic particles possibly detectable at the LHC. In Fig. 2.10 the masses obtained with values of the parameters for which the majority of flavour constraints are satisfied are highlighted; it results that relatively light masses of the lightest flavour boson  $\hat{A}_{24}$  are preferred, while both for low and for high masses of the lightest exotic quark  $t'$  the predictions in the flavour sector can be satisfactory.

- **Comparison with MFV**

Despite the numerous similarities in the principles and in the realization, the GFS model do not satisfy the MFV requirements. This can be seen by noticing that while in MFV in the limit of vanishing Yukawa couplings the full flavour symmetry is restored, in the GFS model there exists a limit in which all Yukawa couplings vanish but flavour-breaking contributions remain finite: when  $M_{u,d} \rightarrow 0$  with all the other parameters, the four-fermion operators, generated by the exchange of the flavour bosons, still break flavour [25].

The deviations from the MFV patterns can be experimentally recognized. Comparing the GFS model with the CMFV frameworks, one observes that in both cases they prefer the exclusive value of  $V_{ub}$ , solving the  $\epsilon_K - S_{\psi K_S}$  tension through the enhancement of  $|\epsilon_K|$ , but worsening the  $\epsilon_K - \Delta M_{d,s}$  agreement. Nevertheless, the distinction can be provided by  $\Delta F = 1$  processes: for example, considering  $\bar{B} \rightarrow X_s \gamma$ , while in the GFS model the NP contributions uniquely enhance the branching ratio, in CMFV this can be also suppressed.

Concerning MFV at large, taking for example the  $2\text{HDM}_{\overline{\text{MFV}}}$ , in the latter NP contributions to  $\epsilon_K$  are tiny and hence the inclusive value of  $|V_{ub}|$  is selected, contrarily to the GFS model.

# Chapter 3

## Theory and phenomenology of 331 models

### 3.1 General theory

#### 3.1.1 Gauge group and fermion representations

We want to build a model with gauge group  $SU(3)_c \times SU(3)_L \times U(1)_X$ . We indicate with  $T^a$  ( $a = 1 \dots 8$ ) the generators of  $SU(3)_L$ , and with  $T^9$  the generator of  $U(1)_X$ , defined as

$$T^a = \frac{1}{2}\lambda^a, \quad T^9 = \frac{1}{\sqrt{6}}I_3, \quad (3.1)$$

where  $\lambda^a$  are the Gell-Mann matrices and  $I_3$  is the  $3 \times 3$  identity matrix, so that the normalization condition

$$\text{Tr}(T^a T^b) = \frac{1}{2}\delta^{ab} \quad (3.2)$$

holds for  $a, b = 1 \dots 9$ .

The electric charge must be a linear combination of the diagonal generators of the  $SU(3)_L \times U(1)_X$  gauge group<sup>1</sup>:

$$\hat{Q} = \hat{T}^3 + \beta \hat{T}^8 + X \hat{I}_3. \quad (3.3)$$

In the specific representations it reads

$$Q = \begin{pmatrix} \frac{1}{2} + \frac{\beta}{2\sqrt{3}} + X & & \\ & -\frac{1}{2} + \frac{\beta}{2\sqrt{3}} + X & \\ & & -\frac{\beta}{\sqrt{3}} + X \end{pmatrix}; \quad (3.4a)$$

$$\bar{Q} = \begin{pmatrix} -\frac{1}{2} - \frac{\beta}{2\sqrt{3}} + X & & \\ & \frac{1}{2} - \frac{\beta}{2\sqrt{3}} + X & \\ & & \frac{\beta}{\sqrt{3}} + X \end{pmatrix}; \quad (3.4b)$$

---

<sup>1</sup>We will denote a general operator  $\hat{O}$  by a hat, to distinguish them from their representations as operator matrices that we will denote by  $O$  for the  $\mathbf{3}$  representation,  $\bar{O}$  for the  $\bar{\mathbf{3}}$  representation, and by  $O_{(r)}$  for other representations.

$$Q_{\mathbf{6}} = \begin{pmatrix} 1 + \frac{\beta}{\sqrt{3}} + 2X & \frac{\beta}{\sqrt{3}} + 2X & \frac{1}{2} - \frac{\beta}{2\sqrt{3}} + 2X \\ \frac{\beta}{\sqrt{3}} & -1 + \frac{\beta}{\sqrt{3}} & -\frac{1}{2} - \frac{\beta}{2\sqrt{3}} + 2X \\ \frac{1}{2} - \frac{\beta}{2\sqrt{3}} + 2X & -\frac{1}{2} - \frac{\beta}{2\sqrt{3}} + 2X & -\frac{2\beta}{\sqrt{3}} + 2X \end{pmatrix}; \quad (3.4c)$$

$$Q_{\mathbf{8}} = \begin{pmatrix} 0 & 1 & \frac{1}{2} + \frac{\sqrt{3}\beta}{2} \\ -1 & 0 & -\frac{1}{2} + \frac{\sqrt{3}\beta}{2} \\ -\left(\frac{1}{2} + \frac{\sqrt{3}\beta}{2}\right) & -\left(-\frac{1}{2} + \frac{\sqrt{3}\beta}{2}\right) & 0 \end{pmatrix}; \quad (3.4d)$$

where we have used the properties  $\hat{T}_a \Phi = \Phi T_a + T_a^T \Phi$  for the symmetric sextet, and  $\bar{T}^a = -(T^a)^T$  and  $T_a^a T^b = [T^a, T^b]$  for the adjoint octet.

The gauge invariance is obtained by building a covariant derivative introducing the gauge bosons  $W_\mu^a$  ( $a = 1 \dots 8$ ) and  $X_\mu$ , and the coupling constants  $g$  and  $g_X$ :

$$D_\mu = \partial_\mu - ig \hat{T}^a W_\mu^a - ig_X \hat{T}^9 X_\mu, \quad (3.5)$$

where the representation of the generators depends on the representation of the objects on which the derivative is applied. The gauge bosons associated to  $SU(3)_L$  transform according to the adjoint representation  $(\mathbf{8}, 0)$  and can be rewritten as

$$W_\mu = W_\mu^a T^a = \frac{1}{2} \begin{pmatrix} W_\mu^3 + \frac{1}{\sqrt{3}} W_\mu^8 & \sqrt{2} W_\mu^+ & \sqrt{2} Y_\mu^{Q_Y} \\ \sqrt{2} W_\mu^- & -W_\mu^3 + \frac{1}{\sqrt{3}} W_\mu^8 & \sqrt{2} V_\mu^{Q_V} \\ \sqrt{2} Y_\mu^{-Q_Y} & \sqrt{2} V_\mu^{-Q_V} & -\frac{2}{\sqrt{3}} W_\mu^8 \end{pmatrix}, \quad (3.6)$$

from which one can recognize one singly-charged boson

$$W_\mu^\pm = \frac{1}{\sqrt{2}} (W_\mu^1 \mp i W_\mu^2), \quad (3.7a)$$

two generically-charged bosons

$$Y_\mu^{\pm Q_Y} = \frac{1}{\sqrt{2}} (W_\mu^4 \mp i W_\mu^5) \quad \text{with} \quad Q_Y = \frac{1}{2} + \frac{\sqrt{3}\beta}{2}, \quad (3.7b)$$

$$V_\mu^{\pm Q_V} = \frac{1}{\sqrt{2}} (W_\mu^6 \mp i W_\mu^7) \quad \text{with} \quad Q_V = -\frac{1}{2} + \frac{\sqrt{3}\beta}{2}, \quad (3.7c)$$

and three neutral states that are linearly-independent combinations of  $W_\mu^3$  and  $W_\mu^8$ .

The lowest possible fermion representations under this gauge group  $SU(3)_L$  are the singlet  $\psi_{(\mathbf{1})}$ , the triplet  $\psi_{(\mathbf{3})}$ , and the antitriplet  $\psi_{(\bar{\mathbf{3}})}$ , that are of quark or of leptonic type depending on if they are respectively triplets or singlets under  $SU(3)_c$ :

$$\psi_{(\mathbf{1})} = \begin{cases} q_{(\mathbf{1})} : (\mathbf{3}, \mathbf{1}, X) \\ \ell_{(\mathbf{1})} : (\mathbf{1}, \mathbf{1}, X) \end{cases}, \quad (3.8a)$$

$$\psi_{(\mathbf{3})} = \begin{cases} q_{(\mathbf{3})} : (\mathbf{3}, \mathbf{3}, X) \rightarrow (\mathbf{3}, \mathbf{2}, Y) \oplus (\mathbf{3}, \mathbf{1}, Y) \\ \ell_{(\mathbf{3})} : (\mathbf{1}, \mathbf{3}, X) \rightarrow (\mathbf{1}, \mathbf{2}, Y) \oplus (\mathbf{1}, \mathbf{1}, Y) \end{cases}, \quad (3.8b)$$

$\psi_L$	$Q_{\psi_L}$	$X_{\psi_L}$	$\psi_R$	$Q_{\psi_R} = X_{\psi_R}$
$q_L^{(m)} = \begin{pmatrix} U^{(m)} \\ D^{(m)} \\ J^{(m)} \end{pmatrix}_L$	$\begin{pmatrix} \frac{2}{3} \\ -\frac{1}{3} \\ \frac{1}{6} - \frac{\sqrt{3}\beta}{2} \end{pmatrix}$	$\frac{1}{6} - \frac{\beta}{2\sqrt{3}}$	$\begin{pmatrix} U_R^{(m)} \\ D_R^{(m)} \\ J_R^{(m)} \end{pmatrix}$	$\begin{pmatrix} \frac{2}{3} \\ -\frac{1}{3} \\ \frac{1}{6} - \frac{\sqrt{3}\beta}{2} \end{pmatrix}$
$q_L^{(m^*)} = \begin{pmatrix} D^{(m^*)} \\ -U^{(m^*)} \\ J^{(m^*)} \end{pmatrix}_L$	$\begin{pmatrix} -\frac{1}{3} \\ \frac{2}{3} \\ \frac{1}{6} + \frac{\sqrt{3}\beta}{2} \end{pmatrix}$	$-\frac{1}{6} - \frac{\beta}{2\sqrt{3}}$	$\begin{pmatrix} D_R^{(m^*)} \\ U_R^{(m^*)} \\ J_R^{(m^*)} \end{pmatrix}$	$\begin{pmatrix} -\frac{1}{3} \\ \frac{2}{3} \\ \frac{1}{6} + \frac{\sqrt{3}\beta}{2} \end{pmatrix}$
$\ell_L^{(n)} = \begin{pmatrix} \nu^{(n)} \\ e^{(n)} \\ E^{(n)} \end{pmatrix}_L$	$\begin{pmatrix} 0 \\ -1 \\ -\frac{1}{2} - \frac{\sqrt{3}\beta}{2} \end{pmatrix}$	$-\frac{1}{2} - \frac{\beta}{2\sqrt{3}}$	$\begin{pmatrix} \nu_R^{(n)} \\ e_R^{(n)} \\ E_R^{(n)} \end{pmatrix}$	$\begin{pmatrix} 0 \\ -1 \\ -\frac{1}{2} - \frac{\sqrt{3}\beta}{2} \end{pmatrix}$
$\ell_L^{(n^*)} = \begin{pmatrix} e^{(n^*)} \\ -\nu^{(n^*)} \\ E^{(n^*)} \end{pmatrix}_L$	$\begin{pmatrix} -1 \\ 0 \\ -\frac{1}{2} + \frac{\sqrt{3}\beta}{2} \end{pmatrix}$	$\frac{1}{2} - \frac{\beta}{2\sqrt{3}}$	$\begin{pmatrix} e_R^{(n^*)} \\ \nu_R^{(n^*)} \\ E_R^{(n^*)} \end{pmatrix}$	$\begin{pmatrix} -1 \\ 0 \\ -\frac{1}{2} + \frac{\sqrt{3}\beta}{2} \end{pmatrix}$

Table 3.1: Generic fermionic content of 331 models, requiring only one lepton and one quark  $SU(3)_L$  multiplet for each generation, and no more than one right-handed singlet for each left-handed field.  $U$  and  $D$  are generic up-type and down-type quarks respectively, as well as  $e$  and  $\nu$  are a generic lepton and neutrino;  $m$  and  $n$  label the quark and lepton left-handed triplets, respectively, while  $m^*$  and  $n^*$  label the antitriplets.

$$\psi_{(\bar{\mathbf{3}})} = \begin{cases} q_{(\bar{\mathbf{3}})} : (\mathbf{3}, \bar{\mathbf{3}}, X) \rightarrow (\mathbf{3}, \mathbf{2}, Y) \oplus (\mathbf{3}, \mathbf{1}, Y) \\ \ell_{(\bar{\mathbf{3}})} : (\mathbf{1}, \bar{\mathbf{3}}, X) \rightarrow (\mathbf{1}, \mathbf{2}, Y) \oplus (\mathbf{1}, \mathbf{1}, Y) \end{cases} ; \quad (3.8c)$$

due to the branching rules  $SU(2) \subset SU(3)$ , after the breaking of  $SU(3)_L$  both the triplet and the antitriplet embed a doublet and a singlet of  $SU(2)_L$ .

Trying to embed the SM fermions in the 331 multiplets, in general one could introduce sets of multiplets with different quantum numbers, meaning that one represents each generation as a set of triplets with particles of the SM plus exotic particles. However, this would at the same time enlarge the exotic spectrum and hugely increase the number of free parameters; hence, we decide as a minimal assumption to associate only one lepton and one quark multiplet for each generation, and at most one right-handed singlet associated with each left-handed fermion. Based on this criterium, the possible fermion multiplets are the ones listed in Tab. 3.1 [143].

From Eq. (3.8b)–(3.8c) it is evident that the SM left-handed doublets can be embedded in  $SU(3)_L$  triplets or antitriplets. Reproducing their correct electric charge fixes the values of the multiplet hypercharge and consequently the ( $\beta$ -dependent) charge of the third exotic component.

### 3.1.2 Spontaneous symmetry breaking

#### Higgs content

Given its great experimental success, a feature of the majority of NP models is to reduce to the SM at low energies. In the case of 331 models, this can be obtained with a first spontaneous symmetry breaking at high energies, followed by the usual electroweak symmetry breaking:

$$\mathrm{SU}(3)_L \times \mathrm{U}(1)_X \rightarrow \mathrm{SU}(2)_L \times \mathrm{U}(1)_Y \rightarrow \mathrm{U}(1)_Q . \quad (3.9)$$

In order to build a reliable Higgs sector, the following conditions must be respected [144].

1. For the first symmetry breaking, there must exist one or more Higgs fields  $\Phi_1$  getting vevs that break the generators in the following way:

$$\left[ \hat{T}^4, \hat{T}^5, \hat{T}^6, \hat{T}^7, \left( \beta \hat{T}^8 - X \hat{I} \right) \right] \langle \Phi_1 \rangle \neq 0 \quad (3.10a)$$

$$\left[ \hat{T}^1, \hat{T}^2, \hat{T}^3, \left( \beta \hat{T}^8 + X \hat{I} \right) \equiv \hat{Y}/2 \right] \langle \Phi_2 \rangle = 0 , \quad (3.10b)$$

where  $\hat{Y}$  is the SM weak hypercharge.

2. Analogously, for the second symmetry breaking, one or more Higgs fields  $\Phi_2$  must get a vev according to

$$\left[ \hat{T}^1, \hat{T}^2, \hat{T}^3 - \hat{Y}/2 \right] \langle \Phi_2 \rangle \neq 0 \quad (3.11a)$$

$$\left[ \hat{T}^3 + \hat{Y}/2 \equiv \hat{Q} \right] \langle \Phi_2 \rangle = 0 . \quad (3.11b)$$

3. The Higgs content must be able to generate appropriate fermion masses through the Yukawa couplings. The Yukawa terms must be invariant, that is singlets, under the gauge group, and this restricts the possible representations of the Higgs fields. If  $\psi_L \sim (\mathbf{3}, X_L)$  and  $\psi_R \sim (\mathbf{1}, X_R)$ , then the following Yukawa terms are possible

$$\overline{\psi}_L^i \psi_R \Phi \Rightarrow \Phi \sim \mathbf{3}_{X_L - X_R} , \quad (3.12a)$$

$$\overline{\psi}_L^i (\psi_L^j)^c \Phi \Rightarrow \Phi \sim \bar{\mathbf{3}}_{2X_L} \oplus \mathbf{6}_{2X_L} , \quad (3.12b)$$

$$\overline{\psi}_R (\psi_R)^c \Rightarrow \Phi \sim \mathbf{1}_{2X_R} , \quad (3.12c)$$

$$\overline{(\psi_R)^c} (\psi_L^i)^c \Phi \Rightarrow \Phi \sim \mathbf{3}_{X_L - X_R} , \quad (3.12d)$$

and their hermitian conjugates, that provide the couplings for fermion antitriplets; in this way there is no difference between a charge conjugated scalar triplet and a scalar antitriplet, and we can omit the latter without loss of generality. Of course these patterns can be realized also by higher Higgs representations, but those multiplets do not give rise to new features.

4. For each step of the spontaneous symmetry breaking, the total number of Higgs components involved must be sufficient to give mass to the relative gauge bosons. As a consequence, the singlet representation is disfavored.

With the guide of the previous conditions, we analyze systematically the possible content of the Higgs sector.

• **First symmetry breaking**

It can be accomplished by a triplet or a sextet with the following quantum numbers and vevs in order to satisfy the Eq. (3.10a)-(3.10b):

$$\chi \sim (\mathbf{3}, \frac{\beta}{\sqrt{3}}) \quad \text{with} \quad \langle \chi \rangle = \frac{1}{\sqrt{2}} \begin{pmatrix} 0 \\ 0 \\ u \end{pmatrix}, \quad (3.13a)$$

$$S_0 \sim (\mathbf{6}, \frac{\beta}{\sqrt{3}}) \quad \text{with} \quad \langle S_0 \rangle = \frac{1}{\sqrt{2}} \begin{pmatrix} 0 & 0 & 0 \\ 0 & 0 & 0 \\ 0 & 0 & u \end{pmatrix}. \quad (3.13b)$$

However, following Eq. (3.12b), this Higgs sextet can generate Yukawa masses only if  $2X_L = X_\Phi \equiv \beta/\sqrt{3}$ , and, as evident from Tab. 3.1, this can be satisfied neither for quarks nor for leptons for any value of  $\beta$ . On the other hand, from Eq. (3.12a)-(3.12d) one has that for the triplet  $X_L - X_R = X_\Phi \equiv \beta/\sqrt{3}$ , which can be obtained from the third component of both quarks and leptons for each value of  $\beta$ , and from the other components for particular values of  $\beta$ .

• **Second symmetry breaking**

The possible fields are

$$\rho \sim (\mathbf{3}, \frac{1}{2} - \frac{\beta}{2\sqrt{3}}) \quad \text{with} \quad \langle \rho \rangle = \frac{1}{\sqrt{2}} \begin{pmatrix} 0 \\ v_1 \\ 0 \end{pmatrix}, \quad (3.14a)$$

$$\eta \sim (\mathbf{3}, -\frac{1}{2} - \frac{\beta}{2\sqrt{3}}) \quad \text{with} \quad \langle \eta \rangle = \frac{1}{\sqrt{2}} \begin{pmatrix} v_2 \\ 0 \\ 0 \end{pmatrix}, \quad (3.14b)$$

$$S_1 \sim (\mathbf{6}, -\frac{1}{4} + \frac{\beta}{4\sqrt{3}}) \quad \text{with} \quad \langle S_1 \rangle = \frac{1}{2} \begin{pmatrix} 0 & 0 & w_1 \\ 0 & 0 & 0 \\ w_1 & 0 & 0 \end{pmatrix}, \quad (3.14c)$$

$$S_2 \sim (\mathbf{6}, -\frac{1}{2} + \frac{\beta}{2\sqrt{3}}) \quad \text{with} \quad \langle S_1 \rangle = \frac{1}{2} \begin{pmatrix} w_2 & 0 & 0 \\ 0 & 0 & 0 \\ 0 & 0 & 0 \end{pmatrix}, \quad (3.14d)$$

$$S_3 \sim (\mathbf{6}, \frac{1}{2} - \frac{\beta}{2\sqrt{3}}) \quad \text{with} \quad \langle S_3 \rangle = \frac{1}{2} \begin{pmatrix} 0 & 0 & 0 \\ 0 & w_3 & 0 \\ 0 & 0 & 0 \end{pmatrix}, \quad (3.14e)$$

$$S_4 \sim (\mathbf{6}, \frac{1}{4} + \frac{\beta}{4\sqrt{3}}) \quad \text{with} \quad \langle S_4 \rangle = \frac{1}{2} \begin{pmatrix} 0 & 0 & 0 \\ 0 & 0 & w_4 \\ 0 & w_4 & 0 \end{pmatrix}; \quad (3.14f)$$

		$\beta = 1/\sqrt{3}$				
$\langle \Phi \rangle$	$\begin{pmatrix} 0 \\ v_2 \\ v_3 \end{pmatrix}$	$\begin{pmatrix} v_1 \\ 0 \\ 0 \end{pmatrix}$	$\begin{pmatrix} 0 & w_2 & w_3 \\ w_2 & 0 & 0 \\ w_3 & 0 & 0 \end{pmatrix}$	$\begin{pmatrix} 0 & 0 & 0 \\ 0 & w_4 & w_5 \\ 0 & w_5 & w_4 \end{pmatrix}$	$\begin{pmatrix} w_1 & 0 & 0 \\ 0 & 0 & 0 \\ 0 & 0 & 0 \end{pmatrix}$	
$X_\Phi$	$\frac{1}{3}$	$-\frac{2}{3}$	$-\frac{1}{6}$	$\frac{1}{3}$	$-\frac{2}{3}$	
		$\beta = -1/\sqrt{3}$				
$\langle \Phi \rangle$	$\begin{pmatrix} 0 \\ v_2 \\ 0 \end{pmatrix}$	$\begin{pmatrix} v_1 \\ 0 \\ v_3 \end{pmatrix}$	$\begin{pmatrix} w_1 & 0 & w_3 \\ 0 & 0 & 0 \\ w_3 & 0 & w_6 \end{pmatrix}$	$\begin{pmatrix} 0 & w_2 & 0 \\ w_2 & 0 & w_5 \\ 0 & w_5 & 0 \end{pmatrix}$	$\begin{pmatrix} 0 & 0 & 0 \\ 0 & w_4 & 0 \\ 0 & 0 & 0 \end{pmatrix}$	
$X_\Phi$	$\frac{2}{3}$	$-\frac{1}{3}$	$-\frac{1}{3}$	$\frac{1}{6}$	$\frac{2}{3}$	
		$\beta = \sqrt{3}$				
$\langle \Phi \rangle$	$\begin{pmatrix} 0 & 0 & w_3 \\ 0 & w_4 & 0 \\ w_3 & 0 & 0 \end{pmatrix}$	$\begin{pmatrix} w_1 & 0 & 0 \\ 0 & 0 & 0 \\ 0 & 0 & 0 \end{pmatrix}$	$\begin{pmatrix} 0 & 0 & 0 \\ 0 & 0 & w_5 \\ 0 & 0 & w_5 \end{pmatrix}$			
$X_\Phi$	0	-1	$\frac{1}{2}$			
		$\beta = -\sqrt{3}$				
$\langle \Phi \rangle$	$\begin{pmatrix} w_1 & 0 & 0 \\ 0 & 0 & w_5 \\ 0 & w_5 & 0 \end{pmatrix}$	$\begin{pmatrix} 0 & 0 & w_3 \\ 0 & 0 & 0 \\ w_3 & 0 & 0 \end{pmatrix}$	$\begin{pmatrix} 0 & 0 & 0 \\ 0 & w_4 & 0 \\ 0 & 0 & 0 \end{pmatrix}$			
$X_\Phi$	0	$-\frac{1}{2}$	1			

Table 3.2: Further Higgs fields valid only for specific values of  $\beta$ .

they are valid for each value of  $\beta$ , while for specific values of  $\beta$  other vacuum alignments are possible, as shown in Tab. 3.2. In general, both these triplets are necessary to give masses to all quarks; however, in some particular cases also a sextet is needed to give masses to the leptons [145, 146], while if a mechanism of dynamical symmetry breaking is implemented a more economical Higgs content can be sufficient [147–155].

The variegate possibilities for the Higgs sector of 331 models have been extensively analyzed [156–164]. According to what we have discussed, in order to perform an analysis as general as possible, in what follows we are going to consider the following Higgs content:

$$\chi = \begin{pmatrix} \chi^{Q_Y} \\ \chi^{Q_V} \\ \chi^0 \end{pmatrix} \sim \left( \mathbf{3}, \frac{\beta}{\sqrt{3}} \right) \quad \text{with} \quad \langle \chi \rangle = \frac{1}{\sqrt{2}} \begin{pmatrix} 0 \\ 0 \\ v_\chi \end{pmatrix}, \quad (3.15a)$$

$$\rho = \begin{pmatrix} \rho^+ \\ \rho^0 \\ \rho^{-Q_V} \end{pmatrix} \sim \left( \mathbf{3}, \frac{1}{2} - \frac{\beta}{2\sqrt{3}} \right) \quad \text{with} \quad \langle \rho \rangle = \frac{1}{\sqrt{2}} \begin{pmatrix} 0 \\ v_\rho \\ 0 \end{pmatrix}, \quad (3.15b)$$

$$\eta = \begin{pmatrix} \eta^0 \\ \eta^- \\ \eta^{-Q_Y} \end{pmatrix} \sim (\mathbf{3}, -\frac{1}{2} - \frac{\beta}{2\sqrt{3}}) \quad \text{with} \quad \langle \eta \rangle = \frac{1}{\sqrt{2}} \begin{pmatrix} v_\eta \\ 0 \\ 0 \end{pmatrix}, \quad (3.15c)$$

$$S = \begin{pmatrix} S^{Q_Y} & S^{Q_V} & S^0 \\ S^{Q_V} & S^{Q_C} & S^- \\ S^0 & S^- & S^{-Q_Y} \end{pmatrix} \sim (\mathbf{6}, \frac{1}{4} + \frac{\beta}{4\sqrt{3}}) \quad \text{with} \quad \langle S \rangle = \frac{1}{2} \begin{pmatrix} 0 & 0 & 0 \\ 0 & 0 & v_S \\ 0 & v_S & 0 \end{pmatrix}, \quad (3.15d)$$

where  $Q_Y, Q_V$  are the charges defined in Eq. (3.7b)-(3.7c), while

$$Q_C = -\frac{3}{2} + \frac{\sqrt{3}\beta}{2}, \quad (3.16)$$

and the vevs are at different energy scales  $v_\chi \gg v_\rho, v_\eta, v_S$ .

### Gauge bosons masses

With the first spontaneous symmetry breaking, the Higgs field  $\chi$  gets a vev, and from its covariant kinetic Lagrangian  $(D_\mu \chi)^\dagger (D^\mu \chi)$  some mass terms arise:

$$m_{W^\pm}^2 = 0, \quad m_{V^\pm Q_V}^2 = g^2 \frac{v_\chi^2}{4}, \quad m_{Y^\pm Q_Y}^2 = g^2 \frac{v_\chi^2}{4}, \quad (3.17a)$$

$$m_{W^3}^2 = 0, \quad m_B^2 = 0, \quad m_{Z'}^2 = g^2 \frac{v_\chi^2}{3} \left( 1 + \frac{\beta^2 g_X^2}{6 g^2} \right); \quad (3.17b)$$

the bosons  $W^\pm$  and  $W^3$  remain massless by construction of the symmetry breaking pattern;  $B$  and  $Z'$  are neutral mass eigenstates obtained from the mixing

$$\begin{pmatrix} B_\mu \\ Z'_\mu \end{pmatrix} = \begin{pmatrix} \cos \theta_{331} & \sin \theta_{331} \\ -\sin \theta_{331} & \cos \theta_{331} \end{pmatrix} \begin{pmatrix} W_\mu^8 \\ X_\mu \end{pmatrix} \quad \text{with} \quad \sin^2 \theta_{331} = \frac{1}{1 + \frac{\beta^2 g_X^2}{6 g^2}}. \quad (3.18)$$

The covariant derivative can be rewritten as

$$D_\mu = \partial_\mu - igW_\mu^\pm \hat{T}_W^\pm - igW_\mu^3 \hat{T}^3 - i\frac{g_Y}{2} B_\mu \hat{Y} \\ - igV_\mu^{\pm Q_V} \hat{T}_V^\pm - igY_\mu^{\pm Q_Y} \hat{T}_Y^\pm - ig_Y Z'_\mu \left( -X \frac{\beta}{\sqrt{6}} \frac{g_X}{g} \hat{I} + \frac{\sqrt{6}g}{g_X} \hat{T}^8 \right), \quad (3.19)$$

where

$$\frac{1}{g_Y^2} = \frac{6}{g_X^2} + \frac{\beta^2}{g^2}, \quad \hat{Y} = \hat{T}^8 + X \hat{I}_3; \quad (3.20)$$

the first row presents the usual SM terms before the electroweak symmetry breaking, while the second row contains the new fields.

When with the second step of spontaneous symmetry breaking also the Higgs fields  $\rho$ ,  $\eta$  and  $S$  get a vev, the masses of the charged gauge bosons become

$$m_{W^\pm}^2 = g^2 \frac{v_+^2}{4}, \quad (3.21a)$$

$$m_{V^\pm Q_V}^2 = g^2 \frac{v_\chi^2}{4} \left( 1 + \frac{v_+^2}{2v_\chi^2} - \frac{v_-^2}{2v_\chi^2} + \frac{4v_S^2}{v_\chi^2} \right), \quad (3.21b)$$

$$m_{Y^\pm Q_Y}^2 = g^2 \frac{v_\chi^2}{4} \left( 1 + \frac{v_+^2}{2v_\chi^2} + \frac{v_-^2}{2v_\chi^2} \right), \quad (3.21c)$$

where  $v_\pm^2 = \pm v_\rho^2 + v_\eta^2 + v_S^2$ . It is evident that, while the charged boson  $W^\pm$  has a mass of the order of the electroweak symmetry breaking scale, and hence should be identified with the SM charged gauge boson, the new bosons are significantly heavier [165].

As regards the neutral bosons, the mass terms read

$$\begin{aligned} & \begin{pmatrix} B^\mu \\ W_\mu^3 \\ Z'_\mu \end{pmatrix}^T \left[ \begin{pmatrix} \frac{v_+^2}{4} g_Y^2 & -\frac{v_+^2}{4} g g_Y & 0 \\ -\frac{v_+^2}{4} g g_Y & \frac{v_+^2}{4} g^2 & 0 \\ 0 & 0 & \frac{g^4}{3(g^2 - g_Y^2 \beta^2)} \left( v_\chi^2 + \frac{v_+^2}{4} \left( 1 + \frac{3g_Y^4 \beta^2}{g^4} \right) + \frac{v_-^2}{4} \frac{\sqrt{3} g_Y^2 \beta}{g^2} \right) \end{pmatrix} \right. \\ & \left. + \frac{g^2}{4\sqrt{3}\sqrt{g^2 - g_Y^2 \beta^2}} \left( v_-^2 + v_+^2 \frac{\sqrt{3} g_Y^2 \beta}{g^2} \right) \begin{pmatrix} 0 & 0 & g_Y \\ 0 & 0 & -g \\ g_Y & -g & 0 \end{pmatrix} \right] \begin{pmatrix} B^\mu \\ W_\mu^3 \\ Z'_\mu \end{pmatrix}; \quad (3.22) \end{aligned}$$

it is evident that the mixing with the  $Z'_\mu$  is small, and with a rotation of

$$\sin \theta_W = \frac{g_Y}{\sqrt{g^2 + g_Y^2}} \quad (3.23)$$

one can recognize the SM neutral bosons  $A_\mu$  and  $Z_\mu$ :

$$\begin{pmatrix} A_\mu \\ Z_\mu \\ Z'_\mu \end{pmatrix} = \begin{pmatrix} \cos \theta_W & \sin \theta_W & 0 \\ -\sin \theta_W & \cos \theta_W & 0 \\ 0 & 0 & 1 \end{pmatrix} \begin{pmatrix} B^\mu \\ W_\mu^3 \\ Z'_\mu \end{pmatrix}; \quad (3.24)$$

the mass eigenstates are obtained with a further rotation of

$$\sin \delta_{Z-Z'} = \frac{\sqrt{3}\sqrt{g^2 + g_Y^2}\sqrt{g^2 - g_Y^2\beta^2}}{4g^2} \left( \frac{\sqrt{3}g_Y^2\beta}{g^2} \frac{v_+^2}{v_\chi^2} + \frac{v_-^2}{v_\chi^2} \right), \quad (3.25)$$

that gives

$$\begin{pmatrix} A_\mu \\ Z_\mu^1 \\ Z_\mu^2 \end{pmatrix} = \begin{pmatrix} 1 & 0 & 0 \\ 0 & \cos \delta_{Z-Z'} & \sin \delta_{Z-Z'} \\ 0 & -\sin \delta_{Z-Z'} & \cos \delta_{Z-Z'} \end{pmatrix} \begin{pmatrix} A_\mu \\ Z_\mu \\ Z'_\mu \end{pmatrix}. \quad (3.26)$$

The phenomenological effects of the  $Z - Z'$  mixing are not relevant, being  $\delta_{Z-Z'} \lesssim \mathcal{O}(10^{-3})$  [166–169], and hence one can approximate  $Z_\mu \approx Z_\mu^1$ ,  $Z'_\mu \approx Z_\mu^2$ , obtaining

the following masses:

$$m_A^2 = 0 , \quad (3.27a)$$

$$m_Z^2 = \frac{v_+^2}{4} \frac{g^2}{\cos^2 \theta_W} , \quad (3.27b)$$

$$m_{Z'}^2 = v_\chi^2 \frac{g^2 \cos^2 \theta_W}{3(1 - \sin^2 \theta_W(1 + \beta^2))} \left[ 1 + \frac{v_+^2}{4v_\chi^2} \left( 1 + \frac{3\beta^2 \sin^4 \theta_W}{\cos^4 \theta_W} \right) + \frac{v_-^2}{4v_\chi^2} \frac{\sqrt{3}\beta \sin^2 \theta_W}{\cos^2 \theta_W} \right] ; \quad (3.27c)$$

the massless boson is identified with the photon, and comparing Eq. (3.21a) and Eq. (3.27b) one observes that

$$\frac{m_W^2}{m_Z^2} = \cos^2 \theta_W , \quad (3.28)$$

and hence  $\theta_W$  is just the SM Weinberg angle; moreover, the mass of the new boson  $Z'$  is at the scale  $v_\chi$ , much larger than the SM masses. It is clear that both  $g_Y$  and

$$\cos \theta_{331} = \beta \tan \theta_W \quad (3.29)$$

are not fundamental parameters, and the neutral mass eigenstates can be written as a function of the original neutral bosons as

$$A_\mu = \sin \theta_W W_\mu^3 + \cos \theta_W \left( \beta \tan \theta_W W_\mu^8 + \sqrt{1 - \beta^2 \tan^2 \theta_W} X_\mu \right) , \quad (3.30a)$$

$$Z_\mu = \cos \theta_W W_\mu^3 - \sin \theta_W \left( \beta \tan \theta_W W_\mu^8 + \sqrt{1 - \beta^2 \tan^2 \theta_W} X_\mu \right) , \quad (3.30b)$$

$$Z'_\mu = -\sqrt{1 - \beta^2 \tan^2 \theta_W} W_\mu^8 + \beta \tan \theta_W X_\mu . \quad (3.30c)$$

Finally, it is very interesting to note the relation between  $g_X$  and  $g$

$$\frac{g_X^2}{g^2} = \frac{6 \sin^2 \theta_W}{1 - (\beta^2 + 1) \sin^2 \theta_W} , \quad (3.31)$$

that, even if obtained at tree level, remains valid at higher orders. It shows that the theory can present a Landau pole at  $\sin^2 \theta_W = 1/(\beta^2 + 1)$ . This is particularly relevant for example in the minimal model, in which  $\beta = \sqrt{3}$ : since  $\sin^2 \theta_W(m_Z) = 0.233$ , the constraint  $\sin^2 \theta_W(m_Z) < 1/4$  would restrict the 331 breaking scale to be of about a few TeV [170–174].

More phenomenological studies on the 331 gauge bosons can be found in [175–183].

### Yukawa interactions

The requirement of being able to obtain  $SU(3)_L \times U(1)_Y$ -invariant Yukawa terms has been used for the construction of the Higgs sector; now, from the comparison of

Tab. 3.1 with Eq. (3.12a)-(3.12d) and Eq. (3.15a)-(3.15d), one obtains directly the most generic Yukawa Lagrangian; in the quark sector this is

$$\begin{aligned} \mathcal{L}_Y^q &= \lambda_{m,m'}^J \bar{Q}^{(m)} \chi J_R^{(m')} + \lambda_{m^*,m'^*}^J \bar{Q}^{(m'^*)} \chi^* J^{(m'^*)} \\ &+ \lambda_{m,i}^D \bar{Q}^{(m)} \rho D_R^{(i)} + \lambda_{m^*,i}^U \bar{Q}^{(m^*)} \rho^* U_R^{(i)} \\ &+ \lambda_{m,i}^U \bar{Q}^{(m)} \eta U_R^{(i)} + \lambda_{m^*,i}^D \bar{Q}^{(m^*)} \eta^* D_R^{(i)} + \text{h.c.} , \end{aligned} \quad (3.32)$$

where the indices  $m, m'$  run over the quark triplets,  $m^*, m'^*$  over the quark antitriplets, and  $i$  over all the quark generations. We observe that the  $\chi$  Higgs boson can only give mass to the third elements of the (anti)triplets  $J^{(m^*)}$ , and hence these exotic quarks get a mass proportional to the high scale  $u$ ; on the contrary, the  $U$ - and  $D$ -type quarks get a mass at the lower scales. As usual, the mass eigenstates can be obtained by diagonalizing the Yukawa couplings for each type of quark with unitary matrices:

$$\begin{pmatrix} U_L^{(1)} \\ \vdots \\ U_L^{(M)} \end{pmatrix} = (V_L^U)^{-1} \begin{pmatrix} U_L^{(1)} \\ \vdots \\ U_L^{(M)} \end{pmatrix} , \quad \begin{pmatrix} D_L^{(1)} \\ \vdots \\ D_L^{(M)} \end{pmatrix} = (V_L^D)^{-1} \begin{pmatrix} D_L^{(1)} \\ \vdots \\ D_L^{(M)} \end{pmatrix} , \quad (3.33a)$$

$$\begin{pmatrix} J_L^{(1)} \\ \vdots \\ J_L^{(k)} \end{pmatrix} = (V_L^J)^{-1} \begin{pmatrix} J_L^{(1)} \\ \vdots \\ J_L^{(k)} \end{pmatrix} , \quad \begin{pmatrix} J_L^{(k+1)} \\ \vdots \\ J_L^{(M)} \end{pmatrix} = (V_L^{J^*})^{-1} \begin{pmatrix} J_L^{(k+1)*} \\ \vdots \\ J_L^{(M)*} \end{pmatrix} ; \quad (3.33b)$$

however, since triplets and antitriplets couple differently with the  $Z'$ , the unitary matrices can appear explicitly in these neutral currents and hence one could not be able to absorb all of them in CKM-like matrices as in the SM [184, 185].

As regards the lepton sector, the form of the Yukawa Lagrangian depends on the presence of right-handed leptons. If right-handed leptons are available to build Yukawa terms, the lepton Yukawa Lagrangian is analogue to the quark one; if the model does not contain them one has to conveniently combine the left-handed multiplets. For example, in the minimal 331 model the most general lepton Yukawa Lagrangian reads

$$\mathcal{L}_Y^\ell = \lambda_{n,n'}^{\ell,\rho} \epsilon^{ijk} \bar{\ell}_i^{(n)} (\ell_j^{(n')})^c \rho_k + \lambda_{n,n'}^{\ell,S} \bar{\ell}^{(n)} S^\dagger (\ell^{(n')})^c + \text{h.c.} , \quad (3.34)$$

where the introduction of the Higgs sextet  $S$  is necessary to give (Majorana) masses to the neutrinos.

### Higgs potential

The most general gauge-invariant renormalizable potential for the Higgs content that we are considering reads

$$\begin{aligned}
V = & \mu_1^2 \chi^\dagger \chi + \mu_2^2 \rho^\dagger \rho + \mu_3^2 \eta^\dagger \eta \\
& + \lambda_1 (\chi^\dagger \chi)^2 + \lambda_2 (\rho^\dagger \rho)^2 + \lambda_3 (\eta^\dagger \eta)^2 \\
& + \lambda_4 (\chi^\dagger \chi) (\rho^\dagger \rho) + \lambda_5 (\rho^\dagger \rho) (\eta^\dagger \eta) + \lambda_6 (\eta^\dagger \eta) (\chi^\dagger \chi) \\
& + \lambda_7 (\chi^\dagger \rho) (\rho^\dagger \chi) + \lambda_8 (\rho^\dagger \eta) (\eta^\dagger \rho) + \lambda_9 (\eta^\dagger \chi) (\chi^\dagger \eta) \\
& + f (\epsilon^{ijk} \chi_i \rho_j \eta_k + \text{h.c.}) \\
& + \mu_4^2 S^\dagger S + \lambda_{10} (S^\dagger S) (\chi^\dagger \chi) + \lambda_{11} (S^\dagger S) (\rho^\dagger \rho) + \lambda_{12} (S^\dagger S) (\eta^\dagger \eta) \\
& + \lambda_{13} (\chi^\dagger S) (S^\dagger \chi) + \lambda_{14} (\rho^\dagger S) (S^\dagger \rho) + \lambda_{15} (\eta^\dagger S) (S^\dagger \eta) \\
& + \lambda_{16} (S^\dagger S)^2 + \lambda_{17} (S^\dagger (S (S^\dagger S))) .
\end{aligned} \tag{3.35}$$

For specific values of  $\beta$ , the fact that some Higgs fields happen to have the same hypercharge imply that other terms are allowed; for example, for  $\beta = 1/\sqrt{3}$  there is the further contribution

$$\begin{aligned}
V_{1/\sqrt{3}} = & + \mu_5^2 (\chi^\dagger \rho + \text{h.c.}) + \lambda_{18} (\chi^\dagger \chi) (\chi^\dagger \rho + \text{h.c.}) + \lambda_{19} (\rho^\dagger \rho) (\chi^\dagger \rho + \text{h.c.}) \\
& + \lambda_{20} (\eta^\dagger \eta) (\chi^\dagger \rho + \text{h.c.}) + \lambda_{21} ((\chi^\dagger \rho) (\chi^\dagger \rho) + \text{h.c.}) + \lambda_{22} ((\eta^\dagger \chi) (\rho^\dagger \eta) + \text{h.c.}) \\
& + f_2 (\chi^\dagger S \chi + \text{h.c.}) + \lambda_{23} (\chi_i S^{ij} \eta^k \rho^l \epsilon_{jkl} + \text{h.c.}) \\
& + \lambda_{24} (S^\dagger S) (\rho^\dagger \chi + \text{h.c.}) + \lambda_{25} (\rho^\dagger (S (S^\dagger \rho)) + \text{h.c.}) ;
\end{aligned} \tag{3.36}$$

however, in these cases there are terms containing combinations like  $\chi^\dagger S \chi$  and  $(\eta^\dagger \chi) (\rho^\dagger \eta)$  that violate leptonic number, and discrete symmetries have to be introduced in order to remove them.

For an overall analysis we are going to consider the case of generic  $\beta$ , and to concentrate on the quark sector in which the  $S$  Higgs boson is never required; hence in what follows the Higgs potential will be the one on Eq. (3.35) without the last three lines. We write the Higgs triplets

$$\chi = \begin{pmatrix} \chi^{Q_Y} \\ \chi^{Q_V} \\ v_\chi + \xi_\chi + i\zeta_\chi \end{pmatrix}, \quad \rho = \begin{pmatrix} \rho^+ \\ v_\rho + \xi_\rho + i\zeta_\rho \\ \rho^{-Q_V} \end{pmatrix}, \quad \eta = \begin{pmatrix} v_\eta + \xi_\eta + i\zeta_\eta \\ \eta^- \\ \eta^{-Q_Y} \end{pmatrix}; \tag{3.37}$$

moreover, from the minimization of the potential, one finds that, in order to obtain a suitable spontaneous symmetry breaking, the first coefficients in the potential must take the form:

$$\mu_1^2 = -\lambda_1 v_\chi^2 - \frac{\lambda_4}{2} v_\rho^2 - \frac{\lambda_6}{2} v_\eta^2 + f \frac{v_\rho v_\eta}{v_\chi}, \tag{3.38a}$$

$$\mu_2^2 = -\lambda_2 v_\rho^2 - \frac{\lambda_4}{2} v_\chi^2 - \frac{\lambda_5}{2} v_\eta^2 + f \frac{v_\chi v_\eta}{v_\rho}, \tag{3.38b}$$

$$\mu_3^2 = -\lambda_3 v_\eta^2 - \frac{\lambda_6}{2} v_\chi^2 - \frac{\lambda_5}{2} v_\rho^2 + f \frac{v_\chi v_\rho}{v_\eta}, \tag{3.38c}$$

Besides, since as we will see some of the Higgs bosons deriving from the first symmetry breaking have a squared mass proportional to  $f v_\chi$ , in order to prevent the introduction of a third energy scale one can assume  $|f| \sim |v_\chi|$ . Then, the spectrum of the Higgs fields results to be the following, where we have defined

$$\sin \beta_{ab} = \frac{v_a}{\sqrt{v_a^2 + v_b^2}} . \quad (3.39)$$

- **Charge 1**

$$\begin{pmatrix} \phi_W^\pm \\ H_1^\pm \end{pmatrix} = \begin{pmatrix} -\sin \beta_{\rho\eta} & \cos \beta_{\rho\eta} \\ \cos \beta_{\rho\eta} & \sin \beta_{\rho\eta} \end{pmatrix} \begin{pmatrix} \rho^\pm \\ \eta^\pm \end{pmatrix} ; \quad (3.40)$$

$$m_{\phi_W^\pm}^2 = 0 , \quad (3.41a)$$

$$m_{H_1^\pm}^2 = \frac{(v_\rho^2 + v_\eta^2)(2f v_\chi + \lambda_8 v_\rho v_\eta)}{2v_\rho v_\eta} \simeq \frac{1}{\sin \beta_{\rho\eta} \cos \beta_{\rho\eta}} f v_\chi . \quad (3.41b)$$

We obtain the Goldstone boson that gives mass to the  $W^\pm$ , and a heavy charged physical Higgs.

- **Charge  $Q_Y$**

$$\begin{pmatrix} \phi_Y^{\pm Q_Y} \\ H_2^{\pm Q_Y} \end{pmatrix} = \begin{pmatrix} -\sin \beta_{\chi\eta} & \cos \beta_{\chi\eta} \\ \cos \beta_{\chi\eta} & \sin \beta_{\chi\eta} \end{pmatrix} \begin{pmatrix} \eta^{\pm Q_Y} \\ \chi^{\pm Q_Y} \end{pmatrix} ; \quad (3.42)$$

$$m_{\phi_Y^{\pm Q_Y}}^2 = 0 , \quad (3.43a)$$

$$m_{H_2^{\pm Q_Y}}^2 = \frac{(v_\chi^2 + v_\eta^2)(2f v_\rho + \lambda_9 v_\chi v_\eta)}{2v_\chi v_\eta} \simeq \tan \beta_{\rho\eta} f v_\chi + \frac{\lambda_9}{2} v_\chi^2 . \quad (3.43b)$$

The Goldstone boson gives mass to the new  $Y^{\pm Q_Y}$  gauge bosons, and there is also a heavy physical Higgs.

- **Charge  $Q_V$**

$$\begin{pmatrix} \phi_V^{\pm Q_V} \\ H_3^{\pm Q_V} \end{pmatrix} = \begin{pmatrix} -\sin \beta_{\chi\rho} & \cos \beta_{\chi\rho} \\ \cos \beta_{\chi\rho} & \sin \beta_{\chi\rho} \end{pmatrix} \begin{pmatrix} \rho^{\pm Q_V} \\ \chi^{\pm Q_V} \end{pmatrix} ; \quad (3.44)$$

$$m_{\phi_V^{\pm Q_V}}^2 = 0 , \quad (3.45a)$$

$$m_{H_3^{\pm Q_V}}^2 = \frac{(v_\chi^2 + v_\rho^2)(2f v_\eta + \lambda_7 v_\chi v_\rho)}{2v_\chi v_\rho} \simeq \cot \beta_{\rho\eta} f v_\chi + \frac{\lambda_7}{2} v_\chi^2 . \quad (3.45b)$$

Again, the Goldstone boson gives mass to the new  $V^{\pm Q_V}$  gauge bosons, and there is another heavy physical Higgs.

- **Neutral pseudoscalars**

The mass matrix of the  $\zeta_\chi, \zeta_\rho, \zeta_\eta$  pseudoscalar fields reads

$$M_\zeta^2 = f \begin{pmatrix} \frac{v_\rho v_\eta}{v_\chi} & v_\eta & v_\rho \\ v_\eta & \frac{v_\chi v_\eta}{v_\rho} & v_\chi \\ v_\rho & v_\chi & \frac{v_\chi v_\rho}{v_\eta} \end{pmatrix}; \quad (3.46)$$

it can be diagonalized, obtaining

$$\begin{pmatrix} \phi_Z^0 \\ \phi_{Z'}^0 \\ H_4^0 \end{pmatrix} \simeq \begin{pmatrix} -1 & 0 & \cot \beta_{\chi\eta} \\ -\cot \beta_{\chi\eta} \cos \beta_{\rho\eta} & \sin \beta_{\rho\eta} & -\cos \beta_{\rho\eta} \\ \cot \beta_{\chi\rho} \cos \beta_{\rho\eta} & \cos \beta_{\rho\eta} & \sin \beta_{\rho\eta} \end{pmatrix} \begin{pmatrix} \zeta_\chi \\ \zeta_\rho \\ \zeta_\eta \end{pmatrix}; \quad (3.47)$$

$$m_{\phi_Z^0}^2 = 0, \quad (3.48a)$$

$$m_{\phi_{Z'}^0}^2 = 0, \quad (3.48b)$$

$$m_{H_4^0}^2 = \frac{f(v_\chi^2 v_\rho^2 + v_\chi^2 v_\eta^2 + v_\rho^2 v_\eta^2)}{v_\chi v_\rho v_\eta} \simeq \frac{1}{\sin \beta_{\rho\eta} \cos \beta_{\rho\eta}} f v_\chi; \quad (3.48c)$$

where two Goldstone bosons give mass to the  $Z$  and  $Z'$ , and a heavy neutral pseudoscalar Higgs fields results too.

- **Neutral scalars**

This time the mass matrix is

$$M_\xi^2 = \begin{pmatrix} 2\lambda_1 v_\chi^2 + f \frac{v_\rho v_\eta}{v_\chi} & \lambda_4 v_\chi v_\rho - f v_\eta & \lambda_6 v_\chi v_\eta - f v_\rho \\ \lambda_4 v_\chi v_\rho - f v_\eta & 2\lambda_2 v_\rho^2 + f \frac{v_\chi v_\eta}{v_\rho} & \lambda_5 v_\rho v_\eta - f v_\chi \\ \lambda_6 v_\chi v_\eta - f v_\rho & \lambda_5 v_\rho v_\eta - f v_\chi & 2\lambda_3 v_\eta^2 + f \frac{v_\chi v_\rho}{v_\eta} \end{pmatrix}. \quad (3.49)$$

The diagonalization is more complicated; keeping only the terms of  $\mathcal{O}(v_\chi^2)$  it becomes block-diagonal:

$$M_\xi = \begin{pmatrix} 2\lambda_1 v_\chi^2 & 0 & 0 \\ 0 & f \frac{v_\chi v_\eta}{v_\rho} & -f v_\chi \\ 0 & -f v_\chi & f \frac{v_\chi v_\rho}{v_\eta} \end{pmatrix}, \quad (3.50)$$

and in the second block higher orders have to be included in order not to lose the light masses. One obtains three neutral scalar fields that are all physical:

$$\begin{pmatrix} H_5^0 \\ H_6^0 \\ H_7^0 \end{pmatrix} \simeq \begin{pmatrix} 1 & 0 & 0 \\ 0 & \sin \beta_{\rho\eta} & \cos \beta_{\rho\eta} \\ 0 & -\cos \beta_{\rho\eta} & \sin \beta_{\rho\eta} \end{pmatrix} \begin{pmatrix} \xi_\chi \\ \xi_\rho \\ \xi_\eta \end{pmatrix}; \quad (3.51)$$

$$m_{H_5^0}^2 \simeq 2\lambda_1 v_\chi^2, \quad (3.52a)$$

$$m_{H_6^0}^2 \simeq \frac{2(\lambda_2 v_\rho^4 + \lambda_3 v_\eta^4 + \lambda_5 v_\rho^2 v_\eta^2)}{v_\rho^2 + v_\eta^2}, \quad (3.52b)$$

$$m_{H_7^0}^2 \simeq \frac{1}{\sin \beta_{\rho\eta} \cos \beta_{\rho\eta}} f v_\chi; \quad (3.52c)$$

while  $H_5^0$  and  $H_7^0$  have mass at the high scale  $v_\chi$ ,  $H_6^0$  gets mass at the electroweak scale and can be identified with the SM Higgs boson.

## 3.2 Aspects of the models

### 3.2.1 Number of generations

We perform the analysis of anomalies in 331 models considering a 331 model with a generic fermion content of  $M$  quark generations and  $N$  lepton generations, transforming as

$$q_L^{(m)} \text{ with } m = \underbrace{1 \dots k}_{3k \text{ triplets}} ; \quad q_L^{(m^*)} \text{ with } m^* = \underbrace{k+1 \dots M}_{3(M-k) \text{ antitriplets}} \quad (3.53a)$$

$$\ell_L^{(n)} \text{ with } n = \underbrace{1 \dots j}_{j \text{ triplets}} ; \quad \ell_L^{(n^*)} \text{ with } n^* = \underbrace{j+1 \dots N}_{N-j \text{ antitriplets}} . \quad (3.53b)$$

As described in the Sec. 2.1.1, we have to consider all the possible combinations of three generators, except the ones that contain a single SU(3) factor.

- $\mathbf{SU(3)}_c \times \mathbf{SU(3)}_c \times \mathbf{SU(3)}_c$

If we require the  $\mathbf{SU(3)}_c$  representations to be vectorlike as in the SM, the fermionic representation is

$$3k \cdot \mathbf{3} + 3k \cdot \bar{\mathbf{3}} + 3(M-k) \cdot \mathbf{3} + 3(M-k) \cdot \bar{\mathbf{3}} + N \cdot \mathbf{1} + (\text{a } \mathbf{1} \text{ term for each right-handed lepton}) , \quad (3.54)$$

that is real and hence do not contribute to the anomaly, in the same way as the SM.

- $\mathbf{SU(3)}_L \times \mathbf{SU(3)}_L \times \mathbf{SU(3)}_L$

As before, we need the  $\mathbf{SU(3)}_L$  representation to be real, that is obtained when the number of left-handed triplets equals the number of left-handed antitriplets. This gives the condition

$$3k + j = 3(M-k) + (N-j) . \quad (3.55)$$

- $\mathbf{U(1)}_X \times \mathbf{SU(3)}_c \times \mathbf{SU(3)}_c$

We have to take the trace of the  $X$ -hypercharges over the colored fermions, obtaining the conditions

$$3X_{q^{(m)}}^L - (X_{U^{(m)}}^R + X_{D^{(m)}}^R + X_{J^{(m)}}^R) = 0 \quad \forall m , \quad (3.56a)$$

$$-3X_{q^{(m^*)}}^L - (X_{U^{(m^*)}}^R + X_{D^{(m^*)}}^R + X_{J^{(m^*)}}^R) = 0 \quad \forall m^* ; \quad (3.56b)$$

since they are already satisfied by the SM left-handed doublets, they are automatically satisfied by the 331 left-handed triplets when we embed the doublets and impose the charge.

- $U(1)_X \times SU(3)_L \times SU(3)_L$

This time the trace runs over the  $X$ -hypercharges of the left-handed triplets:

$$\sum_{n=1}^j (X_{\ell^{(n)}}^L) + \sum_{n^*=j+1}^N (-X_{\ell^{(n^*)}}^L) + 3 \sum_{m=1}^k (X_{q^{(m)}}^L) + 3 \sum_{m^*=k+1}^M (-X_{q^{(m^*)}}^L) = 0, \quad (3.57)$$

which, substituting the actual values of the hypercharges, gives the condition

$$-\frac{3}{2}M + \frac{3\sqrt{3}\beta}{2}(M - 2k) = -\frac{3}{2}N + \frac{\sqrt{3}\beta}{2}(N - 2j). \quad (3.58)$$

- $U(1)_X \times [\mathbf{Grav}] \times [\mathbf{Grav}]$

Since gravity acts on all the fields, the anomaly is

$$\begin{aligned} & 3 \sum_{n=1}^j (X_{\ell^{(n)}}^L) + 3 \sum_{n^*=j+1}^N (-X_{\ell^{(n^*)}}^L) + 9 \sum_{m=1}^k (X_{q^{(m)}}^L) + 9 \sum_{m^*=k+1}^M (-X_{q^{(m^*)}}^L) \\ & - \sum_{n=1}^j (X_{\nu^{(n)}}^R + X_{e^{(n)}}^R + X_{E^{(n)}}^R) - \sum_{n^*=j+1}^N (X_{\nu^{(n^*)}}^R + X_{e^{(n^*)}}^R + X_{E^{(n^*)}}^R) \\ & - 3 \sum_{m=1}^k (X_{U^{(m)}}^R + X_{D^{(m)}}^R + X_{J^{(m)}}^R) - 3 \sum_{m^*=k+1}^M (X_{U^{(m^*)}}^R + X_{D^{(m^*)}}^R + X_{J^{(m^*)}}^R) = 0. \end{aligned} \quad (3.59)$$

Now, while for each left-handed quark its right-handed partner must always be present, this is not necessary for leptons, not only for right-handed neutrinos but also for the other leptons, since in some cases a right-handed lepton could be embedded into the third place of a left-handed triplet, or because the exotic fermion could be neutral. The right-handed neutrinos, being electrically neutral, do not contribute to the anomalies, but we have to take into account the possible absence of right-handed charged leptons, by introducing the symbol

$$\Theta_\ell \equiv \begin{cases} 1 & \text{for models with charged } \ell_R \\ 0 & \text{for models without charged } \ell_R \end{cases}. \quad (3.60)$$

With this notation we substitute the hyper charges obtaining

$$\begin{aligned} -\frac{3}{2}N + \frac{\sqrt{3}\beta}{2}(N - 2j) &= -j\Theta_{e^{(1)}} - j \left( \frac{1}{2} + \frac{\sqrt{3}\beta}{2} \right) \Theta_{E^{(1)}} \\ &\quad - (N - j)\Theta_{e^{(j+1)}} - (N - j) \left( \frac{1}{2} - \frac{\sqrt{3}\beta}{2} \right) \Theta_{E^{(j+1)}}, \end{aligned} \quad (3.61)$$

that is a condition on the lepton sector.

- $U(1)_{\mathbf{X}} \times U(1)_{\mathbf{X}} \times U(1)_{\mathbf{X}}$

Similarly to the previous case, we get

$$\begin{aligned}
& 3 \sum_{n=1}^j (X_{\ell(n)}^L)^3 + 3 \sum_{n^*=j+1}^N (-X_{\ell(n^*)}^L)^3 + 9 \sum_{m=1}^k (X_{q(m)}^L)^3 + 9 \sum_{m^*=k+1}^M (-X_{q(m^*)}^L)^3 \\
& - \sum_{n=1}^j ((X_{\nu(n)}^R)^3 + (X_{e(n)}^R)^3 + (X_{E(n)}^R)^3) \\
& - \sum_{n^*=j+1}^N ((X_{\nu(n^*)}^R)^3 + (X_{e(n^*)}^R)^3 + (X_{E(n^*)}^R)^3) \\
& - 3 \sum_{m=1}^k ((X_{U(m)}^R)^3 + (X_{D(m)}^R)^3 + (X_{J(m)}^R)^3) \\
& - 3 \sum_{m^*=k+1}^M ((X_{U(m^*)}^R)^3 + (X_{D(m^*)}^R)^3 + (X_{J(m^*)}^R)^3) = 0 ,
\end{aligned} \tag{3.62}$$

and from it

$$\begin{aligned}
& -\frac{3}{4}(1+\beta^2) \left( \frac{1}{2}N + M \right) + \frac{\sqrt{3}\beta(9+\beta^2)}{24}(N-2j) - \sqrt{3}\beta^3(M-2k) = \\
& -j\Theta_{e^{(1)}} + j \left( \frac{1}{2} + \frac{\sqrt{3}\beta}{2} \right)^3 \Theta_{E^{(1)}} - (N-j)\Theta_{e^{(j+1)}} - (N-j) \left( \frac{1}{2} - \frac{\sqrt{3}\beta}{2} \right)^3 \Theta_{E^{(j+1)}} .
\end{aligned} \tag{3.63}$$

From the requirement of anomaly cancellation we have obtained the four conditions in Eq. (3.55), Eq. (3.58), Eq. (3.61) and Eq. (3.63). Combining the first two, they simplify in

$$N = M; \tag{3.64}$$

$$j + 3k = 2N, \tag{3.65}$$

the first one saying that, as in the SM, the number of quark and lepton generations must be the same, while the second is a constraint on the subdivision of the multiplets in triplets and antitriplets, whose possible solutions are reported in Tab. 3.3 for the relevant values of  $N$ , i.e.  $N \geq 3$  in order to fit all the SM generations and  $N \leq 5$  in order to obtain asymptotic freedom [123].

Now, substituting the first three conditions into the fourth, this becomes

$$j(\Theta_{e^{(1)}} - \Theta_{E^{(1)}}) = (j - N)(\Theta_{e^{(j+1)}} - \Theta_{E^{(j+1)}}) , \tag{3.66}$$

and, together with the condition in Eq. (3.61), represents a constraint in the building of the lepton sector; once the latter have been consistently defined, the quark sector is fixed by Eq. (3.64)-(3.65). Moreover, despite the freedom left by the  $\Theta_{\ell}$

$N = M$	triplets
3	$j = 0; \quad k = 2$
	$j = 3; \quad k = 1$
4	$j = 2; \quad k = 2$
5	$j = 1; \quad k = 3$
	$j = 4; \quad k = 2$

Table 3.3: Anomaly-free subdivision of  $SU(3)_L$  triplets and antitriplets for the possible numbers of generations. We notice that the different possibilities for a single number of generations are symmetric for the interchange of triplets and antitriplets.

parameters, in the lepton sector one has to ensure to include for each charged lepton its corresponding conjugate in the spectrum in order to build up the corresponding Dirac Lagrangian. Hence we perform a systematic analysis of all the possible structures of the lepton sector.

- **N = 3**

- **j = 0**

Since there are no left-handed triplets, we cannot have the relative right-handed singlets and hence  $\Theta_{e^{(1)}} = \Theta_{E^{(1)}} = 0$ . Then the two conditions in Eq. (3.61)-(3.66) become respectively

$$\Theta_{e^{(j+1)}} + \left( \frac{1}{2} - \frac{\sqrt{3}\beta}{2} \right) \Theta_{E^{(j+1)}} = \frac{3}{2} - \frac{\sqrt{3}\beta}{2}, \quad (3.67a)$$

$$\Theta_{e^{(j+1)}} - \Theta_{E^{(j+1)}} = 0, \quad (3.67b)$$

that admit the solutions

$$\Theta_{e^{(j+1)}} = \Theta_{E^{(j+1)}} = 0 \quad \text{with} \quad \beta = \sqrt{3}, \quad (3.68a)$$

$$\Theta_{e^{(j+1)}} = \Theta_{E^{(j+1)}} = 1 \quad \forall \beta. \quad (3.68b)$$

- **j = 3**

Symmetrically with respect to the previous case, we have  $\Theta_{e^{(j+1)}} = \Theta_{E^{(j+1)}} = 0$  and the solutions

$$\Theta_{e^{(1)}} = \Theta_{E^{(1)}} = 0 \quad \text{with} \quad \beta = \sqrt{3}, \quad (3.69a)$$

$$\Theta_{e^{(1)}} = \Theta_{E^{(1)}} = 1 \quad \forall \beta. \quad (3.69b)$$

- **N = 4, j = 2**

This time there are no a priori conditions on the  $\Theta_\ell$ 's, and they are constrained by

$$\Theta_{e^{(1)}} + \left( \frac{1}{2} + \frac{\sqrt{3}\beta}{2} \right) \Theta_{E^{(1)}} + \Theta_{e^{(j+1)}} + \left( \frac{1}{2} - \frac{\sqrt{3}\beta}{2} \right) \Theta_{E^{(j+1)}} = 3, \quad (3.70a)$$

$$\Theta_{e^{(1)}} - \Theta_{E^{(1)}} = -(\Theta_{e^{(j+1)}} - \Theta_{E^{(j+1)}}) , \quad (3.70b)$$

whose possible solutions are

$$(\Theta_{e^{(1)}}, \Theta_{E^{(1)}}, \Theta_{e^{(j+1)}}, \Theta_{E^{(j+1)}}) = (0, 0, 1, 1) \quad \text{with } \beta = -\sqrt{3} , \quad (3.71a)$$

$$(\Theta_{e^{(1)}}, \Theta_{E^{(1)}}, \Theta_{e^{(j+1)}}, \Theta_{E^{(j+1)}}) = (0, 1, 1, 0) \quad \text{with } \beta = \sqrt{3} , \quad (3.71b)$$

$$(\Theta_{e^{(1)}}, \Theta_{E^{(1)}}, \Theta_{e^{(j+1)}}, \Theta_{E^{(j+1)}}) = (1, 0, 0, 1) \quad \text{with } \beta = -\sqrt{3} , \quad (3.71c)$$

$$(\Theta_{e^{(1)}}, \Theta_{E^{(1)}}, \Theta_{e^{(j+1)}}, \Theta_{E^{(j+1)}}) = (1, 1, 0, 0) \quad \text{with } \beta = \sqrt{3} , \quad (3.71d)$$

$$(\Theta_{e^{(1)}}, \Theta_{E^{(1)}}, \Theta_{e^{(j+1)}}, \Theta_{E^{(j+1)}}) = (1, 1, 1, 1) \quad \forall \beta . \quad (3.71e)$$

- **N = 5**

- **j = 1**

The two conditions read

$$\Theta_{e^{(1)}} + \left( \frac{1}{2} + \frac{\sqrt{3}\beta}{2} \right) \Theta_{E^{(1)}} + 4\Theta_{e^{(j+1)}} + 4 \left( \frac{1}{2} - \frac{\sqrt{3}\beta}{2} \right) \Theta_{E^{(j+1)}} = \frac{15}{2} - \frac{3\sqrt{3}\beta}{2} , \quad (3.72a)$$

$$\Theta_{e^{(1)}} - \Theta_{E^{(1)}} = -4(\Theta_{e^{(j+1)}} - \Theta_{E^{(j+1)}}) , \quad (3.72b)$$

with solutions

$$(\Theta_{e^{(1)}}, \Theta_{E^{(1)}}, \Theta_{e^{(j+1)}}, \Theta_{E^{(j+1)}}) = (0, 0, 0, 0) \quad \text{with } \beta = -\frac{5}{\sqrt{3}} , \quad (3.73a)$$

$$(\Theta_{e^{(1)}}, \Theta_{E^{(1)}}, \Theta_{e^{(j+1)}}, \Theta_{E^{(j+1)}}) = (0, 0, 1, 1) \quad \text{with } \beta = -\sqrt{3} , \quad (3.73b)$$

$$(\Theta_{e^{(1)}}, \Theta_{E^{(1)}}, \Theta_{e^{(j+1)}}, \Theta_{E^{(j+1)}}) = (1, 1, 0, 0) \quad \text{with } \beta = \sqrt{3} , \quad (3.73c)$$

$$(\Theta_{e^{(1)}}, \Theta_{E^{(1)}}, \Theta_{e^{(j+1)}}, \Theta_{E^{(j+1)}}) = (1, 1, 1, 1) \quad \forall \beta ; \quad (3.73d)$$

however, the first solution is not physical because it implies the presence of right-handed leptons with charge different from the one of the relative left-handed ones.

- **j = 4**

Symmetrically, the possible configurations are

$$(\Theta_{e^{(1)}}, \Theta_{E^{(1)}}, \Theta_{e^{(j+1)}}, \Theta_{E^{(j+1)}}) = (0, 0, 1, 1) \quad \text{with } \beta = -\sqrt{3} , \quad (3.74)$$

$$(\Theta_{e^{(1)}}, \Theta_{E^{(1)}}, \Theta_{e^{(j+1)}}, \Theta_{E^{(j+1)}}) = (1, 1, 0, 0) \quad \text{with } \beta = \sqrt{3} , \quad (3.75)$$

$$(\Theta_{e^{(1)}}, \Theta_{E^{(1)}}, \Theta_{e^{(j+1)}}, \Theta_{E^{(j+1)}}) = (1, 1, 1, 1) \quad \forall \beta . \quad (3.76)$$

In summary, some representatives of possible matter contents for which a model with gauge group  $SU(3)_c \times SU(3)_L \times U(1)_X$  is anomaly-free are listed in Tab. 3.4 and Tab. 3.5, with the only assumption to associate only one lepton and one quark multiplet for each generation, and at most one right-handed singlet associated with each left-handed fermion.

A few considerations are worth. We notice from the first row of Tab. 3.4 that for a certain value of  $\beta$  the third place of the leptonic left-handed (anti)triplets

$N = 3, \quad j = 0, \quad (\Theta_{e^{(1)}}, \Theta_{E^{(1)}}, \Theta_{e^{(j+1)}}, \Theta_{E^{(j+1)}}) = (0, 0, 0, 0), \quad \beta = \sqrt{3}$			
$\ell_L^{(1^*)} = \begin{pmatrix} e^{(1^*)} \\ -\nu^{(1^*)} \\ (e^{(1^*)})^c \end{pmatrix}_L$		$\ell_L^{(2^*)} = \begin{pmatrix} e^{(2^*)} \\ -\nu^{(2^*)} \\ (e^{(2^*)})^c \end{pmatrix}_L$	
$\ell_L^{(3^*)} = \begin{pmatrix} e^{(3^*)} \\ -\nu^{(3^*)} \\ (e^{(3^*)})^c \end{pmatrix}_L$			
$q_L^{(1)} = \begin{pmatrix} U^{(1)} \\ D^{(1)} \\ J^{(1)} \end{pmatrix}_L$	$\begin{matrix} U_R^{(1)} \\ D_R^{(1)} \\ J_R^{(1)} \end{matrix}$	$q_L^{(2)} = \begin{pmatrix} U^{(2)} \\ D^{(2)} \\ J^{(2)} \end{pmatrix}_L$	$\begin{matrix} U_R^{(2)} \\ D_R^{(2)} \\ J_R^{(2)} \end{matrix}$
$q_L^{(3^*)} = \begin{pmatrix} D^{(3^*)} \\ -U^{(3^*)} \\ J^{(3^*)} \end{pmatrix}_L$	$\begin{matrix} D_R^{(3^*)} \\ U_R^{(3^*)} \\ J_R^{(3^*)} \end{matrix}$		
$N = 3, \quad j = 1, \quad (\Theta_{e^{(1)}}, \Theta_{E^{(1)}}, \Theta_{e^{(j+1)}}, \Theta_{E^{(j+1)}}) = (0, 0, 1, 1), \quad \forall \beta$			
$\ell_L^{(1^*)} = \begin{pmatrix} e^{(1^*)} \\ -\nu^{(1^*)} \\ E^{(1^*)} \end{pmatrix}_L$	$\begin{matrix} e_R^{(1^*)} \\ [\nu_R^{(1^*)}] \\ E_R^{(1^*)} \end{matrix}$	$\ell_L^{(2^*)} = \begin{pmatrix} e^{(2^*)} \\ -\nu^{(2^*)} \\ E^{(2^*)} \end{pmatrix}_L$	$\begin{matrix} e_R^{(2^*)} \\ [\nu_R^{(2^*)}] \\ E_R^{(2^*)} \end{matrix}$
$\ell_L^{(3^*)} = \begin{pmatrix} e^{(3^*)} \\ -\nu^{(3^*)} \\ E^{(3^*)} \end{pmatrix}_L$	$\begin{matrix} e_R^{(3^*)} \\ [\nu_R^{(3^*)}] \\ E_R^{(3^*)} \end{matrix}$		
$q_L^{(1)} = \begin{pmatrix} U^{(1)} \\ D^{(1)} \\ J^{(1)} \end{pmatrix}_L$	$\begin{matrix} U_R^{(1)} \\ D_R^{(1)} \\ J_R^{(1)} \end{matrix}$	$q_L^{(2)} = \begin{pmatrix} U^{(2)} \\ D^{(2)} \\ J^{(2)} \end{pmatrix}_L$	$\begin{matrix} U_R^{(2)} \\ D_R^{(2)} \\ J_R^{(2)} \end{matrix}$
$q_L^{(3^*)} = \begin{pmatrix} D^{(3^*)} \\ -U^{(3^*)} \\ J^{(3^*)} \end{pmatrix}_L$	$\begin{matrix} D_R^{(3^*)} \\ U_R^{(3^*)} \\ J_R^{(3^*)} \end{matrix}$		

Table 3.4: Possible fermionic contents for  $N = 3$  generations; also the two solutions obtained for the exchange of triplets with antitriplets are admissible.

acquires the right charge to fit the antiparticle of the charged lepton, avoiding at all the introduction of right-handed leptons, compatibly with the anomaly cancellation. Historically, this configuration was used for the very first formulations of the 331 model [39, 40], and led to the derivation of very interesting properties. In fact, if one assumes that all the leptons behave in the same way, it is evident from Tab. 3.3 that the theory is anomaly free only for 3 generations of leptons, offering a solution to a long-debated question; moreover, in this case there is one quark generation that behaves differently from the other two, giving a starting point to explain the large hierarchy of the third quark generation [186]. On the other hand, the limits of this configuration emerged soon, and the cases with right-handed neutrinos [187–189]

$N = 4, \quad j = 2, \quad (\Theta_{e^{(1)}}, \Theta_{E^{(1)}}, \Theta_{e^{(j+1)}}, \Theta_{E^{(j+1)}}) = (0, 0, 1, 1), \quad \beta = -\sqrt{3}$			
$\ell_L^{(1)} = \begin{pmatrix} \nu^{(1)} \\ e^{(1)} \\ (e^{(1)})^c \end{pmatrix}_L$	$\ell_L^{(2)} = \begin{pmatrix} \nu^{(2)} \\ e^{(2)} \\ (e^{(2)})^c \end{pmatrix}_L$	$\ell_L^{(3^*)} = \begin{pmatrix} e^{(3^*)} \\ -\nu^{(3^*)} \\ E^{(3^*)} \end{pmatrix}_L$	$\ell_L^{(4^*)} = \begin{pmatrix} e^{(4^*)} \\ -\nu^{(4^*)} \\ E^{(4^*)} \end{pmatrix}_L$
$q_L^{(1)} = \begin{pmatrix} U^{(1)} \\ D^{(1)} \\ J^{(1)} \end{pmatrix}_L$	$q_L^{(2)} = \begin{pmatrix} U^{(2)} \\ D^{(2)} \\ J^{(2)} \end{pmatrix}_L$	$q_L^{(3^*)} = \begin{pmatrix} D^{(3^*)} \\ -U^{(3^*)} \\ J^{(3^*)} \end{pmatrix}_L$	$q_L^{(4^*)} = \begin{pmatrix} D^{(4^*)} \\ -U^{(4^*)} \\ J^{(4^*)} \end{pmatrix}_L$
	$e_R^{(3^*)}$ $\begin{bmatrix} \nu_R^{(3^*)} \\ E_R^{(3^*)} \end{bmatrix}$ $U_R^{(1)}$ $D_R^{(1)}$ $J_R^{(1)}$ $D_R^{(3^*)}$ $U_R^{(3^*)}$ $J_R^{(3^*)}$		$e_R^{(4^*)}$ $\begin{bmatrix} \nu_R^{(4^*)} \\ E_R^{(4^*)} \end{bmatrix}$ $U_R^{(2)}$ $D_R^{(2)}$ $J_R^{(2)}$ $D_R^{(4^*)}$ $U_R^{(4^*)}$ $J_R^{(4^*)}$
$N = 4, \quad j = 2, \quad (\Theta_{e^{(1)}}, \Theta_{E^{(1)}}, \Theta_{e^{(j+1)}}, \Theta_{E^{(j+1)}}) = (1, 1, 1, 1), \quad \forall \beta$			
$\ell_L^{(1)} = \begin{pmatrix} \nu^{(1)} \\ e^{(1)} \\ E^{(1)} \end{pmatrix}_L$	$\ell_L^{(2)} = \begin{pmatrix} \nu^{(2)} \\ e^{(2)} \\ E^{(2)} \end{pmatrix}_L$	$\ell_L^{(3^*)} = \begin{pmatrix} e^{(3^*)} \\ -\nu^{(3^*)} \\ E^{(3^*)} \end{pmatrix}_L$	$\ell_L^{(4^*)} = \begin{pmatrix} e^{(4^*)} \\ -\nu^{(4^*)} \\ E^{(4^*)} \end{pmatrix}_L$
$q_L^{(1)} = \begin{pmatrix} U^{(1)} \\ D^{(1)} \\ J^{(1)} \end{pmatrix}_L$	$q_L^{(2)} = \begin{pmatrix} U^{(2)} \\ D^{(2)} \\ J^{(2)} \end{pmatrix}_L$	$q_L^{(3^*)} = \begin{pmatrix} D^{(3^*)} \\ -U^{(3^*)} \\ J^{(3^*)} \end{pmatrix}_L$	$q_L^{(4^*)} = \begin{pmatrix} D^{(4^*)} \\ -U^{(4^*)} \\ J^{(4^*)} \end{pmatrix}_L$
	$\begin{bmatrix} \nu_R^{(1)} \\ e_R^{(1)} \\ E_R^{(1)} \end{bmatrix}$ $e_R^{(3^*)}$ $\begin{bmatrix} \nu_R^{(3^*)} \\ E_R^{(3^*)} \end{bmatrix}$ $U_R^{(1)}$ $D_R^{(1)}$ $J_R^{(1)}$ $D_R^{(3^*)}$ $U_R^{(3^*)}$ $J_R^{(3^*)}$		$\begin{bmatrix} \nu_R^{(2)} \\ e_R^{(2)} \\ E_R^{(2)} \end{bmatrix}$ $e_R^{(4^*)}$ $\begin{bmatrix} \nu_R^{(4^*)} \\ E_R^{(4^*)} \end{bmatrix}$ $U_R^{(2)}$ $D_R^{(2)}$ $J_R^{(2)}$ $D_R^{(4^*)}$ $U_R^{(4^*)}$ $J_R^{(4^*)}$

Table 3.5: Some of the possible fermionic contents for  $N = 4$  generations; the solutions obtained for the exchange of triplets with antitriplets and some solutions with different positions of the right-handed singlets are also possible.

and mirror fermions have been considered as well [143], [190], and the role of the anomalies in the scalar sector has been investigated [191, 192].

### 3.2.2 Peccei-Quinn symmetry

In the limit of vanishing masses for the  $u$  and  $d$  quark, the QCD Lagrangian for these two flavours presents a global  $U(2)_V \times U(2)_A$  (vector-axial) symmetry. Experimentally, while the vector symmetry is respected to a very good approximation

(in fact  $U(2)_V = SU(2)_I \times U(1)_B$ ), this is not true for the axial symmetry: quark condensates with  $\langle \bar{u}u \rangle = \langle \bar{d}d \rangle \neq 0$  form, breaking down the axial symmetry spontaneously; four pseudo-Goldstone bosons would be expected, but, apart for the pions, there are no signs of another light state in the hadronic spectrum.

A possible solution to this problem seems to be provided by the breaking of the  $U(2)_A$  symmetry at loop level. In fact, considering the triangle loop of an axial current with two gluons, one finds the anomalous current

$$\partial_\mu j^{\mu 5} = \frac{g^2}{32\pi^2} G_a^{\mu\nu} \tilde{G}_{a\mu\nu} , \quad (3.77)$$

with  $\tilde{G}_{a\mu\nu} = \frac{1}{2}\epsilon_{\mu\nu\alpha\beta} G_a^{\alpha\beta}$ . One can notice that the pseudoscalar density entering this anomaly is a total divergence:

$$G_a^{\mu\nu} \tilde{G}_{a\mu\nu} = \partial_\mu K^\mu \quad \text{with} \quad K^\mu = \epsilon^{\mu\alpha\beta\gamma} A_{a\alpha} \left[ G_{a\beta\gamma} - \frac{g}{3} f_{abc} A_{b\beta} A_{c\gamma} \right] ; \quad (3.78)$$

however, this do not vanish when integrated into the action, because the usual boundary condition  $A_a^\mu = 0$  at spatial infinity is not gauge invariant; the correct boundary condition to use is that any gauge transformation of  $A_a^\mu$  should vanish at the spatial infinity [193]. This nontrivial structure of the QCD vacuum brings out a free parameter  $\theta$  from the gauge transformation, with the result of adding to the Lagrangian the effective contribution

$$\mathcal{L}_\theta = \theta \frac{g^2}{32\pi^2} G_a^{\mu\nu} \tilde{G}_{a\mu\nu} . \quad (3.79)$$

Moreover, when electroweak interactions are included, the diagonalization of the mass matrix  $M$  implies a chiral transformation that changes  $\theta \rightarrow \bar{\theta} = \theta + \arg(\det M)$ . The term in Eq. (3.79) is  $C$ -conserving and  $P$ - and  $T$ -violating, and hence violates  $CP$ . It is directly linked to the neutron electric dipole moment  $d_n \simeq e\theta m_q/m_N^2$ , and the strong bounds on the latter,  $|d_n| < 2.9 \text{ e}\cdot\text{cm}$  [194] imply that the phase  $\theta$  is extremely small, if not vanishing; this is known as the *strong CP problem* and it is an open problem of the SM.

The most popular solution to the CP problem is the introduction of the *Peccei-Quinn symmetry* [120, 195] and hence of the *axion* [196, 197]. If the theory presents a global axial symmetry  $U(1)_{PQ}$  that is spontaneously broken, the relative Goldstone boson, called the axion, exhibits a triangle anomaly that, due to the effective potential generated by the interaction with the gluons, exactly cancels the axial anomaly. Due to the anomaly, the axion acquires a mass and hence is not incompatible with experiments.

A theory that naturally presents such a symmetry has the appealing advantage of not suffering of the strong CP problem. This is the case of at least some realizations of the 331 model [198–201].

- In its minimal version [39, 40], with 3 generations without right-handed lepton singlets and  $\beta = \sqrt{3}$ , the fermion content of the model is

$$\ell_L^{(1^*, 2^*, 3^*)} \sim (\mathbf{1}, \bar{\mathbf{3}}, 0), \quad Q_L^{(1, 2)} \sim \left( \mathbf{3}, \mathbf{3}, -\frac{1}{3} \right), \quad Q_L^{(3^*)} \sim \left( \mathbf{3}, \bar{\mathbf{3}}, \frac{2}{3} \right) ; \quad (3.80a)$$

$$U_R^{(1, 2, 3^*)} \sim \left( \mathbf{3}, \mathbf{1}, \frac{2}{3} \right), \quad D_R^{(1, 2, 3^*)} \sim \left( \mathbf{3}, \mathbf{1}, -\frac{1}{3} \right); \quad (3.80b)$$

$$J_R^{(1, 2)} \sim \left( \mathbf{3}, \mathbf{1}, -\frac{4}{3} \right), \quad J_R^{(3^*)} \sim \left( \mathbf{3}, \mathbf{1}, \frac{5}{3} \right); \quad (3.80c)$$

while the Higgs sector contains

$$\chi \sim (\mathbf{1}, \mathbf{3}, 1), \quad \rho \sim (\mathbf{1}, \mathbf{3}, 0), \quad \eta \sim (\mathbf{1}, \mathbf{3}, -1), \quad S \sim (\mathbf{1}, \mathbf{6}, 0); \quad (3.81)$$

the most general Yukawa Lagrangian is

$$\begin{aligned} \mathcal{L}_Y = & \lambda_{ab}^{\ell, \rho} \epsilon^{ijk} \bar{\ell}_{ia} \ell_{jb}^c \rho_k + \lambda_{ab}^{\ell, S} \bar{\ell}_a S^\dagger \ell_b^c \\ & + \lambda_{ij}^{Q, \chi} \bar{Q}_L^i \chi J_R^j + \lambda_3^{Q, \chi} \bar{Q}_L^3 \chi^\dagger T_R \\ & + \lambda_{ia}^{Q, \rho} \bar{Q}_L^i \rho d_R^a + \lambda_3^{Q, \rho} \bar{Q}_L^3 \rho^\dagger u_R \\ & + \lambda_{ia}^{Q, \eta} \bar{Q}_L^i \eta u_R^a + \lambda_3^{Q, \eta} \bar{Q}_L^3 \eta^\dagger d_R + \text{h.c.}; \end{aligned} \quad (3.82)$$

and the most general Higgs potential

$$\begin{aligned} V = & \lambda_1 (\chi^\dagger \chi - v_\chi^2)^2 + \lambda_2 (\rho^\dagger \rho - v_\rho^2)^2 + \lambda_3 (\eta^\dagger \eta - v_\eta^2)^2 + \lambda_4 (\text{Tr}(S^\dagger S) - v_S^2)^2 \\ & + \lambda_5 (\text{Tr}(S^\dagger S S^\dagger S) - v_S^4) + \lambda_6 (\chi^\dagger \chi \rho^\dagger \rho - v_\chi^2 v_\rho^2) + \lambda_7 (\rho^\dagger \rho \eta^\dagger \eta - v_\rho^2 v_\eta^2) \\ & + \lambda_8 (\eta^\dagger \eta \chi^\dagger \chi - v_\eta^2 v_\chi^2) + \lambda_9 (\chi^\dagger \chi \text{Tr}(S^\dagger S) - v_\chi^2 v_S^2) + \lambda_{10} (\rho^\dagger \rho \text{Tr}(S^\dagger S) - v_\rho^2 v_S^2) \\ & + \lambda_{11} (\eta^\dagger \eta \text{Tr}(S^\dagger S) - v_\eta^2 v_S^2) + \lambda_{12} (\chi^\dagger \chi \rho^\dagger \rho) + \lambda_{13} (\rho^\dagger \rho \eta^\dagger \eta) + \lambda_{14} (\eta^\dagger \eta \chi^\dagger \chi) \\ & + \mu_1 \eta \rho \chi + \mu_2 \rho^T S^\dagger \chi + \text{h.c.} . \end{aligned} \quad (3.83)$$

The gauge Lagrangian and the Yukawa Lagrangian are invariant with respect to the global chiral U(1) symmetry [198]

Multiplet	$\ell_L^{(i^*)}$	$Q_L^{(i)}$	$Q_L^{(3^*)}$	$q_R$	$\chi, \eta, \rho$	$S$
Charge	1	1	-1	0	1	2

as well as the Higgs potential, with the exception of the trilinear term  $\eta \rho \chi$  that can be dropped out without consequences.

This scenario presents therefore a symmetry of the type advocated by Peccei-Quinn. However the model is not realistic in this way: at the high scale  $v_\chi$ , although the  $U(1)_{PQ}$  breaks, the combination  $U(1)_{PQ} + U(1)_X$  is unbroken and acts as a Peccei-Quinn symmetry; hence the axion emerges at the lower scale  $v_\rho \sim v_\eta$  and this is ruled out by experiments. The model has to be extended in order to make the axion invisible.

- If one wants to include right-handed neutrinos, one can choose  $\beta = -1/\sqrt{3}$  and a fermionic content

$$\ell_L^{(1, 2, 3)} \sim \left( \mathbf{1}, \bar{\mathbf{3}}, -\frac{1}{3} \right), \quad Q_L^{(1^*, 2^*)} \sim (\mathbf{3}, \bar{\mathbf{3}}, 0), \quad Q_L^{(3)} \sim \left( \mathbf{3}, \mathbf{3}, \frac{1}{3} \right) \quad (3.84a)$$

$$e_R^{(1,2,3)} \sim (\mathbf{1}, \mathbf{1}, -1) ; \quad (3.84b)$$

$$U_R^{(1^*, 2^*, 3)}, J_R^{(3)} \sim \left( \mathbf{3}, \mathbf{1}, \frac{2}{3} \right), \quad D_R^{(1^*, 2^*, 3)}, J_R^{(1^*, 2^*)} \sim \left( \mathbf{3}, \mathbf{1}, -\frac{1}{3} \right) ; \quad (3.84c)$$

the Higgs sector is reduced to

$$\chi \sim \left( \mathbf{1}, \mathbf{3}, -\frac{1}{3} \right), \quad \rho \sim \left( \mathbf{1}, \mathbf{3}, \frac{2}{3} \right), \quad \eta \sim \left( \mathbf{1}, \mathbf{3}, -\frac{1}{3} \right) ; \quad (3.85)$$

the Yukawa Lagrangian and the Higgs potential<sup>2</sup> read respectively

$$\begin{aligned} \mathcal{L}_Y = & \lambda_{ij}^{\ell, LL} \ell_L^i \ell_L^j \rho + \lambda_{ij}^{\ell, LR} \bar{\ell}_L^i \ell_R^j \rho \\ & + \lambda_{ij}^{Q, \chi} \bar{Q}_L^i \chi^\dagger J_R^j + \lambda_3^{Q, \chi} \bar{Q}_L^3 \chi T_R \\ & + \lambda_{ia}^{Q, \rho} \bar{Q}_L^i \rho^\dagger d_R^a + \lambda_3^{Q, \rho} \bar{Q}_L^3 \rho u_R \\ & + \lambda_{ia}^{Q, \eta} \bar{Q}_L^i \eta^\dagger u_R^a + \lambda_3^{Q, \eta} \bar{Q}_L^3 \eta d_R + \text{h.c.} ; \end{aligned} \quad (3.86)$$

$$\begin{aligned} V = & \lambda_1 (\chi^\dagger \chi - v_\chi^2)^2 + \lambda_2 (\rho^\dagger \rho - v_\rho^2)^2 + \lambda_3 (\eta^\dagger \eta - v_\eta^2)^2 \\ & + \lambda_4 (\chi^\dagger \chi - v_\chi^2) (\eta^\dagger \eta - v_\eta^2) + \lambda_5 (\eta^\dagger \eta - v_\eta^2) (\rho^\dagger \rho - v_\rho^2) \\ & + \lambda_6 (\rho^\dagger \rho - v_\rho^2) (\chi^\dagger \chi - v_\chi^2) + \lambda_7 (\chi^\dagger \eta + \eta^\dagger \chi)^2 \\ & + \lambda_8 (\chi^\dagger \eta) (\eta^\dagger \chi) + \lambda_9 (\eta^\dagger \rho) (\rho^\dagger \eta) + \lambda_{10} (\rho^\dagger \chi) (\chi^\dagger \rho) . \end{aligned} \quad (3.87)$$

Also in this case there is a Peccei-Quinn symmetry [198]

Multiplet	$\ell_L^{(i)}$	$\ell_R^{(i)}$	$Q_L^{(i^*)}$	$Q_L^{(3)}$	$q_R$	$\chi, \eta, \rho$
Charge	$-\frac{1}{2}$	$-\frac{3}{2}$	-1	1	0	1

which however presents the same axion problem as the previous scenario.

## 3.3 The $\overline{331}$ model

### 3.3.1 Model content

As we have discussed in the previous sections, a specific realization of a 331 model is defined by a value of the  $\beta$  parameter and by the assignment of a consequent non-anomalous fermionic content. The specific scenario that we are going to consider, that we will call  $\overline{331}$  model, has

$$\beta = \frac{1}{\sqrt{3}} \quad (3.88)$$

and the fermionic content listed in Tab. 3.6. We introduce three fermion generations; the three lepton families are arranged into antitriplets, and their third component can fit the charged-conjugated neutrinos, so that neutrinos can get a mass without the explicit introduction of their right-handed component; on the other hand, the

<sup>2</sup>In [187] the following discrete symmetry is imposed:  $\chi \rightarrow -\chi, T_R \rightarrow -T_R, D_R^j \rightarrow D_R^j$ .

$\psi_L$	$Q_{\psi_L}$	$\psi_R$	$Q_{\psi_R}$
$Q_L^{(1,2)} = \begin{pmatrix} u \\ d \\ D \end{pmatrix}_L, \begin{pmatrix} c \\ s \\ S \end{pmatrix}_L$	$\begin{pmatrix} \frac{2}{3} \\ -\frac{1}{3} \\ -\frac{1}{3} \end{pmatrix}$	$u_R, c_R \\ d_R, s_R \\ D_R, S_R$	$\frac{2}{3} \\ -\frac{1}{3} \\ -\frac{1}{3}$
$Q_L^{(3^*)} = \begin{pmatrix} b \\ -t \\ T \end{pmatrix}_L$	$\begin{pmatrix} -\frac{1}{3} \\ \frac{2}{3} \\ \frac{2}{3} \end{pmatrix}$	$b_R \\ t_R \\ T_R$	$-\frac{1}{3} \\ \frac{2}{3} \\ \frac{2}{3}$
$\ell_L^{(1^*, 2^*, 3^*)} = \begin{pmatrix} e \\ -\nu_e \\ (\nu_e)^c \end{pmatrix}_L, \begin{pmatrix} \mu \\ -\nu_\mu \\ (\nu_\mu)^c \end{pmatrix}_L, \begin{pmatrix} \tau \\ -\nu_\tau \\ (\nu_\tau)^c \end{pmatrix}_L$	$\begin{pmatrix} -1 \\ 0 \\ 0 \end{pmatrix}$	$e_R, \mu_R, \tau_R$	$-1$

Table 3.6: Fermionic content of the  $\overline{331}$  model.

right-handed components are introduced necessarily for the charged leptons. Concerning the quark sector, in order to build an anomaly-free model, according to Tab. 3.3 two families must be arranged into triplets and one into an antitriplet; in order to obtain a realistic phenomenology, the third generation is chosen to be the antitriplet [186]. Three new quarks are present: two of down-type and one of up-type. Notice that the sign of the  $b$  or of the  $t$  quark has to be reversed to get the proper couplings to the charged SM gauge bosons, which has no effect on the diagonal couplings to the neutral gauge bosons. However, this affects the couplings of  $b$  and  $t$  to the heavy  $T$  and thus has physical consequences, but the ambiguity cannot be resolved up to now as the effect enters only in loops with the heavy  $T$  and it is not strong enough to significantly influence measured quantities. In the lepton sector, the minus sign can be assigned to the neutrino or to the charged lepton indifferently because all couplings are independent of the choice. The choice of  $\beta = 1/\sqrt{3}$  implies that no exotic charges are present, neither in the fermionic nor in the gauge sector [202–204].

The gauge bosons, in the mass basis, are

$$W_\mu^\pm = \frac{1}{\sqrt{2}}(W_\mu^1 \mp i W_\mu^2), \quad m_W^2 = g^2 \frac{v_\rho^2 + v_\eta^2}{4}, \quad (3.89a)$$

$$Y_\mu^\pm = \frac{1}{\sqrt{2}}(W_\mu^4 \mp i W_\mu^5), \quad m_Y^2 = g^2 \frac{v_\chi^2 + v_\rho^2}{4}, \quad (3.89b)$$

$$V_\mu^0, \bar{V}_\mu^0 = \frac{1}{\sqrt{2}}(W_\mu^6 \mp i W_\mu^7), \quad m_V^2 = g^2 \frac{v_\chi^2 + v_\eta^2}{4}, \quad (3.89c)$$

$$A_\mu = c_W W_\mu^3 + c_W \left( \frac{t_W}{\sqrt{3}} W_\mu^8 + \sqrt{1 - \frac{t_W^2}{3}} X_\mu \right), \quad m_A^2 = 0, \quad (3.89d)$$

$$Z_\mu = c_W W_\mu^3 + s_W \left( \frac{t_W}{\sqrt{3}} W_\mu^8 + \sqrt{1 - \frac{t_W^2}{3}} X_\mu \right), \quad m_Z^2 = g^2 \frac{v_\rho^2 + v_\eta^2}{4c_W^2}, \quad (3.89e)$$

$$Z'_\mu = -\sqrt{1 - \frac{t_W^2}{3}} W_\mu^8 + \frac{t_W}{\sqrt{3}} X_\mu, \quad (3.89f)$$

$$m_{Z'}^2 \simeq \frac{g^2 c_W^2}{3 - 4s_W^2} \left[ v_\chi^2 + \frac{v_\rho^2}{4} \left( t_W^2 + \frac{1}{c_W^4} \right) + \frac{v_\eta^2}{4} \left( 1 + \frac{1}{c_W^4} \right) \right].$$

$W_\mu^\pm, A_\mu, Z_\mu$  are the gauge bosons of the SM, while  $Y_\mu^\pm, V_\mu^0, \bar{V}_\mu^0$  and  $Z'_\mu$  are new heavy gauge bosons.

The scalar sector contains the three triplets

$$\chi = \begin{pmatrix} \chi_A^+ \\ \chi_B^0 \\ v_\chi + \xi_\chi + i\zeta_\chi \end{pmatrix}, \quad \rho = \begin{pmatrix} \rho_A^+ \\ v_\rho + \xi_\rho + i\zeta_\rho \\ \rho_B^0 \end{pmatrix}, \quad \eta = \begin{pmatrix} v_\eta + \xi_\eta + i\zeta_\eta \\ \eta_A^- \\ \eta_B^- \end{pmatrix}, \quad (3.90)$$

for which the mass eigenstates are

$$\phi_W^\pm = -s_\beta \rho_A^\pm + c_\beta \eta_A^\pm, \quad m_{\phi_W}^2 = 0, \quad (3.91a)$$

$$\phi_Y^\pm \simeq -\eta_B^\pm, \quad m_{\phi_Y}^2 = 0, \quad (3.91b)$$

$$\phi_V^0, \bar{\phi}_V^0 \simeq -\rho_B^0, -\bar{\rho}_B^0, \quad m_{\phi_V}^2 = 0, \quad (3.91c)$$

$$\phi_Z^0 \simeq -\zeta_\chi, \quad m_{\phi_Z}^2 = 0, \quad (3.91d)$$

$$\phi_{Z'}^0 \simeq s_\beta \zeta_\rho - c_\beta \zeta_\eta, \quad m_{\phi_{Z'}}^2 = 0, \quad (3.91e)$$

$$H_1^\pm = c_\beta \rho_A^\pm + s_\beta \eta_A^\pm, \quad m_{H_1}^2 = \frac{1}{s_\beta c_\beta} f v_\chi, \quad (3.91f)$$

$$H_2^\pm \simeq \chi_A^\pm, \quad m_{H_2}^2 = t_\beta f v_\chi + \frac{\lambda_9}{2} v_\chi^2, \quad (3.91g)$$

$$H_3^0, \bar{H}_3^0 \simeq \chi_B^0, \bar{\chi}_B^0, \quad m_{H_3}^2 = \frac{1}{t_\beta} f v_\chi + \frac{\lambda_7}{2} v_\chi^2, \quad (3.91h)$$

$$H_4^0 \simeq c_\beta \zeta_\rho + s_\beta \zeta_\eta, \quad m_{H_4}^2 = \frac{1}{s_\beta c_\beta} f v_\chi, \quad (3.91i)$$

$$H_5^0 \simeq \xi_\chi, \quad m_{H_5}^2 = 2\lambda_1 v_\chi^2, \quad (3.91j)$$

$$H_6^0 \simeq s_\beta \xi_\rho + c_\beta \xi_\eta, \quad m_{H_6}^2 = \frac{2(\lambda_2 v_\rho^4 + \lambda_4 v_\eta^4 + \lambda_5 v_\rho^2 v_\eta^2)}{v_\rho^2 + v_\eta^2}, \quad (3.91k)$$

$$H_7^0 \simeq -c_\beta \xi_\rho + s_\beta \xi_\eta, \quad m_{H_7}^2 = \frac{1}{s_\beta c_\beta} f v_\chi, \quad (3.91l)$$

$$(3.91m)$$

where  $s_\beta \equiv \sin \beta_{\rho\eta} = \frac{v_\rho}{\sqrt{v_\rho^2 + v_\eta^2}}$ . The  $\phi$ 's are the Goldstone bosons that give mass to the five gauge bosons,  $H_6$  is the neutral scalar field that can be identified with the SM Higgs boson, while  $H_1 \dots H_5$  and  $H_7$  are heavy (pseudo)scalar fields.

The Feynman rules of the  $\overline{331}$  model are listed in Appendix B. It is interesting to notice that the SM quark sector is strictly not affected by the effects of the gauge group enlargement, in the sense that, if we consider only the SM quarks and gauge bosons, their interactions are exactly the same as in the SM. On the contrary, in the lepton sector the new gauge bosons can couple two SM leptons; they are assigned

lepton number  $L = \mp 2$ , but carry no lepton generation number since they can mediate lepton-flavour violating processes at tree level. Consequently, strict bounds on the model come from the upper bounds on the  $\mu \rightarrow e\gamma$  decay set by the MEG experiment [205]; detailed studies on lepton-flavour violation have been performed in [206–211], and more insights into lepton masses, see-saw mechanisms and neutrino physics in 331 models can be found in [212–226].

We mention here that, in addition to consider realizations of the 331 model with different values of  $\beta$  and different fermionic contents, a variety of extensions with more NP features has been studied: supersymmetric extensions [227–242], the additions of further symmetries [243–251], the inclusion into GUTs [252–256], the dark matter candidates [257–259].

### 3.3.2 Quark mixing and FCNCs

The most general gauge-invariant Yukawa Lagrangian in the quark sector is

$$\begin{aligned} \mathcal{L}_Y^q &= \lambda_{ij}^J \bar{Q}_{i,L} \chi J_{j,R} + \lambda_{33}^J \bar{Q}_{3,L} \chi^* T_R \\ &+ \lambda_{ia}^D \bar{Q}_{i,L} \rho d_{a,R} + \lambda_{3a}^D \bar{Q}_{3,L} \eta^* d_{a,R} \\ &+ \lambda_{ia}^U \bar{Q}_{i,L} \eta u_{a,R} + \lambda_{3a}^U \bar{Q}_{3,L} \rho^* u_{a,R} + \text{h.c.} , \end{aligned} \quad (3.92)$$

where  $i = 1, 2$  so that  $J_j = D, S$ , while  $a = 1, 2, 3$  so that  $u_a = u, c, t$  and  $d_a = d, s, b$ . The pattern is similar to the 2HDM or to the SUSY one, with up- and down- quarks getting mass from different Higgs multiplets; instead, the new quarks get mass from another different multiplet at a different scale.

As in the SM, the mass eigenstates of the SM quarks can be obtained through unitary transformations of the left-handed multiplets:

$$\begin{pmatrix} u'_L \\ c'_L \\ t'_L \end{pmatrix} = U_L^{-1} \begin{pmatrix} u_L \\ c_L \\ t_L \end{pmatrix} , \quad \begin{pmatrix} d'_L \\ s'_L \\ b'_L \end{pmatrix} = V_L^{-1} \begin{pmatrix} d_L \\ s_L \\ b_L \end{pmatrix} . \quad (3.93)$$

As regards the exotic quarks, obviously the  $D$  and  $S$  quarks do not mix with the differently charged  $T$  quark; on the other hand, the mixing of  $D$  and  $S$  can be reabsorbed by a suitable parametrization of the rotation matrices. In fact, the exotic mass matrix  $M_J$  can be diagonalized by two block-diagonal unitary matrices  $W_L$  and  $W_R$ , and  $W_R$  can be removed by a redefinition of the right-handed heavy quark fields, while  $W_L$  can be absorbed into the definition of  $U_L$  and  $V_L$ . As a consequence, one can treat  $D, S, T$  as physical fields.

The rotation of the SM quarks affects the charged currents: the  $W$ -mediated current becomes

$$J_W^\mu = \bar{u}_L \gamma^\mu U_L^\dagger V_L d_L , \quad (3.94)$$

and hence the relevant matrix is the combination

$$V_{\text{CKM}} \equiv U_L^\dagger V_L , \quad (3.95)$$

that is just the SM CKM matrix. Nonetheless, differently from the SM, the  $U_L$  and  $V_L$  matrices are physical quantities: first of all they appear explicitly in the vertices

of the  $Y$  and  $V$  gauge bosons, but moreover they have also an important impact on the neutral currents. In fact, the quark mixing has no consequences on the  $A$  and  $Z$  interactions, as in the SM, but this is not true for the  $Z'$ , due to its different treatment of the third generation. Explicitly, we consider the  $Z'$ -mediated current, keeping only the phenomenologically interesting contributions, i.e. the left handed ones leaving out the exotic quarks that are too heavy as external states:

$$\begin{aligned}
J_{Z'}^\mu &= \bar{u}_L \gamma^\mu U_L^\dagger \begin{pmatrix} -1 + \frac{4}{3}s_W^2 & & \\ & -1 + \frac{4}{3}s_W^2 & \\ & & 1 - \frac{2}{3}s_W^2 \end{pmatrix} U_L u \\
&\quad + \bar{d}_L \gamma^\mu V_L^\dagger \begin{pmatrix} -1 + \frac{4}{3}s_W^2 & & \\ & -1 + \frac{4}{3}s_W^2 & \\ & & 1 - \frac{2}{3}s_W^2 \end{pmatrix} V_L d \\
&= (-1 + \frac{4}{3}s_W^2)(\bar{u}_L \gamma^\mu u_L + \bar{d}_L \gamma^\mu d_L) \\
&\quad + 2c_W^2 \bar{u}_L \gamma^\mu U_L^\dagger \begin{pmatrix} 0 & \\ & 0 \\ & & 1 \end{pmatrix} U_L u_L + 2c_W^2 \bar{d}_L \gamma^\mu V_L^\dagger \begin{pmatrix} 0 & \\ & 0 \\ & & 1 \end{pmatrix} V_L d_L,
\end{aligned} \tag{3.96}$$

i.e. the  $Z'$  can mediate tree-level FCNCs governed by the  $U_L$  and  $V_L$  matrices, introducing new sources of CP violation. This holds for all the 3-generations 331 models, since by construction two generations are treated equally and differently from the third. On the other hand, the universality of the coupling of the  $Z'$  to right-handed quarks implies that the FCNCs are purely left-handed, and the universality of its coupling to leptons guarantees that no FCNCs show up in this case. In addition, we underline that instead the new  $V^0$  gauge boson does not generate tree-level FCNCs between SM quarks, since it only mediates interactions between SM and exotic quarks. FCNCs in 331 models have been analyzed theoretically and phenomenologically in [260–271], and CP violation in [272–274].

In order to analyze the structure of these matrices, it is convenient to take  $V_L$  and  $V_{\text{CKM}}$  as the independent matrices. The structure of the CKM matrix is the same as in the SM since the form of the  $W$ -vertex is exactly the same and one can still rotate five independent, unphysical phases. The matrix  $V_L$  is a unitary matrix as well and therefore it is determined by nine parameters. As there are three new quarks in the theory, three phases are unphysical, and in  $V_L$  six parameters remain, three angles and three mixing phases. In order to draw out a parametrization of  $V_L$ , one has to analyze the structure of the other vertices in which it appears, i.e. with the currents

$$J_V^\mu = \bar{d}_L^i \gamma^\mu V_L^\dagger \begin{pmatrix} 1 & 0 \\ 0 & 1 \\ 0 & 0 \end{pmatrix}_{ia} D_L^a + \bar{T}_L \gamma^\mu (0 \ 0 \ 1)_i U_L u_L^i, \tag{3.97a}$$

$$J_Y^\mu = \bar{u}_L^i \gamma^\mu U_L^\dagger \begin{pmatrix} 1 & 0 \\ 0 & 1 \\ 0 & 0 \end{pmatrix}_{ia} D_L^a - \bar{T}_L \gamma^\mu (0 \ 0 \ 1)_i V_L d_L^i; \tag{3.97b}$$

from the second term in Eq. (3.97b) we see that rotating  $T$  by a complex phase  $\theta$  amounts to multiplying the third line in  $V_L$  by  $\theta$ ; in the first term in Eq. (3.97a) one can rotate the first and second line of  $V_L$  through an arbitrary phase rotation of each  $D$  and  $S$ . Therefore the transformations allowed for the  $V_L$  matrix are an independent phase rotation in every line. It is convenient to choose a parameterization that has a simple structure and as little parameters as possible in the third line, since these are the elements that will occur in the down-type FCNCs. Moreover, the parametrization must be compatible with the choice to treat  $D$  and  $S$  both as masses and interaction eigenstates. We will use the following parametrization [263]:

$$V_L = \begin{pmatrix} c_{12}c_{13} & s_{12}c_{23}e^{i\delta_3} - c_{12}s_{13}s_{23}e^{i(\delta_1-\delta_2)} & c_{12}c_{23}s_{13}e^{i\delta_1} + s_{12}s_{23}e^{i(\delta_2+\delta_3)} \\ -c_{13}s_{12}e^{-i\delta_3} & c_{12}c_{23} + s_{12}s_{13}s_{23}e^{i(\delta_1-\delta_2-\delta_3)} & -s_{12}s_{13}c_{23}e^{i(\delta_1-\delta_3)} - c_{12}s_{23}e^{i\delta_2} \\ -s_{13}e^{-i\delta_1} & -c_{13}s_{23}e^{-i\delta_2} & c_{13}c_{23} \end{pmatrix}. \quad (3.98)$$

Moreover, we will use the following notation for the  $Z'$ -mediated FCNCs of down quarks:

$$i\mathcal{L}_{\text{FCNC}} = i [\Delta^{sd}(s_L\gamma^\mu d_L) + \Delta^{bd}(b_L\gamma^\mu d_L) + \Delta^{bs}(b_L\gamma^\mu s_L)] Z'_\mu, \quad (3.99)$$

and similarly  $\Delta_{L,R}^{\mu\bar{\mu}}$  and  $\Delta^{\nu\bar{\nu}}$  for the couplings of  $Z'$  to leptons. For a generic 331 model with 3 generations the  $\Delta$ 's are

$$\Delta^{ij} = \frac{gc_W^2}{\sqrt{3}c_W\sqrt{1-(1+\beta^2)s_W^2}} v_{3i}^* v_{3j}, \quad (3.100a)$$

$$\Delta^{ji} = (\Delta^{ij})^*, \quad (3.100b)$$

$$\Delta_L^{\mu\bar{\mu}} = \frac{g[1-(1+\sqrt{3}\beta)s_W^2]}{2\sqrt{3}c_W\sqrt{1-(1+\beta^2)s_W^2}}, \quad (3.100c)$$

$$\Delta_R^{\mu\bar{\mu}} = \begin{cases} \frac{-gs_W^2}{c_W\sqrt{1-(1+\beta^2)s_W^2}} & \beta \neq \sqrt{3} \\ \frac{g\sqrt{1-4s_W^2}}{\sqrt{3}c_W} & \beta = \sqrt{3} \end{cases}, \quad (3.100d)$$

$$\Delta^{\nu\bar{\nu}} = \Delta_L^{\mu\bar{\mu}}, \quad (3.100e)$$

$$(3.100f)$$

where  $v_{ij} = (V_L)_{ij}$ ; in particular, in the  $\overline{331}$  model and using the value of the Weinberg angle, they read

$$\Delta^{sd} = 0.61gs_{13}s_{23}c_{13}e^{i(\delta_2-\delta_1)}, \quad (3.101a)$$

$$\Delta^{bd} = -0.61gs_{13}c_{13}c_{23}e^{-i\delta_1}, \quad (3.101b)$$

$$\Delta^{bs} = -0.61gs_{23}c_{13}^2c_{23}e^{-i\delta_2}, \quad (3.101c)$$

$$\Delta_L^{\mu\bar{\mu}} = 0.213g, \quad (3.101d)$$

$$\Delta_R^{\mu\bar{\mu}} = -0.183g, \quad (3.101e)$$

$$\Delta^{\nu\bar{\nu}} = 0.213g. \quad (3.101f)$$

## 3.4 Phenomenology of the $\overline{331}$ model

The previous phenomenological analyses of different kinds of 331 models can be found in [275–290] for hadron colliders and in [291–299] for lepton colliders.

### 3.4.1 Impact on the master functions

#### General structure

The key observation about the structure of the  $\overline{331}$  model is that it presents the same operators as the SM: neither left-right nor right-right effective vertices are introduced, and, neglecting the Higgs-mediated transition, the left-left operator is vectorial. As a consequence, the penguin-box expansion approach can be used without the definition of new master functions. However, the presence of the  $V_L$  matrix elements is a new source of both flavour violation and CP violation, and this implies that the master functions loose respectively their universality and their realness. In summary, the phenomenological effects of the  $\overline{331}$  model can be incorporated into the SM formulae for the relevant observables simply by performing a substitution of the master functions

$$F(x_t) \rightarrow F_i(x_t; \rho_{\overline{331}}) \equiv |F_i| e^{i\theta_F^i} , \quad (3.102)$$

where  $\rho_{\overline{331}}$  indicates the new parameters of the model, the  $i$  index indicates that the master function is flavour-dependent, and the  $\theta_F^i$  are the new CP-violating phases.

#### $\Delta F = 2$ transitions

The master function involved is  $S$ , that becomes

$$S_i(x_t; m_{Z'}, V_L) = S_0(x_t) + \Delta S_i^{(Z')} (m_{Z'}, V_L) + \Delta S_i^{(\text{Box})} \equiv |S_i| e^{i\theta_S^i} , \quad (3.103)$$

where  $S_0$  is the SM contribution,  $\Delta S_i^{(Z')}$  is the contribution due to the tree-level  $Z'$  exchange, and  $\Delta S_i^{(\text{Box})}$  is the contribution coming from the exchange of the new particles into the box diagram.

As regards the first contribution, from Fig. 3.1a we find

$$\Delta S_{\{sd,bd,bs\}}^{(Z')} (m_{Z'}, V_L) = \left[ \frac{\Delta_{\{sd,bd,bs\}}}{\lambda_t^{(sd,bd,bs)}} \right]^2 \frac{4\tilde{r}}{g_{\text{SM}}^2 m_{Z'}^2} , \quad (3.104)$$

where we have defined

$$\lambda_t^{(ij)} = (V_{\text{CKM}})^*_{ti} (V_{\text{CKM}})_{tj} , \quad g_{\text{SM}}^2 = \frac{2G_F \alpha}{\sqrt{2}\pi \sin^2 \theta_W} . \quad (3.105)$$

The  $\tilde{r}$  coefficient includes the renormalization group effects. It reads

$$\tilde{r} = \frac{C_1^{VLL}(m_{Z'})}{0.985} \eta_6^{6/21} \left[ 1 + 1.371 \frac{\alpha_s^{(6)}(m_t)}{4\pi} (1 - \eta_6) \right] , \quad (3.106)$$

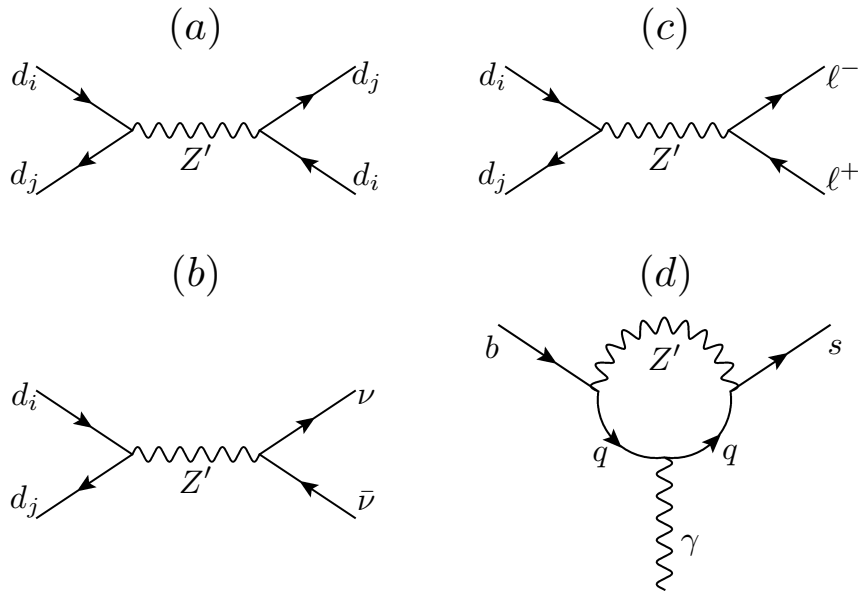


Figure 3.1:  $Z'$  contribution to: (a)  $\Delta F = 2$  transitions; (b)  $d_i \rightarrow d_j \ell^+ \ell^-$ ; (c)  $d_i \rightarrow d_j \nu \bar{\nu}$ ; (d)  $b \rightarrow s \gamma$ .

where

$$C_1^{VLL}(\mu) = 1 + \frac{\alpha_s}{4\pi} \left( -2 \log \frac{m_{Z'}^2}{\mu^2} \frac{11}{3} \right) \quad (3.107)$$

represents  $\mathcal{O}(\alpha_s)$  QCD corrections to  $Z'$  tree-level exchange [300] and the two factors involving

$$\eta_6 = \frac{\alpha_s^{(6)}(m_{Z'})}{\alpha_s^{(6)}(m_t)} \quad (3.108)$$

represent together NLO QCD renormalization group evolution from  $m_t$  to  $m_{Z'}$  as given in [138]; the renormalization scheme dependence of this evolution is cancelled by the one of  $C_1^{VLL}$ . The departure of  $\tilde{r}$  from unity is governed by the renormalization group effects between  $\mu_t$  and  $\mu_{Z'} = \mathcal{O}(m_{Z'})$ , absent in the SM, and by the difference in matching conditions between full and effective theories, involving tree diagrams in the 331 models while box diagrams in the SM. These are represented by  $C_1^{VLL}(m_{Z'})$  and the numerical factor 0.985 [53], respectively. The latter factor describes flavour universal QCD correction to  $S_0(x_t)$  in the SM and is usually included in  $\eta_B$  and  $\eta_2$  [53]. The coefficient 1.371, calculated in [138], corresponds to the effective theory with six flavours. We implicitly assume that the new fermions  $D, S, T$  are heavier than  $Z'$ ; their inclusion into this formula would have a very small impact on  $\tilde{r}$ . Note that  $\tilde{r}$  is free from hadronic uncertainties; it is also flavour universal, as the flavour dependence is already included in  $\eta_2$ ,  $\eta_B$ ,  $\hat{B}_q$  and  $\hat{B}_K$ , which have been factored out. The numerical values for  $\tilde{r}$ , for the values of  $m_{Z'}$  that we will use in the numerical analysis, are

$$\tilde{r}(m_{Z'} = 1 \text{ TeV}) = 0.985, \quad \tilde{r}(m_{Z'} = 3 \text{ TeV}) = 0.9534. \quad (3.109)$$

In principle one should also include new box diagram contributions with new charged and neutral gauge bosons and new quark exchanges; charged Higgs particles can also contribute. However it is possible to show that these contributions are negligible even without explicit calculations. Indeed, compared to the SM contributions, the new box contributions are suppressed automatically by a factor  $m_W^2/m_V^2 \leq 0.006$ , where  $m_V \geq 1$  TeV stands for the masses of the new gauge bosons. In models with new left-right operators this suppression could be compensated by enhanced hadronic matrix elements of new operators and QCD renormalization group effects; however, in 331 models only the SM operator is present and such enhancements are absent. Another enhancement could be present through increased values of the elements of the mixing matrix  $V_L$ , but our analysis shows that, in order to suppress sufficiently tree-level  $Z'$  contributions to  $\Delta F = 2$  processes, the hierarchical structure of  $V_L$  resembles the structure of the CKM matrix. Box diagrams are also suppressed with respect to the tree-level contributions by a loop factor  $1/(16\pi^2)$  and two additional vertices. In summary, it is safe to keep only  $Z'$  contributions; this simplifies significantly the analysis as new box diagrams depend generally on many more new parameters, like masses of new gauge bosons and fermions and new mixing angles.

### $\Delta F = 1$ transitions

According to what we have just discussed, we will neglect the loop contributions also in this case.

- $d_i \rightarrow d_j \nu \bar{\nu}$

In the SM, the  $Z$ -penguin and the box diagram that contribute to this process are contained in the  $X$  master function, which with the  $Z'$  contribution in Fig. 3.1c becomes here

$$X_{\{sd,bd,bs\}}(m_t; m_{Z'}, V_L) = X(x_t) + \frac{\Delta^{\nu\bar{\nu}}}{g_{\text{SM}}^2 m_{Z'}^2} \frac{\Delta^{\{sd,bd,bs\}}}{\lambda_t^{\{sd,bd,bs\}}} \equiv |X_i| e^{i\theta_X^i} . \quad (3.110)$$

- $d_i \rightarrow d_j \ell^+ \ell^-$

In this transition the relevant loop functions is the  $Y$ , which in the SM is a linear combination of the  $V - A$  component of the  $Z$ -penguin and the box diagrams with final leptons with weak isospin  $T_3 = -1/2$ , and  $Z$ , which is a linear combination of the vector component of the  $Z$ -penguin and the  $\gamma$  penguin; they are modified as follows by the contribution in Fig. 3.1b:

$$Y_{\{sd,bd,bs\}}(m_t; m_{Z'}, V_L) = Y(x_t) + \frac{\Delta_A^{\mu\bar{\mu}}}{g_{\text{SM}}^2 m_{Z'}^2} \frac{\Delta^{\{sd,bd,bs\}}}{\lambda_t^{\{sd,bd,bs\}}} \equiv |Y_i| e^{i\theta_Y^i} , \quad (3.111)$$

$$Z_{\{sd,bd,bs\}}(m_t; m_{Z'}, V_L) = Z(x_t) + \frac{2}{4 \sin^2 \theta_W} \frac{\Delta_R^{\mu\bar{\mu}}}{g_{\text{SM}}^2 m_{Z'}^2} \frac{\Delta^{\{sd,bd,bs\}}}{\lambda_t^{\{sd,bd,bs\}}} \equiv |Z_i| e^{i\theta_Z^i} , \quad (3.112)$$

where we have defined  $\Delta_A^{\mu\bar{\mu}} = \Delta_R^{\mu\bar{\mu}} + \Delta_L^{\mu\bar{\mu}}$ .

- $\mathbf{b} \rightarrow \mathbf{s} \gamma$

Very detailed analyses of  $B \rightarrow X_s \gamma$  decay in 331 models have been presented in [260], [266], and it has been found that the dominant NP contributions come from the Higgs sector. In the numerical analysis that we are going to perform, we will not consider the parameters involved in this sector, which being particularly rich do not provide significant predictions. Similarly, the subleading contributions involving the new gauge bosons  $V^0$  and  $Y^\pm$  and the new heavy quarks involve new parameters and their contributions can be suppressed if necessary without any impact on our analysis. The only contributing diagram that involves only the  $Z'$  as a new particle is shown in Fig. 3.1d; we have performed a novel analysis regarding its QCD corrections, founding that it determines a correction of  $\mathcal{O}(10^{-4})$  with respect to the SM prediction, and hence is negligible as expected [301].

### 3.4.2 Correlations

The  $\overline{331}$  model does not satisfy Constrained Minimal Flavour Violation, since the master functions are neither flavour universal nor real; the pattern of flavour violation can be investigated by looking at the deviation from unity of the  $r$  parameters, that in this case read:

$$r(\Delta M) = \left| \frac{S_{bd}}{S_{bs}} \right|, \quad r(\mu^+ \mu^-) = \left| \frac{Y_{bd}}{Y_{bs}} \right|^2, \quad r(\nu \bar{\nu}) = \left| \frac{X_{bd}}{X_{bs}} \right|^2. \quad (3.113)$$

On the other hand, due to the small number of new parameters, a noticeable pattern of correlations can be recognized. In fact, we make the following observations.

- The good consistence of the CKM theory with experiments implies that the angles and the phases of the new  $V_L$  matrix should be very small; as a consequence, it is a good approximation to set  $c_{12} \simeq c_{13} \simeq c_{23} \simeq 1$ , provided that a post-check is made with the obtained values of the relative sine terms. Then, fixing the mass of the  $Z'$ , the  $\overline{331}$  contributions depend only on four new parameters:

$$s_{13}, \quad s_{23}, \quad \delta_1, \quad \delta_2. \quad (3.114)$$

- Going further, we notice that:
  - $\Delta^{bd}$  depends only on  $s_{13}$  and  $\delta_1$ . As a consequence, we expect direct correlations between the  $B_d$ -related observables, such as  $\Delta M_d$ ,  $S_{\psi K_S}$  in the mixing,  $B_d \rightarrow \mu^+ \mu^-$ ,  $S_{\mu^+ \mu^-}^d$  in the dimuon decay.
  - $\Delta^{bs}$  depends only on  $s_{33}$  and  $\delta_2$ . As a consequence, analogously to the previous case, we expect direct correlations between the  $B_s$ -related observables, i.e.  $\Delta M_s$ ,  $S_{\psi \phi}$  in the mixing,  $B_s \rightarrow \mu^+ \mu^-$ ,  $S_{\mu^+ \mu^-}^s$ ,  $A_{\Delta \Gamma}^\lambda$  in the dimuon decay, the rare decays  $B \rightarrow X_s \nu \bar{\nu}$ .

- $\Delta^{ds}$  depends on all the four parameters, and (weaker) correlations can be expected between the observables in the  $K$  system. Moreover, when experimental constraints are taken into account, this will provide indirect correlations between the  $B_d$ - and  $B_s$ -observables.

Given the simple structure of the  $Z'$  contribution, the form of these correlations can be derived in analytical form even for arbitrary values of  $\beta$ .

- In order to estimate the correlation between the mixing in the  $K$  sector and in the  $B_{d,s}$  sector, we consider the ratio

$$\frac{\Delta S_{sd}}{\Delta S_{bd} \Delta S_{bs}^*} = \frac{m_{Z'}^2 g_{\text{SM}}^2}{4\tilde{r}} \left[ \frac{\Delta^{sd}}{\Delta^{bd}(\Delta^{bs})^*} \right]^2 = 0.41 \left( \frac{m_{Z'}}{\text{TeV}} \right)^2 \frac{1 - (1 + \beta^2) s_W^2}{\tilde{r}} \xrightarrow{\beta=1/\sqrt{3}} 0.28 \left( \frac{m_{Z'}}{\text{TeV}} \right)^2 \frac{1}{\tilde{r}}. \quad (3.115)$$

This relation implies that after the experimental constraints on  $\Delta M_{d,s}$  have been taken into account, the effects in  $\epsilon_K$  are smaller than in  $\Delta M_{d,s}$  for values  $m_{Z'} \leq 3$  TeV. Indeed, NP contributions in  $\Delta M_{d,s}$  are constrained to be at most 10% of the SM values and therefore the absolute values of  $\Delta^{\{bd,bs\}}$  can be at most 0.25. As  $\tilde{r} \approx 1$ , we find  $\Delta^{\{ds\}} \leq 0.16$ , which implies a correction of at most 6%. However, for much larger values of  $m_{Z'}$  these effects can increase significantly.

- In order to estimate the impact of the variation in the mixing observables to the  $\nu\bar{\nu}$  decays, the relevant comparison is

$$\frac{\Delta X_{\{bd,bs\}}}{\sqrt{\Delta S_{\{bd,bs\}}^*}} = \{\pm\} \frac{\Delta^{\nu\bar{\nu}}}{\sqrt{\tilde{r}} g_{\text{SM}} m_{Z'}} = \{\mp\} 0.255 \left( \frac{\text{TeV}}{m_{Z'}} \right) \frac{1 - (1 + \sqrt{3}\beta) s_W^2}{\tilde{r} \sqrt{1 - (1 + \beta^2) s_W^2}} \xrightarrow{\beta=1/\sqrt{3}} \{\mp\} 0.165 \left( \frac{m_{Z'}}{\text{TeV}} \right) \frac{1}{\sqrt{\tilde{r}}}. \quad (3.116)$$

This result implies that NP effects in the processes with  $\nu\bar{\nu}$  in the final state are rather small for  $m_{Z'} = 3$  TeV: requiring again that  $\Delta^{\{bd,bs\}} \leq 0.25$  we find that only effects of at most 5% on branching ratios are expected for  $b \rightarrow s\nu\bar{\nu}$  transitions; these effects are even smaller for the  $K$  decays. For  $m_{Z'} = 1$  TeV the relevant mixing parameters  $s_{13}$  and  $s_{23}$  have to be lowered by roughly a factor of 3 to satisfy the  $\Delta M_{d,s}$  constraint. The inspection of the dependence on mixing angles shows that the decrease of the latter is compensated approximately by the decrease of  $m_{Z'}$  in the case of  $K^+ \rightarrow \pi^+ \nu\bar{\nu}$  and  $K_L \rightarrow \pi^0 \nu\bar{\nu}$ , and it is overcompensated in the case of  $b \rightarrow s\nu\bar{\nu}$  transitions, so that modifications of the branching ratios by 15% are possible in this case.

- As regards the correlation between the decays with  $\nu\bar{\nu}$  and  $\mu^+ \mu^-$  in the final state, the ratio

$$\frac{\Delta Y_i}{\Delta X_i} = - \frac{1 - (1 - \sqrt{3}\beta) s_W^2}{1 - (1 + \sqrt{3}\beta) s_W^2} \xrightarrow{\beta=1/\sqrt{3}} -1.86 \quad (3.117)$$

implies that NP effects in the  $\mu^+\mu^-$  decays can be larger than in the case of  $\nu\bar{\nu}$ . This is not only because of the factor  $-1.9$  in this relation, but also because, concerning the SM contributions,  $Y(x_t)$  is smaller than  $X(x_t)$ ; thus for  $m_{Z'} = 3$  TeV effects of 10-15% on the branching ratio are still allowed in  $B_{d,s} \rightarrow \mu^+\mu^-$  and these effects are expected to increase up to 30% for  $m_{Z'} = 1$  TeV. Interestingly the NP effects in  $B_{d,s} \rightarrow \mu^+\mu^-$  and  $B \rightarrow X_s\nu\bar{\nu}$  are anticorrelated, and similarly for  $K^+ \rightarrow \pi^+\nu\bar{\nu}$  and  $K_L \rightarrow \mu^+\mu^-$ ; unfortunately, due to small NP effects in decays with  $\nu\bar{\nu}$  in the final states, these anticorrelations will be difficult to test.

Moreover, these relations allow to point out that, once the constraints on  $\Delta M_{d,s}$  are taken into account, the NP effects for  $\beta = \sqrt{3}$  both in  $\epsilon_K$  and in all rare decays are so small that it will be difficult to distinguish this model from the SM on the basis of flavour violation in meson decays.

### 3.4.3 Numerical analysis

#### Strategy

Since in all the  $\overline{331}$  contributions that we are going to consider the key role is played by the new  $Z'$  boson, first of all it is fundamental to determine a plausible working range for its mass. Lower bounds on  $m_{Z'}$  within 331 models were discussed in literature, from the study of  $\mu$  decay [165, 186, 206],  $Z'$  decays to  $e^+e^-$  or  $\mu^+\mu^-$  [302], or from the analysis of  $S$ ,  $T$ ,  $U$  parameters [167]; however, the resulting bounds are model dependent, since they depend also on the entries of the matrices that transform the quark gauge eigenstates into mass eigenstates. Concerning the direct lower bound on  $m_{Z'}$  from collider experiments, the most stringent bounds are provided by CMS experiment [303]; the precise value depends on the model considered: while for the so-called sequential  $Z'$  the lower bound for  $m_{Z'}$  is of about 2.5 TeV, in other models values as low as 1 TeV are still possible, and we will use the latter in order to be more general. As regards the upper bounds on  $m_{Z'}$ , as we have discussed about Eq. (3.31), some realization of the 331 model present the interesting feature of an upper limit to the breaking scale and consequently to the mass of the  $Z'$ ; however, it can be seen that this is not the case of the models with  $\beta = 1/\sqrt{3}$ . Hence we choose to investigate the range  $1 \text{ TeV} \leq m_{Z'} \leq 3 \text{ TeV}$ , that is testable in the nearby future by present experiments, and we will discuss the case in which  $Z'$  is beyond the LHC reach at the end.

As our discussion about the correlations in the  $\overline{331}$  model indicates, the imposition of the experimental constraints on  $\Delta M_{d,s}$  for the chosen range of  $m_{Z'}$  implies very small effects in  $\epsilon_K$ . Moreover, in the  $\overline{331}$  model there are no new tree-level contributions to  $B^+ \rightarrow \tau^+\nu_\tau$ . Both these aspects favor a value of  $|V_{ub}|$  that is closer to inclusive determinations, i.e. to what we have called Scenario 2, in which  $\epsilon_K$  is in good agreement with data and  $B^+ \rightarrow \tau^+\nu_\tau$  is closer to the experimental value than in the SM. Therefore we perform our numerical analysis setting  $|V_{ub}| = 4.0 \cdot 10^{-3}$ , and the other three CKM input parameters  $|V_{us}|$ ,  $|V_{cb}| = 0.0406$ ,  $\gamma$  at their central values measured in tree level decays; we checked that varying  $|V_{ub}|$  within  $\pm 5\%$  has

only minor impact on our results. Once four parameters have been fixed, we derive the other entries requiring the unitarity of the CKM matrix; defining [45]

$$\lambda = |V_{us}|, \quad A = \frac{|V_{cb}|}{\lambda^2}, \quad (3.118a)$$

$$R_b = \left(1 - \frac{\lambda^2}{2}\right) \frac{1}{A\lambda^3} |V_{ub}|, \quad R_t = \sqrt{1 + R_b^2 - 2R_b \cos \gamma}. \quad (3.118b)$$

the elements that we are going to use are:

$$|V_{td}| = A\lambda^3 R_t = 8.49 \cdot 10^{-3}, \quad (3.118c)$$

$$\beta = -\arg(V_{td}) = \arctan\left(\frac{R_b \sin \gamma}{1 - R_b \sin \gamma}\right) = 25.2^\circ, \quad (3.118d)$$

$$|V_{ts}| = \left| -A\lambda^2 \left[ \left(1 - \frac{\lambda^2}{2}\right) + \left(\frac{2\lambda^2}{2 - \lambda^2}\right) (1 - R_t e^{i\beta}) \right] \right| = 0.0399, \quad (3.118e)$$

$$\beta_s = \arg(-V_{ts}) = 1.2^\circ, \quad (3.118f)$$

$$V_{tb} = 1 - \frac{1}{2} A^2 \lambda^4 = 0.9992. \quad (3.118g)$$

Now, having fixed the CKM matrix and a range for  $m_{Z'}$ , the goals of our numerical analysis are: (i) to explore the space of the new parameters in order to see if it is constrained by the experimental data; (ii) to study if the freedom in the allowed regions permits to solve the anomalies in the flavour data. The first step can be realized in an elegant and straightforward way by using the particular pattern of dependences that we have recognized in the previous section, and in particular using only the experimental limits on the two pairs of observables  $(\Delta M_d, S_{\psi K_S})$  and  $(\Delta M_s, S_{\psi\phi})$ , which constrain separately the pairs of parameters  $(s_{13}, \delta_1)$  and  $(s_{23}, \delta_2)$  respectively. Once the possible regions of the parameter space have been identified in this way, we let the parameters vary into them and study the impact of this on all the other relevant observables in the  $K$ ,  $B_d$ ,  $B_s$  mixing and decays, in order to verify where their experimental limits are respected and then if the present tensions can be relaxed.

### Identification of the space parameter regions

As we have anticipated, in order to perform a first analysis of the parameter space, we consider the  $\Delta F = 2$  pairs of observables  $(\Delta M_s, S_{\psi\phi})$  and  $(\Delta M_d, S_{\psi K_S})$  independently. We set all the other input parameters at their central values, and in order to take partially hadronic and experimental uncertainties into account we require the  $\overline{331}$  model to reproduce the data for  $\Delta M_{s,d}$  within  $\pm 5\%$  and the data on  $S_{\psi\{\phi, K_S\}}$  within experimental  $2\sigma$ , i.e. we allow the ranges

$$1.112 \cdot 10^{-11} \text{ GeV} \leq \Delta M_s \leq 1.231 \cdot 10^{-11} \text{ GeV} \quad -0.18 \leq S_{\psi\phi} \leq 0.18, \quad (3.119a)$$

$$3.159 \cdot 10^{-13} \text{ GeV} \leq \Delta M_d \leq 3.488 \cdot 10^{-13} \text{ GeV} \quad 0.64 \leq S_{\psi K_S} \leq 0.72. \quad (3.119b)$$

We underline that in this scenario for  $V_{ub}$  the SM predictions for both  $\Delta M_d$  and  $\Delta M_s$  and also for  $S_{\psi K_S}$  fall outside this ranges; in fact, one of our aims is to see if the

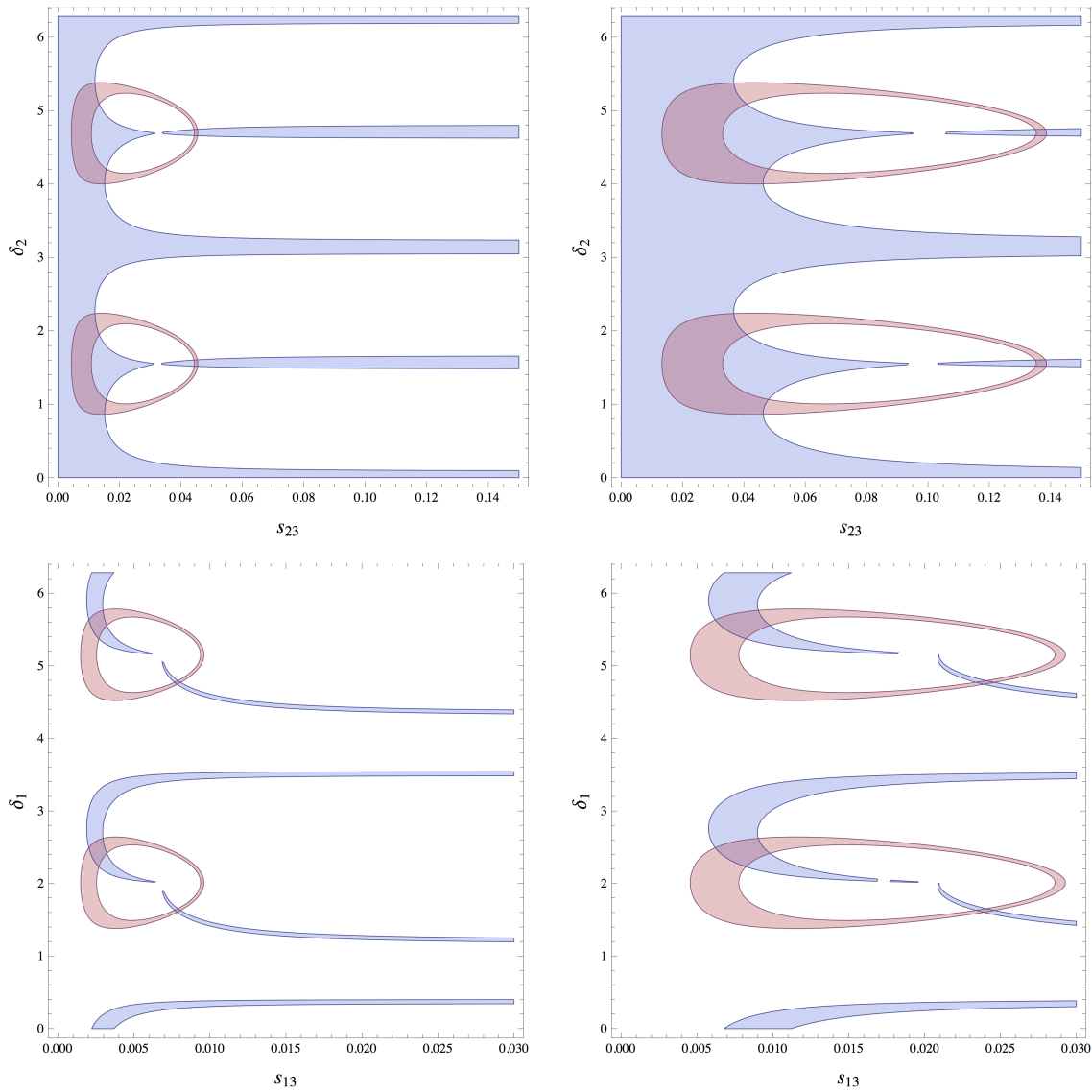


Figure 3.2: Conditions of consistency of the  $\overline{331}$  parameters  $s_{13}, s_{23}, \delta_1, \delta_2$  with the experimental data of  $\Delta M_d, \Delta M_s, S_{\psi K_s}, S_{\psi\phi}$ . In the upper panel the shaded areas of  $(s_{23}, \delta_2)$  are the ones allowed by the conditions on  $\Delta M_s$  (red) and  $S_{\psi\phi}$  (blue). Analogously, in the lower panel they are the ones of  $(s_{13}, \delta_1)$  allowed by the conditions on  $\Delta M_d$  (red) and  $S_{\psi K_s}$  (blue). The plots on the left are obtained for  $m_{Z'} = 1$  TeV, the ones on the right for  $m_{Z'} = 3$  TeV.

$\overline{331}$  model can improve the performance of the SM. Now, these conditions, for fixed  $m_{Z'} = 1$  TeV and  $m_{Z'} = 3$  TeV, select the regions of the parameter space shown in Fig. 3.2. We can see that each couple of conditions is satisfied in four disjoint regions in the two planes of parameters; being the conditions and the parameters independent, we obtain therefore 16 distinct intervals of parameters. We will denote as  $A_i(m_{Z'}/\text{TeV})$  and  $B_i(m_{Z'}/\text{TeV})$  the allowed regions in the  $(s_{23}, \delta_2)$  and  $(s_{13}, \delta_1)$  respectively, as illustrated in Fig. 3.3; the numerical bounds of these regions are

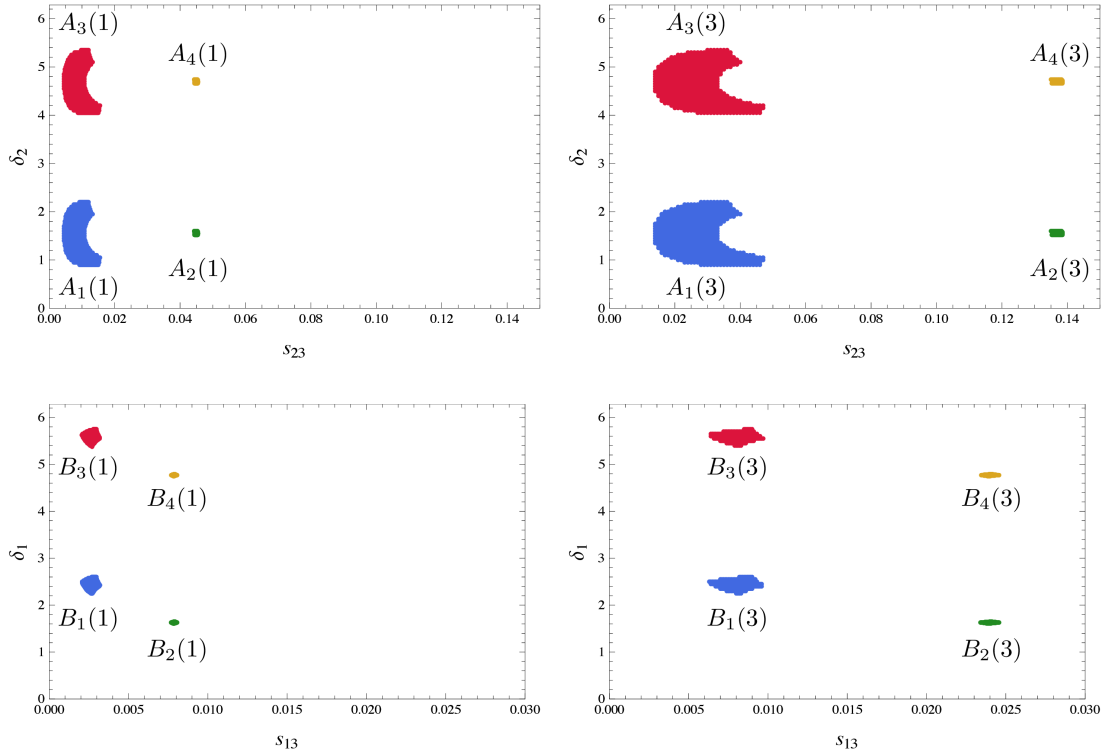


Figure 3.3: Allowed regions in the  $(s_{23}, \delta_2)$  plane (upper panel) and  $(s_{13}, \delta_1)$  plane (lower panel). The plots on the left are obtained for  $m_{Z'} = 1$  TeV, the ones on the right for  $m_{Z'} = 3$  TeV. The used names for the region are shown, as well as their numerical sampling.

	$s_{23}$	$\delta_2$		$s_{13}$	$\delta_1$
$A_1(1)$	[0.004, 0.016]	[49°, 129°]	$B_1(1)$	[0.0019, 0.0033]	[126°, 152°]
$A_2(1)$	[0.044, 0.046]	[83°, 95°]	$B_2(1)$	[0.0075, 0.0081]	[89°, 97°]
$A_3(1)$	[0.004, 0.016]	[229°, 308°]	$B_3(1)$	[0.0019, 0.0033]	[306°, 352°]
$A_4(1)$	[0.044, 0.046]	[263°, 275°]	$B_4(1)$	[0.0075, 0.0081]	[269°, 277°]
$A_1(3)$	[0.012, 0.048]	[49°, 129°]	$B_1(3)$	[0.006, 0.010]	[126°, 152°]
$A_2(3)$	[0.13, 0.15]	[83°, 95°]	$B_2(3)$	[0.022, 0.024]	[89°, 97°]
$A_3(3)$	[0.012, 0.048]	[229°, 308°]	$B_3(3)$	[0.006, 0.010]	[306°, 352°]
$A_4(3)$	[0.13, 0.15]	[263°, 275°]	$B_4(3)$	[0.022, 0.024]	[269°, 277°]

Table 3.7: Allowed intervals for  $(s_{23}, \delta_2)$  and  $(s_{13}, \delta_1)$ .

listed in Tab. 3.7.

Two immediate considerations are that the regions with  $i = 2, 4$  are very small, and that for each allowed region with a given  $\delta_i$  the one with  $\delta_i$  shifted by 180° is allowed too. As regards the dependence on the mass of the  $Z'$ , we notice that the increase of  $m_{Z'}$  by a factor of three allows to increase  $s_{13}$  and  $s_{23}$  by the same factor; this structure is evident from the formulae for  $\Delta S_{bq}$ . Conversely, the ranges

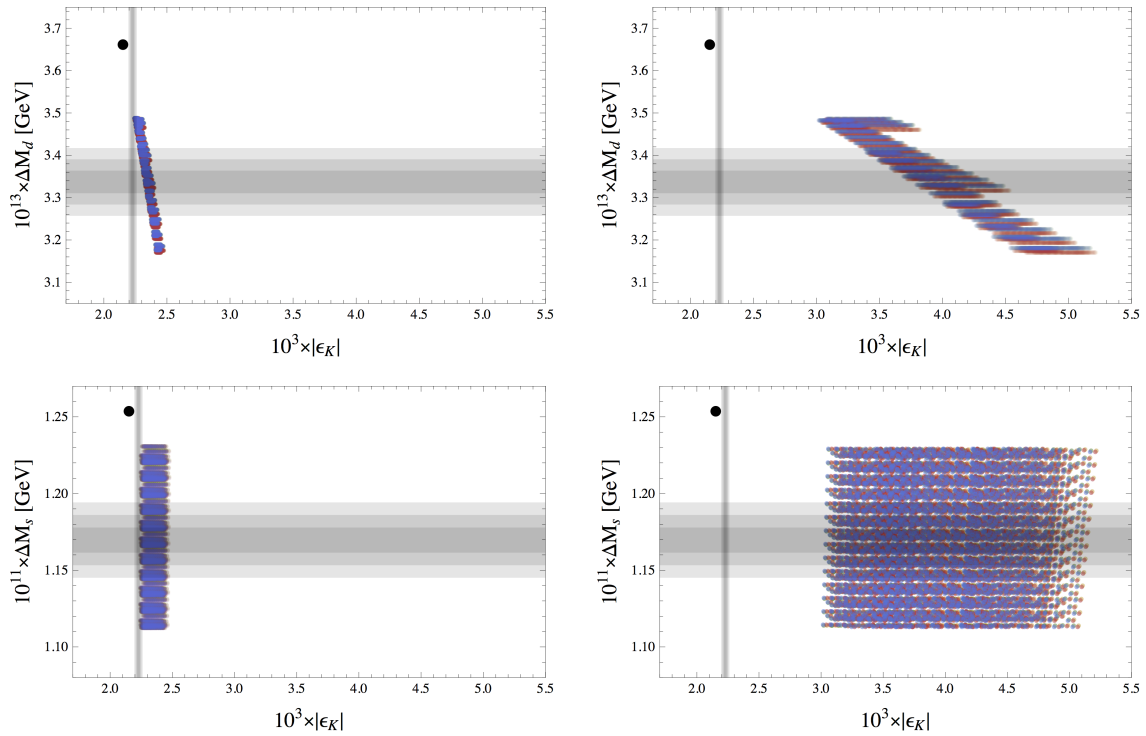


Figure 3.4:  $\epsilon_K$  versus  $\Delta M_d$  (upper panel) and  $\Delta M_s$  (lower panel), for  $m_{Z'} = 1$  TeV (left plots) and  $m_{Z'} = 3$  TeV (right plots). The parameters  $(s_{23}, \delta_2; s_{13}, \delta_1)$  vary in the regions  $(A_2, B_1)$  (blue),  $(A_4, B_1)$  (red),  $(A_2, B_3)$  (green),  $(A_4, B_3)$  (yellow), all superposed. The shaded grey regions are the experimental  $1\sigma - 3\sigma$  error ranges, while the black points are the central values of the SM predictions.

for  $\delta_i$  are not affected by the variation of  $m_{Z'}$ .

### Indications from other observables

- $\epsilon_K$

Once we have considered the observables of the  $\Delta F = 2$  transitions in the  $B_d$  and  $B_s$  systems to constrain independently two planes of the parameter space, we turn to the  $K$  system that involves all the observables; in particular, the  $\Delta F = 2$  observable  $\epsilon_K$  provides very useful indications.

First of all we consider the four small regions between the allowed ones. It turns out that they correspond to NP contributions to  $M_{12}^d$  and  $M_{12}^s$  that are larger than their SM values roughly by a factor of two, but carry opposite signs; as  $\Delta M_{d,s}$  involve the absolute values of the mixing amplitudes, these regions cannot be eliminated on the basis of them, and to this aim other observables have to be invoked. In fact, it turns out that, when  $(s_{23}, \delta_2)$  vary in the small regions  $A_2$  and  $A_4$ , the predictions for  $\epsilon_K$  are well above its experimental measurement, worsening with the increase of  $m_{Z'}$ , as shown in Fig. 3.4. As a consequence, if we require only that  $\epsilon_K$  does not differ more than 5% with respect to the experimental central value (a bound even larger

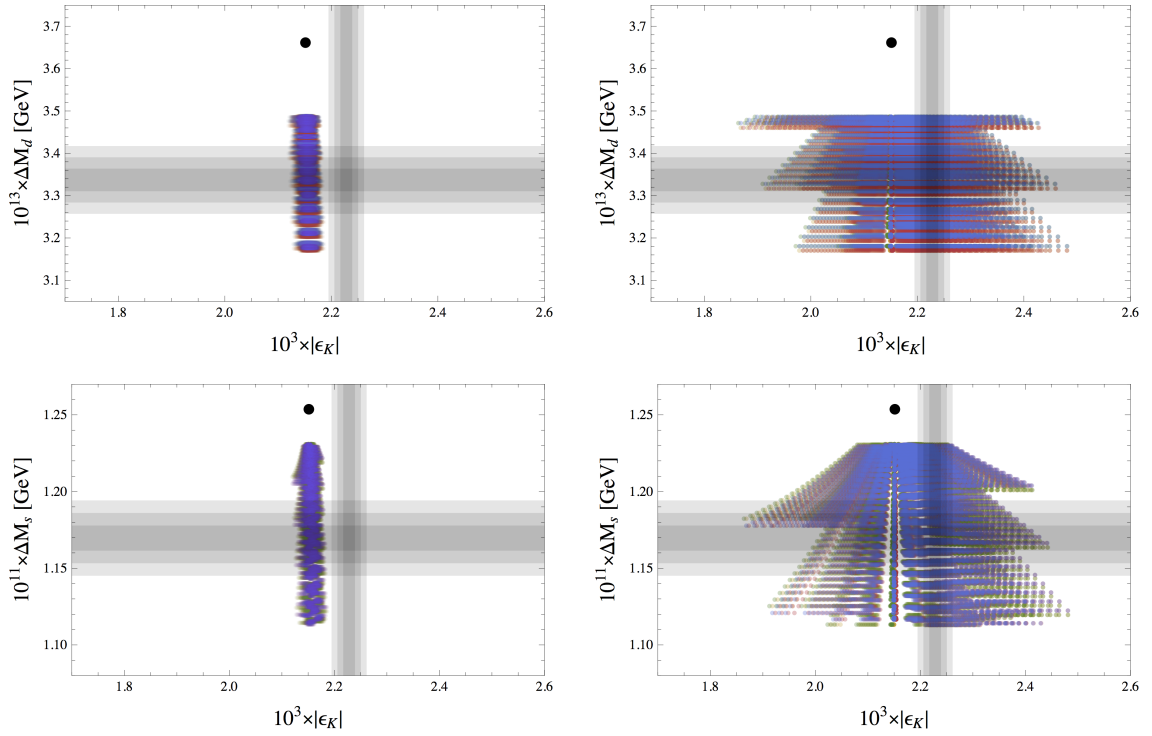


Figure 3.5:  $\epsilon_K$  versus  $\Delta M_d$  (upper plots) and  $\Delta M_s$  (lower plots), for  $m_{Z'} = 1$  TeV (left plots) and  $m_{Z'} = 3$  TeV (right plots). The parameters  $(s_{23}, \delta_2; s_{13}, \delta_1)$  vary in the regions  $(A_1, B_1)$  (blue),  $(A_3, B_1)$  (red),  $(A_1, B_3)$  (green),  $(A_3, B_3)$  (yellow), all superposed. The shaded grey regions are the experimental  $1\sigma - 3\sigma$  error ranges, while the black points are the central values of the SM predictions.

than the experimental uncertainty), these parameter regions can be excluded, provided the theoretical and parametric uncertainties in  $\epsilon_K$  could be lowered down to 5%; this is clearly not the case at present, especially due to  $V_{cb}^4$  dependence present in  $\epsilon_K$ , but could become realistic in the second half of this decade. At the end we are left with 8 possible combinations of regions  $(A_i, B_j)$ .

The second interesting feature arises when we let the parameters vary into the large regions  $A_1, A_3$  and  $B_1, B_3$ ; the results are shown in Fig. 3.5. It is evident how imposing that  $\Delta M_d$  and  $\Delta M_s$  are in agreement with their experimental values and hence lower than their SM prediction does not have a strong impact on  $\epsilon_K$ , that stays within a few percents from the experimental central value and SM prediction; as expected, in this case the room for NP contributions is larger for larger  $Z'$  mass. Thus these plots show that this model does not suffer from the  $\Delta M_{s,d} - |\epsilon_K|$  tension that has been identified in CMFV models.

- $\mathbf{B}_{d,s} \rightarrow \mu^+ \mu^-$

The data from the superstar decays of the flavour physics at LHC will be fundamental in order to univocally select the region of the parameters of the  $\overline{331}$  model and to provide additional stringent tests.

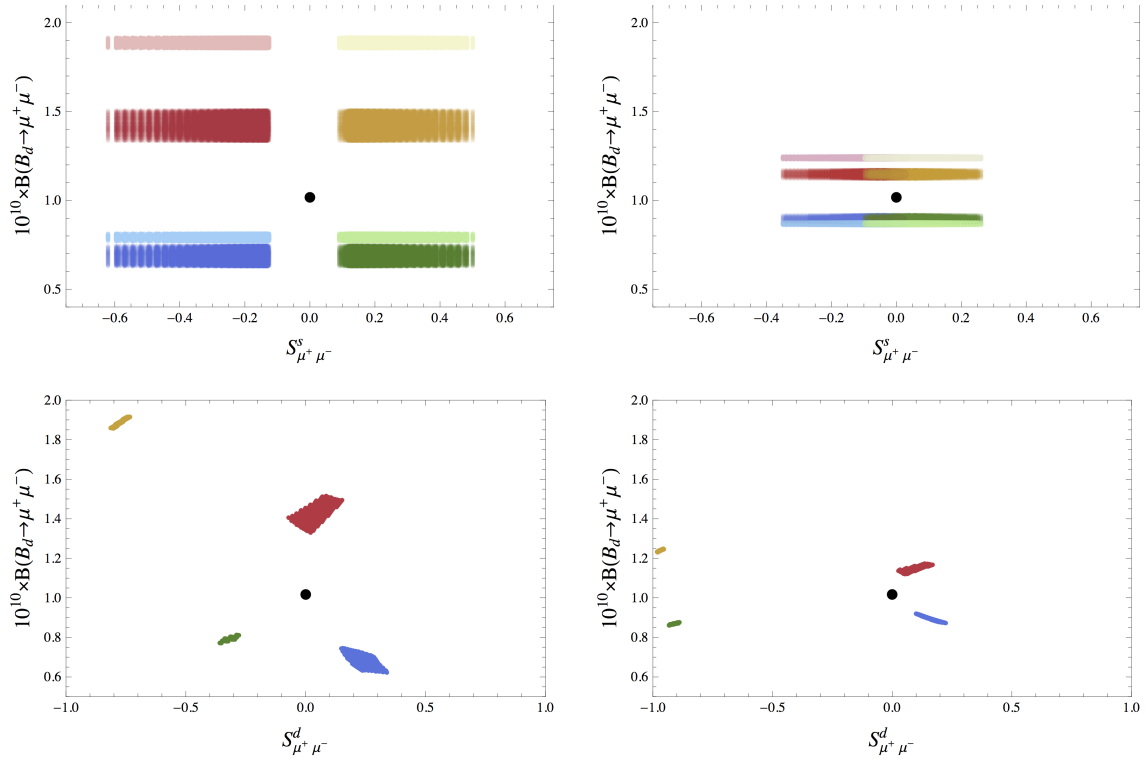


Figure 3.6: Upper panel:  $\mathcal{B}(B_d \rightarrow \mu^+ \mu^-)$  versus  $S_{\mu^+ \mu^-}^s$ , for  $m_{Z'} = 1$  TeV (left) and  $m_{Z'} = 3$  TeV (right). The parameters  $(s_{23}, \delta_2; s_{13}, \delta_1)$  vary in the regions  $(A_1, B_1)$  (blue),  $(A_1, B_3)$  (red),  $(A_3, B_1)$  (green),  $(A_3, B_3)$  (yellow),  $(A_1, B_2)$  (light red),  $(A_1, B_4)$  (light blue),  $(A_3, B_2)$  (light yellow),  $(A_3, B_4)$  (light green). Lower panel:  $\mathcal{B}(B_d \rightarrow \mu^+ \mu^-)$  versus  $S_{\mu^+ \mu^-}^d$ , when the parameters  $(s_{13}, \delta_1)$  vary in the regions  $B_1$  (blue),  $B_3$  (red),  $B_2$  (green),  $B_4$  (yellow). The black points are the central values of SM predictions.

We have found a very powerful way to distinguish the effects from the different parameter regions when looking simultaneously at the two observables  $S_{\mu^+ \mu^-}^s$  and  $\mathcal{B}(B_d \rightarrow \mu^+ \mu^-)$ . In fact, as shown in the upper plots of Fig. 3.6, when these quantities will be measured, possible deviations from the SM prediction would select one large region and one small region between the 8 we are left with. In particular:

- $(A_1, B_1)$  and  $(A_1, B_4)$  are chosen when  $S_{\mu^+ \mu^-}^s < 0$  and  $\mathcal{B}(B_d \rightarrow \mu^+ \mu^-) < \mathcal{B}(B_d \rightarrow \mu^+ \mu^-)_{\text{SM}}$ ;
- $(A_1, B_3)$  and  $(A_1, B_2)$  are chosen when  $S_{\mu^+ \mu^-}^s < 0$  and  $\mathcal{B}(B_d \rightarrow \mu^+ \mu^-) > \mathcal{B}(B_d \rightarrow \mu^+ \mu^-)_{\text{SM}}$ ;
- $(A_3, B_1)$  and  $(A_3, B_4)$  are chosen when  $S_{\mu^+ \mu^-}^s > 0$  and  $\mathcal{B}(B_d \rightarrow \mu^+ \mu^-) < \mathcal{B}(B_d \rightarrow \mu^+ \mu^-)_{\text{SM}}$ ;
- $(A_3, B_3)$  and  $(A_3, B_2)$  are chosen when  $S_{\mu^+ \mu^-}^s > 0$  and  $\mathcal{B}(B_d \rightarrow \mu^+ \mu^-) > \mathcal{B}(B_d \rightarrow \mu^+ \mu^-)_{\text{SM}}$ .

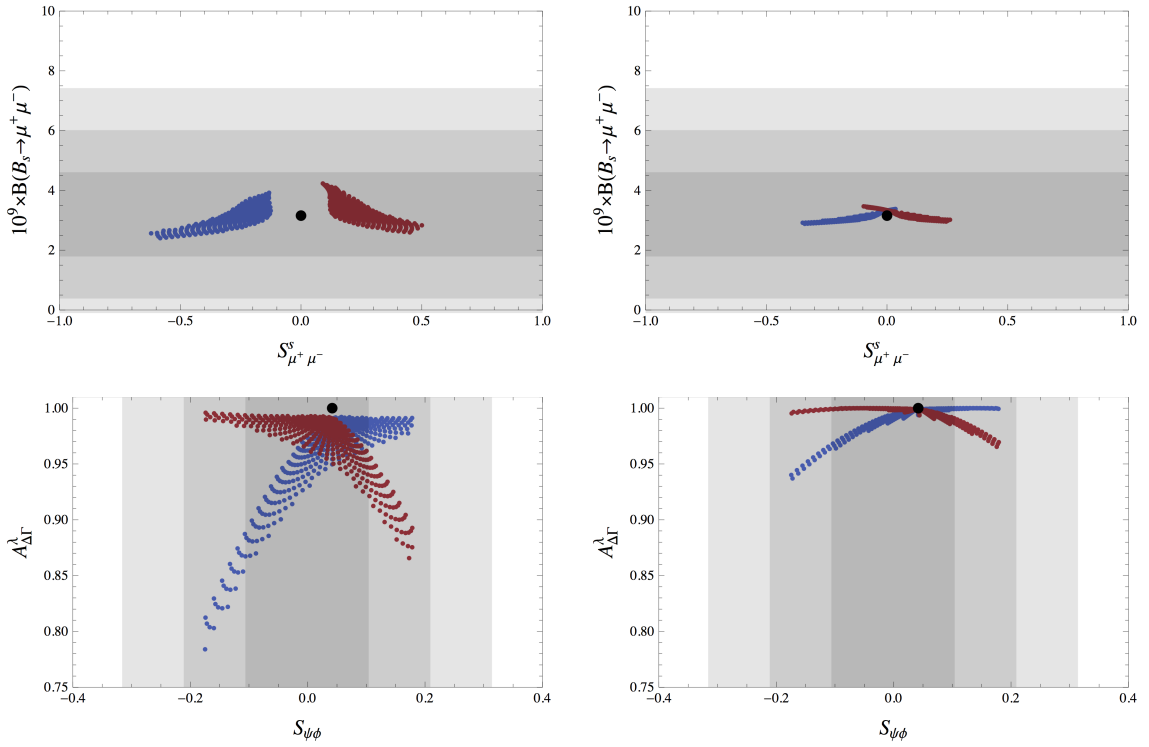


Figure 3.7: Upper panel:  $\mathcal{B}(B_s \rightarrow \mu^+ \mu^-)$  versus  $S_{\mu^+ \mu^-}^s$ , when the parameters  $(s_{23}, \delta_2)$  vary in the regions  $A_1$  (blue),  $A_3$  (red). In both rows the left plots are obtained for  $m_{Z'} = 1$  TeV, the right ones for  $m_{Z'} = 3$  TeV. Lower panel:  $S_{\psi\phi}$  versus  $A_{\Delta\Gamma}^\lambda$ , for  $m_{Z'} = 1$  TeV (left) and  $m_{Z'} = 3$  TeV (right), when the parameters  $(s_{23}, \delta_2)$  vary in the regions  $A_1$  (blue),  $A_3$  (red). The shaded grey regions are the experimental  $1\sigma$ – $3\sigma$  error ranges, while the black points are the central values of the SM predictions.

The fact that  $S_{\mu^+ \mu^-}^s$  and  $\mathcal{B}(B_d \rightarrow \mu^+ \mu^-)$  are very powerful in identifying the optimal parameter space region can be understood as follows.  $S_{\mu^+ \mu^-}^s$  is governed by the phase of the function  $Y^{bs}$  that originates in the  $Z'$  contribution. It can distinguish between  $A_1$  and  $A_3$  because the new phase  $\delta_2$  in these two regions differs by  $180^\circ$  and consequently  $\sin \delta_2$ , which is relevant for this asymmetry, differs by sign in the two regions. Calculating the imaginary part of  $Y^{bs}$  and taking into account that it is  $\Delta^{sb}$  and not  $\Delta^{bs}$  that enters  $Y^{bs}$ , one can understand the origin of the definite sign of  $S_{\mu^+ \mu^-}^s$  in  $A_1$  and  $A_3$  regions, as stated above.

The most evident distinction between the large regions and the small regions of the parameters  $(s_{13}, \delta_1)$  is possible by adding  $S_{\mu^+ \mu^-}^d$  to the previous set of observables, as shown in the lower plots of Fig. 3.6. Explicitly:

- The large regions are chosen when  $S_{\mu^+ \mu^-}^d > 0$ ;
- The small regions are chosen when  $S_{\mu^+ \mu^-}^d < 0$ .

In summary, the future measurements of  $\mathcal{B}(B_d \rightarrow \mu^+ \mu^-)$ ,  $S_{\mu^+ \mu^-}^d$  and  $S_{\mu^+ \mu^-}^s$

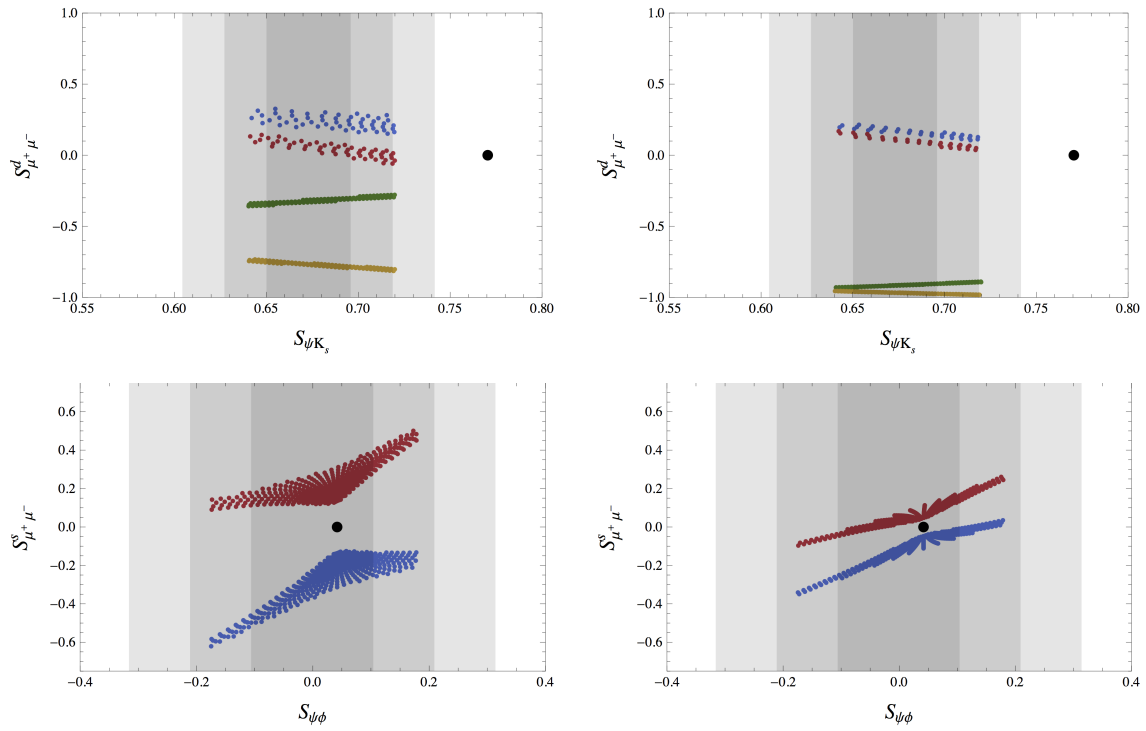


Figure 3.8: Upper panel:  $S_{\psi K_S}$  versus  $S_{\mu^+\mu^-}^d$ , when the parameters  $(s_{13}, \delta_1)$  vary in the regions  $B_1$  (blue),  $B_3$  (red),  $B_2$  (green),  $B_4$  (yellow). Lower panel:  $S_{\psi\phi}$  versus  $S_{\mu^+\mu^-}^s$ , when the parameters  $(s_{23}, \delta_2)$  vary in the regions  $A_1$  (blue),  $A_3$  (red). In both rows the left plots are obtained for  $m_{Z'} = 1$  TeV, the right ones for  $m_{Z'} = 3$  TeV. The shaded grey regions are the experimental  $1\sigma - 3\sigma$  error ranges, while the black points are the central values of the SM predictions.

will be able to select univocally one region of the parameter space of the  $\overline{331}$  model. Once this region has been fixed, the other observables and correlations that we are going to show provide stringent tests to the validity of the model.

For completeness, in the upper plots of Fig. 3.7 we show the relation between  $S_{\mu^+\mu^-}^s$  and  $\mathcal{B}(B_s \rightarrow \mu^+\mu^-)$ , while in the lower plots of the same figure we consider the observable  $\mathcal{A}_{\Delta\Gamma}^\lambda$ . Only for  $m_{Z'} = 1$  TeV and  $S_{\psi\phi}$  significantly different from zero  $\mathcal{A}_{\Delta\Gamma}^\lambda$  differs significantly from unity.

In Fig. 3.8 we show the CP violation in the  $B_q \rightarrow \psi\{qs\}$  decays versus the one in the  $B_q \rightarrow \mu^+\mu^-$  decays. In the lower plots it is evident that the requirement of suppression of  $\Delta M_s$  requires  $S_{\mu^+\mu^-}^s$  to be non-zero. In both scenarios the sign of  $S_{\psi\phi}$  is not fixed yet but it will be fixed by invoking  $\mathcal{B}(B_s \rightarrow \mu^+\mu^-)$ . It is particularly remarkable that  $|S_{\mu^+\mu^-}^s|$  can reach high values for the extreme values of  $S_{\psi\phi}$ .

In Fig. 3.9 we compare instead the branching ratios of the  $B_q \rightarrow \mu^+\mu^-$  decays with the CP asymmetries in the  $B_q \rightarrow \psi\{qs\}$ . In the upper plots, it is evident that the requirements on  $S_{\psi K_S}$  and  $\Delta M_d$  forces  $\mathcal{B}(B_d \rightarrow \mu^+\mu^-)$  to differ from the SM value, but the sign of this departure depends on the parameter region

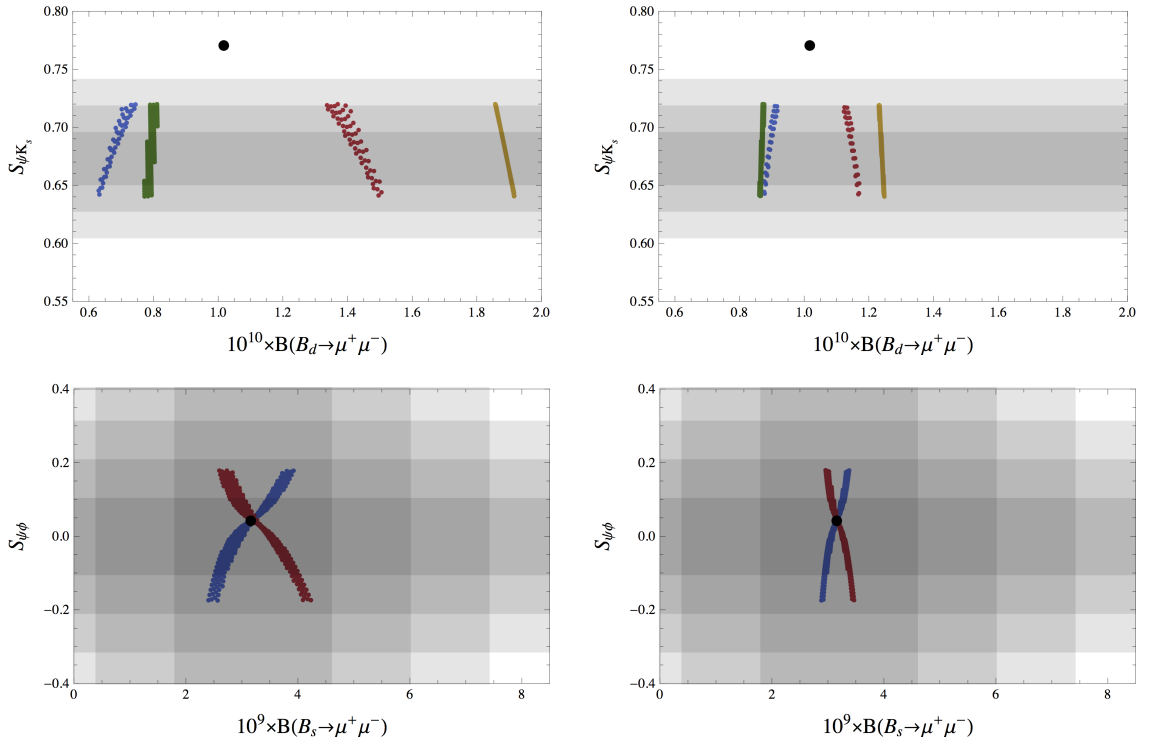


Figure 3.9: Upper panel:  $\mathcal{B}(B_d \rightarrow \mu^+ \mu^-)$  versus  $S_{\psi K_S}$ , when the parameters  $(s_{13}, \delta_1)$  vary in the regions  $B_1$  (blue),  $B_3$  (red),  $B_2$  (green),  $B_4$  (yellow). Lower panel:  $\mathcal{B}(B_s \rightarrow \mu^+ \mu^-)$  versus  $S_{\psi\phi}$ , when the parameters  $(s_{23}, \delta_2)$  vary in the regions  $A_1$  (blue),  $A_3$  (red). In both rows the left plots are obtained for  $m_{Z'} = 1$  TeV, the right ones for  $m_{Z'} = 3$  TeV. The shaded grey regions are the experimental  $1\sigma - 3\sigma$  error ranges, while the black points are the central values of the SM predictions.

considered, and the effect increases with decreasing  $S_{\psi K_S}$ . Since  $\mathcal{B}(B_d \rightarrow \mu^+ \mu^-)$  is correlated with  $S_{\psi K_S}$  which is already well determined, the range of  $\delta_1$  cannot be large.  $\mathcal{B}(B_d \rightarrow \mu^+ \mu^-)$  can then distinguish between the  $B_1$  and  $B_3$  regions because  $\cos \delta_1$  differs by sign in these two regions. We find then destructive interference of  $Z'$  contribution with the SM contribution in  $B_1$  and constructive interference in  $B_3$  implying the results exposed above. It should be noted that on the basis of  $\Delta F = 2$  processes such a distinction between these regions cannot be made because the relevant amplitudes are governed by  $2\delta_1$  and  $2\delta_2$  which differ by  $360^\circ$ . The reason why  $\mathcal{B}(B_s \rightarrow \mu^+ \mu^-)$  cannot be presently as powerful as  $\mathcal{B}(B_d \rightarrow \mu^+ \mu^-)$  in the selection of the regions is the significant experimental error on  $S_{\psi\phi}$  with which this branching ratio is correlated. However, inspecting this correlation in a given region constitutes an important test of the model, as we can see in the lower plots. While in the region  $A_1$   $S_{\psi\phi}$  increases (decreases) uniquely with increasing (decreasing)  $\mathcal{B}(B_s \rightarrow \mu^+ \mu^-)$ , in the region  $A_3$  the increase of  $S_{\psi\phi}$  implies uniquely a decrease of  $\mathcal{B}(B_s \rightarrow \mu^+ \mu^-)$ . Therefore, while  $\mathcal{B}(B_s \rightarrow \mu^+ \mu^-)$  alone cannot uniquely determine the optimal region, it can do it together with  $S_{\psi\phi}$ . If the favored region will be found to differ from the one found comparing  $S_{\mu^+\mu^-}^s$  and  $\mathcal{B}(B_d \rightarrow$

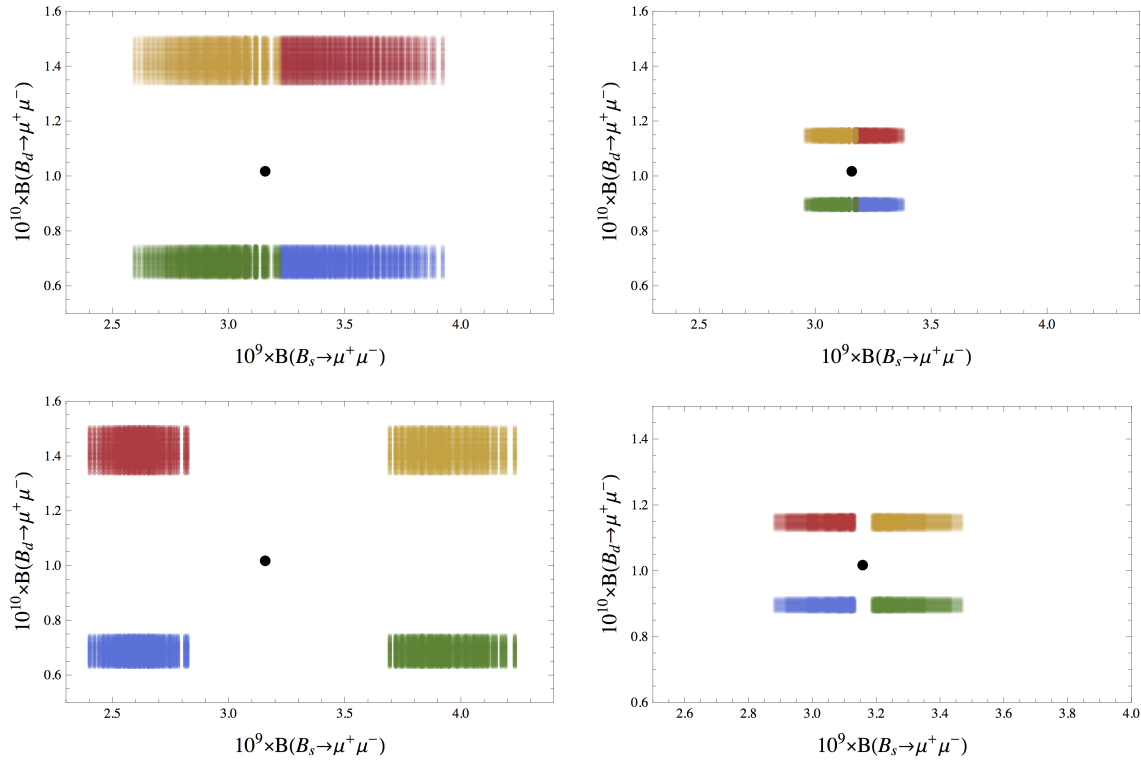


Figure 3.10:  $\mathcal{B}(B_s \rightarrow \mu^+ \mu^-)$  versus  $\mathcal{B}(B_d \rightarrow \mu^+ \mu^-)$ , for  $S_{\psi\phi} > 0.05$  (upper panel) and  $S_{\psi\phi} < -0.05$  (lower panel). The parameters  $(s_{23}, \delta_2; s_{13}, \delta_1)$  vary in the regions  $(A_1, B_1)$  (blue),  $(A_1, B_3)$  (red),  $(A_3, B_1)$  (green),  $(A_3, B_3)$  (yellow). In both rows the left plots are obtained for  $m_{Z'} = 1$  TeV, the right ones for  $m_{Z'} = 3$  TeV. The black point is the central value of SM prediction.

$\mu^+ \mu^-$ ), the  $\overline{331}$  model will be in trouble. This discussion shows that we have a triple correlation  $S_{\mu^+ \mu^-}^s - S_{\psi\phi} - \mathcal{B}(B_s \rightarrow \mu^+ \mu^-)$  in this model: once the sign of  $S_{\mu^+ \mu^-}^s$  is known, a unique correlation  $S_{\psi\phi} - \mathcal{B}(B_s \rightarrow \mu^+ \mu^-)$  is found; if in addition one of these three observables is precisely known, the other two can be strongly constrained.

The relation between  $\mathcal{B}(B_d \rightarrow \mu^+ \mu^-)$  and  $\mathcal{B}(B_s \rightarrow \mu^+ \mu^-)$  with the sign  $S_{\psi\phi}$  is shown in Fig. 3.10, in case  $S_{\psi\phi}$  will be find significantly different from zero.

- $\mathbf{B} \rightarrow \mathbf{X}_s \nu \bar{\nu}, K^+ \rightarrow \pi^+ \nu \bar{\nu}, K_L \rightarrow \pi^0 \nu \bar{\nu}$

We consider some rare decays to final states containing a neutrino-antineutrino pair, and we start with the inclusive channel  $B \rightarrow X_s \nu \bar{\nu}$ , whose results are shown in the upper plots of Fig. 3.11. The sharp correlation found between its branching ratio and the one of  $B_s \rightarrow \mu^+ \mu^-$  is valid in any region of the parameter space, due to the independence of both  $\Delta^{\mu\bar{\mu}}$  and  $\Delta^{\nu\bar{\nu}}$  from the  $V_L$  matrix. As expected, NP effects are significantly larger in  $\mathcal{B}(B_s \rightarrow \mu^+ \mu^-)$  than in  $\mathcal{B}(B \rightarrow X_s \nu \bar{\nu})$ .

Moving to the  $K$  sector, in the lower plots of the same figure we show the relation between  $\mathcal{B}(K^+ \rightarrow \pi^+ \nu \bar{\nu})$  and  $\mathcal{B}(K_L \rightarrow \pi^0 \nu \bar{\nu})$ . It turns out that there

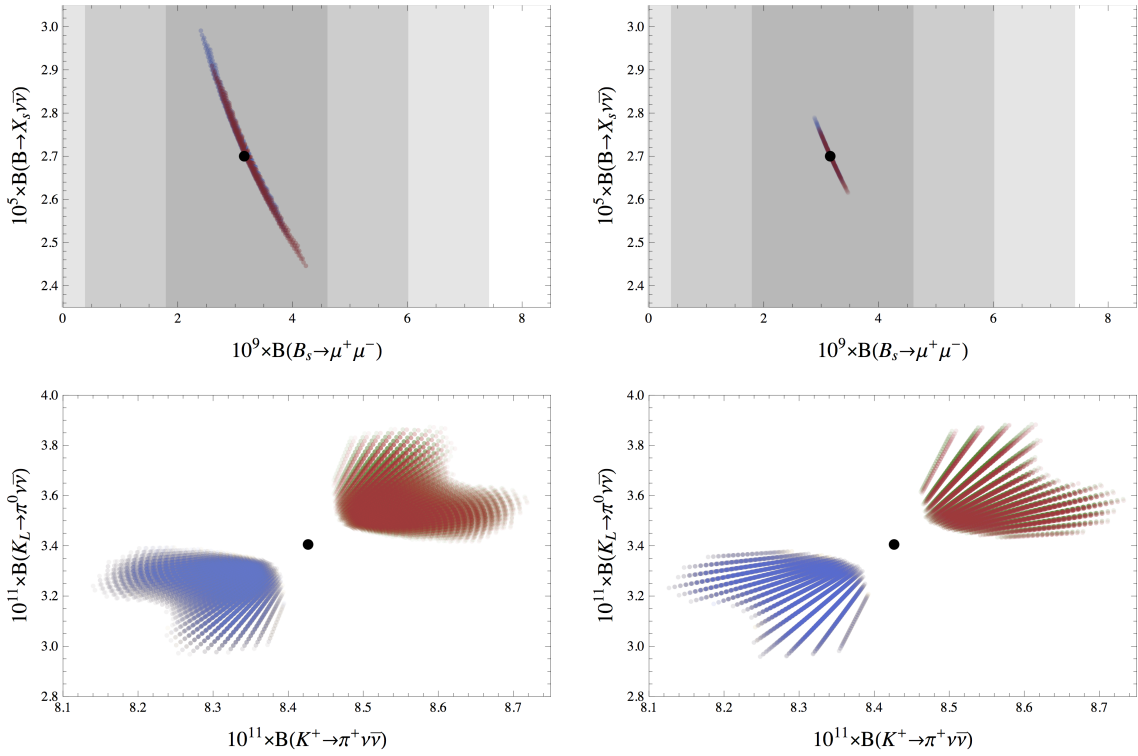


Figure 3.11: Upper panel:  $\mathcal{B}(B_s \rightarrow \mu^+\mu^-)$  versus  $\mathcal{B}(B \rightarrow X_s\nu\bar{\nu})$ , when the parameters  $(s_{23}, \delta_2)$  vary in the regions  $A_1$  (blue) and  $A_3$  (red). Lower panel:  $\mathcal{B}(K^+ \rightarrow \pi^+\nu\bar{\nu})$  versus  $\mathcal{B}(K_L \rightarrow \pi^0\nu\bar{\nu})$ , when the parameters  $(s_{23}, \delta_2; s_{13}, \delta_1)$  vary in the regions  $(A_1, B_1)$  and  $(A_3, B_3)$  (blue and yellow, superposed),  $(A_1, B_3)$  and  $(A_3, B_1)$  (red and green, superposed). In both rows the left plots are obtained for  $m_{Z'} = 1$  TeV, the right ones for  $m_{Z'} = 3$  TeV. The shaded grey regions are the experimental  $1\sigma - 3\sigma$  error ranges, while the black points are the central values of the SM predictions.

are two regions in which both branching ratios are suppressed with respect to the SM values, and two in which they are both enhanced. The measurements of these branching ratios could in principle constitute an important test of the model, but unfortunately the deviations from SM expectations are at most 5% at the level of the branching ratios, so that these correlations cannot be tested in a near future; on the other hand, finding experimentally both branching ratios significantly different from SM expectations would put the model in trouble. As expected, the NP effects basically do not depend on the mass of the  $Z'$ .

- **Correlations**

The calculation of the various observables that we have performed within the  $\overline{331}$  model allows us to discuss the departure from CMFV master correlations, and therefore to recognize the different pattern of flavour violation. We show the analysis of two of the three  $r$ -parameters in the upper plots of Fig. 3.12. We

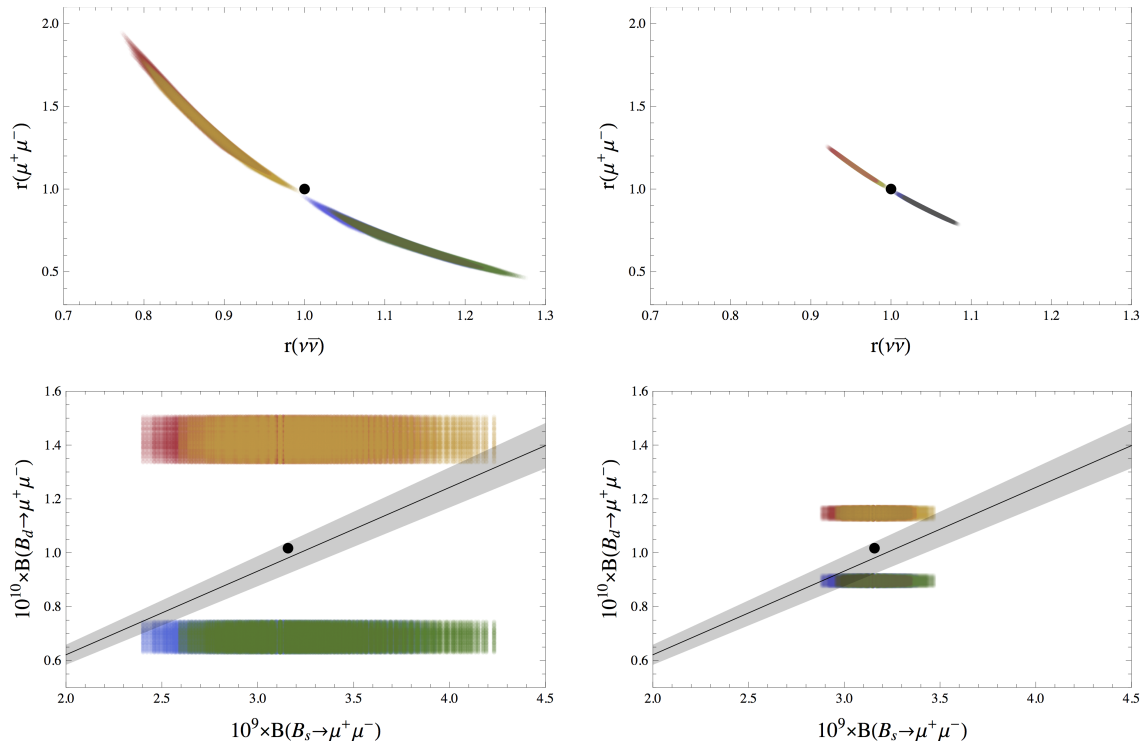


Figure 3.12: Upper panel: violation of the CMFV relations in the parameters  $r(\nu\bar{\nu})$  and  $r(\mu^+\mu^-)$ , obtained in the regions  $(A_1, B_1)$  (blue),  $(A_1, B_3)$  (red),  $(A_3, B_1)$  (green),  $(A_3, B_3)$  (yellow), all almost superposed. Lower panel:  $\mathcal{B}(B_s \rightarrow \mu^+\mu^-)$  versus  $\mathcal{B}(B_d \rightarrow \mu^+\mu^-)$ , in the regions  $(A_1, B_1)$  (blue),  $(A_1, B_3)$  (red),  $(A_3, B_1)$  (green),  $(A_3, B_3)$  (yellow); the gray band is the correlation predicted in the CMFV scenarios. In both rows the left plots are obtained for  $m_{Z'} = 1$  TeV, the right ones for  $m_{Z'} = 3$  TeV. The black point is the central value of SM prediction.

observe that deviation of  $r(\Delta M)$  from 1 is approximately 10%, irrespective of the value of  $m_{Z'}$ ;  $r(\nu\bar{\nu})$  can deviate by almost 20% from 1 for  $m_{Z'} = 1$  TeV, but only 6% for  $m_{Z'} = 3$  TeV;  $r(\mu^+\mu^-)$  is by far the function that mostly deviates from CMFV prediction: its values can differ from 1 by 60% for  $m_{Z'} = 1$  TeV, and almost 20% for  $m_{Z'} = 3$  TeV. The departure of these functions from 1 is anti-correlated in the case of  $r(\mu^+\mu^-)$  and  $r(\nu\bar{\nu})$ ; the largest possible values of  $r(\nu\bar{\nu})$  are obtained when  $(\tilde{s}_{13}, \delta_1) \in B_1$ , while  $r(\mu^+\mu^-)$  is larger when  $(\tilde{s}_{13}, \delta_1) \in B_3$ . The case in which the parameters belong to the small regions is not displayed in these figures for the sake of readability. However, we report that for  $m_{Z'} = 1$  TeV, the values of  $r(\nu\bar{\nu})$  can be larger, while  $r(\mu^+\mu^-)$  can reach even the value 2.2 in the region  $(A_1, B_2)$ . For  $m_{Z'} = 3$  TeV the effects are almost indistinguishable from the ones of the large regions, except for the fact that  $r(\mu^+\mu^-)$  and  $r(\nu\bar{\nu})$  can be as large as 1.3 and 1.1, respectively.

A very clear indication of the different flavour patterns is given by the comparison between  $\mathcal{B}(B_s \rightarrow \mu^+\mu^-)$  and  $\mathcal{B}(B_d \rightarrow \mu^+\mu^-)$ , for which CMFV predicts a precise correlation. In the lower plots of Fig. 3.12 we include the errors on

the experimental determinations of  $\Delta M_s$ ,  $\Delta M_d$ ,  $\tau(B_s)$ ,  $\tau(B_d)$ , and as regards the non-perturbative inputs we used the central value of the last lattice determinations but we reduced the size of the uncertainty. An improvement in this direction would indeed substantially help understanding if and how much CMFV relations are violated in the  $\overline{331}$  model.

The correlations of the  $\overline{331}$  model allow also to distinguish it from general MFV scenarios. Taking as a reference example the  $2\text{HDM}_{\overline{\text{MFV}}}$ , in both cases the NP contributions to  $\epsilon_K$  are small, favoring the inclusive value of  $|V_{ub}|$ . However, while in the  $2\text{HDM}_{\overline{\text{MFV}}}$  the data on  $S_{\psi K_S}$  imply then automatically a positive value of  $S_{\psi\phi} \geq 0.15$  [79], in the  $\overline{331}$  model this is not required, and any value within the LHCb range is still possible. Concerning  $\Delta F = 1$  transitions, in the  $2\text{HDM}_{\overline{\text{MFV}}}$  there is a tendency for which with increasing  $S_{\psi\phi}$  also the lower bound on  $\mathcal{B}(B_s \rightarrow \mu^+\mu^-)$  increases; in the  $\overline{331}$  model the correlation between  $S_{\psi\phi}$  and  $\mathcal{B}(B_s \rightarrow \mu^+\mu^-)$  is much more transparent. In both models  $\mathcal{B}(B_s \rightarrow \mu^+\mu^-)$  can be smaller or larger than the SM value, but in  $2\text{HDM}_{\overline{\text{MFV}}}$  the deviations can be larger, a characteristic property of scalar currents.

### More inspections

- Until now we have considered the case in which the  $Z'$  is detectable by the LHC, but the only indirect effects of a heavier mass are of course worth of investigation as well.

As we can see from the trend in Fig. 3.2, increasing the mass of the  $Z'$  implies that the allowed regions of the space parameter are shifted in order to satisfy the constraints of the  $\Delta F = 2$   $B_{d,s}$ -observables; in particular,  $s_{13}$  and  $s_{23}$  have to be increased proportionally. Since  $\Delta^{sd}$  depends on the product  $s_{13}s_{23}$ , the effects on  $\epsilon_K$  increase with  $m_{Z'}$ , as evident from Fig 3.5; on the contrary, since  $\Delta^{\mu\bar{\mu}}$  and  $\Delta^{\nu\bar{\nu}}$  do not depend on these parameters, the NP contributions to the considered rare decays are suppressed by the mass of the FCNC-mediating  $Z'$  boson.

The consideration that a heavy  $Z'$  can significantly modify  $\epsilon_K$  respecting the experimental bounds on the  $B$ -observables suggests that the experimental value of  $\epsilon_K$  could be even obtained in the context of the Scenario 1, i.e. using the exclusive determination of  $|V_{ub}|$ . In fact, using the representative value of  $m_{Z'} = 10$  TeV, and imposing the additional constraints

$$\left| \frac{\Delta M_K}{(\Delta M_K)_{\text{exp}}} \right| < 25\% , \quad 2.0 \cdot 10^{-3} \leq |\epsilon_K| \leq 2.5 \cdot 10^{-3} , \quad (3.120)$$

which are necessary because of the strong effects on the  $K$  sector, we find that the Scenario 1 with  $|V_{ub}| = 3.1 \cdot 10^{-3}$  is allowed for approximately

$$0.05 \leq s_{23} \leq 0.12 , \quad 0.016 \leq s_{13} \leq 0.030 , \quad (3.121)$$

to be compared with the ranges in Tab. 3.7.

When  $\Delta^{sd}$  reaches its maximal value, further increase of  $m_{Z'}$  will also decrease NP contributions to  $\epsilon_K$ , so that for very large masses of the  $Z'$  SM-like results are obtained as required by decoupling of NP; however, this happens only for  $m_{Z'} \geq 3000$  TeV. This result is just a confirmation of the known fact that if the FCNC  $Z'$  couplings to quarks are  $\mathcal{O}(1)$ ,  $\epsilon_K$  puts very strong constraints on the scale of NP.

- In our analysis we have used the most recent lattice inputs, for which the SM values for  $\Delta M_s$  and  $\Delta M_d$  are significantly above the data, when the hadronic and CKM uncertainties are reduced down to  $\pm 5\%$ . However, some of the correlations that we have found would change if  $\Delta M_s$  and  $\Delta M_d$  were both found below the data instead. For example, if the values of  $\hat{B}_{B_q}$  were reduced by 20%, the values of the allowed  $\delta_i$  would change significantly, going close to  $0^\circ$  or  $180^\circ$ . This changes radically the quantitative and sometimes the qualitative results of the  $\overline{331}$  analysis; for example, in the  $B_d$  meson system, the general structure of correlations is unchanged, but this time the NP effects in  $B_d \rightarrow \mu^+ \mu^-$  are found to be much larger than in  $S_{\mu^+ \mu^-}^d$ ; the impact on the  $B_s$  system is much larger; now the roles of  $B_s \rightarrow \mu^+ \mu^-$  and  $S_{\mu^+ \mu^-}^s$  in the search for the optimal space parameter region are interchanged, and  $\mathcal{B}(B_s \rightarrow \mu^+ \mu^-)$  is bound to be different from the SM values [301]. These considerations show clearly the importance of precise determinations of flavour observables within the SM in order to be able to search indirectly for NP.

# Conclusions and outlook

The LHC has just concluded its first run, and despite all the strong efforts and the accurate analyses, it has not given us any direct hint of NP. Therefore, the complementary research of indirect signatures in precision physics represents the only viable route at least waiting for higher energies. In particular, the flavour sector represents an especially interesting field of investigation, both because its origin is an open question of the SM, and because the accuracy of the available data together with the improvements of the SM predictions provide a powerful starting point.

In this thesis we have considered two NP models, particularly interesting because they provide some answers about the nature of flavour using as only assumption an extended gauge symmetry. We have found that the phenomenological analysis of these models, as well as of several other NP models, returns very interesting signatures, like deviations and correlations, that unfortunately are washed out because of the relatively large uncertainties of some non-perturbative parameters and some experimental values. We have chosen therefore to adopt an approach that is in some sense a bit futuristic: we have tried to understand how these NP model will face the future more precise data. We have done this by considering independent limiting scenarios with small errors that together cover the majority of the ranges allowed by the present uncertainties.

The GFS model [25] provides an elegant description of flavour as a spontaneously broken gauge symmetry; moreover, it is particularly elegant the fact that the minimal non-anomalous fermion content generates a mechanism of inverted hierarchy of the Yukawa couplings that automatically suppresses FCNCs in an effective way.

In this work we have first of all retraced the complete building of the model in the quark sector, from the gauge group to the Feynman rules; the main concrete features of the model are the presence of six new quarks associated to the SM ones, the presence of 24 new neutral flavour gauge bosons that mediate tree-level FCNCs and introduce new CP-violating phases, the facts that the CKM matrix is not unitary and that the couplings of the SM quarks with the  $Z$  boson and with the Higgs boson are modified. As regards in particular the  $\Delta F = 2$  and  $\Delta F = 1$  transitions between down-type quarks, we have calculated all the new contributions, both the ones due to the tree-level exchange of the flavour bosons and the ones due to the exchange of the new heavy quarks into the box diagrams.

In order to put the basis of a phenomenological analysis, we have first explored the parameter space, consisting in nine new parameters, looking for constraints com-

ing from consistency, reasonableness and from the strictest experimental bounds, like the lower limits to the  $b'$  and  $t'$  quark masses and the restrictions from electroweak precision physics. Then we have moved to a more detailed and systematic scan of the allowed regions of the parameter space, finding the following results [142].

- In the most favorite regions of the parameter space, the masses of exotic quarks  $b'$  and  $t'$  as well as of the lightest flavour boson (which for all practical purposes it corresponds to a flavour non-universal leptophobic  $Z'$ ), can be within the reach of LHC. On the other hand, even in the absence of direct detections, there are anyway good regions of parameters in which these exotic particles are much heavier.
- $|\epsilon_K|$  is enhanced by the new box-diagram contributions and suppressed by the tree exchange of flavour bosons; on the other hand,  $S_{\psi K_S}$  can only be slightly suppressed by the left-left tree-level contributions. As a consequence, choosing the exclusive determination of  $|V_{ub}|$ , the GFS model can be able to remove the  $\epsilon_K - S_{\psi K_S}$  tension present in the SM.
- The box diagrams that enhance  $|\epsilon_K|$  enhance also both  $\Delta M_d$  and  $\Delta M_s$ , which are almost unaffected by the tree-level contributions. This implies that, where the  $\epsilon_K - S_{\psi K_S}$  tension is solved, the weak SM equilibrium between  $\epsilon_K$  and  $\Delta M_{d,s}$  is automatically worsened.
- Concerning other relevant observables: (i) the branching ratio of  $\bar{B} \rightarrow X_s \gamma$  is generally enhanced, but only very small modifications are allowed by the  $\Delta F = 2$  bounds; (ii) also the dimuon asymmetry  $A_{sl}^b$ , which could receive large contributions from the tree-level flavour boson diagrams, remains close to the SM prediction if  $|\epsilon_K|$  is required to be in agreement with data; (iii) the branching ratio of  $B^+ \rightarrow \tau^+ \nu$  is modified through the modified CKM matrix, and hence provides important constraints in the parameter space.
- This model does not satisfy MFV, and its signatures can prove this. In fact, even if, by choosing the exclusive  $|V_{ub}|$  and by allowing an enhancement of  $|\epsilon_K|$ , it resembles the CMFV behavior, as well as for the worsening of the  $\epsilon_K - \Delta M_{d,s}$  tension,  $\Delta F = 1$  processes can provide a distinction: for example,  $\mathcal{B}(\bar{B} \rightarrow X_s \gamma)$  can be suppressed in CMFV models. On the other hand, taking as an example of MFV at large the  $2\text{HDM}_{\overline{\text{MFV}}}$ , the GFS model can be easily distinguished from it: in the latter only tiny contributions to  $|\epsilon_K|$  are allowed and hence the inclusive value of  $|V_{ub}|$  is required.

In summary, besides its appealing theoretical form, a great virtue of the GFS model is that it presents a relatively small number of free parameters, the structure of which makes it well predictive. A first decisive test for it will be a more unambiguous determination of  $|V_{ub}|$ : if this will be found to be closer to its present inclusive value, the GFS model will be definitely in difficulty. On the other hand, even with the exclusive value of  $|V_{ub}|$  the model is not able to correctly describe all the flavour

data at the same time; in this case, because of its sensitivity to the non-perturbative parameters, improved calculations of them will play a key role.

The group  $SU(3)_c \times SU(3)_L \times U(1)_X$  is the simplest non-abelian extension of the SM gauge group; some realizations of these so-called 331 models [39, 40] provide an explanation about why there are just three generations of fermions.

In this work we have presented a complete theoretical treatment of 331 models in their most general form; in particular, we have performed a detailed analysis of anomaly cancellation in order to obtain a list of the possible realizations, given by specific combinations of electric charges with fermion content. Subsequently, we have chosen a particular realization, which we have indicated as  $\overline{331}$ , characterized by interesting phenomenological features, and we have studied its gauge and symmetry-breaking structure in detail up to the derivation of the Feynman rules. In the  $\overline{331}$  model there are three exotic quarks, two of down-type and one of up-type, generally very heavy; there are moreover three new gauge bosons, and between them a  $Z'$ , which can have mass at the electroweak scale, mediates FCNCs; finally, the CKM matrix is flanked by a new unitary mixing matrix. The impact on  $\Delta F = 2$  and  $\Delta F = 1$  transitions is due only to the contribution of the  $Z'$  tree-level exchange, and since there are no new local operators it can be implemented by modifications of the master loop functions.

In the phenomenological analysis five free parameters are relevant: the mass of the  $Z'$  and four angles of the new mixing matrix. We have chosen two representative and significant values for  $m_{Z'}$ , namely 1 TeV and 3 TeV, and we have proceeded as follows [301].

- As a preliminary consideration, we have shown that only small contributions to  $|\epsilon_K|$  are possible, and hence the inclusive determination of  $|V_{ub}|$  is preferred.
- Requiring the predictions of the model to be in agreement with the experimental bounds of the two pairs of observables  $(\Delta M_d, S_{\psi K_S})$  and  $(\Delta M_s, S_{\psi\phi})$  of the  $B_{d,s}$  mixing, there are  $4 \times 4$  limited regions in the parameter space of the mixing matrix that are allowed. Requiring also  $|\epsilon_K|$  to be in agreement with data reduces the allowed regions to 8. This means that in these regions the experimental values of  $|\epsilon_K|$ ,  $S_{\psi K_S}$  and  $\Delta M_{d,s}$  are all simultaneously accommodated, differently from the SM.
- Precise data from the decays  $B_{d,s} \rightarrow \mu^+ \mu^-$  will be able to provide more definitive statements about the model. In fact, we have shown that the three observables  $\mathcal{B}(B_d \rightarrow \mu^+ \mu^-)$ ,  $S_{\mu\mu}^s$  and  $S_{\mu\mu}^d$  provide  $2^3 = 8$  combinations of possible deviations from the SM predictions that would be able to univocally select one between the remaining allowed regions.
- Other characteristics of the model are a well defined correlation between  $B_s \rightarrow \mu^+ \mu^-$  and  $S_{\psi\phi}$ , an anti-correlation between  $B_s \rightarrow \mu^+ \mu^-$  and  $\mathcal{B}(B \rightarrow X_s \nu \bar{\nu})$ , small contributions to the transitions  $B \rightarrow X_s \nu \bar{\nu}$ ,  $K^+ \rightarrow \pi^+ \nu \bar{\nu}$ ,  $K_L \rightarrow \pi^0 \nu \bar{\nu}$ .

- 331 models are not included in the MFV framework. In particular, the typical correlations of CMFV are clearly violated in the  $\overline{331}$ , especially the one between the  $B_{d,s} \rightarrow \mu^+ \mu^-$  decays. On the other hand, in contrast to the  $2\text{HDM}_{\overline{\text{MFV}}}$ , it does not present a correlation between  $S_{\psi K_S}$  and  $S_{\psi\phi}$ .

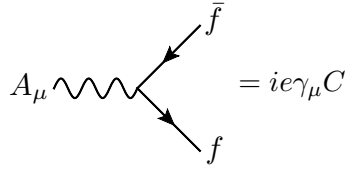
In summary, the  $\overline{331}$  model presents a very interesting phenomenology that, despite the small number of free parameters, could be able to solve the main tensions between the flavor prediction of the SM and the experimental data. The experimental deep investigation of different observables in  $B_{d,s} \rightarrow \mu^+ \mu^-$ , which will be most likely performed in the next future, will be able to provide some conclusive information about this model at least at the TeV scale, which should be also explored searching for the possible  $Z'$  boson.

We are aware that we are living during the most exciting years for particle physics since decades. We have found the Higgs boson and the LHC is warming up to hit the smallest distances ever explored. In spite of this, at least in the last years the search of NP has been quite frustrating, because it has consisted only in feeble hints that have been timely retracted. Nevertheless we believe that NP is around the corner, and with the work of this thesis we have shown how the flavour physics community is preparing itself to face all the surprises that the future experiments are saving for us.

# Appendix A

## Feynman rules of the GFS model

We present here the Feynman rules for the interaction vertices of quarks with gauge bosons and the electroweak Higgs boson and Goldstone bosons.  $V$  is the SM CKM matrix;  $\lambda^a, a = 1, \dots, 8$  are the Gell-Mann matrices while  $\lambda_{u,d}$  are the parameters of the theory;  $P_{L,R} = (1 \mp \gamma_5)/2$ .



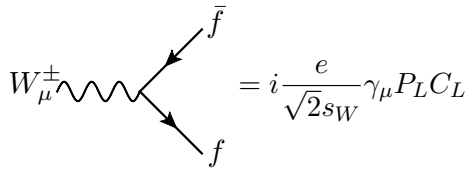
$$A_\mu \rightsquigarrow \begin{array}{l} \nearrow \bar{f} \\ \searrow f \end{array} = ie\gamma_\mu C$$

$$A\bar{u}_i u_i : C = Q_u$$

$$A\bar{u}'_i u'_i : C = Q_u$$

$$A\bar{d}_i d_i : C = Q_d$$

$$A\bar{d}'_i d'_i : C = Q_d$$



$$W_\mu^+ \rightsquigarrow \begin{array}{l} \nearrow \bar{f} \\ \searrow f \end{array} = i \frac{e}{\sqrt{2} s_W} \gamma_\mu P_L C_L$$

$$W^+ \bar{u}_i d_j : C_L = c_{uLi} V_{ij} c_{dLj}$$

$$W^+ \bar{u}'_i d'_j : C_L = s_{uLi} V_{ij} s_{dLj}$$

$$W^+ \bar{u}_i d'_j : C_L = c_{uLi} V_{ij} s_{dLj}$$

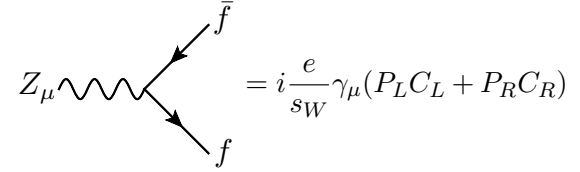
$$W^+ \bar{u}'_i d_j : C_L = s_{uLi} V_{ij} c_{dLj}$$

$$W^- \bar{d}_j u_i : C_L = c_{uLi} V_{ij}^* c_{dLj}$$

$$W^- \bar{d}'_j u_i : C_L = s_{uLi} V_{ij}^* s_{dLj}$$

$$W^- \bar{d}_j u'_i : C_L = s_{uLi} V_{ij}^* c_{dLj}$$

$$W^- \bar{d}'_j u'_i : C_L = c_{uLi} V_{ij}^* s_{dLj}$$



$$Z_\mu \rightsquigarrow \begin{array}{l} \nearrow \bar{f} \\ \searrow f \end{array} = i \frac{e}{s_W} \gamma_\mu (P_L C_L + P_R C_R)$$

$$Z\bar{u}_i u_i : \begin{cases} C_L = \frac{T_u^3 c_{uLi}^2 - s_W^2 Q_u}{c_W} \\ C_R = -\frac{s_W^2}{c_W} Q_u \end{cases}$$

$$Z\bar{u}'_i u'_i : \begin{cases} C_L = +\frac{T_u^3 s_{uLi}^2 - s_W^2 Q_u}{c_W} \\ C_R = -\frac{s_W^2}{c_W} Q_u \end{cases}$$

$$Z\bar{u}_i u'_i : \begin{cases} C_L = +\frac{T_u^3}{c_W} c_{uLi} s_{uLi} \\ C_R = 0 \end{cases}$$

$$Z\bar{u}'_i u_i : \begin{cases} C_L = +\frac{T_u^3}{c_W} c_{uLi} s_{uLi} \\ C_R = 0 \end{cases}$$

$$Z\bar{d}_i d_i : \begin{cases} C_L = \frac{T_d^3 c_{dLi}^2 - s_W^2 Q_d}{c_W} \\ C_R = -\frac{s_W^2}{c_W} Q_d \end{cases}$$

$$Z\bar{d}'_i d'_i : \begin{cases} C_L = +\frac{T_d^3 s_{dLi}^2 - s_W^2 Q_d}{c_W} \\ C_R = -\frac{s_W^2}{c_W} Q_d - \frac{s_W^2}{c_W} Q_d \end{cases}$$

$$Z\bar{d}_i d'_i : \begin{cases} C_L = +\frac{T_d^3}{c_W} c_{dLi} s_{dLi} \\ C_R = 0 \end{cases}$$

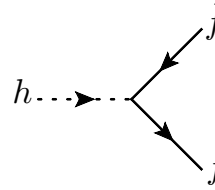
$$Z\bar{d}'_i d_i : \begin{cases} C_L = +\frac{T_d^3}{c_W} c_{dLi} s_{dLi} \\ C_R = 0 \end{cases}$$

$$G^0 \bar{d}_i d_i : C_L = C_R = +i\lambda_d s_{dRi} c_{dLi}$$

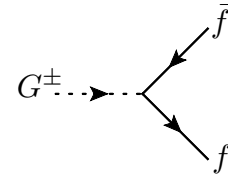
$$G^0 \bar{d}'_i d'_i : C_L = C_R = -i\lambda_d c_{dRi} s_{dLi}$$

$$G^0 \bar{d}_i d'_i : C_L = C_R = -i\lambda_d c_{dRi} c_{dLi}$$

$$G^0 \bar{d}'_i d_i : C_L = C_R = +i\lambda_d s_{dRi} s_{dLi}$$



$$= i\frac{1}{\sqrt{2}}(P_L C_L + P_R C_R)$$



$$= i(P_L C_L + P_R C_R)$$

$$h\bar{u}_i u_i : C_L = C_R = +\lambda_u s_{uRi} c_{uLi}$$

$$h\bar{u}'_i u'_i : C_L = C_R = -\lambda_u c_{uRi} s_{uLi}$$

$$h\bar{u}_i u'_i : C_L = C_R = -\lambda_u c_{uRi} c_{uLi}$$

$$h\bar{u}'_i u_i : C_L = C_R = +\lambda_u s_{uRi} s_{uLi}$$

$$G^+ \bar{u}_i d_j : \begin{cases} C_L = -\lambda_u s_{uRi} V_{ij} c_{dLj} \\ C_R = +\lambda_d c_{uLi} V_{ij} s_{dRj} \end{cases}$$

$$G^+ \bar{u}'_i d'_j : \begin{cases} C_L = +\lambda_u c_{uRi} V_{ij} s_{dLj} \\ C_R = -\lambda_d s_{uLi} V_{ij} c_{dRj} \end{cases}$$

$$G^+ \bar{u}_i d'_j : \begin{cases} C_L = +\lambda_u c_{uRi} V_{ij} c_{dLj} \\ C_R = -\lambda_d c_{uLi} V_{ij} c_{dRj} \end{cases}$$

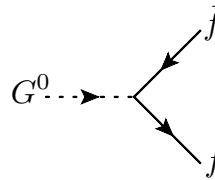
$$G^+ \bar{u}'_i d_j : \begin{cases} C_L = -\lambda_u s_{uRi} V_{ij} s_{dLj} \\ C_R = +\lambda_d s_{uLi} V_{ij} s_{dRj} \end{cases}$$

$$h\bar{d}_i d_i : C_L = C_R = +\lambda_d s_{dRi} c_{dLi}$$

$$h\bar{d}'_i d'_i : C_L = C_R = -\lambda_d c_{dRi} s_{dLi}$$

$$h\bar{d}_i d'_i : C_L = C_R = -\lambda_d c_{dRi} c_{dLi}$$

$$h\bar{d}'_i d_i : C_L = C_R = +\lambda_d s_{dRi} s_{dLi}$$



$$= i\frac{1}{\sqrt{2}}(P_L C_L + P_R C_R)$$

$$G^- \bar{d}_j u_i : \begin{cases} C_L = +\lambda_d c_{uLi} V_{ij}^* s_{dRj} \\ C_R = -\lambda_u s_{uRi} V_{ij}^* c_{dLj} \end{cases}$$

$$G^- \bar{d}'_j u'_i : \begin{cases} C_L = -\lambda_d s_{uLi} V_{ij}^* c_{dRj} \\ C_R = +\lambda_u c_{uRi} V_{ij}^* s_{dLj} \end{cases}$$

$$G^- \bar{d}_j u'_i : \begin{cases} C_L = -\lambda_d c_{uLi} V_{ij}^* c_{dRj} \\ C_R = +\lambda_u c_{uRi} V_{ij}^* c_{dLj} \end{cases}$$

$$G^- \bar{d}'_j u_i : \begin{cases} C_L = +\lambda_d s_{uLi} V_{ij}^* s_{dRj} \\ C_R = -\lambda_u s_{uRi} V_{ij}^* s_{dLj} \end{cases}$$

$$G^0 \bar{u}_i u_i : C_L = C_R = -i\lambda_u s_{uRi} c_{uLi}$$

$$G^0 \bar{u}'_i u'_i : C_L = C_R = +i\lambda_u c_{uRi} s_{uLi}$$

$$G^0 \bar{u}_i u'_i : C_L = C_R = +i\lambda_u c_{uRi} c_{uLi}$$

$$G^0 \bar{u}'_i u_i : C_L = C_R = -i\lambda_u s_{uRi} s_{uLi}$$

$$(A_Q)_\mu^a \text{ (wavy line)} \begin{cases} \nearrow \bar{f} \\ \searrow f \end{cases} = i \frac{g_Q}{\sqrt{2}} \gamma_\mu (P_L C_L + P_R C_R) \quad (A_U)_\mu^a \text{ (wavy line)} \begin{cases} \nearrow \bar{f} \\ \searrow f \end{cases} = i \frac{g_U}{\sqrt{2}} \gamma_\mu (P_L C_L + P_R C_R)$$

$$\begin{aligned}
 A_Q^a \bar{u}_i u_j &: \begin{cases} C_L = +c_{uLi} (V \lambda^a V^\dagger)_{ij} s_{uLj} \\ C_R = +s_{uRi} (V \lambda^a V^\dagger)_{ij} s_{uRj} \end{cases} & A_U^a \bar{u}_i u_j &: \begin{cases} C_L = +s_{uLi} (\lambda^a)_{ij} s_{uLj} \\ C_R = +c_{uRi} (\lambda^a)_{ij} c_{uRj} \end{cases} \\
 A_Q^a \bar{u}'_i u'_j &: \begin{cases} C_L = +s_{uLi} (V \lambda^a V^\dagger)_{ij} s_{uLj} \\ C_R = +c_{uRi} (V \lambda^a V^\dagger)_{ij} c_{uRj} \end{cases} & A_U^a \bar{u}'_i u'_j &: \begin{cases} C_L = +c_{uLi} (\lambda^a)_{ij} c_{uLj} \\ C_R = +s_{uRi} (\lambda^a)_{ij} s_{uRj} \end{cases} \\
 A_Q^a \bar{u}_i u'_j &: \begin{cases} C_L = +c_{uLi} (V \lambda^a V^\dagger)_{ij} s_{uLj} \\ C_R = -s_{uRi} (V \lambda^a V^\dagger)_{ij} c_{uRj} \end{cases} & A_U^a \bar{u}_i u'_j &: \begin{cases} C_L = -s_{uLi} (\lambda^a)_{ij} c_{uLj} \\ C_R = +c_{uRi} (\lambda^a)_{ij} s_{uRj} \end{cases} \\
 A_Q^a \bar{u}'_i u_j &: \begin{cases} C_L = +s_{uLi} (V \lambda^a V^\dagger)_{ij} c_{uLj} \\ C_R = -c_{uRi} (V \lambda^a V^\dagger)_{ij} s_{uRj} \end{cases} & A_U^a \bar{u}'_i u_j &: \begin{cases} C_L = -c_{uLi} (\lambda^a)_{ij} s_{uLj} \\ C_R = +s_{uRi} (\lambda^a)_{ij} c_{uRj} \end{cases}
 \end{aligned}$$

$$(A_D)_\mu^a \text{ (wavy line)} \begin{cases} \nearrow \bar{f} \\ \searrow f \end{cases} = i \frac{g_D}{\sqrt{2}} \gamma_\mu (P_L C_L + P_R C_R)$$

$$\begin{aligned}
 A_Q^a \bar{d}_i d_j &: \begin{cases} C_L = +c_{dLi} (\lambda^a)_{ij} c_{dLj} \\ C_R = +s_{dRi} (\lambda^a)_{ij} s_{dRj} \end{cases} & A_D^a \bar{d}_i d_j &: \begin{cases} C_L = +s_{dLi} (\lambda^a)_{ij} s_{dLj} \\ C_R = +c_{dRi} (\lambda^a)_{ij} c_{dRj} \end{cases} \\
 A_Q^a \bar{d}'_i d'_j &: \begin{cases} C_L = +s_{dLi} (\lambda^a)_{ij} s_{dLj} \\ C_R = +c_{dRi} (\lambda^a)_{ij} c_{dRj} \end{cases} & A_D^a \bar{d}'_i d'_j &: \begin{cases} C_L = +c_{dLi} (\lambda^a)_{ij} c_{dLj} \\ C_R = +s_{dRi} (\lambda^a)_{ij} s_{dRj} \end{cases} \\
 A_Q^a \bar{d}_i d'_j &: \begin{cases} C_L = +c_{dLi} (\lambda^a)_{ij} s_{dLj} \\ C_R = -s_{dRi} (\lambda^a)_{ij} c_{dRj} \end{cases} & A_D^a \bar{d}_i d'_j &: \begin{cases} C_L = -s_{dLi} (\lambda^a)_{ij} c_{dLj} \\ C_R = +c_{dRi} (\lambda^a)_{ij} s_{dRj} \end{cases} \\
 A_Q^a \bar{d}'_i d_j &: \begin{cases} C_L = +s_{dLi} (\lambda^a)_{ij} c_{dLj} \\ C_R = -c_{dRi} (\lambda^a)_{ij} s_{dRj} \end{cases} & A_D^a \bar{d}'_i d_j &: \begin{cases} C_L = +s_{dRi} (\lambda^a)_{ij} c_{dRj} \\ C_R = -c_{dLi} (\lambda^a)_{ij} s_{dLj} \end{cases}
 \end{aligned}$$



# Appendix B

## Feynman rules of the $\overline{331}$ model

We present here the Feynman rules for the interaction vertices of quarks and leptons with gauge bosons. We use the following compact notation:  $u_{1,2,3} = u, c, t$ ;  $d_{1,2,3} = d, s, b$ ;  $D_{1,2} = D, S$ ;  $u_{ij} = (U_L)_{ij}$ ;  $v_{ij} = (V_L)_{ij}$ ;  $P_{L,R} = (1 \mp \gamma_5)/2$ .

$$A_\mu \text{ wavy line} \begin{cases} \nearrow \bar{f} \\ \searrow f \end{cases} = ie\gamma_\mu C$$

$$Y_\mu^\pm \text{ wavy line} \begin{cases} \nearrow \bar{f} \\ \searrow f \end{cases} = i\frac{e}{\sqrt{2}s_W}\gamma_\mu P_L C_L$$

$$A\bar{u}_i u_i : C = 2/3$$

$$A\bar{d}_i d_i : C = -1/3$$

$$A\bar{D}_i D_i : C = -1/3$$

$$A\bar{T} T : C = 2/3$$

$$Y^+ \bar{u}_i D_j : C_L = u_{ij}^*$$

$$Y^+ \bar{T} d_i : C_L = -v_{3i}$$

$$Y^+ \bar{\nu}_i^c \ell_i : C_L = -1$$

$$A\bar{\ell}_i \ell_i : C = -1$$

$$(\bar{V})_\mu^0 \text{ wavy line} \begin{cases} \nearrow \bar{f} \\ \searrow f \end{cases} = i\frac{e}{\sqrt{2}s_W}\gamma_\mu P_L C_L$$

$$W_\mu^\pm \text{ wavy line} \begin{cases} \nearrow \bar{f} \\ \searrow f \end{cases} = i\frac{e}{\sqrt{2}s_W}\gamma_\mu P_L C_L$$

$$V^0 \bar{d}_i D_j : C_L = v_{ij}^*$$

$$V^0 \bar{T} u_i : C_L = u_{3i}$$

$$W^+ \bar{u}_i d_j : C_L = (V_{CKM})_{ij}$$

$$V^0 \bar{\nu}_i^c \nu_i : C_L = 1$$

$$W^+ \bar{\nu}_i \ell_j : C_L = 1$$

$$\begin{array}{cc}
\begin{array}{c} \bar{f} \\ \nearrow \\ Z_\mu \text{ wavy line} \\ \searrow \\ f \end{array} & = i \frac{e}{2s_W c_W} \gamma_\mu (P_L C_L + P_R C_R) & 
\begin{array}{c} \bar{f} \\ \nearrow \\ Z'_\mu \text{ wavy line} \\ \searrow \\ f \end{array} & = i \frac{e}{2s_W c_W \sqrt{3 - 4s_W^2}} \gamma_\mu (P_L C_L + P_R C_R)
\end{array}$$

$$Z\bar{u}_i u_i : \begin{cases} C_L = 1 - \frac{4}{3}s_W^2 \\ C_R = -\frac{4}{3}s_W^2 \end{cases}$$

$$Z\bar{d}_i d_i : \begin{cases} C_L = -1 + \frac{2}{3}s_W^2 \\ C_R = \frac{2}{3}s_W^2 \end{cases}$$

$$Z\bar{D}_i D_i : C_L = C_R = \frac{1}{3}$$

$$Z\bar{T} T : C_L = C_R = -\frac{2}{3}$$

$$Z\bar{u}_i u_j : \begin{cases} C_L = (-1 + \frac{4}{3}s_W^2) \delta_{ij} + 2c_W^2 u_{3i}^* u_{3j} \\ C_R = \frac{4}{3}s_W^2 \delta_{ij} \end{cases}$$

$$Z\bar{d}_i d_j : \begin{cases} C_L = (-1 + \frac{4}{3}s_W^2) \delta_{ij} + 2c_W^2 v_{3i}^* v_{3j} \\ C_R = -\frac{2}{3}s_W^2 \delta_{ij} \end{cases}$$

$$Z\bar{D}_i D_i : \begin{cases} C_L = 2(1 - \frac{4}{3}s_W^2) \\ C_R = -\frac{2}{3}s_W^2 \end{cases}$$

$$Z\bar{T} T : \begin{cases} C_L = 2(-1 + \frac{5}{3}s_W^2) \\ C_R = \frac{4}{3}s_W^2 \end{cases}$$

$$Z\bar{\ell}_i \ell_i : \begin{cases} C_L = -1 + 2s_W^2 \\ C_R = 2s_W^2 \end{cases}$$

$$Z\bar{\ell}_i \ell_i : \begin{cases} C_L = 1 - 2s_W^2 \\ C_R = -2s_W^2 \end{cases}$$

$$Z\bar{\nu}_i \nu_i : \begin{cases} C_L = 1 \\ C_R = 0 \end{cases}$$

$$Z\bar{\nu}_i \nu_i : \begin{cases} C_L = 1 - 2s_W^2 \\ C_R = 0 \end{cases}$$

# Appendix C

## Input Values

Constants		
$\alpha(m_Z)$	1/127.9	[65]
$\alpha_s(m_Z)$	1.1184(7)	[65]
$G_F$	$1.1663787(6) \times 10^{-5} \text{ GeV}^{-2}$	[65]
$\sin^2 \theta_W$	0.23116(12)	[65]
Masses and lifetimes		
$m_W$	80.399(23) GeV	[65]
$m_u(2 \text{ GeV})^1$	$2.3^{+0.7}_{-0.5} \times 10^{-3} \text{ GeV}$	[65]
$m_d(2 \text{ GeV})^1$	$4.8^{+0.7}_{-0.3} \times 10^{-3} \text{ GeV}$	[65]
$m_s(2 \text{ GeV})^1$	$95(5) \times 10^{-3} \text{ GeV}$	[65]
$m_c(m_c)^1$	1.275(25) GeV	[65]
$m_b(m_b)^1$	4.18(3) GeV	[65]
$m_t(m_t)^1$	$160.0^{+4.8}_{-4.3} \text{ GeV}$	[65]
$m_t$ (direct)	$(173.5 \pm 0.6 \pm 0.8) \text{ GeV}$	[65]
$m_\mu$	$105.6583715(35) \times 10^{-3} \text{ GeV}$	[65]
$m_\tau$	1.77682(16) GeV	[65]
$m_{K^0}$	$497.614(24) \times 10^{-3} \text{ GeV}$	[65]
$m_{B_d}$	5.27958(17) GeV	[65]
$m_{B_s}$	5.36677(24) GeV	[65]
$\tau_{B^\pm}$	1.641(8) ps <sup>2</sup>	[65]
$\tau_{B_d}$	1.519(7) ps <sup>2</sup>	[65]
$\tau_{B_s}$	1.497(15) ps <sup>2</sup>	[65]

<sup>1</sup>In the  $\overline{\text{MS}}$  renormalization scheme.

<sup>2</sup>1 ps<sup>-1</sup> =  $6.582 \times 10^{-13} \text{ GeV}/\hbar$ .

CKM matrix		
$ V_{us} $	0.2252(9)	[65]
$ V_{cb} $	$40.9(11) \times 10^{-3}$	[65]
$ V_{ub} ^{(\text{excl.})}$	$4.41(15) \times 10^{-3}$	[65]
$ V_{ub} ^{(\text{incl.})}$	$3.23(31) \times 10^{-3}$	[65]
$\gamma$	$(68_{-11}^{+10})^\circ$	[65]
Renormalization and non-perturbative parameters		
$F_K$	$156.1(11) \times 10^{-3}$ GeV	[61]
$\hat{B}_K$	0.746(10)	[61]
$\eta_1$	1.87(76)	[59]
$\eta_2$	0.5765(65)	[53]
$\eta_3$	0.496(47)	[58]
$\kappa_\epsilon$	0.94(2)	[51]
$\varphi_\epsilon$	$43.51(5)^\circ$	[98]
$F_{B_d}$	$190.6(47) \times 10^{-3}$ GeV	[61]
$\hat{B}_{B_d}$	1.26(11)	[61]
$F_{B_d} \sqrt{\hat{B}_{B_d}}$	$226(15) \times 10^{-3}$ GeV	[61]
$F_{B_s}$	$227.6(50) \times 10^{-3}$ GeV	[61]
$\hat{B}_{B_s}$	1.33(6)	[61]
$F_{B_s} \sqrt{\hat{B}_{B_s}}$	$279(15) \times 10^{-3}$ GeV	[61]
$\xi$	1.237(32)	[61]
$\eta_B$	0.55(1)	[57]
Experimental values of selected observables		
$\Delta M_K$	$3.484(5) \times 10^{-15}$ GeV	[65]
$\Delta M_d$	$3.337(33) \times 10^{-13}$ GeV	[65]
$\Delta M_s$	$1.164(5) \times 10^{-11}$ GeV	[65]
$ \epsilon_K $	$2.228(11) \times 10^{-3}$	[65]
$S_{\psi K_S}$	0.676(21)	[65]
$S_{\psi\phi}$	$-0.001 \pm 0.101 \pm 0.027$	[66]
$A_{sl}^b$	$-0.00957 \pm 0.00251 \pm 0.00146$	[70]
$\mathcal{B}(B_d \rightarrow \mu^+ \mu^-)$	$< 9.4 \times 10^{-10}$ @ 95% CL	[12]
$\mathcal{B}(B_s \rightarrow \mu^+ \mu^-)$	$3.2_{-1.2}^{+1.5} \times 10^{-9}$	[12]
$\mathcal{B}(B^+ \rightarrow \tau^+ \nu_\tau)$	$1.15(23) \times 10^{-4}$	[110]
$\mathcal{B}(\bar{B} \rightarrow X_s \gamma)$	$(3.21 \pm 0.15 \pm 0.29 \pm 0.08) \times 10^{-4}$	[89]
$\mathcal{B}(\bar{B} \rightarrow X_s \nu \bar{\nu})$	$< 6.4 \times 10^{-4}$ @ 90% CL	[91]
$\mathcal{B}(K^+ \rightarrow \pi^+ \nu \bar{\nu})$	$1.73_{-1.05}^{+1.15} \times 10^{-10}$	[95]
$\mathcal{B}(K_L \rightarrow \pi^0 \nu \bar{\nu})$	$< 2.6 \times 10^{-8}$ @ 90% CL	[96]

# Bibliography

- [1] S. Hawking, *Nature of space and time*, hep-th/9409195.
- [2] ATLAS Collaboration, G. Aad et al., *Combined search for the Standard Model Higgs boson using up to  $4.9 \text{ fb}^{-1}$  of  $pp$  collision data at  $\sqrt{s} = 7 \text{ TeV}$  with the ATLAS detector at the LHC*, Phys.Lett. **B710** (2012) 49–66, [arXiv:1202.1408].
- [3] CMS Collaboration, S. Chatrchyan et al., *Combined results of searches for the standard model Higgs boson in  $pp$  collisions at  $\sqrt{s} = 7 \text{ TeV}$* , Phys.Lett. **B710** (2012) 26–48, [arXiv:1202.1488].
- [4] P. Gagnon, *It looks very much like we have “a” Higgs boson*, <http://www.quantumdiaries.org>.
- [5] G. F. Giudice and A. Strumia, *Probing High-Scale and Split Supersymmetry with Higgs Mass Measurements*, Nucl.Phys. **B858** (2012) 63–83, [arXiv:1108.6077].
- [6] A. Arbey, M. Battaglia, A. Djouadi, and F. Mahmoudi, *The Higgs sector of the phenomenological MSSM in the light of the Higgs boson discovery*, JHEP **1209** (2012) 107, [arXiv:1207.1348].
- [7] H. An, T. Liu, and L.-T. Wang, *125 GeV Higgs Boson, Enhanced Di-photon Rate, and Gauged  $U(1)_{PQ}$ -Extended MSSM*, Phys.Rev. **D86** (2012) 075030, [arXiv:1207.2473].
- [8] J. Ellis and T. You, *Global Analysis of the Higgs Candidate with Mass  $\sim 125 \text{ GeV}$* , JHEP **1209** (2012) 123, [arXiv:1207.1693].
- [9] V. Barger and M. Ishida, *Randall-Sundrum Reality at the LHC*, Phys.Lett. **B709** (2012) 185–191, [arXiv:1110.6452].
- [10] B. Grzadkowski, J. F. Gunion, and M. Toharia, *Higgs-Radion interpretation of the LHC data?*, Phys.Lett. **B712** (2012) 70–80, [arXiv:1202.5017].
- [11] K. Cheung and T.-C. Yuan, *Could the excess seen at 124–126 GeV be due to the Randall-Sundrum Radion?*, Phys.Rev.Lett. **108** (2012) 141602, [arXiv:1112.4146].

- 
- [12] **LHCb** Collaboration, R. Aaij et al., *First evidence for the decay  $B_s \rightarrow \mu^+ \mu^-$* , Phys.Rev.Lett. **110** (2013) 021801, [arXiv:1211.2674].
- [13] **LHCb** Collaboration, R. Aaij et al., *Measurement of the CP-violating phase  $\phi_s$  in the decay  $B_s^0 \rightarrow J/\psi \phi$* , Phys.Rev.Lett. **108** (2012) 101803, [arXiv:1112.3183].
- [14] P. Gagnon, *Too early to despair! New physics is bound to show up*, <http://www.quantumdiaries.org>.
- [15] R. P. Feynman, F. B. Morinigo, W. G. Wagner, and B. Hatfield, *Feynman lectures on gravitation*, Westview Press (1995).
- [16] G. F. Giudice, *Naturally Speaking: The Naturalness Criterion and Physics at the LHC*, arXiv:0801.2562.
- [17] E. Gildener and S. Weinberg, *Symmetry Breaking and Scalar Bosons*, Phys.Rev. **D13** (1976) 3333.
- [18] P. Frampton, *Vacuum Instability and Higgs Scalar Mass*, Phys.Rev.Lett. **37** (1976) 1378.
- [19] G. Degrandi, S. Di Vita, J. Elias-Miro, J. R. Espinosa, G. F. Giudice, et al., *Higgs mass and vacuum stability in the Standard Model at NNLO*, JHEP **1208** (2012) 098, [arXiv:1205.6497].
- [20] S. Weinberg, *The Cosmological Constant Problem*, Rev.Mod.Phys. **61** (1989) 1–23.
- [21] N. Cabibbo, *Unitary Symmetry and Leptonic Decays*, Phys.Rev.Lett. **10** (1963) 531–533.
- [22] M. Kobayashi and T. Maskawa, *CP Violation in the Renormalizable Theory of Weak Interaction*, Prog.Theor.Phys. **49** (1973) 652–657.
- [23] S. Glashow, J. Iliopoulos, and L. Maiani, *Weak Interactions with Lepton-Hadron Symmetry*, Phys.Rev. **D2** (1970) 1285–1292.
- [24] G. Isidori, Y. Nir, and G. Perez, *Flavor Physics Constraints for Physics Beyond the Standard Model*, Ann.Rev.Nucl.Part.Sci. **60** (2010) 355, [arXiv:1002.0900].
- [25] B. Grinstein, M. Redi, and G. Villadoro, *Low Scale Flavor Gauge Symmetries*, JHEP **1011** (2010) 067, [arXiv:1009.2049].
- [26] S. M. Barr and A. Zee, *Calculating the electron mass in terms of measured quantities*, Phys.Rev. **D17** (1978) 1854.
- [27] F. Wilczek and A. Zee, *Horizontal Interaction and Weak Mixing Angles*, Phys.Rev.Lett. **42** (1979) 421.

- 
- [28] C. Ong, *Adding a horizontal gauge symmetry to the Weinberg-Salam model: an eight quark model*, Phys.Rev. **D19** (1979) 2738.
- [29] J. Chakrabarti, *Horizontal gauge symmetry and a new picture for the b quark*, Phys.Rev. **D20** (1979) 2411–2415.
- [30] T. Maehara and T. Yanagida, *Gauge Symmetry of Horizontal Flavor*, Prog.Theor.Phys. **61** (1979) 1434.
- [31] A. Davidson, M. Koca, and K. C. Wali,  *$U(1)$  as the minimal horizontal gauge symmetry*, Phys.Rev.Lett. **43** (1979) 92.
- [32] A. Davidson, M. Koca, and K. C. Wali, *Horizontal gauge symmetry as a natural CP violation source at the two generation level*, Phys.Lett. **B86** (1979) 47.
- [33] D.-d. Wu, *Multi-Higgs doublets and a model to calculate KM matrix using horizontal gauge*, High Energy Phys.Nucl.Phys. **4** (1980) 455.
- [34] T. Yanagida, *Horizontal symmetry and mass of the top quark*, Phys.Rev. **D20** (1979) 2986.
- [35] A. Davidson and K. C. Wali, *Horizontal QFD approach to the fermion mass spectrum*, Phys.Rev. **D21** (1980) 787.
- [36] Z. Berezhiani and J. Chkareuli, *Quark-leptonic families in a model with  $SU(5) \times SU(3)$  symmetry. (in Russian)*, Sov.J.Nucl.Phys. **37** (1983) 618–626.
- [37] Z. Berezhiani, *The Weak Mixing Angles in Gauge Models with Horizontal Symmetry: A New Approach to Quark and Lepton Masses*, Phys.Lett. **B129** (1983) 99–102.
- [38] Z. Berezhiani and M. Y. Khlopov, *The Theory of broken gauge symmetry of families. (In Russian)*, Sov.J.Nucl.Phys. **51** (1990) 739–746.
- [39] P. Frampton, *Chiral dilepton model and the flavor question*, Phys.Rev.Lett. **69** (1992) 2889–2891.
- [40] F. Pisano and V. Pleitez, *An  $SU(3) \times U(1)$  model for electroweak interactions*, Phys.Rev. **D46** (1992) 410–417, [hep-ph/9206242].
- [41] K. G. Wilson, *Nonlagrangian models of current algebra*, Phys.Rev. **179** (1969) 1499–1512.
- [42] K. Wilson and W. Zimmermann, *Operator product expansions and composite field operators in the general framework of quantum field theory*, Commun.Math.Phys. **24** (1972) 87–106.
- [43] E. Witten, *Anomalous Cross-Section for Photon - Photon Scattering in Gauge Theories*, Nucl.Phys. **B120** (1977) 189–202.

- [44] G. Buchalla, A. J. Buras, and M. E. Lautenbacher, *Weak decays beyond leading logarithms*, Rev.Mod.Phys. **68** (1996) 1125–1144, [hep-ph/9512380].
- [45] A. J. Buras, *Weak Hamiltonian, CP violation and rare decays*, hep-ph/9806471.
- [46] A. J. Buras, *Minimal flavor violation*, Acta Phys.Polon. **B34** (2003) 5615–5668, [hep-ph/0310208].
- [47] G. Buchalla, A. J. Buras, and M. K. Harlander, *Penguin box expansion: Flavor changing neutral current processes and a heavy top quark*, Nucl.Phys. **B349** (1991) 1–47.
- [48] T. Inami and C. Lim, *Effects of Superheavy Quarks and Leptons in Low-Energy Weak Processes  $K_L \rightarrow \mu^+ \mu^-$ ,  $K^+ \rightarrow \pi^+ \nu \bar{\nu}$  and  $K^0 \leftrightarrow \bar{K}^0$* , Prog.Theor.Phys. **65** (1981) 297.
- [49] V. Weisskopf and E. P. Wigner, *Calculation of the natural brightness of spectral lines on the basis of Dirac's theory*, Z.Phys. **63** (1930) 54–73.
- [50] L.-L. Chau, *Quark Mixing in Weak Interactions*, Phys.Rept. **95** (1983) 1–94.
- [51] A. J. Buras, D. Guadagnoli, and G. Isidori, *On  $\epsilon_K$  beyond lowest order in the Operator Product Expansion*, Phys.Lett. **B688** (2010) 309–313, [arXiv:1002.3612].
- [52] I. Dunietz, R. Fleischer, and U. Nierste, *In pursuit of new physics with  $B_s$  decays*, Phys.Rev. **D63** (2001) 114015, [hep-ph/0012219].
- [53] A. J. Buras, M. Jamin, and P. H. Weisz, *Leading and Next-To-Leading QCD corrections to epsilon parameter and  $B^0 - \bar{B}^0$  mixing in presence of a heavy top quark*, Nucl.Phys. **B347** (1990) 491–536.
- [54] S. Herrlich and U. Nierste, *Enhancement of the  $K_L - K_S$  mass difference by short distance QCD corrections beyond leading logarithms*, Nucl.Phys. **B419** (1994) 292–322, [hep-ph/9310311].
- [55] S. Herrlich and U. Nierste, *Indirect CP violation in the neutral kaon system beyond leading logarithms*, Phys.Rev. **D52** (1995) 6505–6518, [hep-ph/9507262].
- [56] S. Herrlich and U. Nierste, *The Complete  $|\Delta S| = 2$  - Hamiltonian in the next-to-leading order*, Nucl.Phys. **B476** (1996) 27–88, [hep-ph/9604330].
- [57] J. Urban, F. Krauss, U. Jentschura, and G. Soff, *Next-to-leading order QCD corrections for the  $B^0 - \bar{B}^0$  mixing with an extended Higgs sector*, Nucl.Phys. **B523** (1998) 40–58, [hep-ph/9710245].
- [58] J. Brod and M. Gorbahn,  *$\epsilon_K$  at Next-to-Next-to-Leading Order: The Charm-Top-Quark Contribution*, Phys.Rev. **D82** (2010) 094026, [arXiv:1007.0684].

- 
- [59] J. Brod and M. Gorbahn, *Next-to-Next-to-Leading-Order Charm-Quark Contribution to the CP Violation Parameter  $\epsilon_K$  and  $\Delta M_K$* , Phys.Rev.Lett. **108** (2012) 121801, [arXiv:1108.2036].
- [60] **RBC, UKQCD** Collaboration, D. Antonio et al., *Neutral kaon mixing from 2+1 flavor domain wall QCD*, Phys.Rev.Lett. **100** (2008) 032001, [hep-ph/0702042].
- [61] J. Laiho, E. Lunghi, and R. S. Van de Water, *Lattice QCD inputs to the CKM unitarity triangle analysis*, Phys.Rev. **D81** (2010) 034503, [arXiv:0910.2928].
- [62] **HPQCD** Collaboration, E. Gamiz, C. T. Davies, G. P. Lepage, J. Shigemitsu, and M. Wingate, *Neutral B Meson Mixing in Unquenched Lattice QCD*, Phys.Rev. **D80** (2009) 014503, [arXiv:0902.1815].
- [63] C. Bouchard, E. Freeland, C. Bernard, A. El-Khadra, E. Gamiz, et al., *Neutral B mixing from 2 + 1 flavor lattice-QCD: the Standard Model and beyond*, PoS **LATTICE2011** (2011) 274, [arXiv:1112.5642].
- [64] H. Na, C. J. Monahan, C. T. Davies, R. Horgan, G. P. Lepage, et al., *The B and B<sub>s</sub> Meson Decay Constants from Lattice QCD*, Phys.Rev. **D86** (2012) 034506, [arXiv:1202.4914].
- [65] **Particle Data Group** Collaboration, J. Beringer et al., *Review of Particle Physics (RPP)*, Phys.Rev. **D86** (2012) 010001.
- [66] **LHCb** Collaboration, P. Clarke, *Results on CP-violation in B<sub>s</sub> mixing*, LHCb-CONF-2012-002 (2012).
- [67] Y. Grossman, Y. Nir, and G. Raz, *Constraining the phase of B<sub>s</sub> –  $\bar{B}_s$  mixing*, Phys.Rev.Lett. **97** (2006) 151801, [hep-ph/0605028].
- [68] **Heavy Flavor Averaging Group** Collaboration, D. Asner et al., *Averages of b-hadron, c-hadron, and tau-lepton Properties*, arXiv:1010.1589.
- [69] A. Lenz, U. Nierste, J. Charles, S. Descotes-Genon, H. Lacker, et al., *Constraints on new physics in B –  $\bar{B}$  mixing in the light of recent LHCb data*, Phys.Rev. **D86** (2012) 033008, [arXiv:1203.0238].
- [70] **D0** Collaboration, V. M. Abazov et al., *Evidence for an anomalous like-sign dimuon charge asymmetry*, Phys.Rev. **D82** (2010) 032001, [arXiv:1005.2757].
- [71] A. Lenz and U. Nierste, *Theoretical update of B<sub>s</sub> –  $\bar{B}_s$  mixing*, JHEP **0706** (2007) 072, [hep-ph/0612167].
- [72] C. Bobeth, T. Ewerth, F. Kruger, and J. Urban, *Analysis of neutral Higgs boson contributions to the decays  $\bar{B}(s) \rightarrow \ell^+\ell^-$  and  $\bar{B} \rightarrow K\ell^+\ell^-$* , Phys.Rev. **D64** (2001) 074014, [hep-ph/0104284].

- [73] C. Bobeth, A. J. Buras, F. Kruger, and J. Urban, *QCD corrections to  $\bar{B} \rightarrow X_{d,s}\nu\bar{\nu}$ ,  $\bar{B}_{d,s} \rightarrow \ell^+\ell^-$ ,  $K \rightarrow \pi\nu\bar{\nu}$  and  $K_L \rightarrow \mu^+\mu^-$  in the MSSM*, Nucl.Phys. **B630** (2002) 87–131, [hep-ph/0112305].
- [74] A. J. Buras, P. H. Chankowski, J. Rosiek, and L. Slawianowska,  *$\Delta M_{d,s}$ ,  $B^0 d, s \rightarrow \mu^+\mu^-$  and  $B \rightarrow X_s\gamma$  in supersymmetry at large  $\tan\beta$* , Nucl.Phys. **B659** (2003) 3, [hep-ph/0210145].
- [75] A. J. Buras, J. Girrbach, D. Guadagnoli, and G. Isidori, *On the Standard Model prediction for  $BR(B_{s,d} \rightarrow \mu^+\mu^-)$* , Eur.Phys.J. **C72** (2012) 2172, [arXiv:1208.0934].
- [76] S. Descotes-Genon, J. Matias, and J. Virto, *An analysis of  $B_{d,s}$  mixing angles in presence of New Physics and an update of  $B \rightarrow K^{0*}\bar{K}^{0*}$* , Phys.Rev. **D85** (2012) 034010, [arXiv:1111.4882].
- [77] K. De Bruyn, R. Fleischer, R. Kneijens, P. Koppenburg, M. Merk, et al., *Branching Ratio Measurements of  $B_s$  Decays*, Phys.Rev. **D86** (2012) 014027, [arXiv:1204.1735].
- [78] K. De Bruyn, R. Fleischer, R. Kneijens, P. Koppenburg, M. Merk, et al., *Probing New Physics via the  $B_s^0 \rightarrow \mu^+\mu^-$  Effective Lifetime*, Phys.Rev.Lett. **109** (2012) 041801, [arXiv:1204.1737].
- [79] A. J. Buras and J. Girrbach, *BSM models facing the recent LHCb data: A First look*, Acta Phys.Polon. **B43** (2012) 1427–1472, [arXiv:1204.5064].
- [80] A. J. Buras, R. Fleischer, J. Girrbach, and R. Kneijens, *Probing New Physics with the  $B_s \rightarrow \mu + \mu -$  Time-Dependent Rate*, arXiv:1303.3820.
- [81] **LHCb** Collaboration, R. Aaij et al., *Implications of LHCb measurements and future prospects*, arXiv:1208.3355.
- [82] M. Misiak, H. Asatrian, K. Bieri, M. Czakon, A. Czarnecki, et al., *Estimate of  $B(\bar{B} \rightarrow X_s\gamma)$  at  $O(\alpha_s^2)$* , Phys.Rev.Lett. **98** (2007) 022002, [hep-ph/0609232].
- [83] M. Ciuchini, E. Franco, G. Martinelli, L. Reina, and L. Silvestrini, *Scheme independence of the effective Hamiltonian for  $b \rightarrow s\gamma$  and  $b \rightarrow sg$  decays*, Phys.Lett. **B316** (1993) 127–136, [hep-ph/9307364].
- [84] M. Ciuchini, E. Franco, L. Reina, and L. Silvestrini, *Leading order QCD corrections to  $b \rightarrow s\gamma$  and  $b \rightarrow sg$  decays in three regularization schemes*, Nucl.Phys. **B421** (1994) 41–64, [hep-ph/9311357].
- [85] K. G. Chetyrkin, M. Misiak, and M. Munz, *Weak radiative B meson decay beyond leading logarithms*, Phys.Lett. **B400** (1997) 206–219, [hep-ph/9612313].
- [86] E. Lunghi and J. Matias, *Huge right-handed current effects in  $B \rightarrow K^*(K\pi)\ell^+\ell^-$  in supersymmetry*, JHEP **0704** (2007) 058, [hep-ph/0612166].

- 
- [87] S. Pokorski, J. Rosiek, and C. A. Savoy, *Constraints on phases of supersymmetric flavor conserving couplings*, Nucl.Phys. **B570** (2000) 81–116, [[hep-ph/9906206](#)].
- [88] U. Haisch,  $\bar{B} \rightarrow X_s \gamma$ : *Standard Model and Beyond*, [arXiv:0805.2141](#).
- [89] **BABAR** Collaboration, J. Lees et al., *Measurement of  $B(B \rightarrow X_s \gamma)$ , the  $B \rightarrow X_s \gamma$  photon energy spectrum, and the direct CP asymmetry in  $B \rightarrow X_{s+d} \gamma$  decays*, Phys.Rev. **D86** (2012) 112008, [[arXiv:1207.5772](#)].
- [90] W. Altmannshofer, A. J. Buras, D. M. Straub, and M. Wick, *New strategies for New Physics search in  $B \rightarrow K^* \nu \bar{\nu}$ ,  $B \rightarrow K \nu \bar{\nu}$  and  $B \rightarrow X_s \nu \bar{\nu}$  decays*, JHEP **0904** (2009) 022, [[arXiv:0902.0160](#)].
- [91] **ALEPH** Collaboration, R. Barate et al., *Measurements of  $BR(b \rightarrow \tau^- \bar{\nu}_\tau X)$  and  $BR(b \rightarrow \tau^- \bar{\nu}_\tau D^{*+} X)$  and upper limits on  $BR(B^- \rightarrow \tau^- \bar{\nu}_\tau)$  and  $BR(b \rightarrow s \nu \bar{\nu})$* , Eur.Phys.J. **C19** (2001) 213–227, [[hep-ex/0010022](#)].
- [92] A. J. Buras, F. Schwab, and S. Uhlig, *Waiting for precise measurements of  $K^+ \rightarrow \pi^+ \nu \bar{\nu}$  and  $K_L \rightarrow \pi^0 \nu \bar{\nu}$* , Rev.Mod.Phys. **80** (2008) 965–1007, [[hep-ph/0405132](#)].
- [93] F. Mescia and C. Smith, *Improved estimates of rare K decay matrix-elements from  $Kl3$  decays*, Phys.Rev. **D76** (2007) 034017, [[arXiv:0705.2025](#)].
- [94] J. Brod and M. Gorbahn, *Electroweak Corrections to the Charm Quark Contribution to  $K^+ \rightarrow \nu \bar{\nu}$* , Phys.Rev. **D78** (2008) 034006, [[arXiv:0805.4119](#)].
- [95] **E949** Collaboration, A. Artamonov et al., *New measurement of the  $K^+ \rightarrow \pi^+ \nu \bar{\nu}$  branching ratio*, Phys.Rev.Lett. **101** (2008) 191802, [[arXiv:0808.2459](#)].
- [96] **E391a** Collaboration, J. Ahn et al., *Experimental study of the decay  $K_L^0 \rightarrow \pi^0 \nu \bar{\nu}$* , Phys.Rev. **D81** (2010) 072004, [[arXiv:0911.4789](#)].
- [97] E. Lunghi and A. Soni, *Possible Indications of New Physics in  $B_d$  - mixing and in  $\sin(2\beta)$  Determinations*, Phys.Lett. **B666** (2008) 162–165, [[arXiv:0803.4340](#)].
- [98] A. J. Buras and D. Guadagnoli, *Correlations among new CP violating effects in  $\Delta F = 2$  observables*, Phys.Rev. **D78** (2008) 033005, [[arXiv:0805.3887](#)].
- [99] A. J. Buras and D. Guadagnoli, *On the consistency between the observed amount of CP violation in the  $K^-$  and  $B_d$ -systems within minimal flavor violation*, Phys.Rev. **D79** (2009) 053010, [[arXiv:0901.2056](#)].
- [100] **BaBar** Collaboration, J. Lees et al., *Evidence for an excess of  $\bar{B} \rightarrow D^{(*)} \tau^- \bar{\nu}_\tau$  decays*, Phys.Rev.Lett. **109** (2012) 101802, [[arXiv:1205.5442](#)].
- [101] **BaBar** Collaboration, J. Lees et al., *Measurement of an Excess of  $B \rightarrow D^{(*)} \tau \nu$  Decays and Implications for Charged Higgs Bosons*, [arXiv:1303.0571](#).

- [102] S. Fajfer, J. F. Kamenik, and I. Nisandzic, *On the  $B \rightarrow D^* \tau \bar{\nu}_\tau$  Sensitivity to New Physics*, Phys.Rev. **D85** (2012) 094025, [arXiv:1203.2654].
- [103] E. Accomando, A. Akeroyd, E. Akhmetzyanova, J. Albert, A. Alves, et al., *Workshop on CP Studies and Non-Standard Higgs Physics*, hep-ph/0608079.
- [104] **CDF** Collaboration, T. Aaltonen et al., *First Flavor-Tagged Determination of Bounds on Mixing-Induced CP Violation in  $B_s^0 \rightarrow J/\psi \phi$  Decays*, Phys.Rev.Lett. **100** (2008) 161802, [arXiv:0712.2397].
- [105] **DO** Collaboration, V. Abazov et al., *Measurement of  $B_s^0$  mixing parameters from the flavor-tagged decay  $B_s^0 \rightarrow J/\psi \phi$* , Phys.Rev.Lett. **101** (2008) 241801, [arXiv:0802.2255].
- [106] **UTfit** Collaboration, M. Bona et al., *First Evidence of New Physics in  $b \leftrightarrow s$  Transitions*, PMC Phys. **A3** (2009) 6, [arXiv:0803.0659].
- [107] E. Lunghi and A. Soni, *Possible evidence for the breakdown of the CKM-paradigm of CP-violation*, Phys.Lett. **B697** (2011) 323–328, [arXiv:1010.6069].
- [108] **BaBar** Collaboration, J. Lees et al., *Evidence of  $B \rightarrow \tau \nu$  decays with hadronic B tags*, arXiv:1207.0698.
- [109] **Belle** Collaboration, I. Adachi et al., *Measurement of  $B^- \rightarrow \tau^- \bar{\nu}_\tau$  with a Hadronic Tagging Method Using the Full Data Sample of Belle*, Phys. Rev. Lett. **110** (2013) 131801, [arXiv:1208.4678].
- [110] **CKMfitter** Collaboration, J. Charles et al., *Constraint from the  $B^+ \rightarrow \tau^+ \nu$  branching ratio*, ICHEP 2012 (2012).
- [111] G. Isidori, *Kaon decays and the flavor problem*, Annales Henri Poincare **4** (2003) S97–S109, [hep-ph/0301159].
- [112] M. V. Carlucci, *Patterns of flavour violation at the dawn of the LHC era*, arXiv:1210.5419.
- [113] A. Buras, P. Gambino, M. Gorbahn, S. Jager, and L. Silvestrini, *Universal unitarity triangle and physics beyond the standard model*, Phys.Lett. **B500** (2001) 161–167, [hep-ph/0007085].
- [114] M. Blanke, A. J. Buras, D. Guadagnoli, and C. Tarantino, *Minimal Flavour Violation Waiting for Precise Measurements of  $\Delta M_s$ ,  $S_{\psi\phi}$ ,  $A_{SL}$ ,  $|V_{ub}|$ ,  $\gamma$  and  $B_{s,d}^0 \rightarrow \mu^+ \mu^-$* , JHEP **0610** (2006) 003, [hep-ph/0604057].
- [115] A. J. Buras, *Relations between  $\Delta M(s, d)$  and  $B(s, d) \rightarrow \mu \bar{\mu}$  in models with minimal flavor violation*, Phys.Lett. **B566** (2003) 115–119, [hep-ph/0303060].
- [116] M. Blanke and A. J. Buras, *Lower bounds on  $\Delta M(s, d)$  from constrained minimal flavour violation*, JHEP **0705** (2007) 061, [hep-ph/0610037].

- 
- [117] A. J. Buras and J. Girrbach, *Stringent Tests of Constrained Minimal Flavour Violation through  $\Delta F = 2$  Transitions*, arXiv:1304.6835.
- [118] R. S. Chivukula and H. Georgi, *Composite Technicolor Standard Model*, Phys.Lett. **B188** (1987) 99.
- [119] G. D’Ambrosio, G. Giudice, G. Isidori, and A. Strumia, *Minimal flavor violation: An Effective field theory approach*, Nucl.Phys. **B645** (2002) 155–187, [hep-ph/0207036].
- [120] R. Peccei and H. R. Quinn, *Constraints Imposed by CP Conservation in the Presence of Instantons*, Phys.Rev. **D16** (1977) 1791–1797.
- [121] A. J. Buras, M. V. Carlucci, S. Gori, and G. Isidori, *Higgs-mediated FCNCs: Natural Flavour Conservation vs. Minimal Flavour Violation*, JHEP **1010** (2010) 009, [arXiv:1005.5310].
- [122] A. J. Buras, G. Isidori, and P. Paradisi, *EDMs versus CPV in  $B_{s,d}$  mixing in two Higgs doublet models with MFV*, Phys.Lett. **B694** (2011) 402–409, [arXiv:1007.5291].
- [123] M. E. Peskin and D. V. Schroeder, *An Introduction to quantum field theory*, Addison-Wesley (1995).
- [124] S. Weinberg, *The quantum theory of fields. Vol. 2: Modern applications*, Cambridge University Press (2005).
- [125] A. Zee, *Quantum field theory in a nutshell*, Princeton University Press (2003).
- [126] K. Fujikawa, *Path Integral Measure for Gauge Invariant Fermion Theories*, Phys.Rev.Lett. **42** (1979) 1195.
- [127] S. L. Adler and W. A. Bardeen, *Absence of higher order corrections in the anomalous axial vector divergence equation*, Phys.Rev. **182** (1969) 1517–1536.
- [128] L. Alvarez-Gaume and E. Witten, *Gravitational Anomalies*, Nucl.Phys. **B234** (1984) 269.
- [129] **CDF** Collaboration, T. Aaltonen et al., *Search for heavy bottom-like quarks decaying to an electron or muon and jets in  $p\bar{p}$  collisions at  $\sqrt{s} = 1.96$  TeV*, Phys.Rev.Lett. **106** (2011) 141803, [arXiv:1101.5728].
- [130] **CMS** Collaboration, S. Chatrchyan et al., *Search for a Heavy Bottom-like Quark in  $pp$  Collisions at  $\sqrt{s} = 7$  TeV*, Phys.Lett. **B701** (2011) 204–223, [arXiv:1102.4746].
- [131] **ALEPH** Collaboration, D. Decamp et al., *A Search for New Quarks and Leptons from  $Z^0$  Decay*, Phys.Lett. **B236** (1990) 511.

- [132] **ATLAS** Collaboration, G. Aad et al., *Search for New Phenomena in  $t\bar{t}$  Events With Large Missing Transverse Momentum in Proton-Proton Collisions at  $\sqrt{s} = 7$  TeV with the ATLAS Detector*, Phys.Rev.Lett. **108** (2012) 041805, [arXiv:1109.4725].
- [133] **CDF** Collaboration, T. Aaltonen et al., *Search for a Heavy Top-Like Quark in  $p\bar{p}$  Collisions at  $\sqrt{s} = 1.96$  TeV*, Phys.Rev.Lett. **107** (2011) 261801, [arXiv:1107.3875].
- [134] M. E. Peskin and T. Takeuchi, *Estimation of oblique electroweak corrections*, Phys.Rev. **D46** (1992) 381.
- [135] M. Baak, M. Goebel, J. Haller, A. Hoecker, D. Kennedy, et al., *The Electroweak Fit of the Standard Model after the Discovery of a New Boson at the LHC*, Eur.Phys.J. **C72** (2012) 2205, [arXiv:1209.2716].
- [136] C. Collaboration, *First measurement of  $B(t \rightarrow Wb)/B(t \rightarrow Wq)$  in the dilepton channel in  $pp$  collisions at  $\sqrt{s} = 7$  TeV*, .
- [137] **CDF** Collaboration, T. Aaltonen et al., *A Search for resonant production of  $t\bar{t}$  pairs in  $4.8 \text{ fb}^{-1}$  of integrated luminosity of  $p\bar{p}$  collisions at  $\sqrt{s} = 1.96$  TeV*, Phys.Rev. **D84** (2011) 072004, [arXiv:1107.5063].
- [138] A. J. Buras, S. Jager, and J. Urban, *Master formulae for  $\Delta F = 2$  NLO QCD factors in the standard model and beyond*, Nucl.Phys. **B605** (2001) 600–624, [hep-ph/0102316].
- [139] **Belle** Collaboration, K. Ikado et al., *Evidence of the Purely Leptonic Decay  $B^- \rightarrow \tau^- \bar{\nu}_\tau$* , Phys.Rev.Lett. **97** (2006) 251802, [hep-ex/0604018].
- [140] G. Isidori and P. Paradisi, *Hints of large  $\tan\beta$  in flavour physics*, Phys.Lett. **B639** (2006) 499–507, [hep-ph/0605012].
- [141] A. J. Buras, L. Merlo, and E. Stamou, *The Impact of Flavour Changing Neutral Gauge Bosons on  $\bar{B} \rightarrow X_s \gamma$* , JHEP **1108** (2011) 124, [arXiv:1105.5146].
- [142] A. J. Buras, M. V. Carlucci, L. Merlo, and E. Stamou, *Phenomenology of a Gauged  $SU(3)^3$  Flavour Model*, JHEP **1203** (2012) 088, [arXiv:1112.4477].
- [143] R. A. Diaz, R. Martinez, and F. Ochoa,  *$SU(3)_c \times SU(3)_L \times U(1)_X$  models for  $\beta$  arbitrary and families with mirror fermions*, Phys.Rev. **D72** (2005) 035018, [hep-ph/0411263].
- [144] R. A. Diaz, R. Martinez, and F. Ochoa, *The Scalar sector of the  $SU(3)_c \times SU(3)_L \times U(1)_X$  model*, Phys.Rev. **D69** (2004) 095009, [hep-ph/0309280].
- [145] R. Foot, O. F. Hernandez, F. Pisano, and V. Pleitez, *Lepton masses in an  $SU(3)_L \times U(1)_N$  gauge model*, Phys.Rev. **D47** (1993) 4158–4161, [hep-ph/9207264].

- 
- [146] M. Tully and G. C. Joshi, *Generating neutrino mass in the 331 model*, Phys.Rev. **D64** (2001) 011301, [[hep-ph/0011172](#)].
- [147] A. G. Dias, C. de S. Pires, V. Pleitez, and P. Rodrigues da Silva, *Dynamically induced spontaneous symmetry breaking in 3-3-1 models*, Phys.Lett. **B621** (2005) 151–159, [[hep-ph/0503192](#)].
- [148] D. A. Gutierrez, W. A. Ponce, and L. A. Sanchez, *Study of the  $SU(3)_c \times SU(3)_L \times U(1)_X$  model with the minimal scalar sector*, Int.J.Mod.Phys. **A21** (2006) 2217–2235, [[hep-ph/0511057](#)].
- [149] P. V. Dong, H. N. Long, and D. Van Soa, *Higgs-gauge boson interactions in the economical 3-3-1 model*, Phys.Rev. **D73** (2006) 075005, [[hep-ph/0603108](#)].
- [150] P. Dong, D. Huong, T. Huong, and H. N. Long, *Fermion masses in the economical 3-3-1 model*, Phys.Rev. **D74** (2006) 053003, [[hep-ph/0607291](#)].
- [151] P. Dong, H. N. Long, and D. Soa, *Neutrino masses in the economical 3-3-1 model*, Phys.Rev. **D75** (2007) 073006, [[hep-ph/0610381](#)].
- [152] D. Soa, D. Thuy, L. Thuc, and T. Huong, *Charged Higgs boson in the economical 3-3-1 model*, J.Exp.Theor.Phys. **105** (2007) 1107–1118.
- [153] Y. Giraldo, W. A. Ponce, and L. A. Sanchez, *Stability of the Scalar Potential and Symmetry Breaking in the Economical 3-3-1 Model*, Eur.Phys.J. **C63** (2009) 461–475, [[arXiv:0907.1696](#)].
- [154] J. Ferreira, J.G., P. Pinheiro, C. S. Pires, and P. R. da Silva, *The Minimal 3-3-1 model with only two Higgs triplets*, Phys.Rev. **D84** (2011) 095019, [[arXiv:1109.0031](#)].
- [155] A. Doff and A. Natale, *Dynamical Symmetry Breaking in a Minimal 3-3-1 Model*, Int.J.Mod.Phys. **A27** (2012) 1250156, [[arXiv:1210.3390](#)].
- [156] M. Tonasse, *The Scalar sector of 3-3-1 models*, Phys.Lett. **B381** (1996) 191–201, [[hep-ph/9605230](#)].
- [157] T. A. Nguyen, N. A. Ky, and H. N. Long, *The Higgs sector of the minimal 3 3 1 model revisited*, Int.J.Mod.Phys. **A15** (2000) 283–305, [[hep-ph/9810273](#)].
- [158] M. Tully and G. C. Joshi, *The Scalar sector in 331 models*, Int.J.Mod.Phys. **A18** (2003) 1573–1586, [[hep-ph/9810282](#)].
- [159] N. T. Anh, N. A. Ky, and H. N. Long, *The Higgs sector in the minimal 3-3-1 model with the most general lepton number conserving potential*, Int.J.Mod.Phys. **A16** (2001) 541–556, [[hep-ph/0011201](#)].
- [160] A. G. Dias, V. Pleitez, and M. Tonasse, *Realistic extremely flat scalar potential in 3-3-1 models*, [hep-ph/0204121](#).

- [161] W. A. Ponce, Y. Giraldo, and L. A. Sanchez, *Minimal scalar sector of 3-3-1 models without exotic electric charges*, Phys.Rev. **D67** (2003) 075001, [hep-ph/0210026].
- [162] N. A. Ky and N. T. H. Van, *Scalar sextet in the 331 model with right-handed neutrinos*, Phys.Rev. **D72** (2005) 115017, [hep-ph/0512096].
- [163] O. Ravinez, H. Diaz, and D. Romero, *Physical scalar mass particles in the 331 model*, AIP Conf.Proc. **947** (2007) 497–498.
- [164] Y. Giraldo and W. A. Ponce, *Scalar Potential Without Cubic Term in 3-3-1 Models Without Exotic Electric Charges*, Eur.Phys.J. **C71** (2011) 1693, [arXiv:1107.3260].
- [165] D. Ng, *The Electroweak theory of  $SU(3) \times U(1)$* , Phys.Rev. **D49** (1994) 4805–4811, [hep-ph/9212284].
- [166] P. Jain and S. D. Joglekar,  *$Z'$  in the 3-3-1 model*, Phys.Lett. **B407** (1997) 151–154, [hep-ph/9612461].
- [167] H. N. Long and T. Inami,  *$S$ ,  $T$ ,  $U$  parameters in  $SU(3)_c \times SU(3)_L \times U(1)$  model with right-handed neutrinos*, Phys.Rev. **D61** (2000) 075002, [hep-ph/9902475].
- [168] F. Ochoa and R. Martinez,  *$Z$ - $Z'$  mixing in  $SU(3)_c \times SU(3)_L \times U(1)_X$  models with  $\beta$  arbitrary*, hep-ph/0508082.
- [169] D. Cogollo, H. Diniz, C. de S. Pires, and P. Rodrigues da Silva, *Fermion family number and the  $Z - Z'$  mixing in the 3-3-1 model with right-handed neutrinos*, Mod.Phys.Lett. **A23** (2009) 3405–3410, [arXiv:0709.2913].
- [170] A. G. Dias, R. Martinez, and V. Pleitez, *Concerning the Landau pole in 3-3-1 models*, Eur.Phys.J. **C39** (2005) 101–107, [hep-ph/0407141].
- [171] A. G. Dias, *Evading the few TeV perturbative limit in 3-3-1 models*, Phys.Rev. **D71** (2005) 015009, [hep-ph/0412163].
- [172] A. G. Dias, J. Montero, and V. Pleitez, *3-3-1 models at electroweak scale*, Phys.Lett. **B637** (2006) 85–89, [hep-ph/0511084].
- [173] R. Martinez and F. Ochoa, *The Landau pole and  $Z$ -prime decays in the 331 bilepton model*, Eur.Phys.J. **C51** (2007) 701–711, [hep-ph/0606173].
- [174] A. G. Dias and V. Pleitez, *Stabilization of the Electroweak Scale in 3-3-1 Models*, Phys.Rev. **D80** (2009) 056007, [arXiv:0908.2472].
- [175] N. A. Ky, H. N. Long, D. V. Soa, L. P. Trung, and V. T. Van, *Bounds on masses of new gauge bosons in the 3 - 3 - 1 models*, hep-ph/0009187.

- 
- [176] G. Tavares-Velasco and J. Toscano, *Bilepton gauge boson contribution to the static electromagnetic properties of the  $W$  boson in the minimal 331 model*, Phys.Rev. **D65** (2002) 013005, [hep-ph/0108114].
- [177] M. Perez, G. Tavares-Velasco, and J. Toscano, *Two body  $Z'$  decays in the minimal 331 model*, Phys.Rev. **D69** (2004) 115004, [hep-ph/0402156].
- [178] G. Gonzalez-Sprinberg, R. Martinez, and O. Sampayo, *Bilepton and exotic quark mass limits in 331 models from  $Z \rightarrow b\bar{b}$  decay*, Phys.Rev. **D71** (2005) 115003, [hep-ph/0504078].
- [179] J. B. Florez and Y. Giraldo,  *$Z'^0 Z'^0$ ,  $K^+ K^-$  and  $K^0 \bar{K}^0$  boson production with definite helicity amplitudes through  $e^+ e^-$  collisions in the 3-3-1 models without exotic electric charges*, arXiv:0710.1087.
- [180] E. Ramirez Barreto, Y. Coutinho, and J. Sa Borges, *Neutral bilepton boson production in  $p p$  collisions from 3-3-1 model*, Braz.J.Phys. **38** (2008) 495–498.
- [181] A. Flores-Tlalpa, J. Montano, F. Ramirez-Zavaleta, and J. Toscano, *Decays  $X \rightarrow gg\gamma$  and  $Z' \rightarrow gg\gamma$  in the minimal 331 model*, Phys.Rev. **D80** (2009) 077301, [arXiv:0908.3728].
- [182] R. Martinez and F. Ochoa, *Heavy quark signals from radiative corrections to the  $Z'$  boson decay in 3-3-1 models*, Phys.Rev. **D80** (2009) 075020, [arXiv:0909.1121].
- [183] J. Montano, M. Perez, F. Ramirez-Zavaleta, and J. Toscano, *Decays  $Z' \rightarrow \gamma\gamma\gamma$  and  $Z \rightarrow \gamma\gamma\gamma$  in the minimal 331 model*, Phys.Rev. **D85** (2012) 035012, [arXiv:1110.3446].
- [184] J. Florez, W. Ponce, and L. Sanchez, *Fermion mass matrices for a 3-3-1 model*, AIP Conf.Proc. **670** (2003) 323–328.
- [185] C. Alvarado, R. Martinez, and F. Ochoa, *Quark mass hierarchy in 3-3-1 models*, Phys.Rev. **D86** (2012) 025027, [arXiv:1207.0014].
- [186] J. T. Liu, *Generation nonuniversality and flavor changing neutral currents in the 331 model*, Phys.Rev. **D50** (1994) 542–547, [hep-ph/9312312].
- [187] R. Foot, H. N. Long, and T. A. Tran,  *$SU(3)_L \times U(1)_N$  and  $SU(4)_L \times U(1)_N$  gauge models with right-handed neutrinos*, Phys.Rev. **D50** (1994) 34–38, [hep-ph/9402243].
- [188] H. N. Long, *The 331 model with right handed neutrinos*, Phys.Rev. **D53** (1996) 437–445, [hep-ph/9504274].
- [189] H. N. Long,  *$SU(3)_L \times U(1)_N$  model for right-handed neutrino neutral currents*, Phys.Rev. **D54** (1996) 4691–4693, [hep-ph/9607439].

- [190] R. A. Diaz, R. Martinez, and F. Ochoa, *331 vector-like models with mirror fermions as a possible solution for the discrepancy in the b-quark asymmetries, and for the neutrino mass and mixing pattern*, hep-ph/0508051.
- [191] T. Kiyari, T. Maekawa, M. Masuda, and H. Taira, *On nature of right-handed singlet in 331 model and anomalies before and after SSB*, hep-ph/0206180.
- [192] T. Kiyari, T. Maekawa, and S. Yokoi, *Note on triangle anomalies and assignment of singlet in 331 like model*, Mod.Phys.Lett. **A17** (2002) 1813, [hep-ph/0206019].
- [193] G. 't Hooft, *Symmetry Breaking Through Bell-Jackiw Anomalies*, Phys.Rev.Lett. **37** (1976) 8–11.
- [194] C. Baker, D. Doyle, P. Geltenbort, K. Green, M. van der Grinten, et al., *An Improved experimental limit on the electric dipole moment of the neutron*, Phys.Rev.Lett. **97** (2006) 131801, [hep-ex/0602020].
- [195] R. Peccei and H. R. Quinn, *CP Conservation in the Presence of Instantons*, Phys.Rev.Lett. **38** (1977) 1440–1443.
- [196] S. Weinberg, *A New Light Boson?*, Phys.Rev.Lett. **40** (1978) 223–226.
- [197] F. Wilczek, *Problem of Strong P and T Invariance in the Presence of Instantons*, Phys.Rev.Lett. **40** (1978) 279–282.
- [198] P. B. Pal, *The Strong CP question in  $SU(3)_C \times SU(3)_L \times U(1)_N$  models*, Phys.Rev. **D52** (1995) 1659–1662, [hep-ph/9411406].
- [199] A. G. Dias and V. Pleitez, *Stabilizing the invisible axion in 3-3-1 models*, Phys.Rev. **D69** (2004) 077702, [hep-ph/0308037].
- [200] J. Montero and B. Sanchez-Vega, *Natural PQ symmetry in the 3-3-1 model with a minimal scalar sector*, Phys.Rev. **D84** (2011) 055019, [arXiv:1102.5374].
- [201] P. Dong, H. Long, and H. Hung, *Question of Peccei-Quinn symmetry and quark masses in the economical 3-3-1 model*, Phys.Rev. **D86** (2012) 033002, [arXiv:1205.5648].
- [202] W. A. Ponce, J. B. Florez, and L. A. Sanchez, *Analysis of  $SU(3)_c \times SU(3)_L \times U(1)_X$  local gauge theory*, Int.J.Mod.Phys. **A17** (2002) 643–660, [hep-ph/0103100].
- [203] W. A. Ponce, Y. Giraldo, and L. A. Sanchez, *Systematic study of 3-3-1 models*, hep-ph/0201133.
- [204] D. Romero, O. Ravinez, H. Diaz, and J. Reyes, *Exotic gauge bosons in the 331 model*, AIP Conf.Proc. **1123** (2009) 232–234.

- 
- [205] **MEG** Collaboration, J. Adam et al., *New limit on the lepton-flavour violating decay  $\mu^+ \rightarrow e^+\gamma$* , Phys.Rev.Lett. **107** (2011) 171801, [[arXiv:1107.5547](#)].
- [206] J. T. Liu and D. Ng, *Lepton flavor changing processes and CP violation in the 331 model*, Phys.Rev. **D50** (1994) 548–557, [[hep-ph/9401228](#)].
- [207] V. Pleitez, *A Remark on the muonium to anti-muonium conversion in a 331 model*, Phys.Rev. **D61** (2000) 057903, [[hep-ph/9905406](#)].
- [208] A. Gusso, C. de S. Pires, and P. Rodrigues da Silva, *Minimal 3-3-1 model, lepton mixing and muonium - antimuonium conversion*, J.Phys. **G30** (2004) 37–44, [[hep-ph/0208062](#)].
- [209] P. Dong and H. N. Long, *Neutrino masses and lepton flavor violation in the 3-3-1 model with right-handed neutrinos*, Phys.Rev. **D77** (2008) 057302, [[arXiv:0801.4196](#)].
- [210] I. Cortes Maldonado, A. Moyotl, and G. Tavares-Velasco, *Lepton flavor violating decay  $Z \rightarrow l_i l_j$  in the 331 model*, Int.J.Mod.Phys. **A26** (2011) 4171–4185, [[arXiv:1109.0661](#)].
- [211] J. Cabarcas, J. Duarte, and J.-A. Rodriguez, *Lepton Flavor Violation processes in 331 Models*, PoS **HQL2012** (2012) 072, [[arXiv:1212.3586](#)].
- [212] J. Montero, C. A. de Sousa Pires, and V. Pleitez, *Neutrinoless double beta decay with and without Majoron - like boson emission in a 3-3-1 model*, Phys.Rev. **D64** (2001) 096001, [[hep-ph/0003284](#)].
- [213] J. Montero, C. de S. Pires, and V. Pleitez, *Seesaw tau lepton mass and calculable neutrino masses in a 3-3-1 model*, Phys.Rev. **D65** (2002) 093017, [[hep-ph/0103096](#)].
- [214] J. Montero, C. de S. Pires, and V. Pleitez, *Lepton masses from a TeV scale in a 3-3-1 model*, Phys.Rev. **D66** (2002) 113003, [[hep-ph/0112203](#)].
- [215] J. Montero, C. De S. Pires, and V. Pleitez, *Neutrino masses through the seesaw mechanism in 3-3-1 models*, Phys.Rev. **D65** (2002) 095001, [[hep-ph/0112246](#)].
- [216] A. Gusso, C. de S. Pires, and P. Rodrigues da Silva, *Neutrino mixing and the minimal 3-3-1 model*, Mod.Phys.Lett. **A18** (2003) 1849, [[hep-ph/0305168](#)].
- [217] A. G. Dias, A. Doff, C. de S. Pires, and P. Rodrigues da Silva, *Neutrino decay and neutrinoless double beta decay in a 3-3-1 model*, Phys.Rev. **D72** (2005) 035006, [[hep-ph/0503014](#)].
- [218] A. G. Dias, C. de S. Pires, and P. Rodrigues da Silva, *Naturally light right-handed neutrinos in a 3-3-1 model*, Phys.Lett. **B628** (2005) 85–92, [[hep-ph/0508186](#)].

- [219] D. L. Anderson and M. Sher, *3-3-1 models with unique lepton generations*, Phys.Rev. **D72** (2005) 095014, [hep-ph/0509200].
- [220] D. Van Soa, P. V. Dong, T. T. Huong, and H. N. Long, *Bilepton contributions to the neutrinoless double beta decay in the economical 3-3-1 model*, J.Exp.Theor.Phys. **108** (2009) 757–763, [arXiv:0805.4456].
- [221] D. Cogollo, H. Diniz, C. de S. Pires, and P. Rodrigues da Silva, *The Seesaw mechanism at TeV scale in the 3-3-1 model with right-handed neutrinos*, Eur.Phys.J. **C58** (2008) 455–461, [arXiv:0806.3087].
- [222] D. Cogollo, H. Diniz, and C. de S. Pires, *KeV right-handed neutrinos from type II seesaw mechanism in a 3-3-1 model*, arXiv:0903.0370.
- [223] F. Queiroz, C. de S. Pires, and P. R. da Silva, *A minimal 3-3-1 model with naturally sub-eV neutrinos*, Phys.Rev. **D82** (2010) 065018, [arXiv:1003.1270].
- [224] M. Medina and P. de Holanda, *Non-Standard Neutrinos Interactions in A 331 Model with Minimum Higgs Sector*, Adv.High Energy Phys. **2012** (2012) 763829, [arXiv:1108.5228].
- [225] M. Catano, R. Martinez, and F. Ochoa, *Neutrino masses in a 331 model with right-handed neutrinos without doubly charged Higgs bosons via inverse and double seesaw mechanisms*, Phys.Rev. **D86** (2012) 073015, [arXiv:1206.1966].
- [226] W. Caetano, D. Cogollo, C. de S. Pires, and P. Rodrigues da Silva, *Combining type I and type II seesaw mechanisms in the minimal 3-3-1 model*, Phys.Rev. **D86** (2012) 055021, [arXiv:1206.5741].
- [227] M. Capdequi-Peyranere and M. Rodriguez, *Charginos and neutralinos production at 3-3-1 supersymmetric model in  $e^- e^-$  scattering*, Phys.Rev. **D65** (2002) 035001, [hep-ph/0103013].
- [228] J. Montero, V. Pleitez, and M. Rodriguez, *Lepton masses in a supersymmetric 3-3-1 model*, Phys.Rev. **D65** (2002) 095008, [hep-ph/0112248].
- [229] J. Montero, V. Pleitez, and M. Rodriguez, *A Supersymmetric 3-3-1 model*, Phys.Rev. **D65** (2002) 035006, [hep-ph/0012178].
- [230] J. Montero, V. Pleitez, and M. Rodriguez, *Supersymmetric 3-3-1 model with right-handed neutrinos*, Phys.Rev. **D70** (2004) 075004, [hep-ph/0406299].
- [231] M. Rodriguez, *Proton decay in supersymmetric 331 model*, hep-ph/0408153.
- [232] D. Huong and H. Long, *Non-thermal leptogenesis in supersymmetric 3-3-1 model with inflationary scenario*, J.Phys. **G38** (2011) 015202, [arXiv:1004.1246].

- 
- [233] S. Sen and A. Dixit, *A Supersymmetric 3-3-1 model with MSSM-like scalar sector*, hep-ph/0510393.
- [234] M. Rodriguez, *Scalar sector in the minimal supersymmetric 3-3-1 model*, Int.J.Mod.Phys. **A21** (2006) 4303–4322, [hep-ph/0510333].
- [235] P. Dong, T. Huong, N. Thuy, and H. N. Long, *Sfermion masses in the supersymmetric economical 3-3-1 model*, JHEP **0711** (2007) 073, [arXiv:0708.3155].
- [236] P. Dong, D. Huong, M. Rodriguez, and H. N. Long, *Supersymmetric economical 3-3-1 model*, Nucl.Phys. **B772** (2007) 150–174, [hep-ph/0701137].
- [237] H. N. Long, *Right-handed sneutrinos as self-interacting dark matter in supersymmetric economical 3-3-1 model*, Adv.Stud.Theor.Phys. **4** (2010) 173–196, [arXiv:0710.5833].
- [238] D. Huong and H. N. Long, *Neutralinos and charginos in supersymmetric economical 3-3-1 model*, JHEP **0807** (2008) 049, [arXiv:0804.3875].
- [239] P. Dong, D. Huong, N. Thuy, and H. N. Long, *Higgs phenomenology of supersymmetric economical 3-3-1 model*, Nucl.Phys. **B795** (2008) 361–384, [arXiv:0707.3712].
- [240] M. Rodriguez, *Mass Spectrum in the Minimal Supersymmetric 3-3-1 model*, arXiv:1007.0981.
- [241] D. T. Huong and H. N. Long, *Inflationary scenario in the supersymmetric economical 3-3-1 model*, Phys.Atom.Nucl. **73** (2010) 791–804, [arXiv:0807.2346].
- [242] D. Huong, L. Hue, M. Rodriguez, and H. Long, *Supersymmetric reduced minimal 3-3-1 model*, Nucl.Phys.B **870** (2013) 293–322, [arXiv:1210.6776].
- [243] M. Tully and G. C. Joshi, *Fermion masses and mixing in 331 models with horizontal symmetry*, Mod.Phys.Lett. **A13** (1998) 2065–2076, [hep-ph/9807201].
- [244] I. Gogoladze, Y. Mimura, and S. Nandi, *Orbifold breaking of 3-3-1 model*, Phys.Lett. **B554** (2003) 81–91, [hep-ph/0210320].
- [245] A. G. Dias, C. A. de S. Pires, and P. S. R. da Silva, *Discrete symmetries, invisible axion and lepton number symmetry in an economic 3 3 1 model*, Phys.Rev. **D68** (2003) 115009, [hep-ph/0309058].
- [246] N. V. Cortez and M. D. Tonasse, *Calculable lepton masses, seesaw relations and four neutrino mixings in a 3-3-1 model with extra U(1) symmetry*, Phys.Rev. **D72** (2005) 073005, [hep-ph/0510143].
- [247] F. Yin, *Neutrino mixing matrix in the 3-3-1 model with heavy leptons and A(4) symmetry*, Phys.Rev. **D75** (2007) 073010, [arXiv:0704.3827].

- [248] P. Dong, L. Hue, H. Long, and D. Soa, *The 3-3-1 model with  $A_4$  flavor symmetry*, Phys.Rev. **D81** (2010) 053004, [arXiv:1001.4625].
- [249] P. Dong, H. Long, D. Soa, and V. Vien, *The 3-3-1 model with  $S_4$  flavor symmetry*, Eur.Phys.J. **C71** (2011) 1544, [arXiv:1009.2328].
- [250] P. Dong, H. Long, C. Nam, and V. Vien, *The  $S_3$  flavor symmetry in 3-3-1 models*, Phys.Rev. **D85** (2012) 053001, [arXiv:1111.6360].
- [251] P. Dong, V. Huyen, H. Long, and H. Thuy, *Gauge boson mixing in the 3-3-1 models with discrete symmetries*, Adv.High Energy Phys. **2012** (2012) 715038.
- [252] L. A. Sanchez, W. A. Ponce, and R. Martinez,  *$SU(3)_c \times SU(3)_L \times U(1)_X$  as an  $E_6$  subgroup*, Phys.Rev. **D64** (2001) 075013, [hep-ph/0103244].
- [253] R. Martinez, W. A. Ponce, and L. A. Sanchez,  *$SU(3)_c \times SU(3)_L \times U(1)_X$  as an  $SU(6) \times U(1)_X$  subgroup*, Phys.Rev. **D65** (2002) 055013, [hep-ph/0110246].
- [254] R. A. Diaz, D. Gallego, and R. Martinez, *Renormalization group and grand unification with 331 models*, Int.J.Mod.Phys. **A22** (2007) 1849–1874, [hep-ph/0505096].
- [255] R. Gaitan and R. Martinez, *A possible grand unification theory with 331 models*, AIP Conf.Proc. **1116** (2009) 470–472.
- [256] R. Martinez, F. Ochoa, and P. Fonseca, *A 3-3-1 Model with  $SU(8)$  Unification*, arXiv:1105.4623.
- [257] S. Filippi, W. A. Ponce, and L. A. Sanchez, *Dark matter from the scalar sector of 3-3-1 models without exotic electric charges*, Europhys.Lett. **73** (2006) 142–148, [hep-ph/0509173].
- [258] J. Mizukoshi, C. de S. Pires, F. Queiroz, and P. Rodrigues da Silva, *WIMPs in a 3-3-1 model with heavy Sterile neutrinos*, Phys.Rev. **D83** (2011) 065024, [arXiv:1010.4097].
- [259] D. Huong, C. Kim, H. Long, and N. Thuy, *Probing Dark Matter in the Economical 3-3-1 Model*, arXiv:1110.1482.
- [260] J. Agrawal, P. H. Frampton, and J. T. Liu, *The Decay  $b \rightarrow s\gamma$  in the 3-3-1 model*, Int.J.Mod.Phys. **A11** (1996) 2263–2280, [hep-ph/9502353].
- [261] J. A. Rodriguez and M. Sher, *FCNC and rare B decays in 3-3-1 models*, Phys.Rev. **D70** (2004) 117702, [hep-ph/0407248].
- [262] A. Carcamo Hernandez, R. Martinez, and F. Ochoa, *Z and Z' decays with and without FCNC in 331 models*, Phys.Rev. **D73** (2006) 035007, [hep-ph/0510421].

- 
- [263] C. Promberger, S. Schatt, and F. Schwab, *Flavor Changing Neutral Current Effects and CP Violation in the Minimal 3-3-1 Model*, Phys.Rev. **D75** (2007) 115007, [hep-ph/0702169].
- [264] J. Cabarcas, D. Gomez Dumm, and R. Martinez, *Constraints on economical 331 models from mixing of  $K$ ,  $B_d$  and  $B_s$  neutral mesons*, Phys.Rev. **D77** (2008) 036002, [arXiv:0711.2467].
- [265] R. Martinez and F. Ochoa, *Mass-matrix ansatz and constraints on  $B_s^0 - \bar{B}_s^0$  mixing in 331 models*, Phys.Rev. **D77** (2008) 065012, [arXiv:0802.0309].
- [266] C. Promberger, S. Schatt, F. Schwab, and S. Uhlig, *Bounding the Minimal 331 Model through the Decay  $B \rightarrow X_s \gamma$* , Phys.Rev. **D77** (2008) 115022, [arXiv:0802.0949].
- [267] F. Schwab, *Flavor mixing and rare B and K decays in the minimal 331 model*, J.Phys.Conf.Ser. **110** (2008) 072039.
- [268] J. Cabarcas, D. Gomez Dumm, and R. Martinez, *Flavor changing neutral currents in 331 models*, J.Phys. **G37** (2010) 045001, [arXiv:0910.5700].
- [269] R. H. Benavides, Y. Giraldo, and W. A. Ponce, *FCNC in the 3-3-1 model with right-handed neutrinos*, Phys.Rev. **D80** (2009) 113009, [arXiv:0911.3568].
- [270] D. Cogollo, A. V. de Andrade, F. Queiroz, and P. Rebello Teles, *Novel sources of Flavor Changed Neutral Currents in the 331<sub>RHN</sub> model*, Eur.Phys.J. **C72** (2012) 2029, [arXiv:1201.1268].
- [271] V. Huyen, T. Lam, H. Long, and V. Phong, *Neutral currents in reduced minimal 3-3-1 model*, arXiv:1210.5833.
- [272] J. Montero, V. Pleitez, and O. Ravinez, *Concerning CP violation in 331 models*, hep-ph/9804422.
- [273] J. Montero, V. Pleitez, and O. Ravinez, *Soft superweak CP violation in a 331 model*, Phys.Rev. **D60** (1999) 076003, [hep-ph/9811280].
- [274] A. Doff, C. de S. Pires, and P. R. da Silva, *Spontaneous CP violation in the 3-3-1 model with right-handed neutrinos*, Phys.Rev. **D74** (2006) 015014, [hep-ph/0604021].
- [275] P. H. Frampton, J. T. Liu, B. C. Rasco, and D. Ng, *SSC phenomenology of the 331 model of flavor*, Mod.Phys.Lett. **A9** (1994) 1975–1984, [hep-ph/9304294].
- [276] T. Gregoire, *Vector dilepton production at hadron colliders in the 3-3-1 model*, .
- [277] Y. D. A. Coutinho, P. Queiroz Filho, and M. Tonasse, *3-3-1 Exotic quark search at CERN LEP-2 - LHC*, Phys.Rev. **D60** (1999) 115001, [hep-ph/9907553].

- [278] L. D. Ninh and H. N. Long, *SM Higgs boson production at CERN LHC in 3-3-1 model with right-handed neutrinos*, Phys.Rev. **D72** (2005) 075004, [hep-ph/0507069].
- [279] J. Cieza Montalvo, N. V. Cortez, J. Sa Borges, and M. D. Tonasse, *Searching for doubly charged Higgs bosons at the LHC in a 3-3-1 model*, Nucl.Phys. **B756** (2006) 1–15, [hep-ph/0606243].
- [280] N. Gutierrez, R. Martinez, and F. Ochoa, *Z' boson signal at Tevatron and LHC in a 331 model*, arXiv:0802.0310.
- [281] J. Cabarcas, D. Gomez Dumm, and R. Martinez, *Phenomenological aspects of the exotic T quark in 331 models*, Eur.Phys.J. **C58** (2008) 569–578, [arXiv:0809.0821].
- [282] J. Duenas, R. Martinez, and F. Ochoa, *Z' production in 331 models*, Braz.J.Phys. **38** (2008) 421–424.
- [283] J. Cieza Montalvo, N. V. Cortez, and M. Tonasse, *Doubly charged Higgs in 3-3-1 model at the CERN LHC: Prospects for Charged Higgs Discovery at Colliders 16-19 September 2008, Uppsala, Sweden*, arXiv:0812.4000.
- [284] J. Duenas, N. Gutierrez, R. Martinez, and F. Ochoa, *Z' boson signal at Fermilab-Tevatron and CERN-LHC in a 331 model*, Eur.Phys.J. **C60** (2009) 653–659.
- [285] R. Martinez and F. Ochoa, *Neutral currents production in LHC for 331 models*, AIP Conf.Proc. **1259** (2010) 136–145.
- [286] A. Alves, E. R. Barreto, and A. Dias, *Production of Charged Higgs Bosons in a 3-3-1 Model at the CERN LHC*, Phys.Rev. **D84** (2011) 075013, [arXiv:1105.4849].
- [287] A. Alves, E. Ramirez Barreto, A. Dias, C. de S. Pires, F. Queiroz, et al., *Probing 3-3-1 Models in Diphoton Higgs Boson Decay*, Phys.Rev. **D84** (2011) 115004, [arXiv:1109.0238].
- [288] A. Mekahlia, N. Mebarki, and M. Haouchine, *Top anti-top forward-backward asymmetry in the economical 331 model*, AIP Conf.Proc. **1444** (2011) 430–433.
- [289] J. C. Montalvo, R. G. Ramirez, G. R. Ulloa, A. R. Mendoza, and M. Tonasse, *Neutral 3-3-1 Higgs Bosons at LHC*, arXiv:1205.4042.
- [290] R. Martinez and F. Ochoa, *Production of multiple charged Higgs bosons in 3-3-1 models*, Phys.Rev. **D86** (2012) 065030, [arXiv:1208.4085].
- [291] G. Tavares-Velasco and J. Toscano, *Photon photon scattering in a 3-3-1 model*, Europhys.Lett. **53** (2001) 465–470, [hep-ph/9911226].

- 
- [292] E. Ramirez Barreto, Y. D. A. Coutinho, and J. Sa Borges, *Four leptons production in  $e^- e^+$  collisions from 3-3-1 model*, Phys.Lett. **B632** (2006) 675–679, [hep-ph/0509355].
- [293] E. Ramirez Barreto, Y. D. A. Coutinho, and J. Sa Borges, *Bounds for  $Z'$  mass in 3-3-1 Models from  $e^+ e^-$  Collisions at ILC and CLIC Energies*, hep-ph/0605098.
- [294] D. Van Soa and D. Le Thuy, *Study of the singly charged Higgs in the economic at 3-3-1 model at  $e^+ e^-$  colliders*, hep-ph/0610297.
- [295] E. Ramirez Barreto, Y. D. A. Coutinho, and J. Sa Borges, *Extra neutral gauge boson from two versions of the 3-3-1 model in future linear colliders*, Eur.Phys.J. **C50** (2007) 909–917, [hep-ph/0703099].
- [296] J. Cieza Montalvo, N. V. Cortez, and M. Tonasse, *Probing doubly charged Higgs in  $e^+ e^-$  Colliders in 3-3-1 Model*, Phys.Rev. **D78** (2008) 116003, [arXiv:0804.0618].
- [297] J. Cieza Montalvo, N. V. Cortez, and M. Tonasse, *Doubly charged Higgs through photon photon collisions in 3-3-1 models*, Phys.Rev. **D77** (2008) 095015, [arXiv:0804.0033].
- [298] A. Gutierrez-Rodriguez, *Bounds on the dipole moments of the tau-neutrino via the process  $e^+ e^- \rightarrow \nu \bar{\nu} \gamma$  in a 331 model*, Eur.Phys.J. **C71** (2011) 1819, [arXiv:1112.0268].
- [299] J. C. Montalvo, G. R. Ulloa, and M. Tonasse, *Doubly charged Higgs from  $e-\gamma$  scattering in the 3-3-1 Model*, Eur.Phys.J. **C72** (2012) 2210, [arXiv:1205.3822].
- [300] A. J. Buras and J. Gierbach, *Complete NLO QCD Corrections for Tree Level  $\Delta F = 2$  FCNC Processes*, JHEP **1203** (2012) 052, [arXiv:1201.1302].
- [301] A. J. Buras, F. De Fazio, J. Gierbach, and M. V. Carlucci, *The Anatomy of Quark Flavour Observables in 331 Models in the Flavour Precision Era*, JHEP **1302** (2013) 023, [arXiv:1211.1237].
- [302] P. Langacker and M. Plumacher, *Flavor changing effects in theories with a heavy  $Z'$  boson with family nonuniversal couplings*, Phys.Rev. **D62** (2000) 013006, [hep-ph/0001204].
- [303] CMS Collaboration, S. Chatrchyan et al., *Search for narrow resonances in dilepton mass spectra in  $pp$  collisions at  $\sqrt{s} = 7$  TeV*, Phys.Lett. **B714** (2012) 158–179, [arXiv:1206.1849].



# Acknowledgments

The years of Ph.D. school are notoriously a key period during the life of a young aspiring scientist, but I would have never imagined they would have been so crucial for me. At the end of this experience, I would like to thank the people that have been part of it.

I have many reasons to thank with sincere gratitude my ‘Doktorvater’ Andrzej Buras. First of all because he gave me the honor of accepting me as his last doctoral student, giving me the possibility to join his intensely stimulating research group. Then, for teaching me his way of being a great physicist, combining intelligence, passion, deep knowledge of the subjects, indefatigable diligence, and at the same time a great person, rich in wisdom and interests (especially classical music and Chopin). Most important, for really being a fatherly figure for me, with his comprehension and suggestions.

I warmly thank all the people whom for different reasons I have worked with. Fulvia de Fazio for renewing her partnership with me, Gino Isidori for the insightful experience with him, and moreover Jennifer Girrbach, Stefania Gori, Luca Merlo, Emmanuel Stamou for the fruitful collaborations. All the former and present members of the T31 and IAS Fundamental Physics groups for the daily company and discussions. My officemates Björn Duling, Katrin Gemmler, Tillman Heidsieck for the relaxed working environment, as well as Stefan Recksiegel and Elke Krüger for their practical help. Otmar Biebel from the DFG Graduiertenkolleg ‘Particle Physics at the Energy Frontier of New Phenomena’ for his precious support, and Frank Steffen and Monika Goldammer for the wonderful activities at the International Max Planck Research School. Nora Brambilla and Alexander Lenz for the formative experience of the exercise tutorials for their lectures, together with the colleagues I joined for those.

Concerning in particular this work of thesis, I thank very much Marco Bardoscia and Roberto Preghenella for their computational consulting, them together with Andrzej Buras for their critical reading of the drafts, and Jennifer Girrbach for her kind help with the German language.

Finally, and from the deepest of my heart.  
My parents, my unbreakable certainty.  
My brother, refund but always fugitive.  
All my family, especially nonna Mena, whom I feel close as she had never left.  
Aida, always there to remember me that with some purring everything is ok.  
Marco, my anchor and my pole star.  
Roby, a totally unexpected shot of life and emotions.  
My best friends, with whom I always feel at home: Anastasia, Antonella, Felice, Anna, Marco, Nicoletta, Annarita, Ylenia, Alfonso and his family.

